Wind Tunnel Investigation of the Pressures acting on Sheet Clad Scaffolds

Department Report No. 397

Mr. H. Irtaza
Dr. R.G. Beale
Dr. M.H.R. Godley

School of Built-Environment
Oxford Brookes University
Oxford, UK

January 2010

Published October 2010

British Library Cataloguing in Publication Data
A catalogue record for this book is available from the British Library

ISBN: ISBN 978-0-9556254-3-5
Printed in Great Britain by Oxford Brookes University, Oxford, U.K.

Abstract

This report presents the results of wind-tunnel tests on a 1:30 scale model of the Silsoe Full-scale Experimental Building together with two models representing sheeted scaffolding attached around the building, one with the sheeting touching the ground and one with the sheet elevated from the ground at a height corresponding to 1m on the full building.

Pressure contours at various wind orientations to the building together with mean, peak and r.m.s. pressures are given at various points on the surface of the building and on both the inner and the outer faces of the scaffold.

In all cases results are given for two sets of terrain, one corresponding to the terrain at the Silsoe site and one corresponding to a developed site.

CONTENTS

Abstract

1: Introduction 1

2: Full-scale Silsoe data 4

3: Experimental Solution Strategies 7

3.1: Position of experimental tabs 8

4: Testing Facilities and Equipments for Wind Pressure Study 14

5: Experimental Programme 15

6: References 21

Appendix 1: (Experiment 1) *Pressure Coefficients on the Scaled Cubical Silsoe Experimental Building (SEB)* 22

Appendix 2: (Experiment 2) *Pressure Coefficients on theSEB Surrounded by sheeting* 49

Appendix 3: (Experiment 3) *Pressure Coefficients on the SEB Surrounded by elevated sheeting* 76

Appendix 4: (Experiment 4) *Pressure Coefficients on the outer face of the sheeting surrounding the SEB* 103

Appendix 5: (Experiment 5) *Pressure Coefficients on the inner face of the sheeting surrounding the SEB* 118

Appendix 6: (Experiment 6) *Pressure Coefficients on the outer face of elevated sheeting surrounding the SEB* 139

Appendix 7: (Experiment 7) *Pressure Coefficients on the inner face of elevated sheeting surrounding the SEB* 150

Wind Tunnel Investigation of the Pressures acting on Sheet Clad Scaffolds

Department Report No. 397

Mr. H. Irtaza
Dr. R.G. Beale
Dr. M.H.R. Godley

School of Built-Environment
Oxford Brookes University
Oxford, UK

January 2010

Published October 2010

British Library Cataloguing in Publication Data
A catalogue record for this book is available from the British Library

ISBN: ISBN 978-0-9556254-3-5
Printed in Great Britain by Oxford Brookes University, Oxford, U.K.

Abstract

This report presents the results of wind-tunnel tests on a 1:30 scale model of the Silsoe Full-scale Experimental Building together with two models representing sheeted scaffolding attached around the building, one with the sheeting touching the ground and one with the sheet elevated from the ground at a height corresponding to 1m on the full building.

Pressure contours at various wind orientations to the building together with mean, peak and r.m.s. pressures are given at various points on the surface of the building and on both the inner and the outer faces of the scaffold.

In all cases results are given for two sets of terrain, one corresponding to the terrain at the Silsoe site and one corresponding to a developed site.

CONTENTS

Abstract

1: Introduction 1

2: Full-scale Silsoe data 4

3: Experimental Solution Strategies 7

3.1: Position of experimental tabs 8

4: Testing Facilities and Equipments for Wind Pressure Study 14

5: Experimental Programme 15

6: References 21

Appendix 1: (Experiment 1) *Pressure Coefficients on the Scaled Cubical Silsoe Experimental Building (SEB)* 22

Appendix 2: (Experiment 2) *Pressure Coefficients on theSEB Surrounded by sheeting* 49

Appendix 3: (Experiment 3) *Pressure Coefficients on the SEB Surrounded by elevated sheeting* 76

Appendix 4: (Experiment 4) *Pressure Coefficients on the outer face of the sheeting surrounding the SEB* 103

Appendix 5: (Experiment 5) *Pressure Coefficients on the inner face of the sheeting surrounding the SEB* 118

Appendix 6: (Experiment 6) *Pressure Coefficients on the outer face of elevated sheeting surrounding the SEB* 139

Appendix 7: (Experiment 7) *Pressure Coefficients on the inner face of elevated sheeting surrounding the SEB* 150

1 Introduction

Steel scaffolds are extensively used to provide access and support to permanent and temporary works during different stages of construction in the UK and other parts of the world. Figure 1 shows a typical access scaffold system. Scaffold systems are light in weight, easy to maintain, install, and dismantle. They are mostly fabricated from hot rolled steel tubes. The basic components of a tube-and-fitting scaffold are standards, ledgers and transoms. The vertical tubes transfer the entire self weight of the structure and the imposed loads to the ground and are called standards or uprights. Each standard has a base plate underneath to spread the load. In access scaffolds the standards are connected by horizontal tubes which are parallel to the facade called ledgers and perpendicular to the façade called transoms. Transoms are fixed to the ledgers at right angles. The main transoms are placed next to the standards. They hold the standards in place and provide support for boards. Intermediate transoms are those placed between the main transoms to provide extra support for boards. In proprietary scaffolds, other shaped members are used to provide the transom and ledger elements but have the same purpose. The stability for these structures is provided by tie and bracing members. The loading applied to the scaffold consists of the self weight of the structure and imposed loads including men, and materials and wind loads.

Figure 1 A typical tube and fitting scaffold system

Much research, both experimental and computational has been done to determine the exact mechanism of scaffold failure under different conditions of loading. This includes analyses based on the effective length method to more advanced non-linear force displacement effects including both local member imperfections, $P-\delta$, and overall geometric imperfections, $P-\Delta$). These include finite element analyses taking into account the influence of semi-rigid standard-ledger and standard-transom connections taking both material and geometric non-linearity into account. Most of the previous research was directed at obtaining an

understanding of the behaviour of scaffolds under load. Limited research has been reported on the magnitude of loads actually acting on the scaffold particularly wind loading.

Scaffolds are often clad with nets or wind proof sheets to protect both passers-by and the work force from falling debris and also to shield workers from extreme weather. Cladding increases wind loads on the scaffold making scaffold structures susceptible to damage or collapse under stormy conditions. Very little published research has been reported on the effects of wind loads on access scaffolds. The UK Health and Safety Executive has published a few reports of casualties and damage to both scaffold structures and building structures during storms and high winds (Maitra, 1997) but in the current design and analysis of scaffolds the wind loads are derived from experiments conducted on permanent structures and no allowance is made for the presence of the façades of the building to which the scaffold is attached. Limited research using Computational Fluid Dynamics has been reported to determine the wind loads on temporary structures.

The reason why wind-tunnel tests on bare-pole and sheeted scaffold structures have not been undertaken in the past is because of the scaling effect. A scale of 1:50 will lead to the model diameter of a scaffold tube to be less than 1 mm and the thickness of the sheeting to be 0.008 mm. At these sizes it is very difficult to make the stiffness of the scaled scaffold tube proportional to that of the original one. It is also very difficult to fix pressure taps on scaled scaffold tubes and on the nets and sheeting. Ideally the aeroelastic nature of netting and sheeting compels requires aeroelastic wind-tunnel tests on clad scaffolds, because any question regarding the static or dynamic stability of the fabric can only be accurately answered by an aeroelastic wind tunnel test. A rigid model test gives no information regarding the possibility of divergence or flutter, but can be used to predict fluctuating wind pressure due to buffeting.

Keeping all these in mind, wind-tunnel tests were carried out on a scale model of the cubical Silsoe Experimental Building (SEB) as shown in Figure 2 and that on sheet clad scaffolds as shown in Figures 3 and 4surrounding the SEB. The SEB was a (6 m x 6 m x 6 m) cube erected at Silsoe in order to get full-scale data on the wind pressures acting on a building (www.silsoeresearch.org.uk/envir-wind-

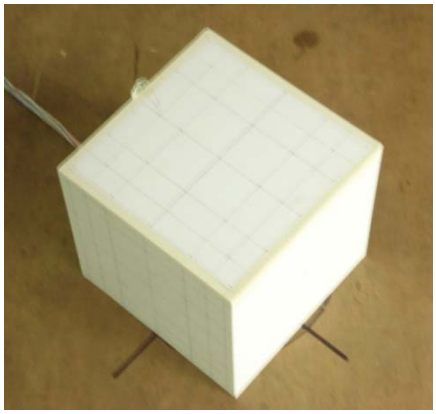

Figure 2 Scaled cubical SEB

waste/wind.html, Richards and Hoxey, 2008).

In the model, the sheeted scaffold surrounding the building was 4 mm thick (with a tapered top) with pressure taps implanted both on the inner and outer face of the sheeting to measure pressure coefficients. The reason for this these experiments was that there was neither full-scale nor model-scale sheeted results available for the SEB. Scale model results for the unsheeted SEB were available for comparison (Richards et al 2007).

The ultimate purpose of wind-tunnel testing of sheeted scaffold models is to contribute significantly to the knowledge of forces due to wind loads that we cannot otherwise assess pertaining, in particular, to wind loads.

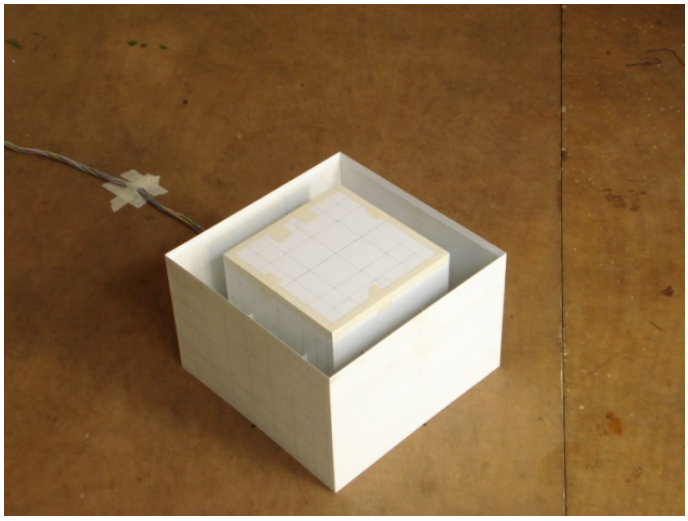

Figure 3 Scaled cubical SEB surrounded by a sheet clad scaffold

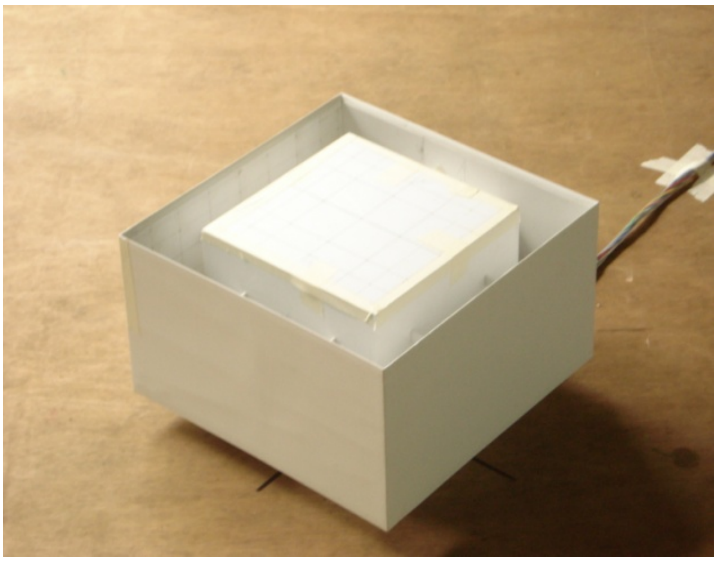

Figure 4 Scaled cubical SEB surrounded by an elevated sheet clad scaffold

These experimental tests have been validated by simulating the above model using Computational Fluid Dynamics (Irtaza, 2009). Although it is new area of study, particularly in its application to external flow, the model has been used to find pressure coefficients on sheets and nets surrounding a scaffold. The net was modelled as a porous media and porous jump boundary conditions were used to simulate a net. Prior to this, wind tunnel tests were conducted on two types of net commonly used in construction industries to determine their permeability.

2 Silsoe Full-Scale Experimental Data

The full scale Silsoe Experimental Building (www.silsoeresearch.org.uk/envir-wind-waste/wind.html) shown in Figure 5 was situated at the Silsoe Research Institute (SRI) in an exposed position in relatively flat terrain in South Bedfordshire, UK. It was constructed in the late 1990s to obtain full-scale data and to allow the comparison of full scale against model scale wind tunnel data. The Silsoe Experimental Building (SEB) was positioned so that the boundary layer was generated from a fetch consisting of short grass with an effective roughness length of 0.006m - 0.01m. Checks undertaken in previous years showed that the effective roughness length of the fetch was constant due to regular cutting of the grass.

(a) Open terrain with full scale buildings **(b) Cubical SEB**

Figure 5 Silsoe Experimental Buildings (Kaspersky and Hoxey, 2008)

The cube could be rotated through 360^{o} and pitched on the horizontal axis by 5^{o}. The cube surface consisted of sheet metal cladding with a smooth plastic coating to afford protection and avoid changes of the surface roughness due to rust. A photograph of the cube can be seen in Figure 5(b).

The cubical SEB was instrumented with surface tapping points on a vertical and horizontal centerline section on the windward face, roof and leeward faces with additional tappings on

one quarter of the roof. Simultaneous measurements could be made of 32 pressures around the cube and the wind dynamic pressure and direction could be derived simultaneously from an ultrasonic anemometer positioned 25 m upstream of the building at roof height. The pressure tap locations could also be used to obtain data when the cube was skewed at 45^o to the incident wind. The tapping points were constructed of simple 7mm diameter holes (a size sufficient to prevent water blocking the tapping points) and the pressure signals were transmitted pneumatically, using a 6mm internal diameter plastic tube to transducers mounted centrally within the cube. Tube lengths of up to 10 metres were used in this system giving a frequency response of 3dB down at 8Hz (Richards and Hoxey, 2008).

The fully recorded information consisting of simultaneous measurements of the pressures at a sampling rate of 4.17 samples per second (~5Hz) together with three components of the wind speed. These were processed to give all the required experimental data including mean, fluctuating and spectral properties and can be found in the work by Richards et al (Richards et al, 2007). 36 minutes record lengths were used (9000 samples) which were sub-divided into three 12 minute segments. For some of the runs the cube was rotated to 45^o clockwise so that the instrumented corner could be towards the prevailing winds. In order to investigate the roof pressure distribution, measurements could be carried out with the corner roof taps in a variety of orientations. A polynomial fit was used to enable actual measurements of wind speed and direction to be manipulated to give a full quasi-steady prediction of surface pressure.

The velocity profile at the Silsoe Research Institute site (as shown in Figure 6a) was measured at various times and is well matched by a simple logarithmic profile with a roughness length z_o = 0.006 - 0.01 m. This means that the cube had a Jensen number of 600-1000. The longitudinal turbulence intensity at the roof height was typically 19-20% as shown in Figure 9b. The **U** and **V** directions were parallel to the ground, **U** being normal to the façade and **V** parallel to the façade. The **W** direction was normal to the ground.

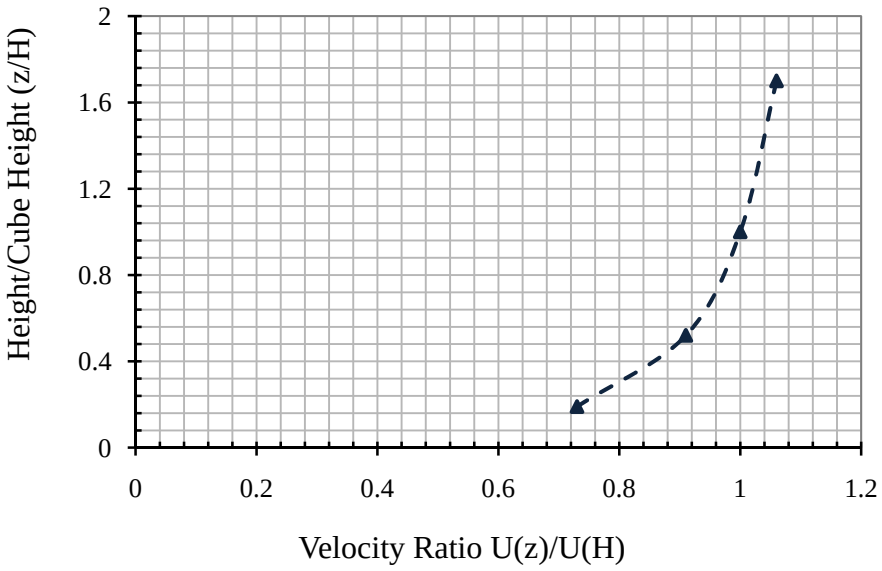

(a) Velocity profile

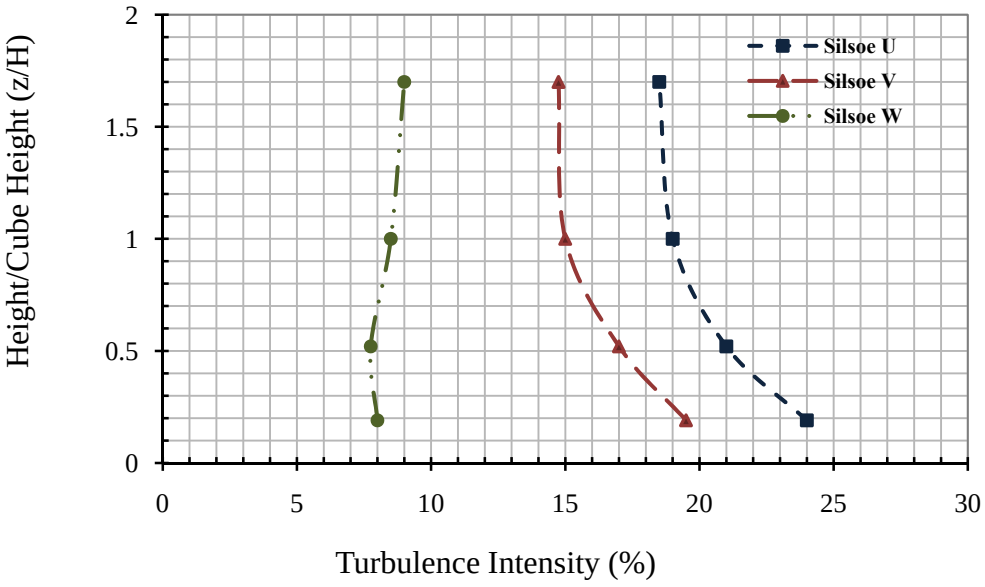

(b) Wind turbulence in all the three directions

Figure 6 Wind profile and wind-turbulence at Silsoe site (Richards et al, 2007)

3 Experimental Solution Strategies

The results of wind-tunnel experiments have been used in this report to determine the forces on the scaled models. The models used in the wind-tunnel experiments are described below:

(i) A scaled cubical SEB and shown in Figure 2.
(ii) A sheet clad scaffold surrounding a scaled SEB and shown in Figure 3.
(iii) An elevated sheet clad scaffold surrounding a scaled SEB and shown in Figure 4.

The elevated sheet in experiment (iii) was constructed to simulate a scaffold which did not have sheeting touching the ground but where the sheeting was terminated 1 m above ground level. This was to investigate the influence of wind flow between scaffold and the building.

Seven sets of experiments were conducted on the models described above. These are:

Experiment-1: Determination of pressure coefficients on the walls and roof of the scaled cubical Silsoe Experimental Building (SEB).

Experiment-2: Determination of pressure coefficients on the wall and roof of the scaled cubical SEB surrounded by the sheet clad scaffold.

Experiment-3: Determination of pressure coefficients on the wall and roof of the scaled cubical SEB surrounded by the elevated sheet clad scaffold.

Experiment-4: Determination of pressure coefficients on the outer face of the sheet clad scaffold surrounding SEB.

Experiment-5: Determination of pressure coefficients on the inner face of the sheet clad scaffold surrounding SEB.

Experiment-6: Determination of pressure coefficients on the outer face of the elevated sheet clad scaffold surrounding SEB.

Experiment-7: Determination of pressure coefficients on the inner face of the elevated sheet clad scaffold surrounding SEB.

For each experiment the following plots/diagrams are given in the appropriate appendices:

- Diagram of experimental set-up
- Pressure tap locations and reference numbers
- For the two experimental velocities and turbulence patterns:

1. Pressure coefficient contours on roof (experiments 1-3); windward, side and leeward faces for wind inclined at 15^o intervals from -45^o to $+45^o$
2. Mean, peak and r.m.s. pressure values at selected taps for wind inclinations varying from 0^o to 360^o (Note that if peak positive pressure went negative it was recorded as zero and correspondingly if the peak negative pressure went positive it was recorded as zero).

3.1 Position of Pressure Taps for the Experimental Models

The building models were fabricated using 2 mm thick white acrylic plastic. The stainless steel tubing pressure taps used were 10 mm long, 1.00 mm external diameter and 0.9 mm internal diameter. They were inserted into holes drilled in the plastic sheeting with one end of the tap flush with the wall/roof surface. The tubing for measuring the pressures consisted of 300 - 400 mm vinyl tubes.

In Experiment-1 the observations were recorded on 1:30 scaled model of the cubical SEB of dimension 200 x 200 x 200 mm as shown in Figure 7 both on the roof and the south walls. The location of pressure taps on the roof and on south vertical wall face are shown in the Figures 8 and 9. The model was tested at every 15 degrees angle of rotation of the turn-table to produce a set of 24 observations around the building. A total of 61 taps (31 taps on the roof + 30 taps on a vertical wall face) were used for the first phase of experiment. The coding that was used throughout the experiments for tap positions was a four digit number.

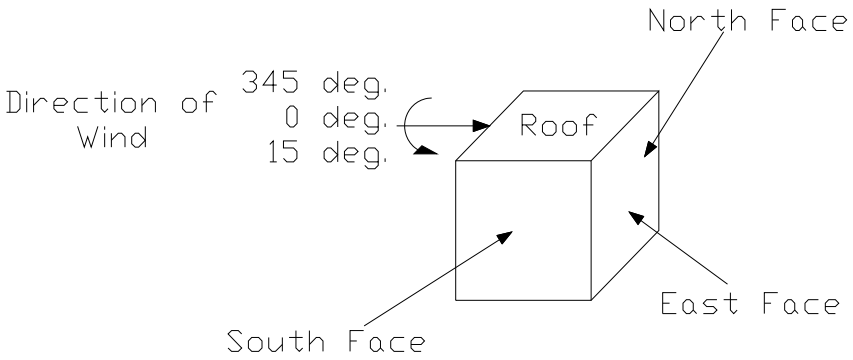

Figure 7 Scaled cubical SEB

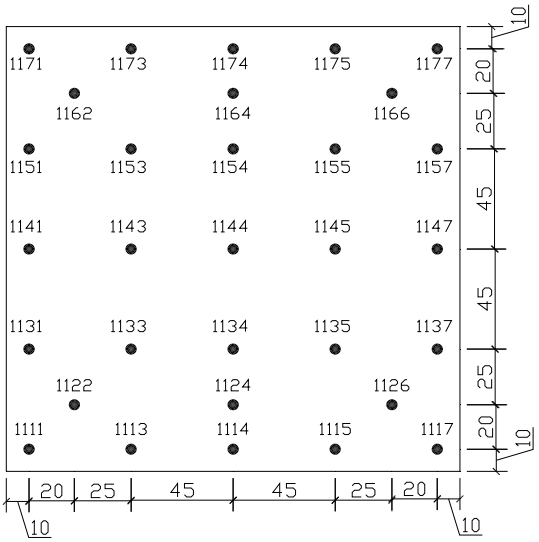

Figure 8 Pressure tap locations on roof

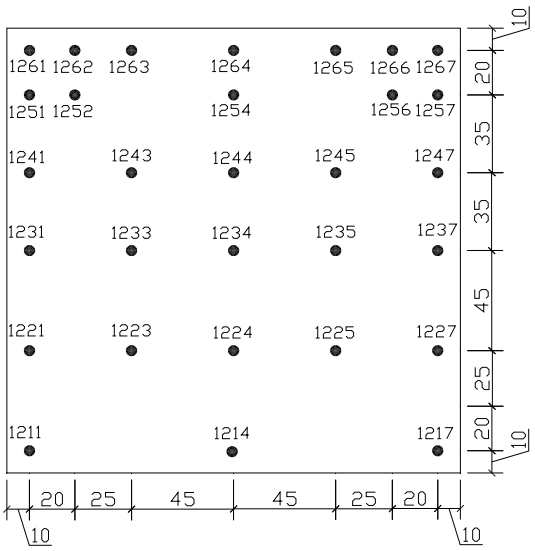

Figure 9 Pressure tap locations on the south wall face

In Experiment-2 and Experiment-3 the observations were also recorded on 1:30 scaled models of the scaled cubical SEB of dimension 200 x 200 x 200 mm surrounded by a sheet clad scaffold (Figure 10) and by an elevated sheet clad scaffold (Figure 13) respectively. The location of pressure taps on the roof and on south vertical wall face are shown in Figures 11 and 12 and Figures 14 and 15 respectively for the two scaffolds. These models were tested at every 15 degrees angle of rotation of the turn-table to produce a set of 24 observations around the building. A total of 61 taps (31 taps on the roof + 30 taps on a vertical wall face) were used for the first phase of experiment. The South face is face of the scaffold which is the windward face when the scaffold is normal to the wind direction as seen in Figure 10. The North face was initially the leeward face and the East face initially a side face.

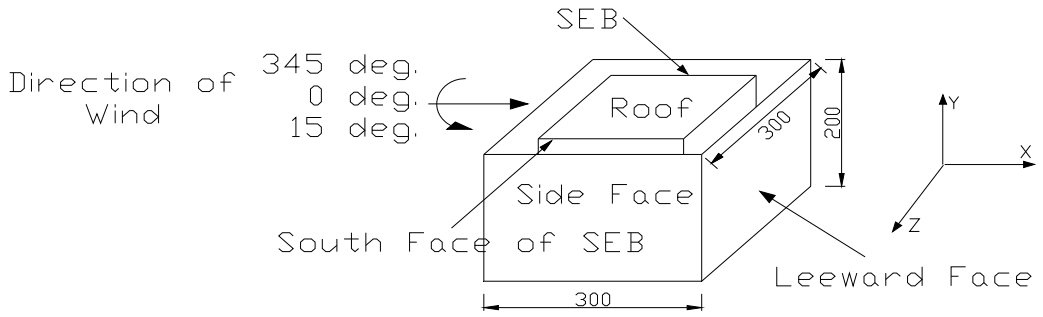

Figure 10 Scaled SEB surrounded by impermeable sheet all around

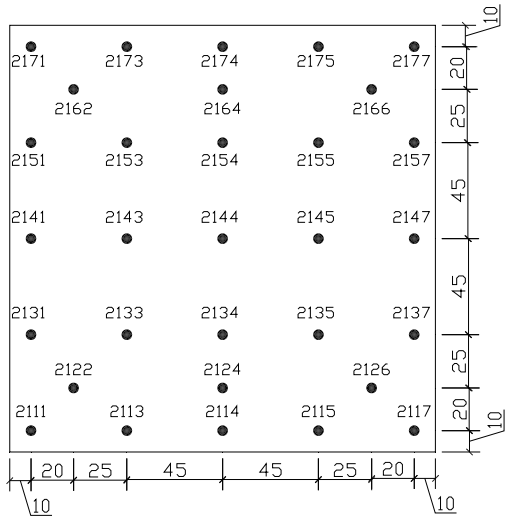

Figure 11 Pressure tap locations on roof

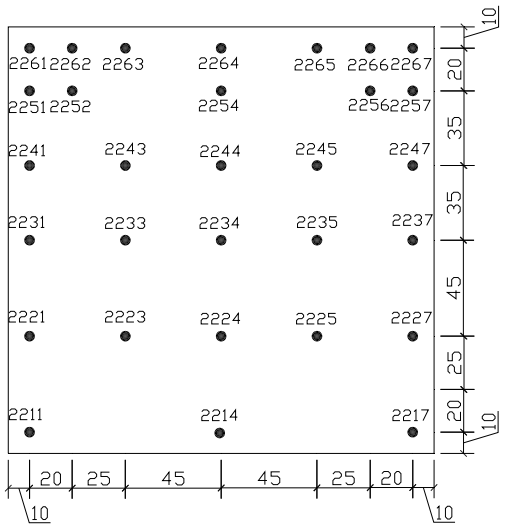

Figure 12 Pressure tap locations on the South wall face

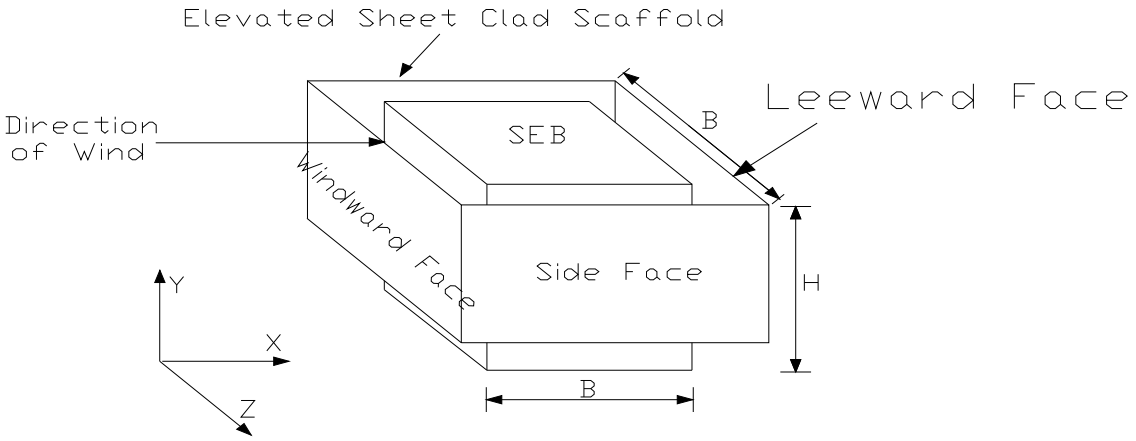

Figure 13 Scaled SEB surrounded by elevated impermeable sheet all around

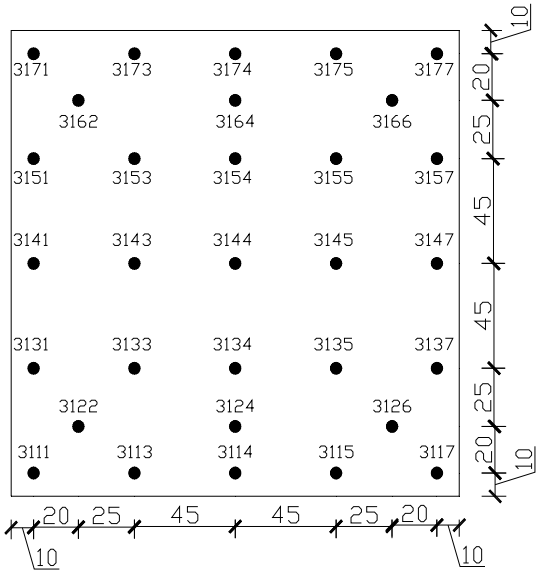

Figure 17 Pressure tap locations on roof

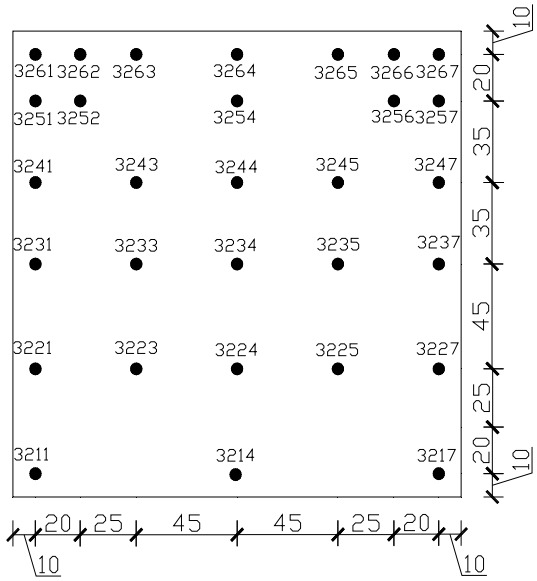

Figure 15 Pressure tap locations on the South wall face

In Experiment-4 and Experiment-5 the observations were recorded on the sheet clad scaffolds surrounding scaled cubical SEB as shown in Figure 13. In Experiment-4 the observations were recorded on the outer South face, whereas, in Experiment-5 the observations were recorded on the inner South face respectively and the location of pressure taps on the outer and inner south face of the sheeting are shown in Figure 16a and Figure 17a. Additional pressure taps were installed on the other two faces (North and East faces) to counter check the recordings of pressures and are shown in Figures 16b, 16c, 17b and 17c respectively. In a similar manner to Experiment 1 the observations were recorded by rotating the models at every 15 degrees until a complete rotation had occurred. In this case a total of 44 taps (36 taps on the outer main face of the sheeting + 4 taps each on the other two face of the sheeting) were used for the experiment.

The distances shown in Figure 20 for the location of pressure taps were from the outer edge of the sheeting. Also the top 7 mm of the sheeting were tapered from the inside as shown by hatched lines.

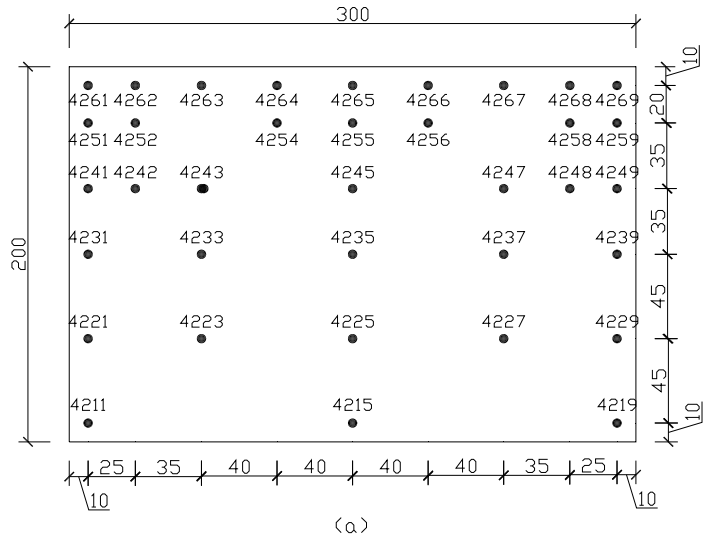

Figure 16a Pressure tap locations on the outer South face of the sheeting corresponding to Figure 10.

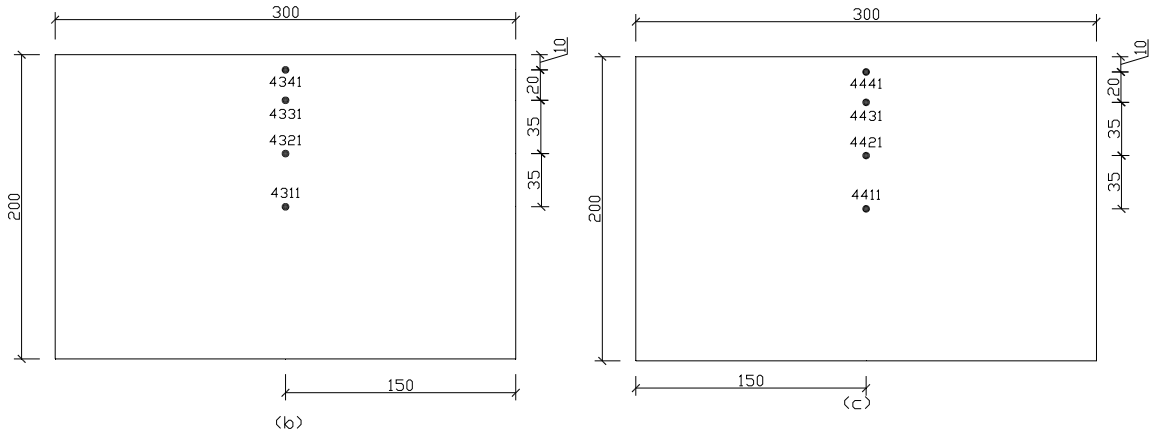

Figure 16b Pressure tap locations on the outer East face of the sheeting corresponding to Figure 10.

Figure 16c Pressure tap locations on the outer North face of the sheeting corresponding to Figure 10.

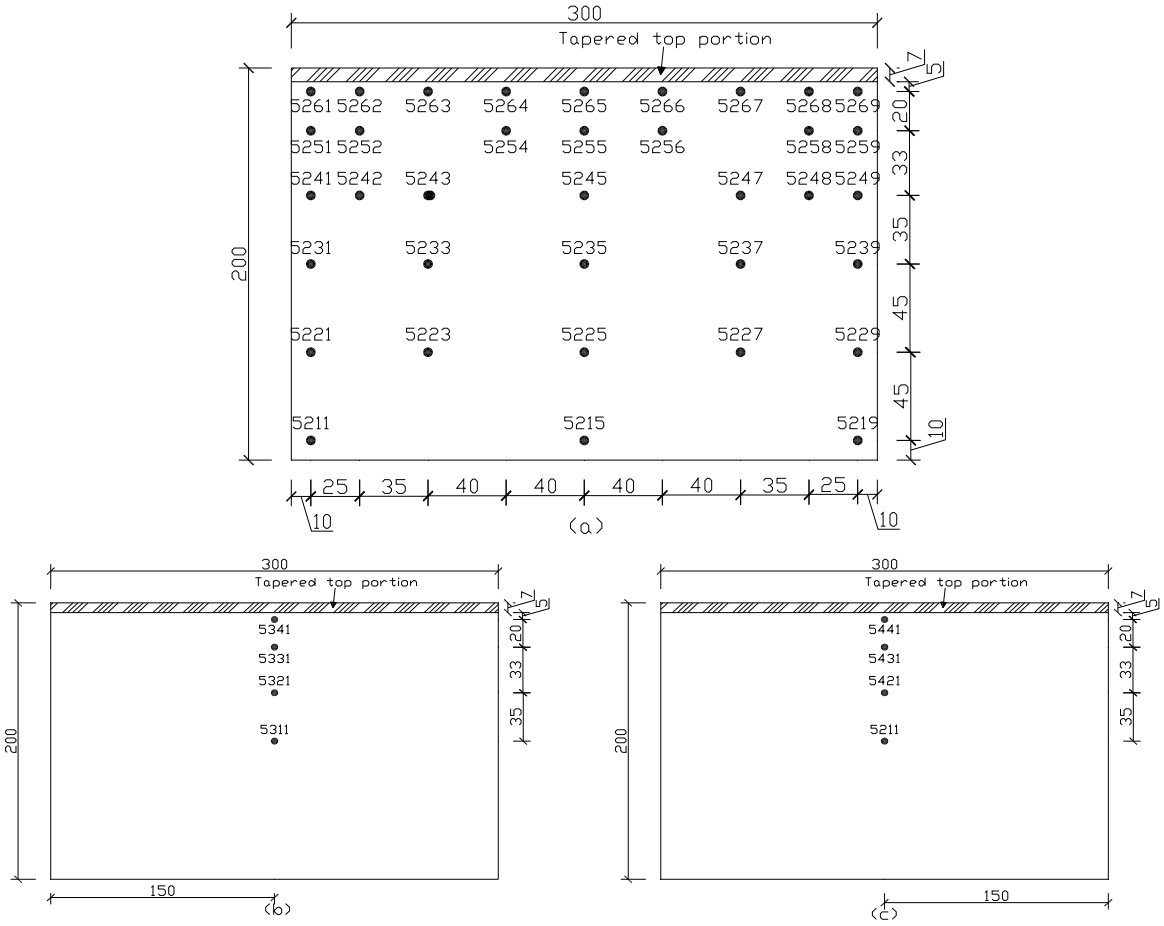

Figure 17a Pressure tap locations on the inner South face of the sheeting corresponding to Figure 10.

Figure 17b Pressure tap locations on the inner East face of the sheeting corresponding to Figure 10.

Figure 17c Pressure tap locations on the inner North face of the sheeting corresponding to Figure 10.

In Experiment-6 and Experiment-7 the observations were recorded on the elevated sheeting surrounding scaled cubical SEB as shown in Figure 13. The bottom 33.3 mm (corresponding to a full-scale prototype of 1 m) of the sheeting was open. In Experiment-6 the observations were recorded on the outer South face, whereas, in Experiment-7 the observations were recorded on the inner South face respectively and the location of pressure taps on the outer and inner South face of the sheeting are shown in Figures 18a and 19a. Once again, additional pressure taps were installed on the other two faces (North and East face) to counter check the recordings of pressures and are shown in Figures 18b, 18c, 19b and 19c respectively.

The distances of the pressure taps shown in Figure 19 were from the outer edge of the sheeting. The top 7 mm and bottom 7 mm of the sheeting were tapered from the inside. The models were again tested at every 15 degrees angle of rotation of the turn-table. In this case a total of 61 taps (47 taps on South inner face of the sheeting + 7 taps each on North and East vertical face of the sheeting) were used for the experiment.

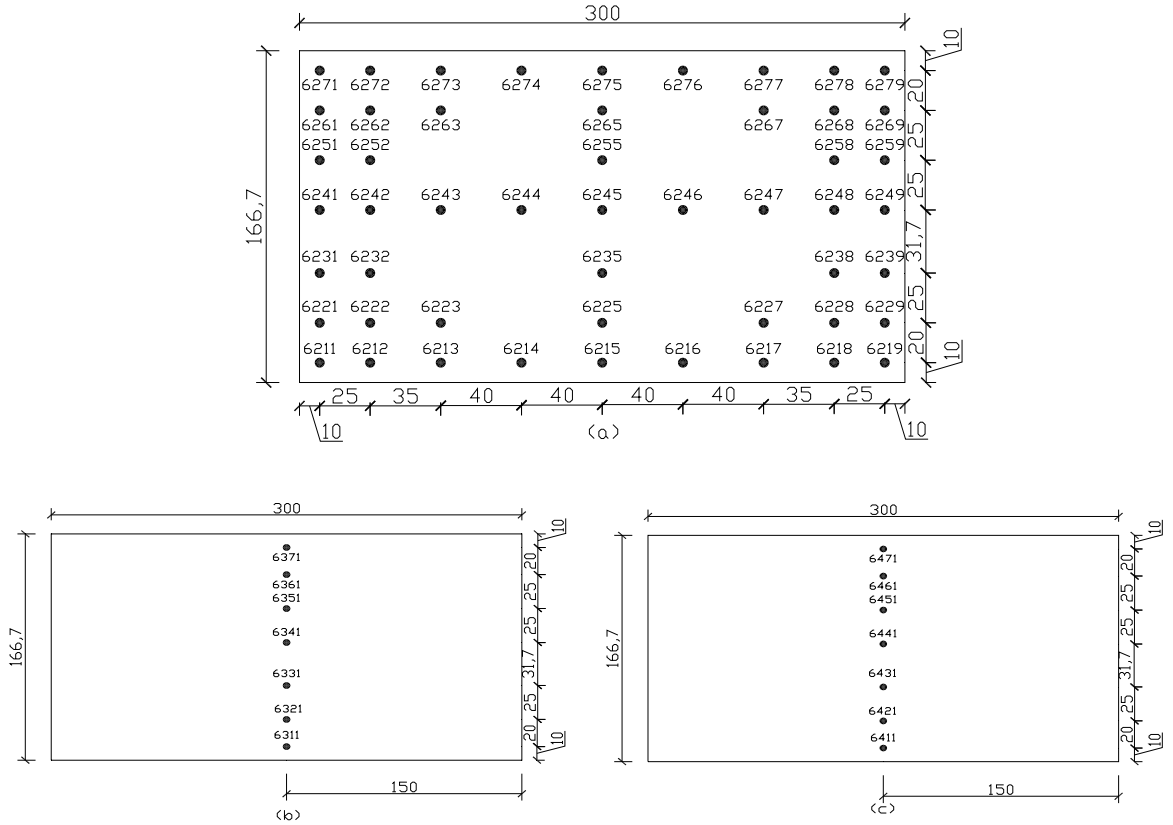

Figure 18a Pressure tap locations on the outer South face of the sheeting corresponding to Figure 13.

Figure 18b Pressure tap locations on the outer North face of the sheeting corresponding to Figure 13.

Figure 18c Pressure tap locations on the outer East face of the sheeting corresponding to Figure 13.

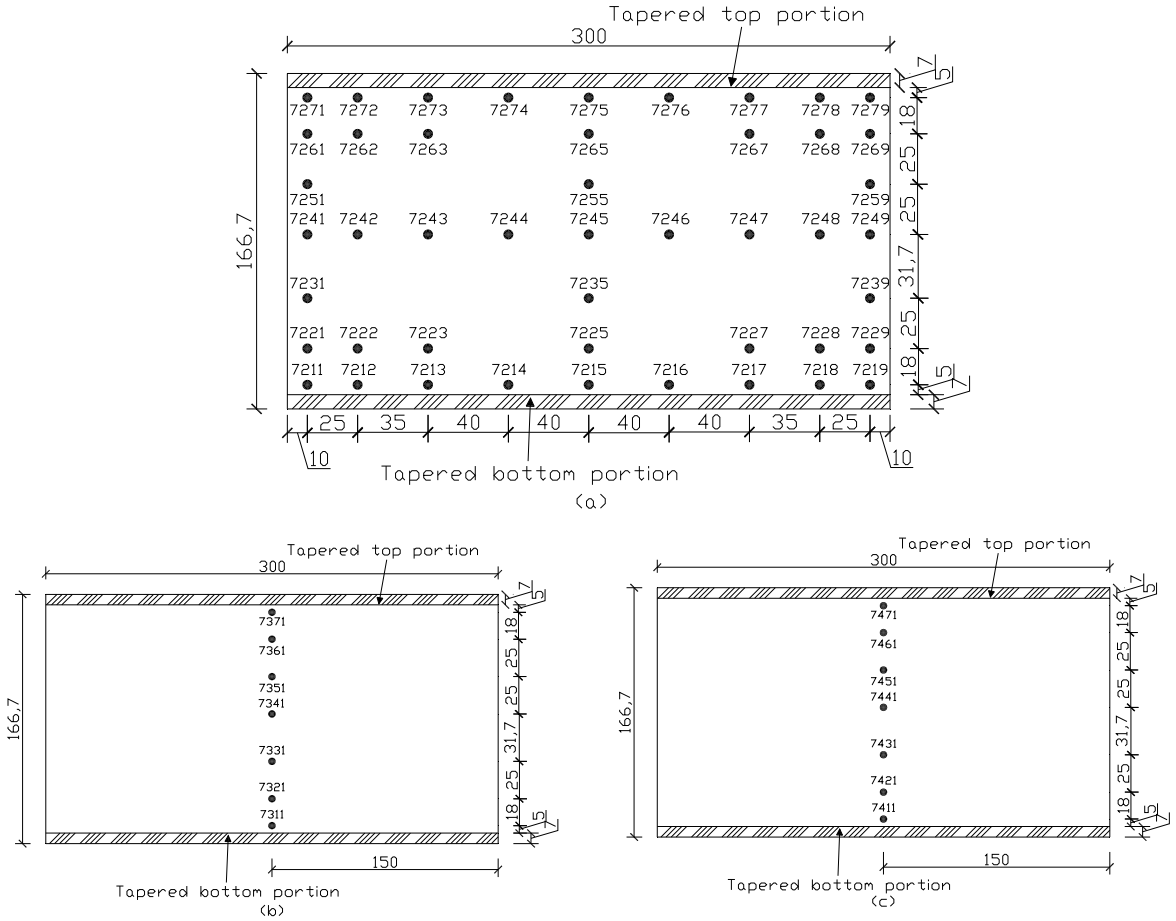

Figure 19a Pressure tap locations on the inner South face of the sheeting corresponding to Figure 13.

Figure 19b Pressure tap locations on the inner North face of the sheeting corresponding to Figure 13.

Figure 19c Pressure tap locations on the inner East face of the sheeting corresponding to Figure 13.

4 Testing Facilities and Equipments for Wind Pressure Study

The wind-tunnel used for testing the models was a 26m long atmospheric boundary layer type as shown in Figure 20. This wind-tunnel was operated by Red Consultants Ltd, Hong Kong, working under the auspices of Department of Civil Engineering, Hong Kong Polytechnic University, Hong Kong. The test section was 17.5 m long, 3.3 m wide and 2.2 m high. The roof of the test section could be raised up to a maximum height of 0.6 m to keep the pressure constant in the longitudinal direction if required. The diameter of the turn table was 2.80 m. The maximum wind speed in the test section was around 15 m/s. The atmospheric boundary layer was simulated by using artificial roughness as shown in Figure 24 with spires and baffles as shown in Figure 22. The wind pressures were measured by a high frequency Esterline's electronic pressure scanner as shown in Figure 23. Simultaneous measurement of wind pressure up to 64 locations could be achieved with this pressure scanner.

Figure 20 Wind-tunnel

Figure 21 Artificial roughness

Figure 22 Spires and baffles in wind-tunnel

Figure 23 Esterline's pressure scanner

5 Experimental Programme

To obtain the wind pressure distribution on the exterior cladding of the structures, 1:30 scale acrylic models of the structures were constructed to include all surface details. Sufficient numbers of pressure transducers were installed on the model structures to comply with the requirement. It was the rainy season in Hong Kong during experimental work. Most of the time it was either raining or the humidity of the air was more than 90% during recording of most of the observations in the wind-tunnel.

Natural wind was developed for the 1:30 scale model to simulate the wind over open country terrain using roughness blocks of different sizes. The simulation was done on the basis of Silsoe Research Institute (SRI) full-scale data. The velocity profile and the longitudinal turbulence intensities simulated in the wind-tunnel and data obtained from SRI site and

shown in Figure 24 and 25. The wind history at model height recorded for 60 seconds in wind-tunnel is shown in Figure 26. Pressure measurements were carried out by using Esterline's 64 port electronic pressure scanner. The outputs of the sensors were electronically multiplexed through a single onboard instrumentation amplifier at rates up to 20,000 Hz using binary addressing. The multiplexed amplified analog output was capable of being driven through long lengths of cable to a remote A/D converter. The sampling rate was kept at 100 samples per second per channel and the duration of each run was kept to 249 seconds. This was equivalent to one hour data in the field.

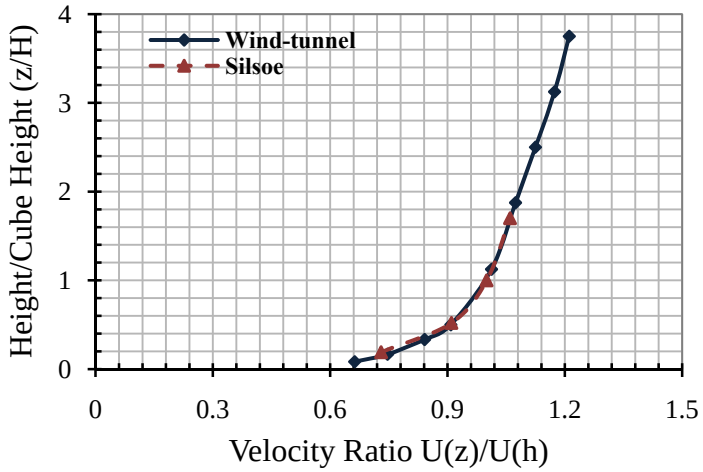

Figure 24 Mean velocity profile of full-scale and wind-tunnel

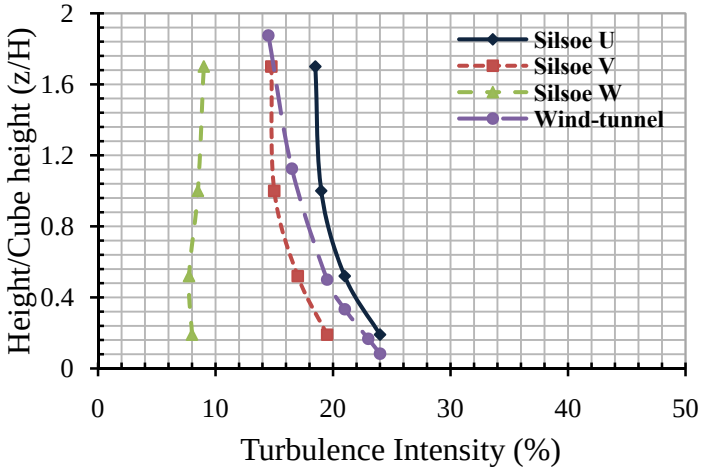

Figure 25 Turbulent intensity profile comparison between full-scale and wind-tunnel

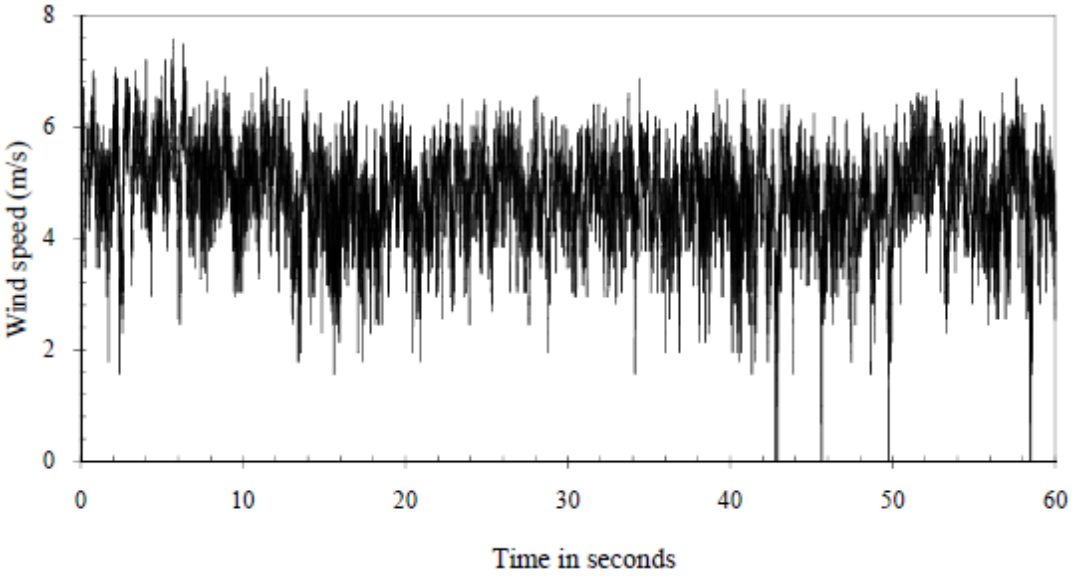

Figure 26 Time history at model height

The mean longitudinal wind speed profile measured in the wind-tunnel was in good agreement with the SRI full-scale profile with a power-law exponent of 0.17. The longitudinal turbulence was slightly less than the SRI full-scale data. Many iterations (by changing the size and position of roughness) were done to achieve the same turbulence at model heights as occurred in the Silsoe building during the testing process but it was not possible to achieve the exact turbulence.

The small-scale turbulence content (S) which is defined as $S = \left[nS_u(n) / \sigma_u^2 \right] \cdot \left[\sigma_u / U \right]^2 \times 10^6$ evaluated at $n = 10U / L_p$ where, n is frequency, $S_u(n)$ is spectral density, σ_u is the standard deviation of the longitudinal mean velocity (U) and L_p is the characteristic model dimension, was found to be 89. The model eave height was taken as the characteristic dimension. The reduced spectra plot at the model eave height is shown in Figure 27. The integral scale in the wind tunnel was also evaluated at the model eave height for the longitudinal wind speed and found to be 0.30 m. The auto-correlation plot to find the integral scale is shown in Figure 28. The integral scale is defined as area under the auto-correlation curve of the fluctuating velocity component. Since the auto-correlation measurements are usually temporal measurements at a fixed point, the Taylor hypothesis can be used to convert the area under the auto-correlation function into a unit of length as given by the equation given below:

$$L_{ux} = U \int_0^\infty R(\tau) d\tau \qquad (1)$$

where L_{ux} is the integral length scale, U is the mean wind speed, τ is the time and $\int_0^\infty R(\tau)d\tau$ is the area under the auto-correlation curve (Tieleman et al, 1996).

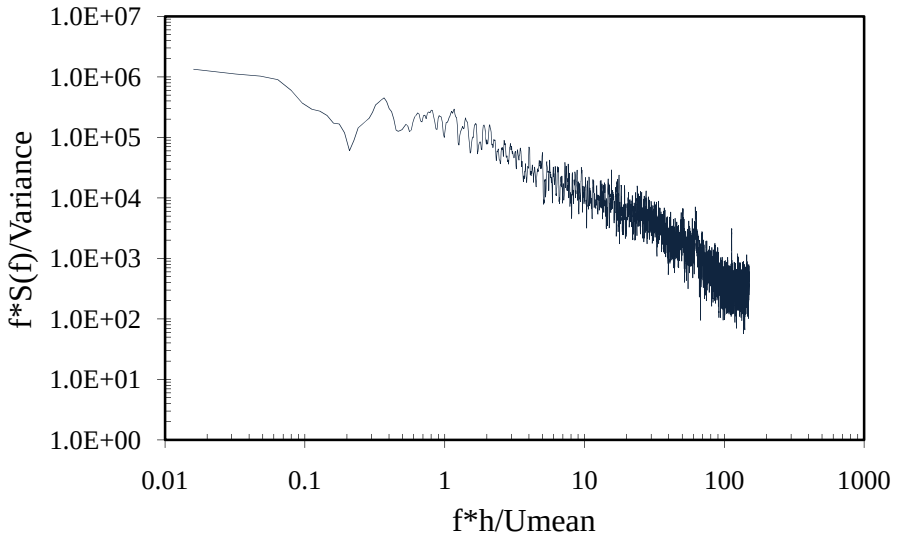

Figure 27 Normalized reduced spectrum plot at eave height

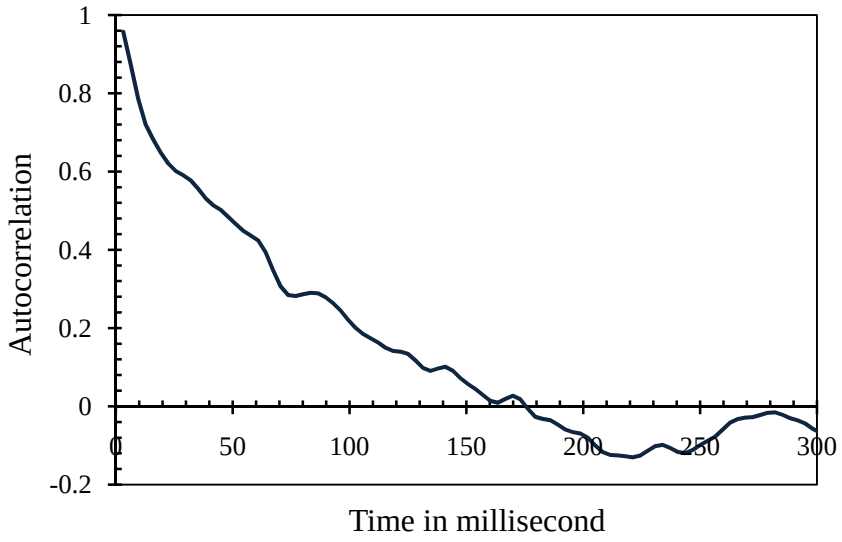

Figure 28 Auto-correlation plot at eave height

The major problem with this integral scale method is that the auto-correlation function is often highly oscillatory, and the area under the curve tends to cancel out, which will give an unrealistically small length scale. A common method of overcoming this problem is to define the integral scale as the area under the auto-correlation curve for the value occurring before

the first zero crossing and this procedure was adopted to calculate the integral length scale of the wind-tunnel experiments (Tieleman et al, 1996).

Apart from the wind profile similar to the Silsoe Experimental site, an artificial site corresponding to the urban habitat was also developed. The mean longitudinal wind speed profile developed in the wind-tunnel had a power-law exponent of 0.308. The longitudinal turbulence was also generated corresponding to an urban developed area. The mean velocity profile and turbulence intensities for this set of experiments (called Terrain Type B) are given in Figures 29 and 30 respectively.

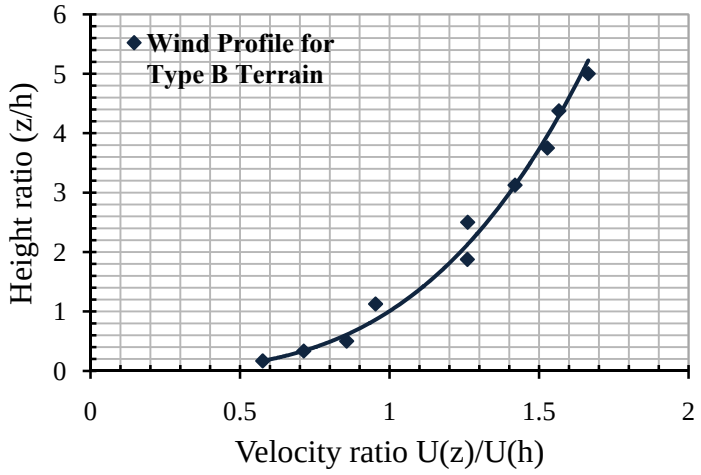

Figure 29 Mean velocity profile developed in the wind-tunnel for Type B Terrain

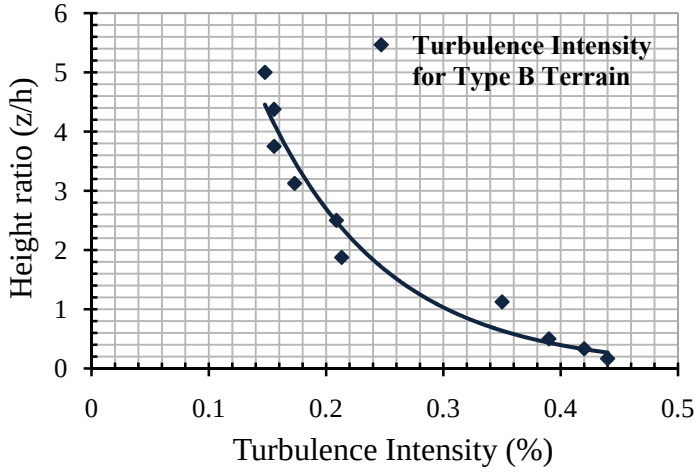

Figure 30 Turbulent intensity profile developed in wind-tunnel for Type B Terrain

The reduced spectra plot at the model eave height is shown in Figure 31. The integral scale in the wind tunnel was also evaluated at the model eave height for the longitudinal wind speed

and found to be 0.34 m. The auto-correlation plot for Type B Terrain to find the integral scale is shown in Figure 32.

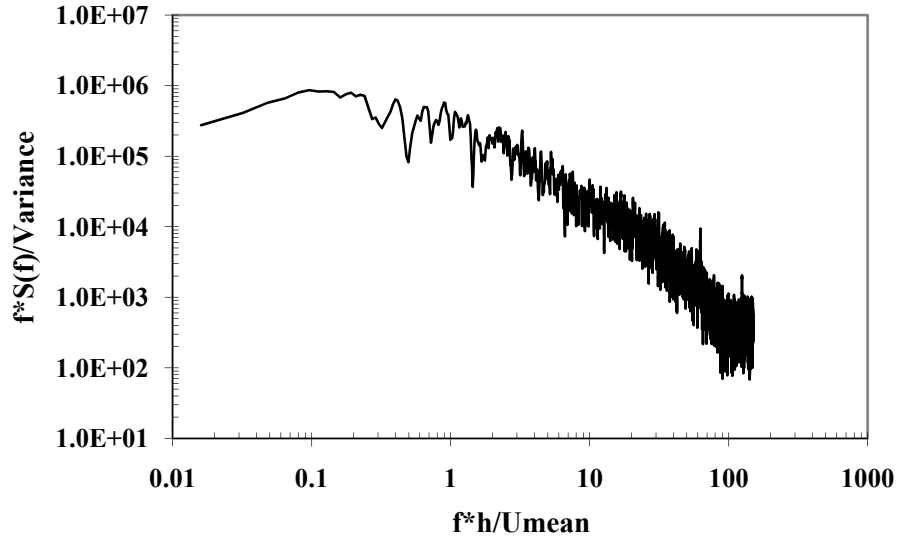

Figure 31 Normalised reduced spectrum plot at eave height for Type B Terrain

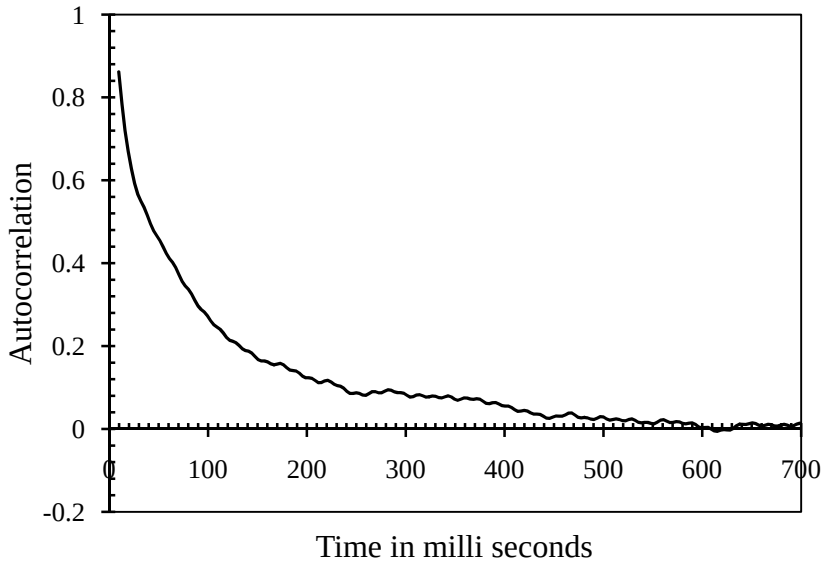

Figure 32 Auto-correlation plot at eave height for Type B Terrain

For each run, wind pressures measured on the models were expressed in the form of a non-dimensional pressure coefficient, defined as follows:

$$C_p(t) = \frac{p(t) - p_0}{\frac{1}{2}\rho U^2} \quad (2)$$

where, p_0 is the static (ambient/atmospheric) reference pressure, U the mean longitudinal wind speed at the reference height (eave height) and ρ the air density.

The instantaneous wind pressures at each location were measured at 24 wind directions in 15 degree intervals. The mean, r.m.s. (root-mean-square) and the maximum and minimum pressure coefficients, with reference to the gradient wind pressure, were derived from the wind tunnel data. The maximum and minimum pressures were determined by using the method proposed by Cook and Mayne (Cook and Mayne, 1979). The maximum and minimum pressures are representative of the wind pressure of 4 minutes 9 seconds (equal to hourly wind data in the field) averages.

The results of all the experiments are given in Appendices 1-7. As described in Section 3 plots of pressure contours and extreme pressure values for selected points are given.

6 References

Cook, N.J. and Mayne, J.R. 1981, 'A novel working approach to the assessment of wind loads for equivalent static design a refined working approach to the assessment of wind loads for equivalent static design', Journal of Wind Engineering and Industrial Aerodynamics, **8**, 299-301.

Irtaza, H. 2009, 'Experimental and Computational Determination of Wind Loads on Sheeted/Netted Scaffold', PhD Thesis, Oxford Brookes University, Oxford, UK.

Kasperski, M. and Hoxey, R.P. 2008, 'Extreme-value analysis for observed peak pressures on the Silsoe cube', Journal of Wind Engineering and Industrial Aerodynamics, **96,** 994-1002.

Maitra, A. 1997, 'Accidents associated with scaffolding in the UK', Technical Seminar, Design and use of temporary structures, Institution of Civil Engineers, London.

Richards, P.J., Hoxey, R.P. Connell, B.D. and Lander, D.P. 2007, 'Wind-tunnel modelling of Silsoe Cube', Journal of Wind Engineering and Industrial Aerodynamics, **95**, 1384-1399.

Richards, P.J. and Hoxey, R.P, 2008, 'Wind loads on the roof of a 6 m cube', Journal of Wind Engineering and Industrial Aerodynamics, **96**, 984-993.

Tieleman, H.W., Surry, D. and Mehta, K.C. 1996, 'Full/model scale comparison of surface pressures on Texas Tech. experimental building', Journal of Wind Engineering and Industrial Aerodynamics, **61,** 1-23,1996.

www.silsoeresearch.org.uk/envir-wind-waste/wind.html (Site visited 17.07.2009).

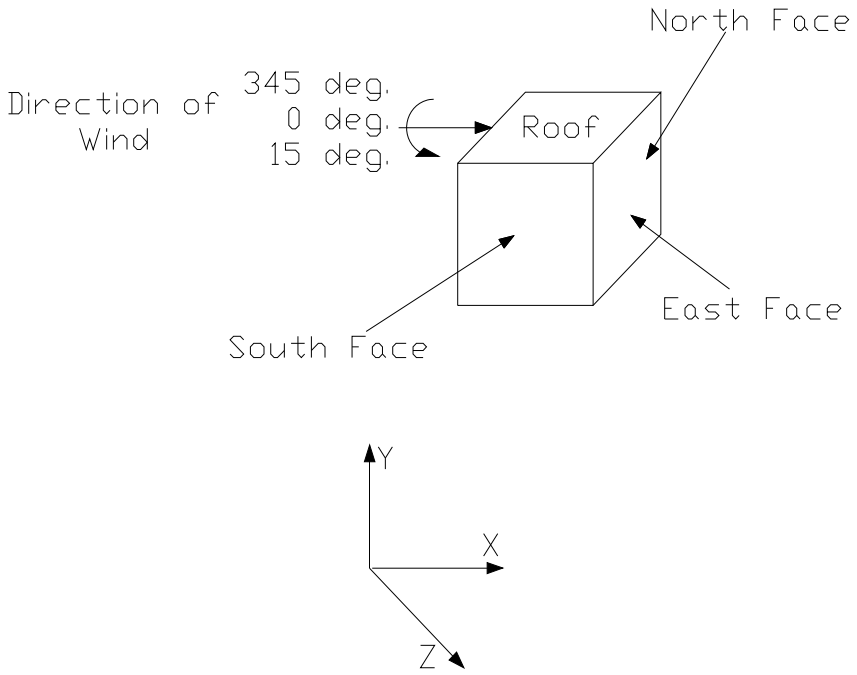

Figure 1.1 Scaled cubical SEB

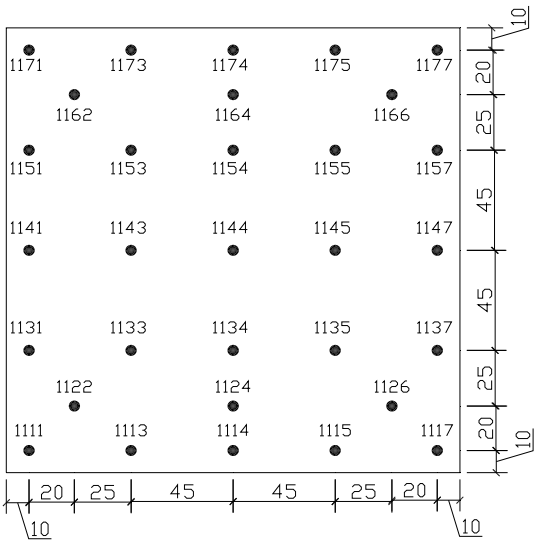

Figure 1.2 Pressure tap locations on roof

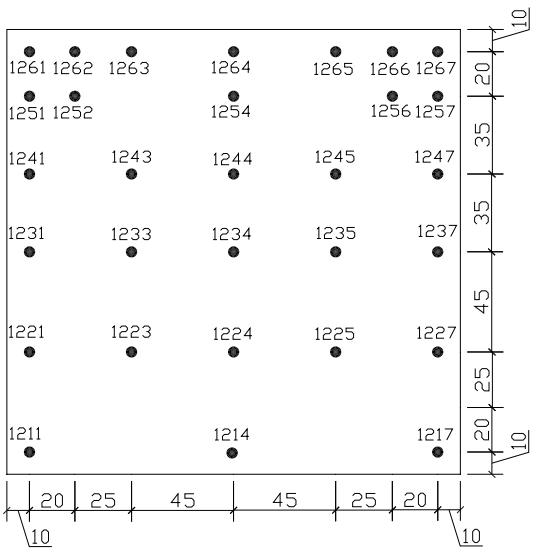

Figure 1.3 Pressure tap locations on the south wall face

Pressure Coefficient Contours on Roof of SEB for Type A Terrain

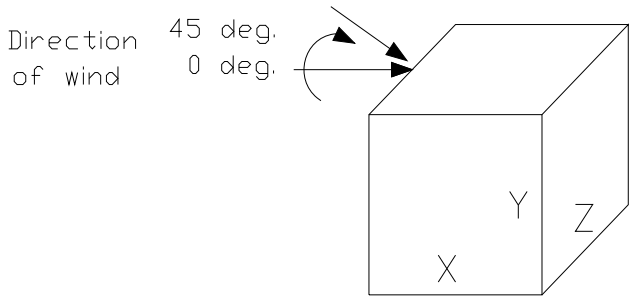

Figure 1A.1 Angle of attack of wind on roof of the SEB , direction of which varies from 0° to +45°

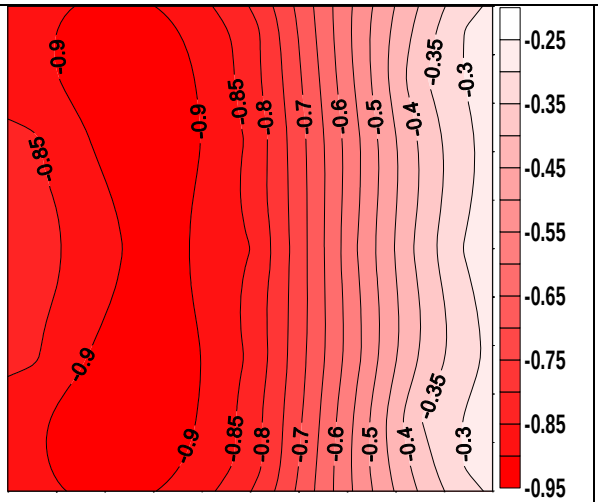

Figure 1A.2 Pressure coefficient contours on the roof of the SEB when θ= 0°

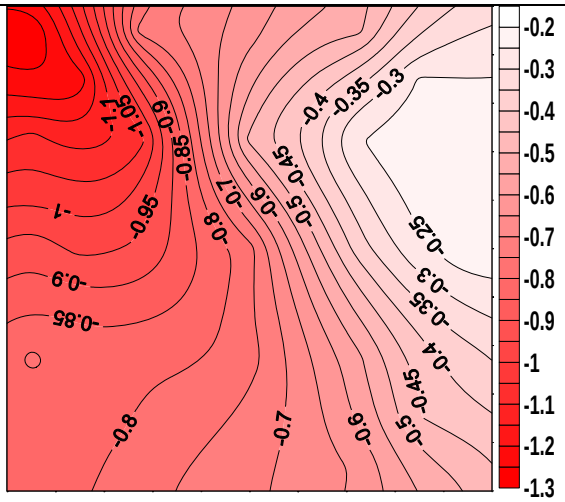

Figure 1A.3 Pressure coefficient contours on the roof of the SEB when θ= 15°

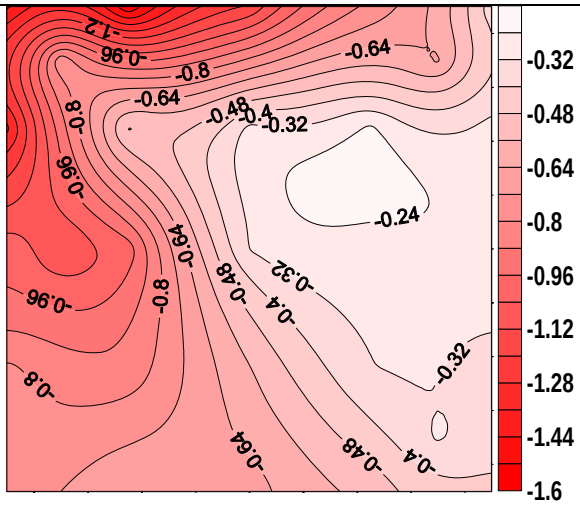

Figure 1A.4 Pressure coefficient contours on the roof of the SEB when θ= 30°

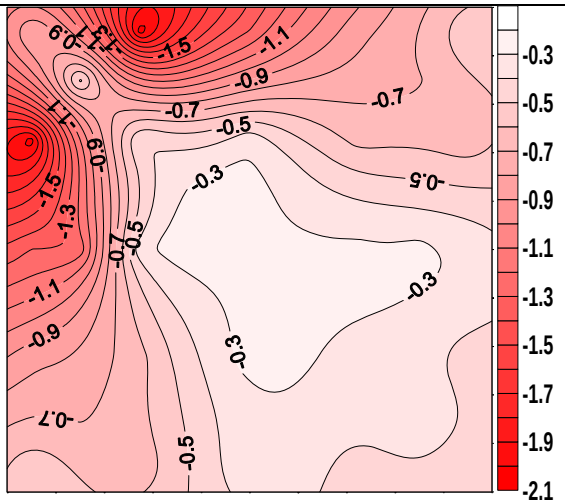

Figure 1A.5 Pressure coefficient contours on the roof of the SEB when θ= 45°

Pressure Coefficient Contours on Windward Face of SEB for Type A Terrain

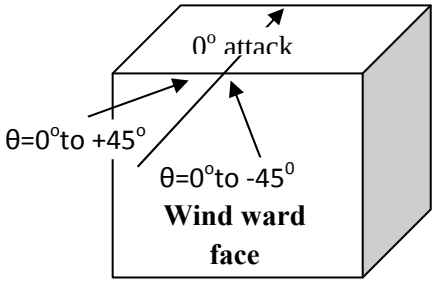

Figure 1A.6 Angle of attack of wind on windward wall of SEB, direction of which varies from -45° to +45°

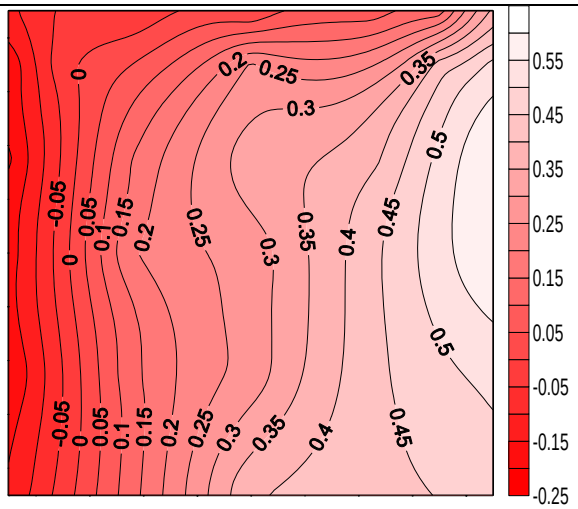

Figure 1A.7 Pressure coefficient contours on the windward face of the SEB when θ= -45°

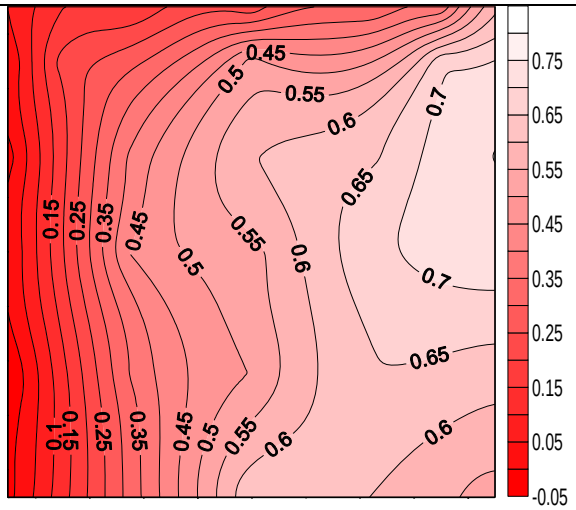

Figure 1A.8 Pressure coefficient contours on the windward face of the SEB when θ= -30°

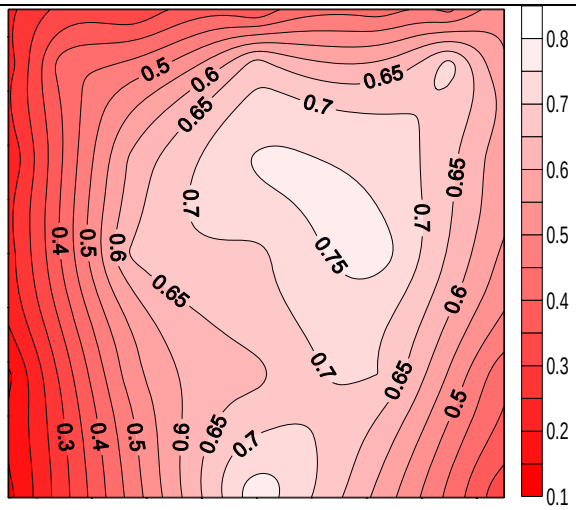

Figure 1A.9 Pressure coefficient contours on the windward face of the SEB when θ= -15°

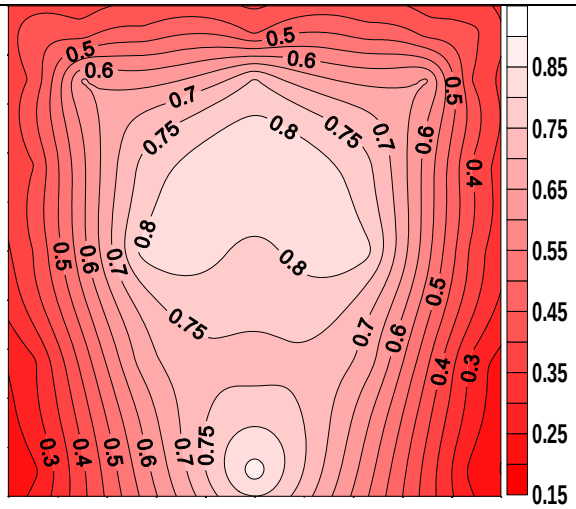

Figure 1A.10 Pressure coefficient contours on the windward face of the SEB when θ=0°

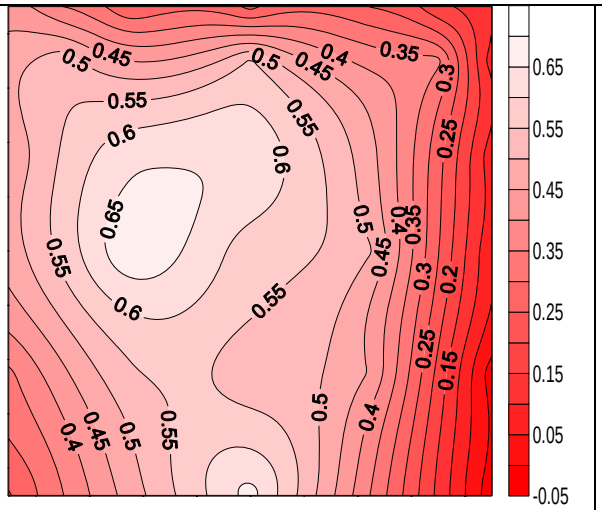

Figure 1A.11 Pressure coefficient contours on the windward face of the SEB when θ=+15^o

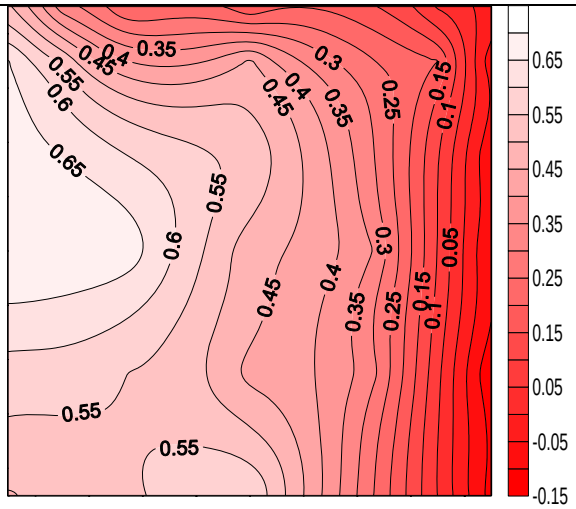

Figure 1A.12 Pressure coefficient contours on the windward face of the SEB when θ=+30^o

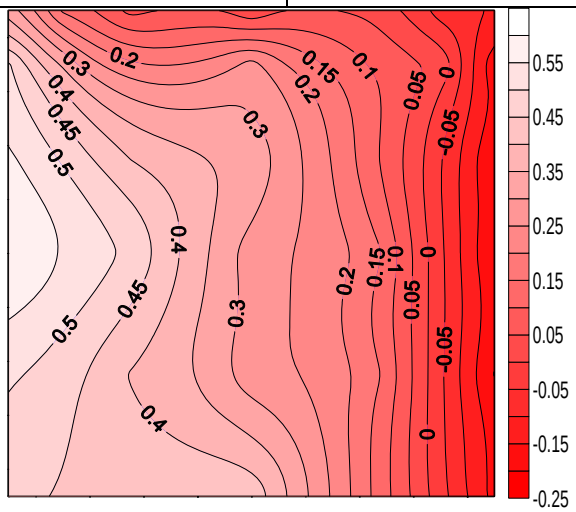

Figure 1A.13 Pressure coefficient contours on the windward face of the SEB when θ=+45^o

Pressure Coefficient Contours on Side Face of SEB for Type A Terrain

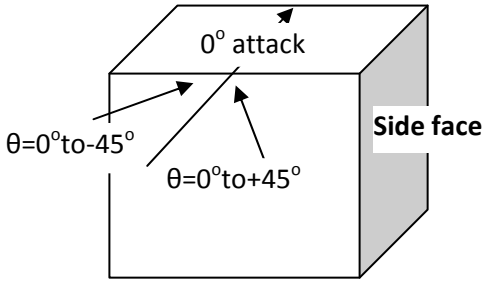

Figure 1A.14 Angle of attack of wind on windward wall of SEB, direction of which varies from -45^o to +45^o

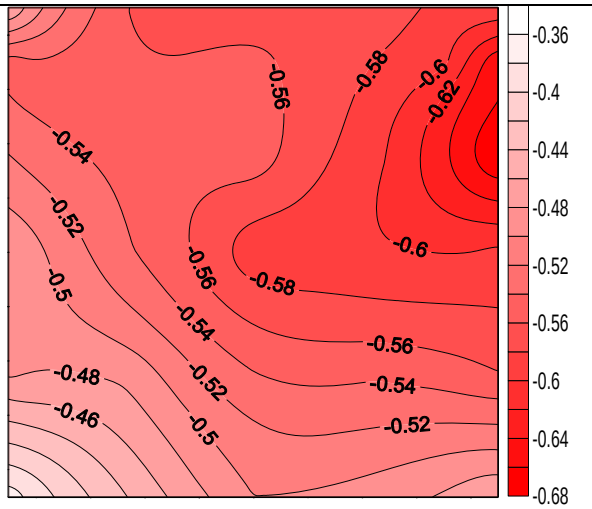

Figure 1A.15 Pressure coefficient contours on the side face of the SEB when θ= -45°

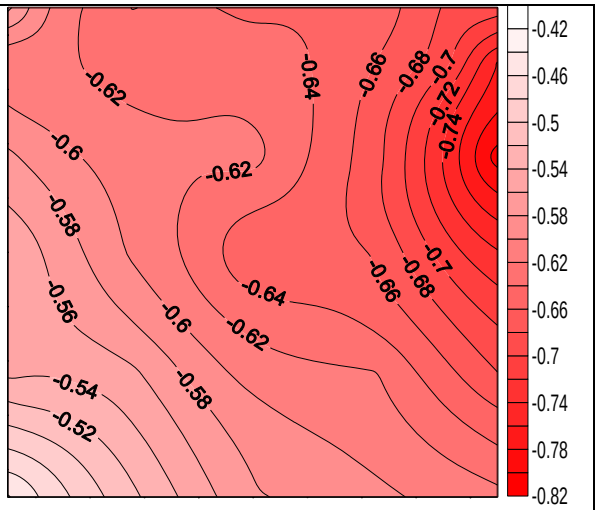

Figure 1A.16 Pressure coefficient contours on the side face of the SEB when θ= -30°

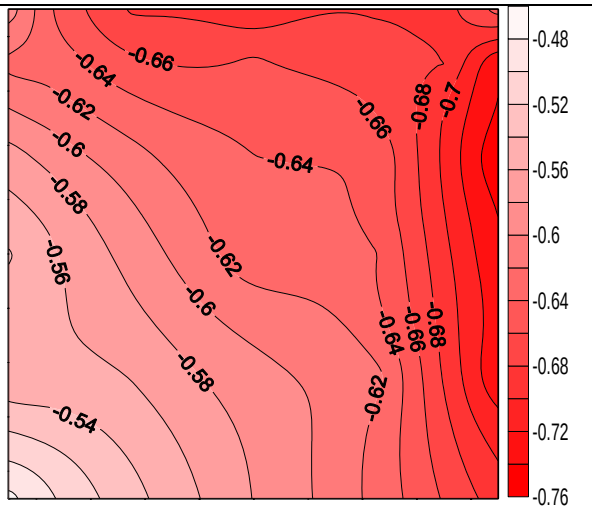

Figure 1A.17 Pressure coefficient contours on the side face of the SEB when θ= -15°

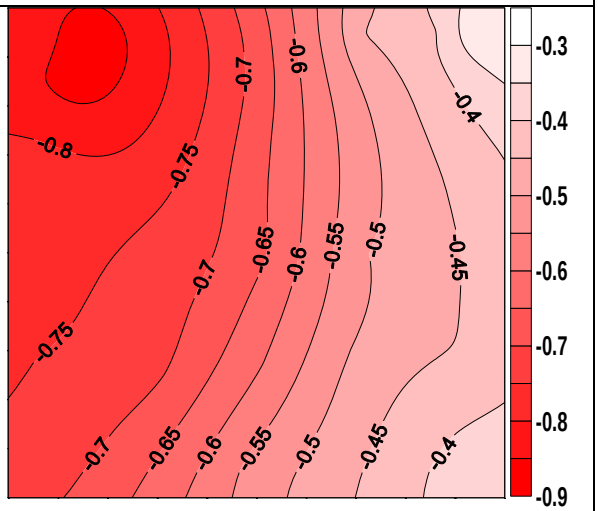

Figure 1A.18 Pressure coefficient contours on the side face of the building when θ= 0°

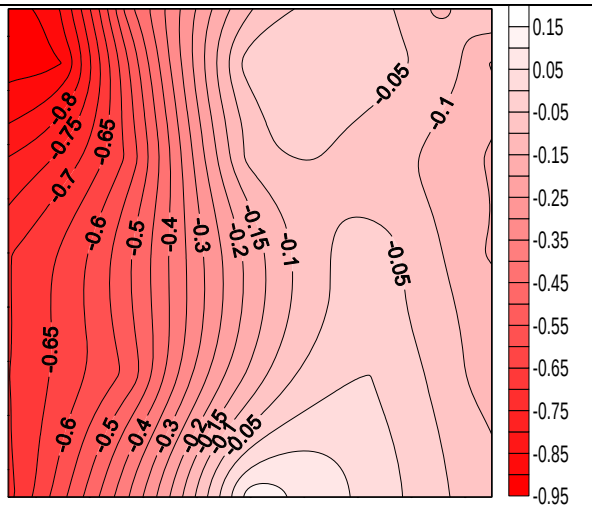

Figure 1A.19 Pressure coefficient contours on the side face of the SEB when θ=+15°

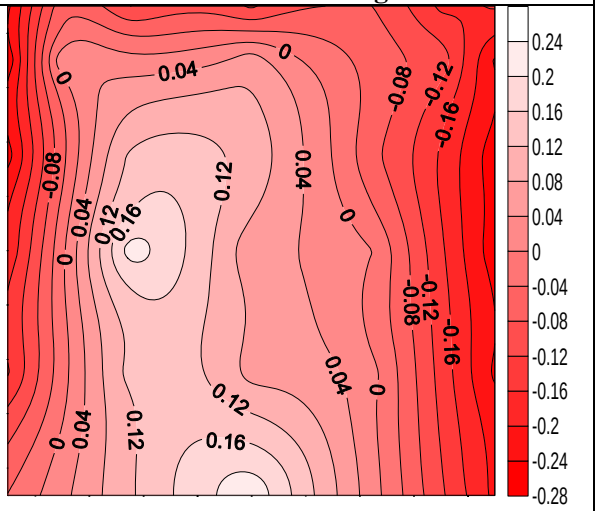

Figure 1A.20 Pressure coefficient contours on the side face of the SEB when θ=+30°

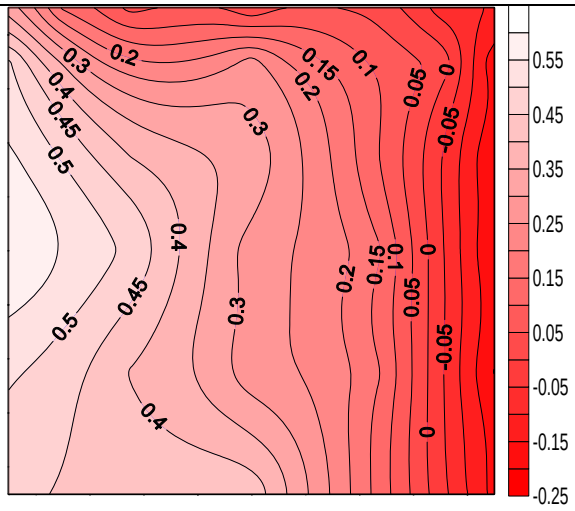

Figure 1A.21 Pressure coefficient contours on the side face of the SEB when θ=+45^o

Pressure Coefficient Contours on Leeward Face of SEB for Type A Terrain

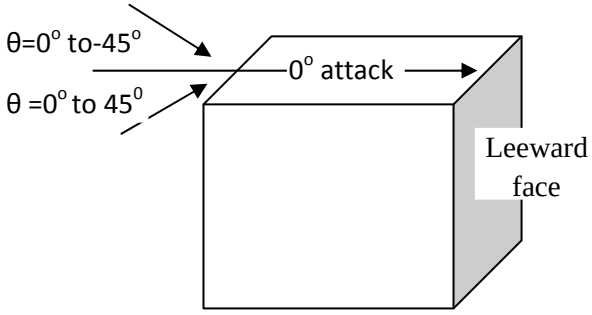

Figure 1A.22 Angle of attack of wind on windward wall of SEB, direction of which varies from -45^o to +45^o

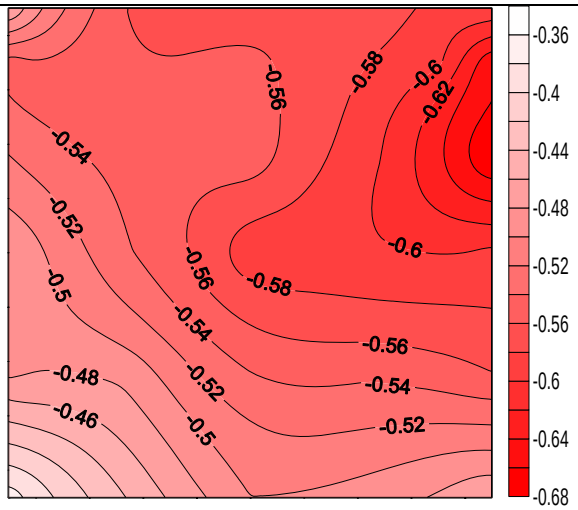

Figure 1A.23 Pressure coefficient contours on the leeward face of the SEB when θ= -45^o

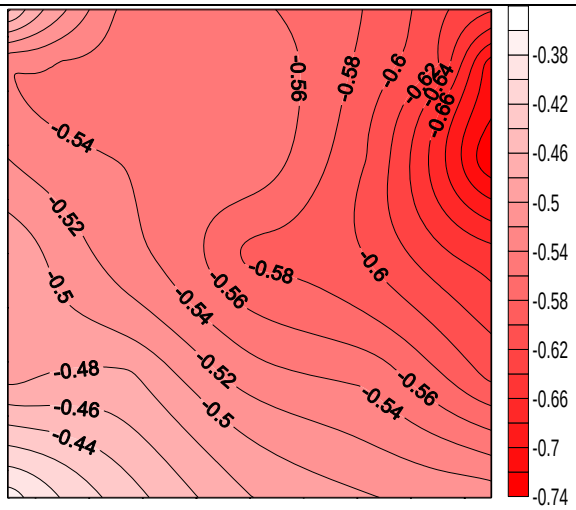

Figure 1A.24 Pressure coefficient contours on the leeward face of the SEB when θ= -30^o

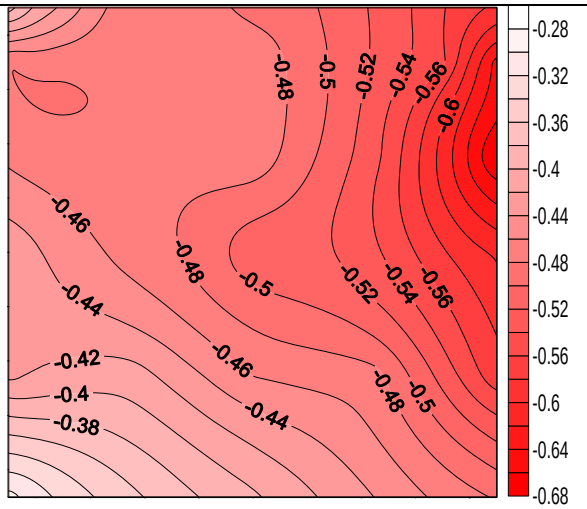

Figure 1A.25 Pressure coefficient contours on the leeward face of the SEB when θ= -15°

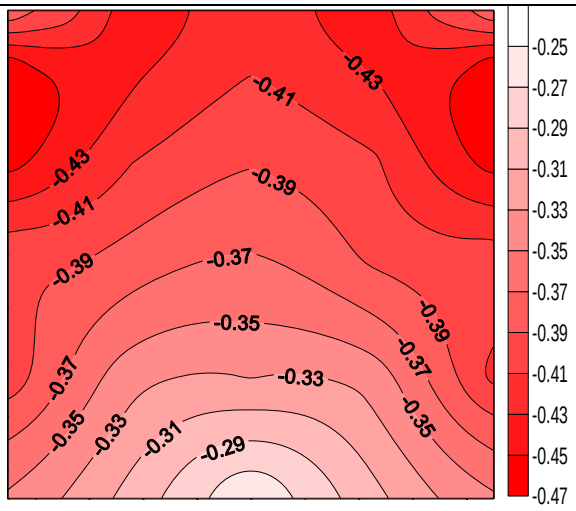

Figure 1A.26 Pressure coefficient contours on the leeward face of the SEB when θ= 0°

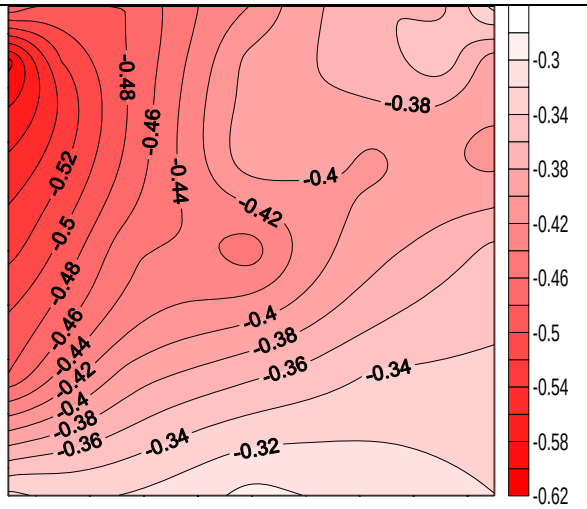

Figure 1A.27 Pressure coefficient contours on the leeward face of the SEB when θ= +15°

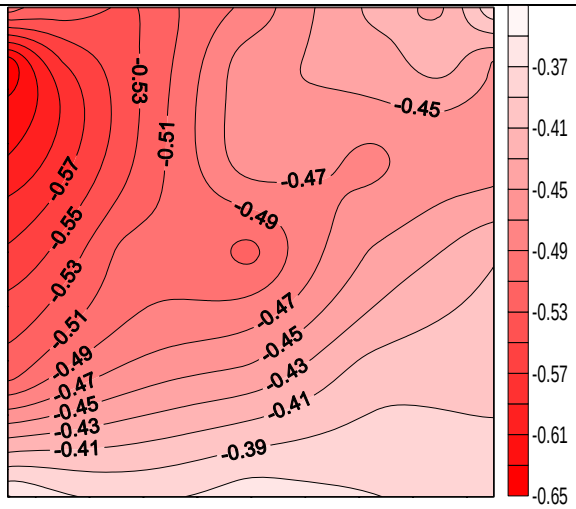

Figure 1A.28 Pressure coefficient contours on the leeward face of the SEB when θ= +30°

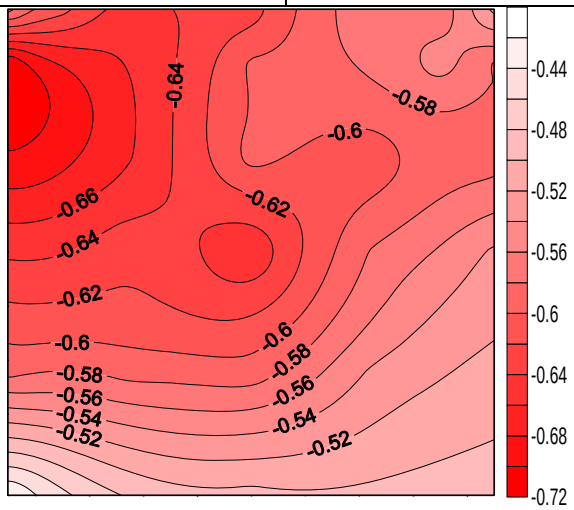

Figure 1A.29 Pressure coefficient contours on the leeward face of the SEB when θ= +45°

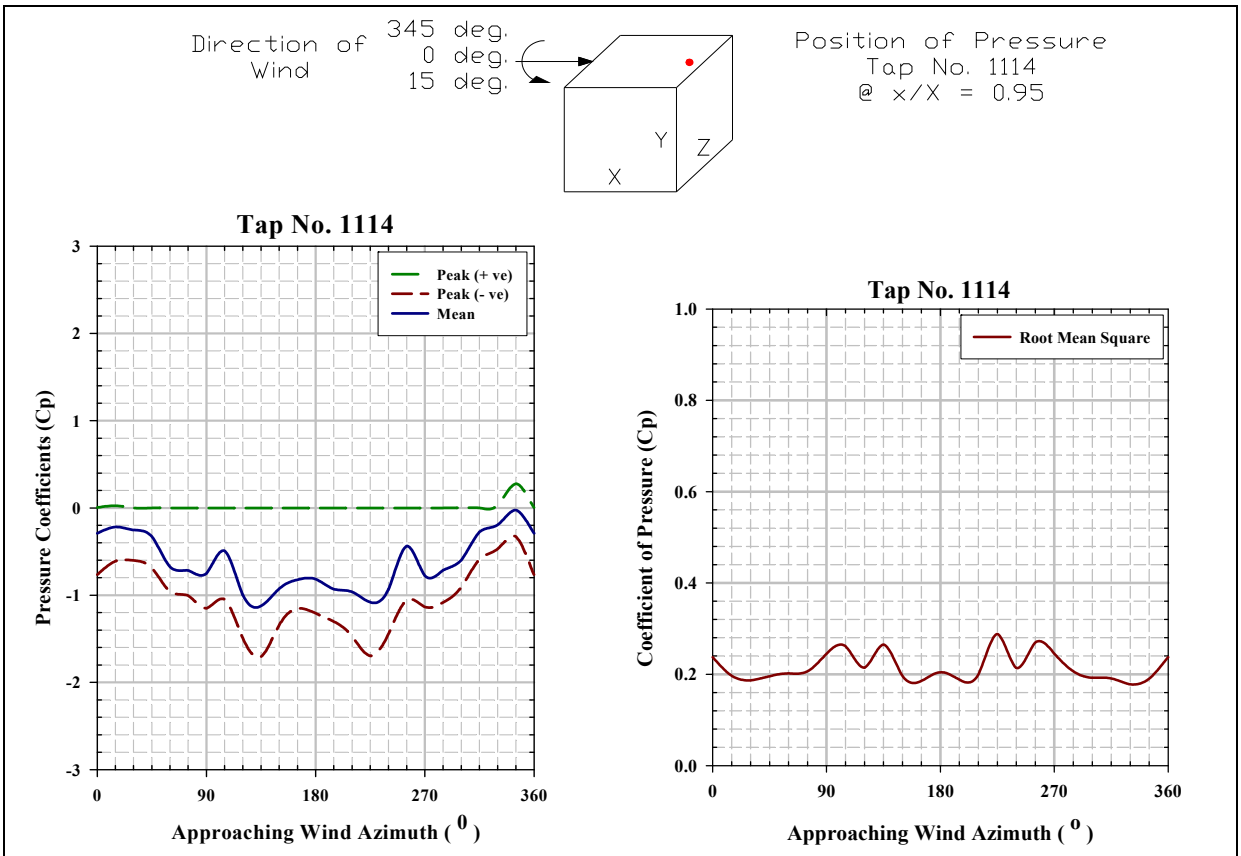

Figure 1A.30 Mean, peak and rms pressure coefficients for the tap number 1114

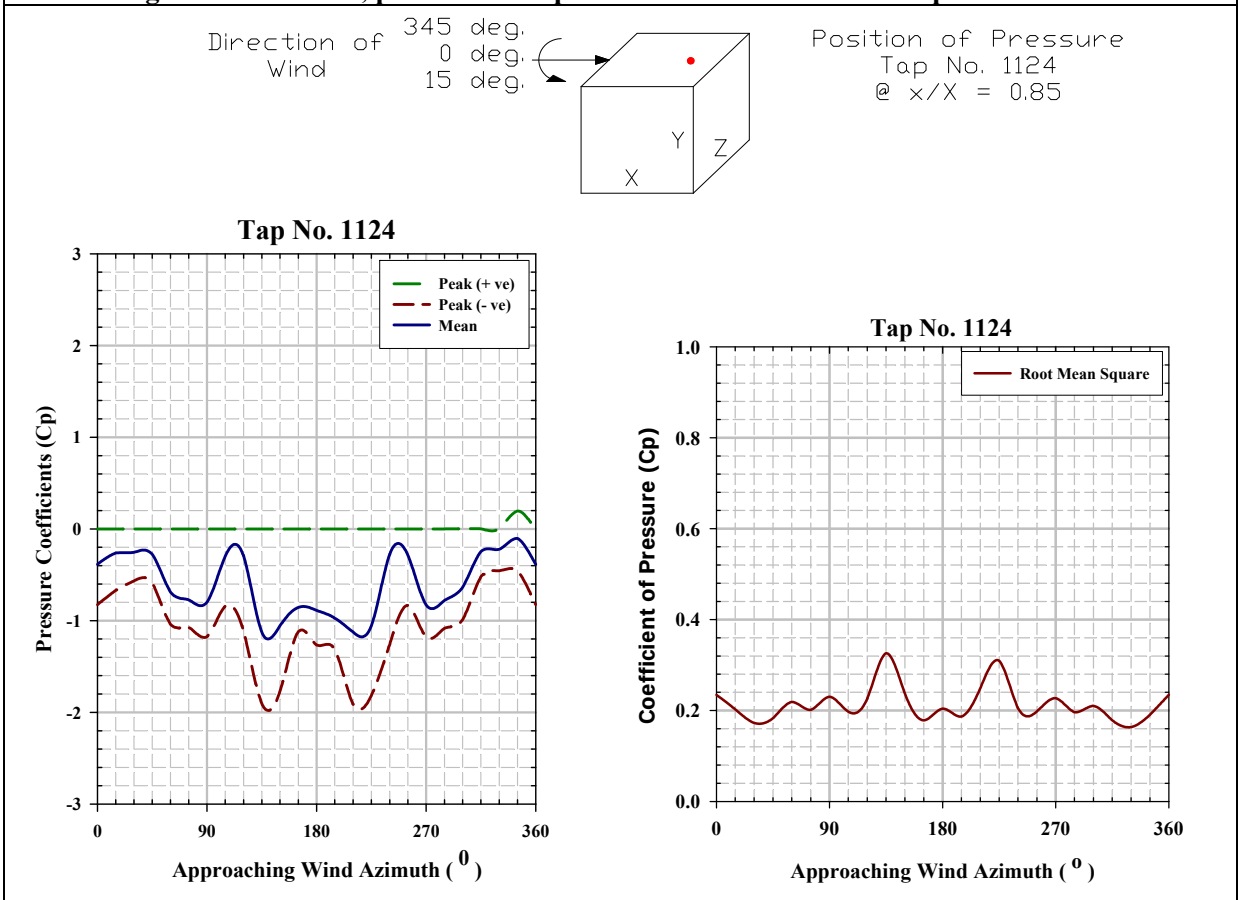

Figure 1A.31 Mean, peak and rms pressure coefficients for the tap number 1124

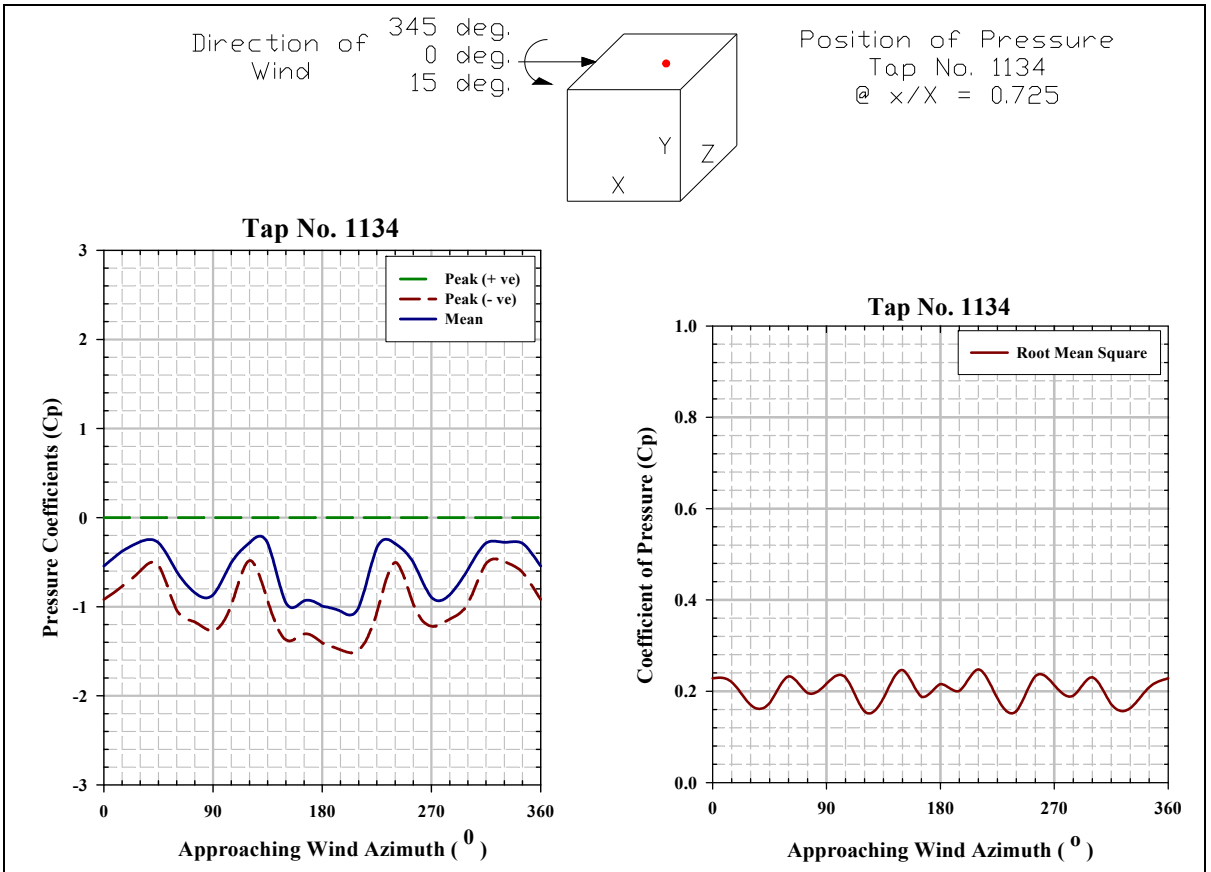

Figure 1A.32 Mean, peak and rms pressure coefficients for the tap number 1134

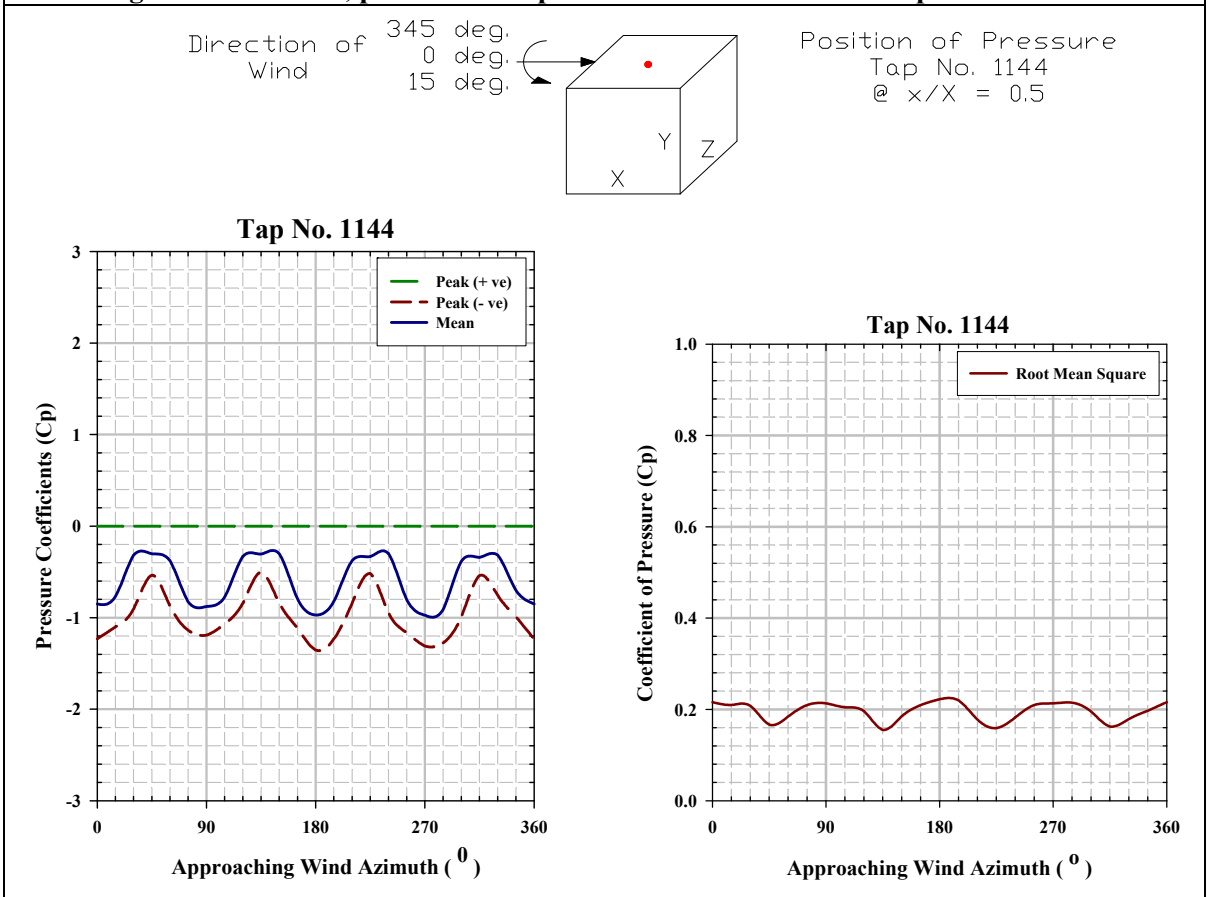

Figure 1A.33 Mean, peak and rms pressure coefficients for the tap number 1144

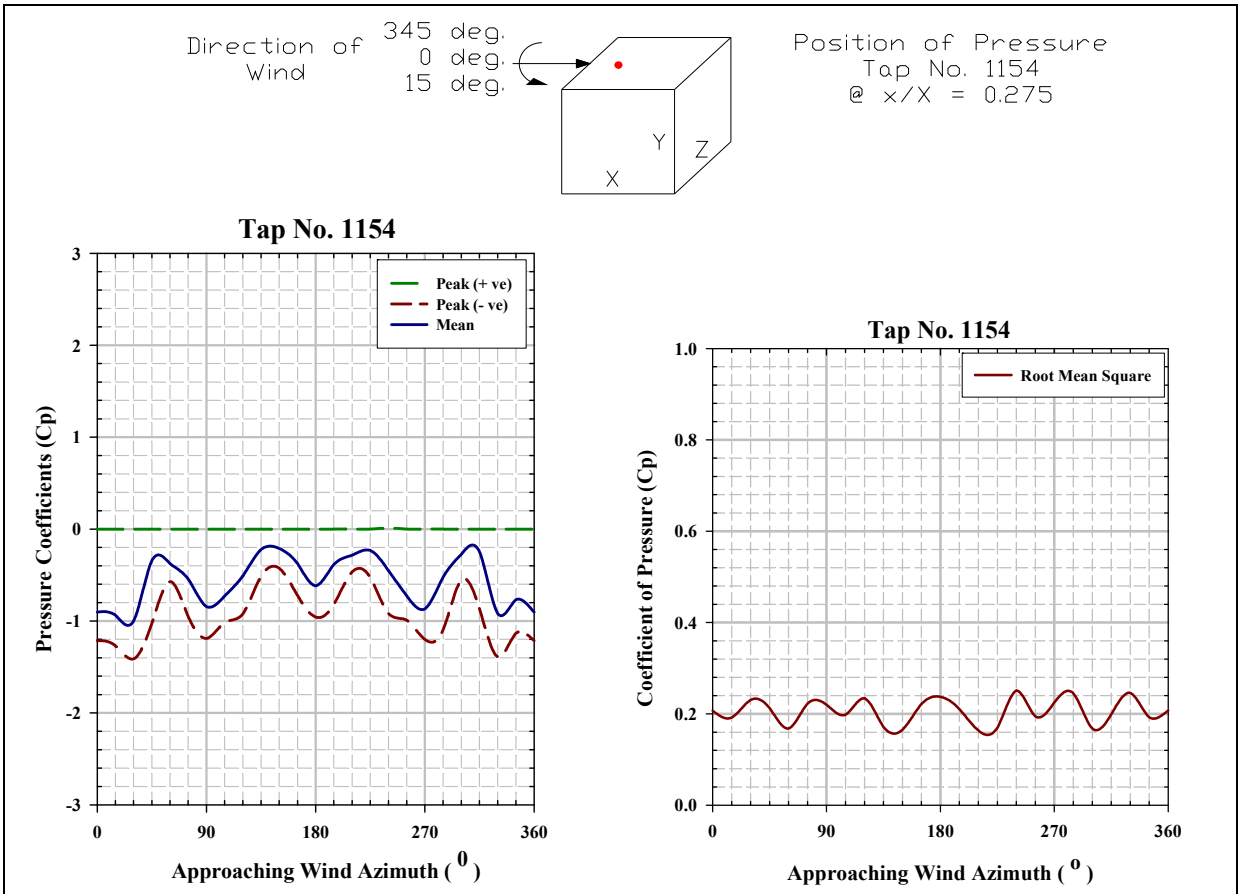

Figure 1A.34 Mean, peak and rms pressure coefficients for the tap number 1154

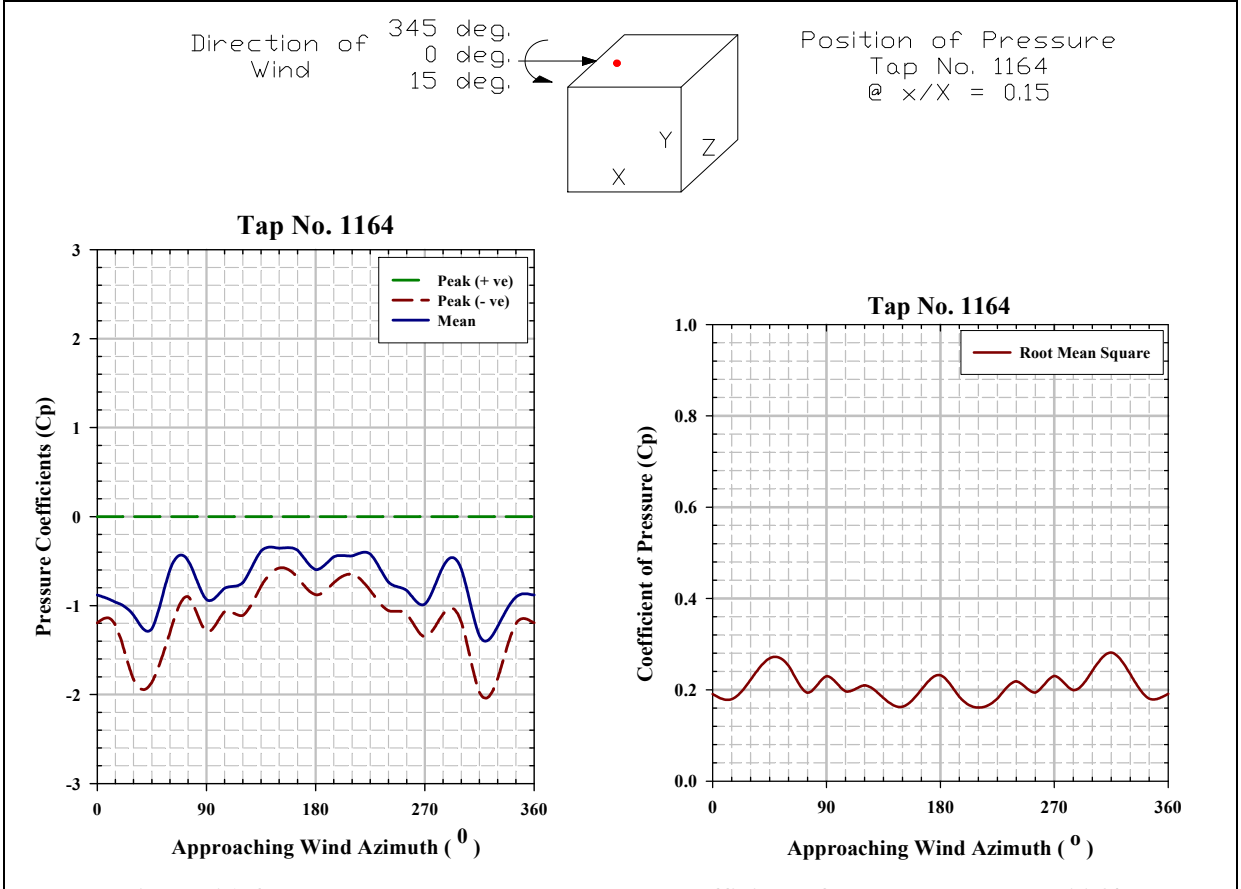

Figure 1A.35 Mean, peak and rms pressure coefficients for the tap number 1164

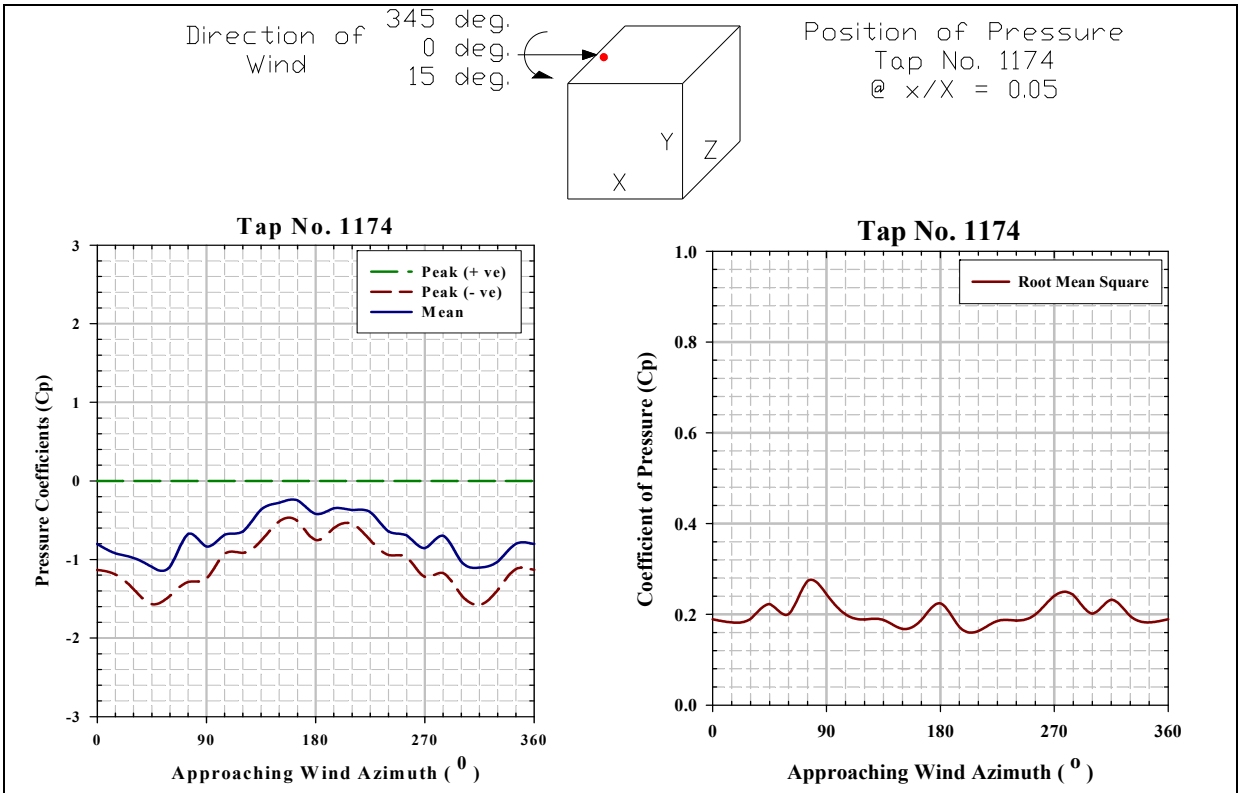

Figure 1A.36 Mean, peak and rms pressure coefficients for the tap number 1174

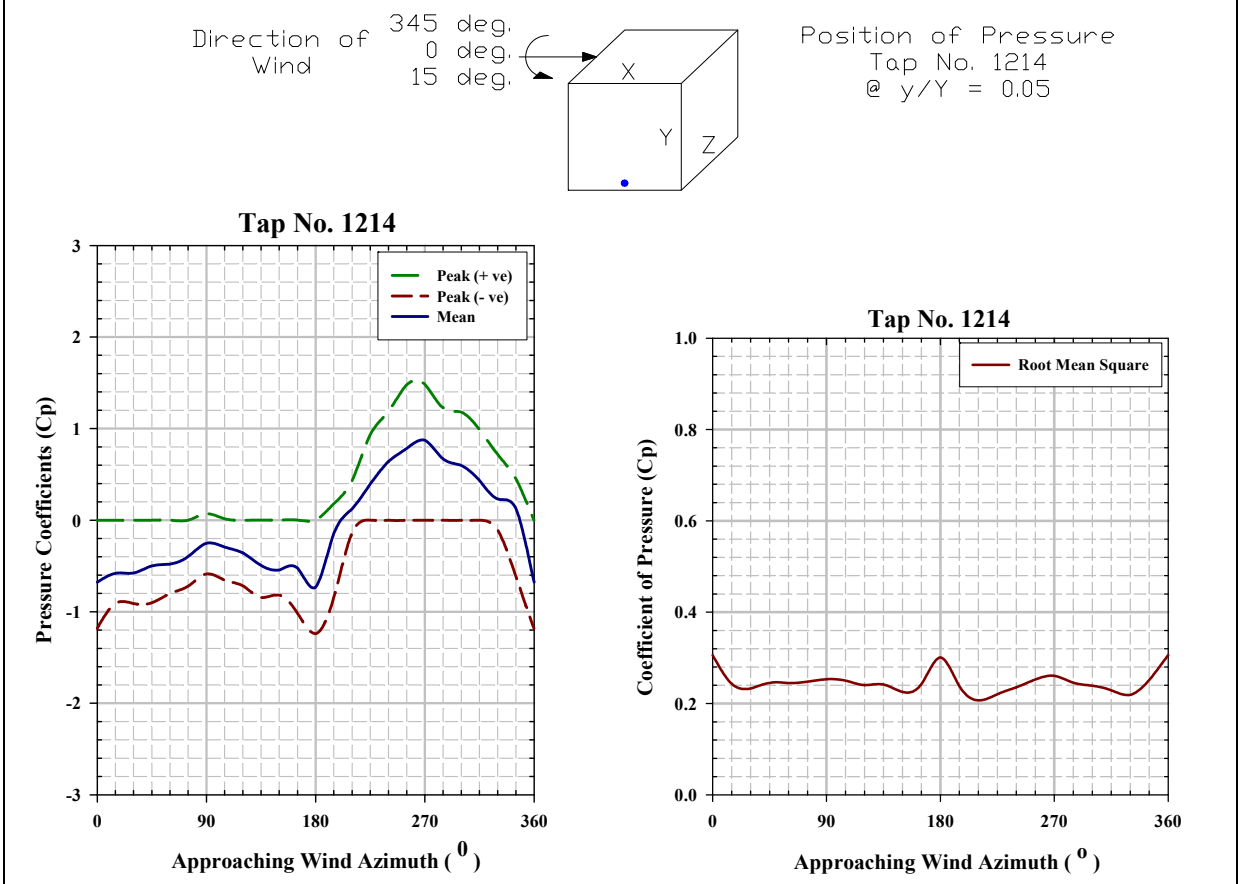

Figure 1A.37 Mean, peak and rms pressure coefficients for the tap number 1214

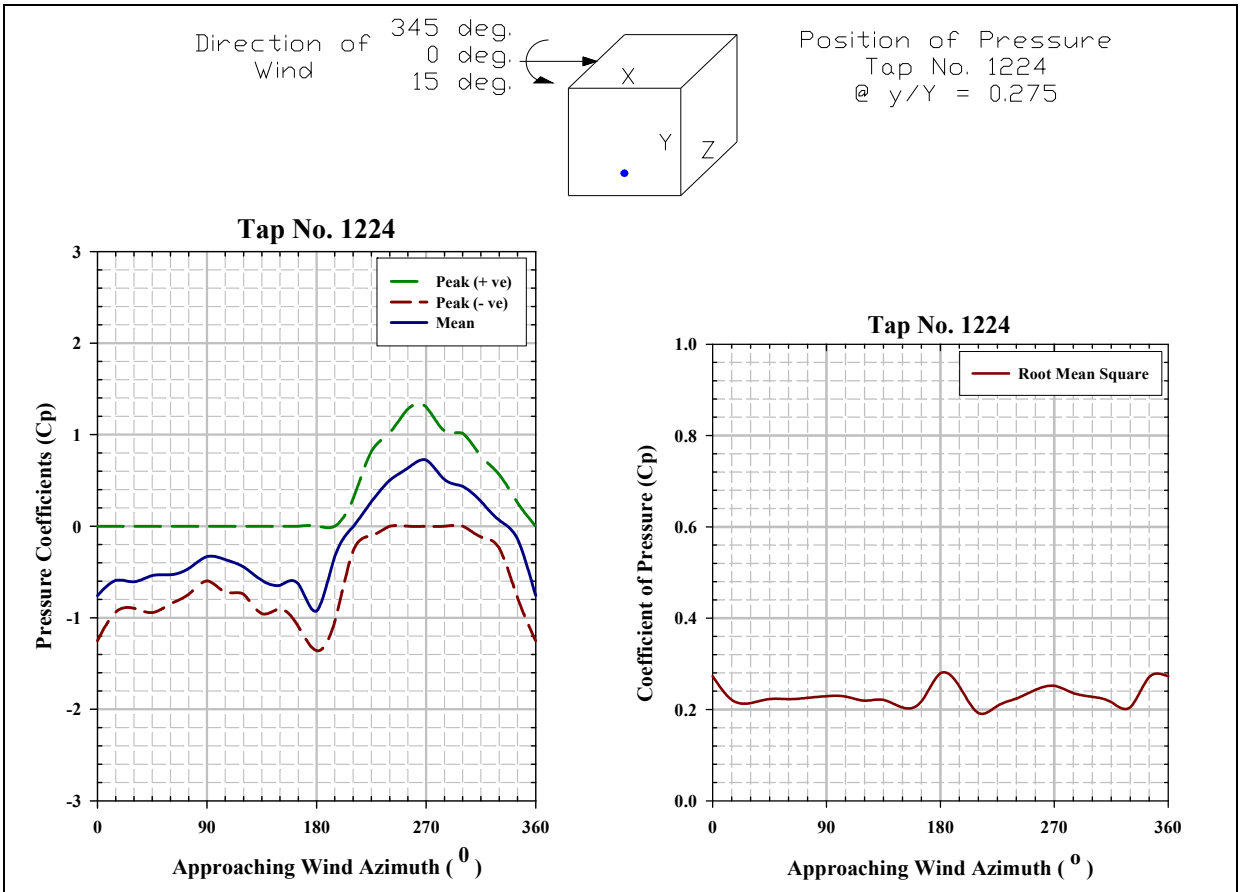

Figure 1A.38 Mean, peak and rms pressure coefficients for the tap number 1224

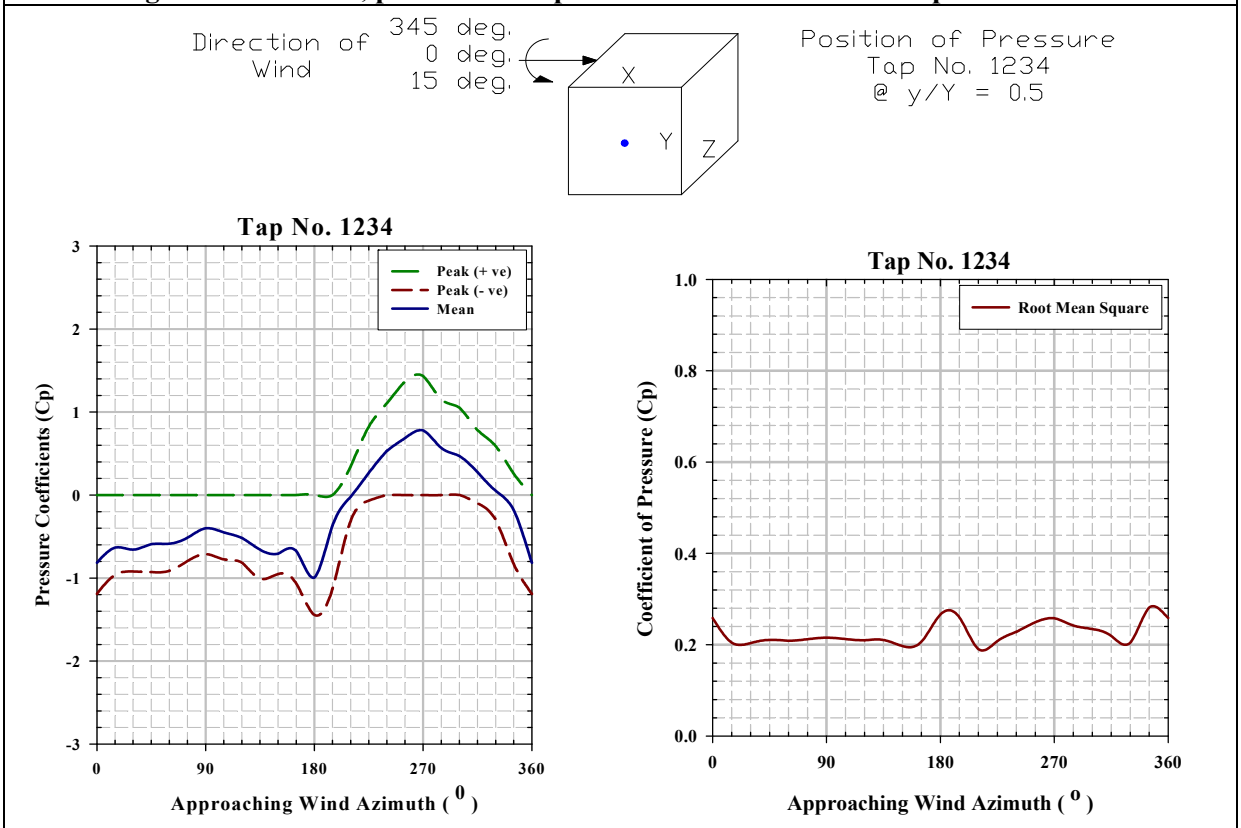

Figure 1A.39 Mean, peak and rms pressure coefficients for the tap number 1234

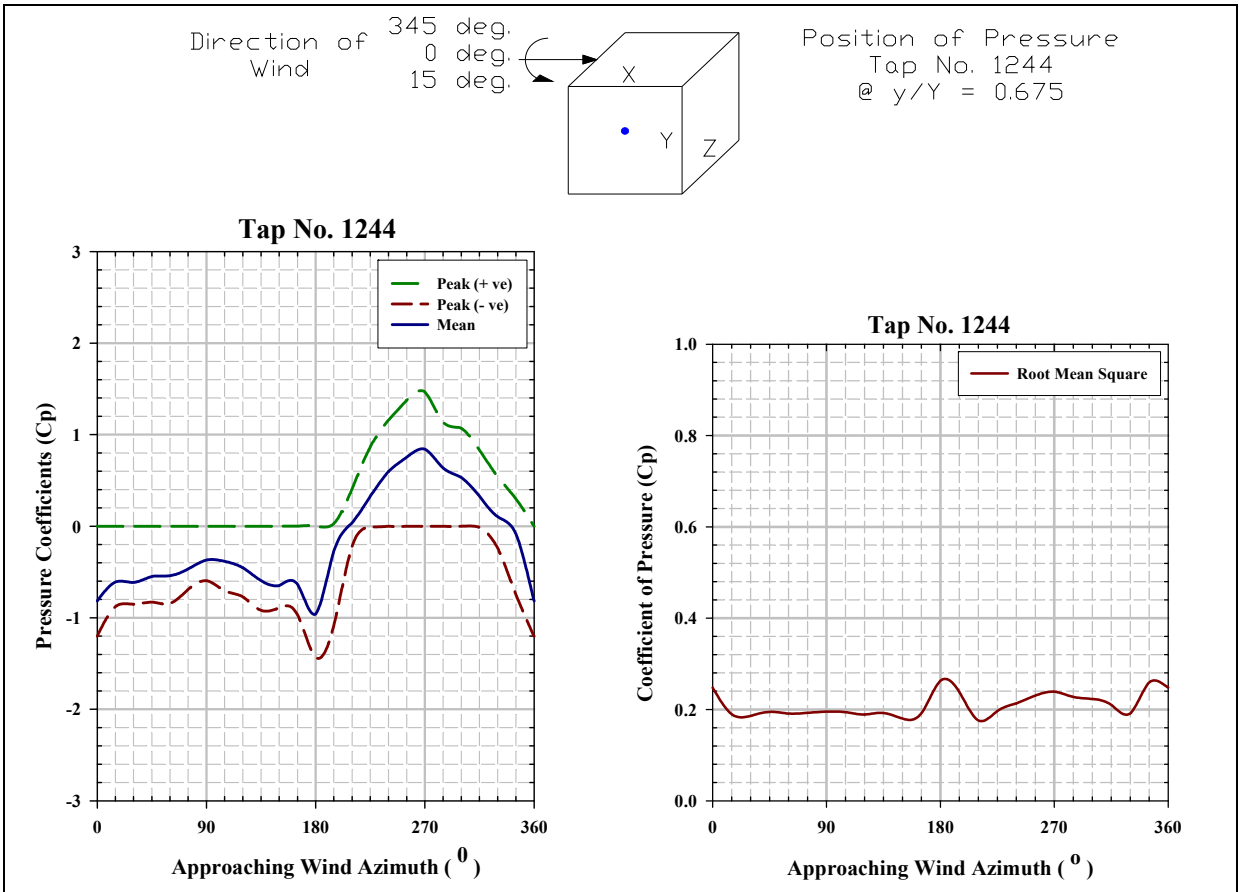

Figure 1A.40 Mean, peak and rms pressure coefficients for the tap number 1244

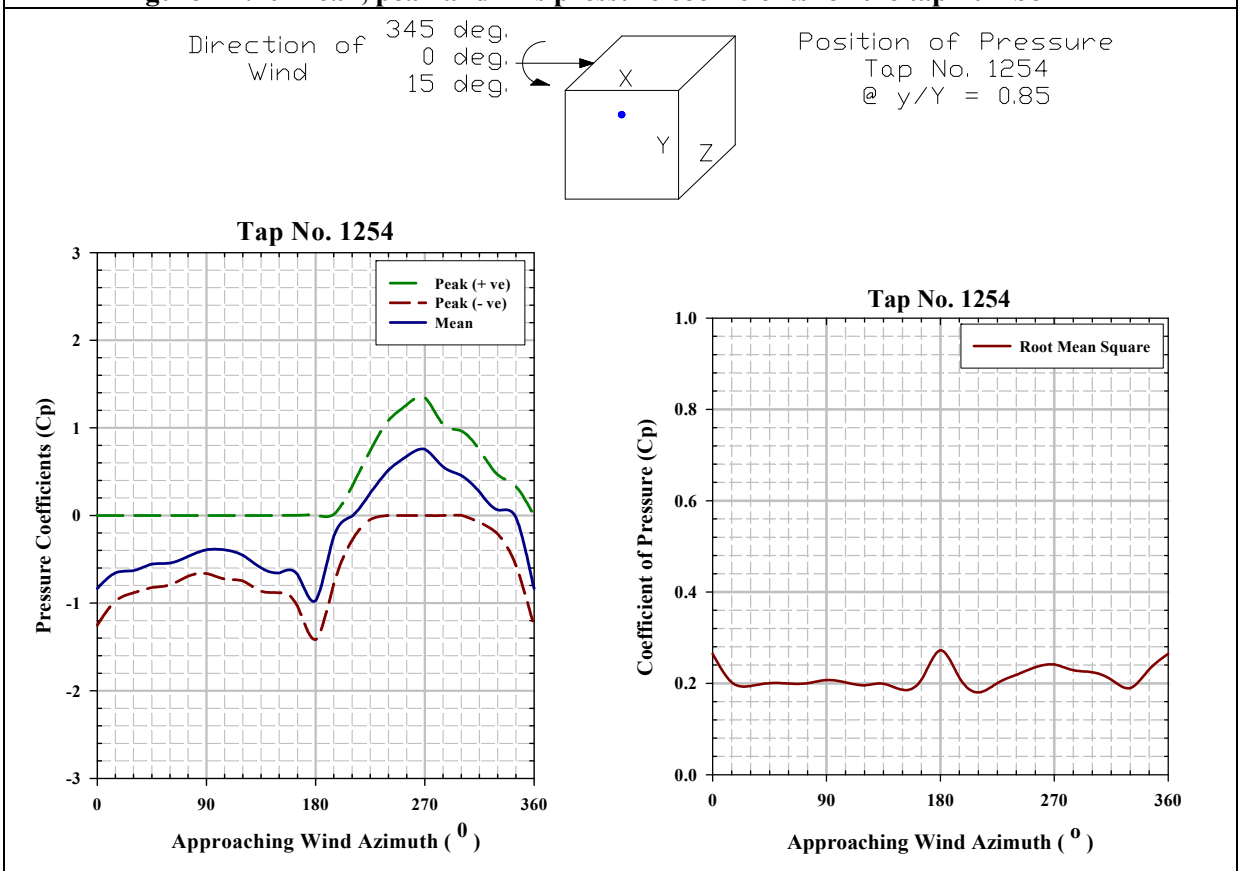

Figure 1A.41 Mean, peak and rms pressure coefficients for the tap number 1254

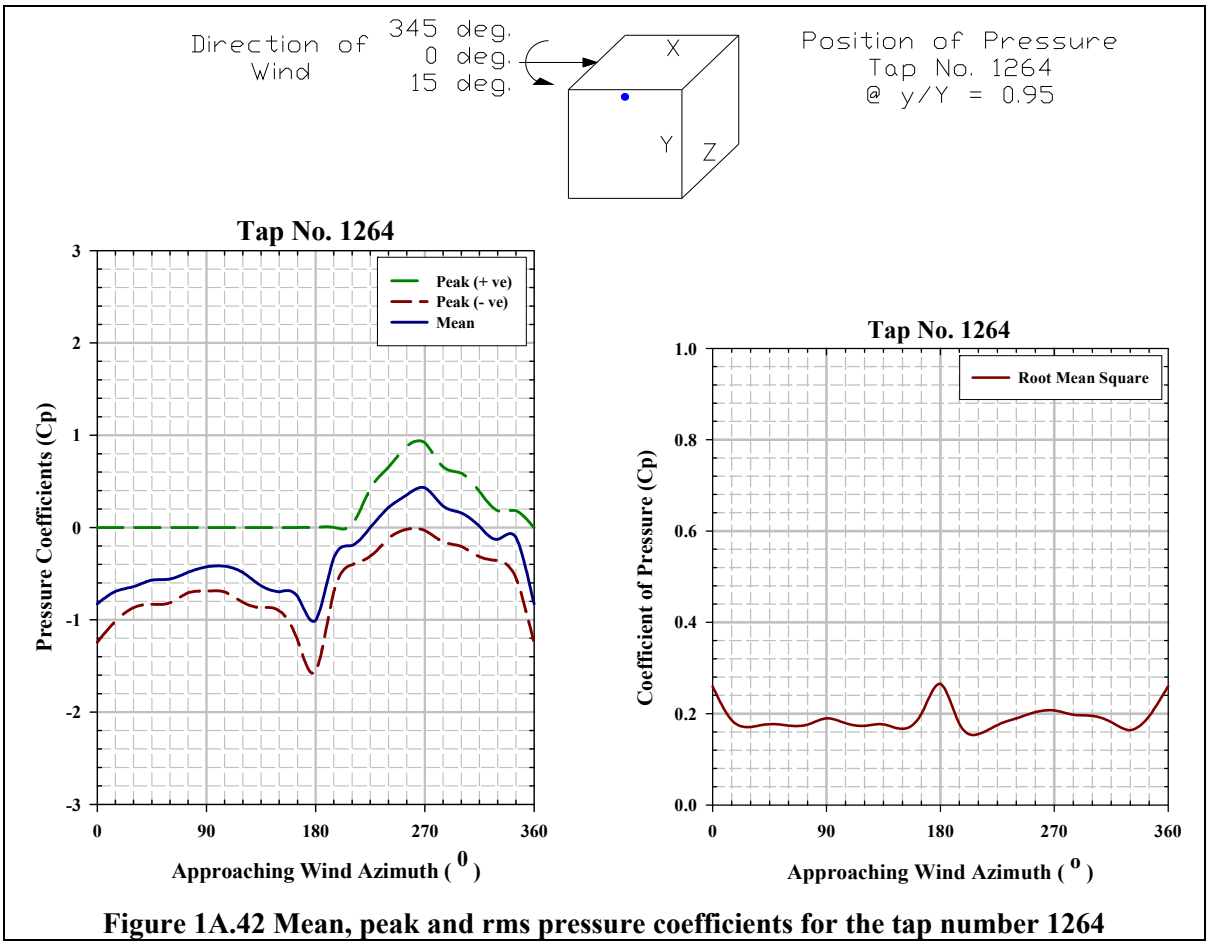

Figure 1A.42 Mean, peak and rms pressure coefficients for the tap number 1264

Pressure Coefficient Contours on Roof of SEB for Type B Terrain

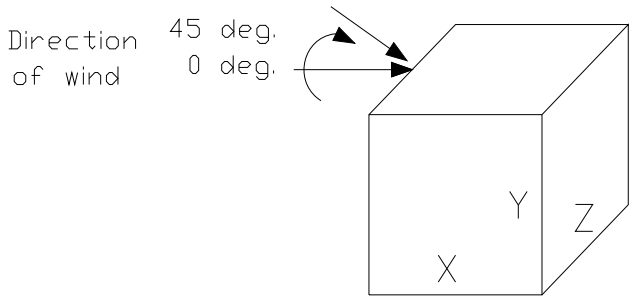

Figure 1B.1 Angle of attack of wind on roof of the SEB , direction of which varies from 0° to +45°

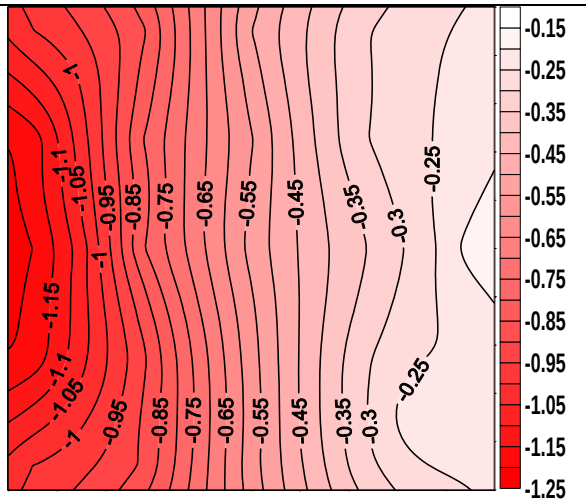

Figure 1B.2 Pressure coefficient contours on the roof of the SEB when θ= 0°

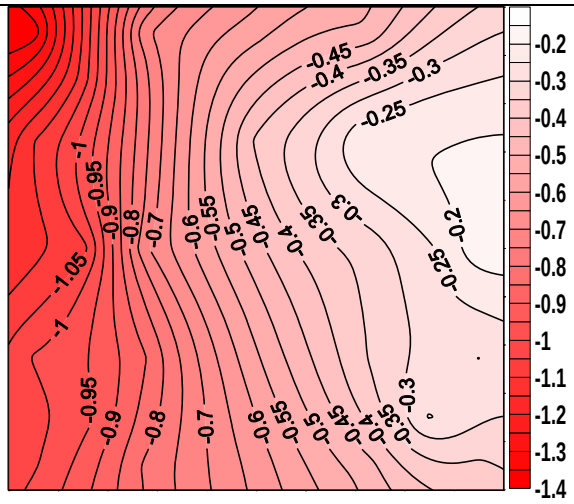

Figure 1B.3 Pressure coefficient contours on the roof of the SEB when θ= 15°

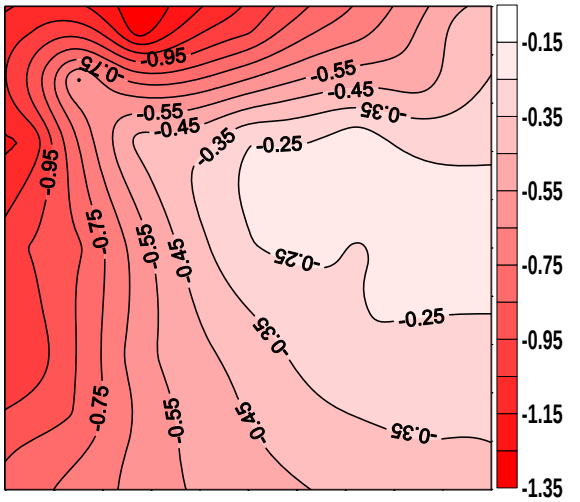

Figure 1B.4 Pressure coefficient contours on the roof of the SEB when θ= 30°

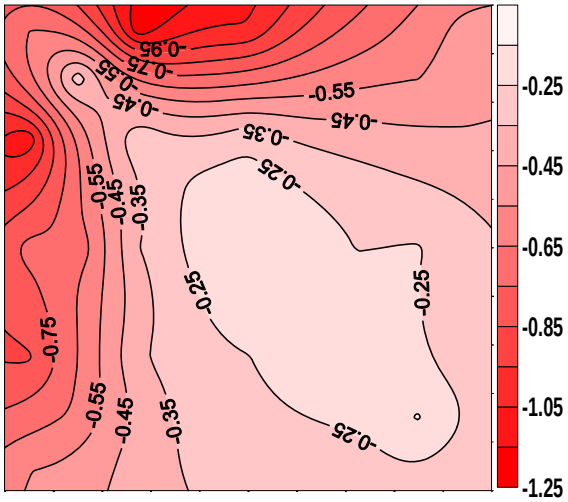

Figure 1B.5 Pressure coefficient contours on the roof of the SEB when θ= 45°

Pressure Coefficient Contours on Windward Face of SEB for Type B Terrain

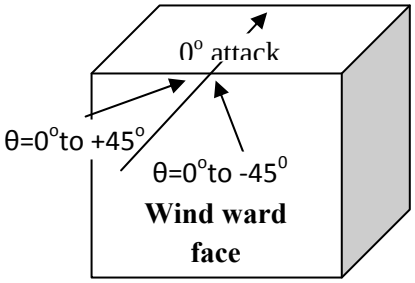

Figure 1B.6 Angle of attack of wind on windward wall of SEB, direction of which varies from -45° to +45°

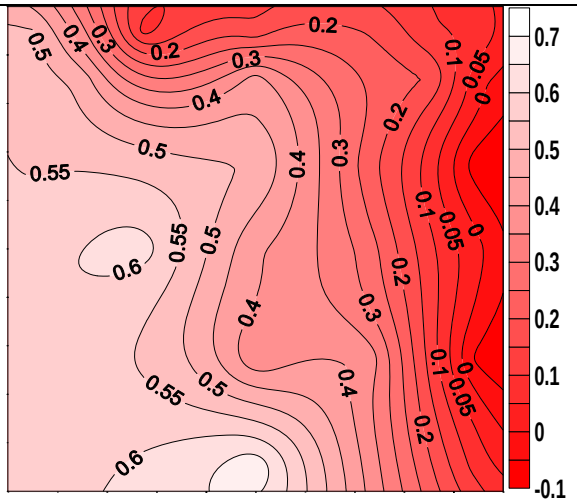

Figure 1B.7 Pressure coefficient contours on the windward face of the SEB when θ= -45°

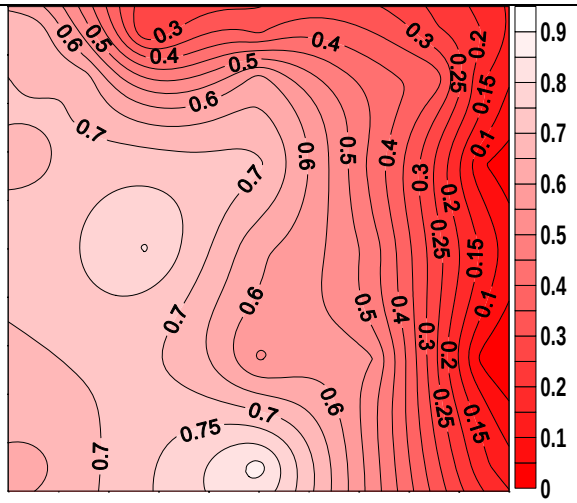

Figure 1B.8 Pressure coefficient contours on the windward face of the SEB when θ= -30°

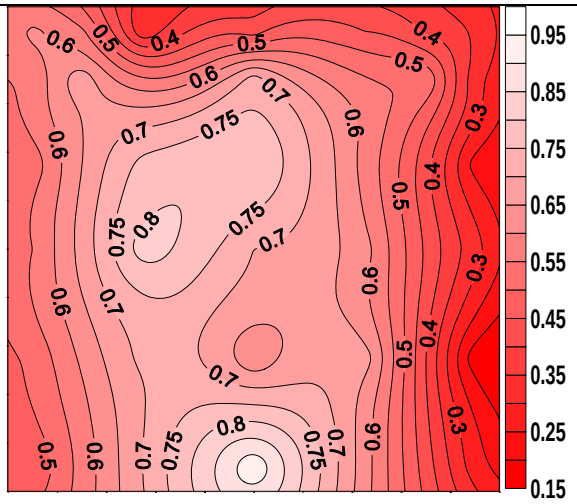

Figure 1B.9 Pressure coefficient contours on the windward face of the SEB when θ= -15°

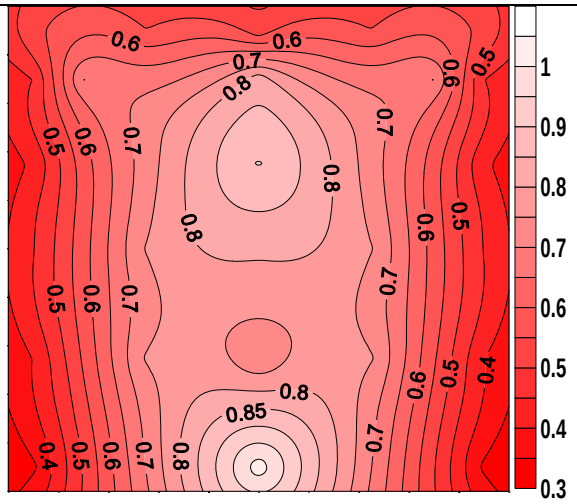

Figure 1B.10 Pressure coefficient contours on the windward face of the SEB when θ=0°

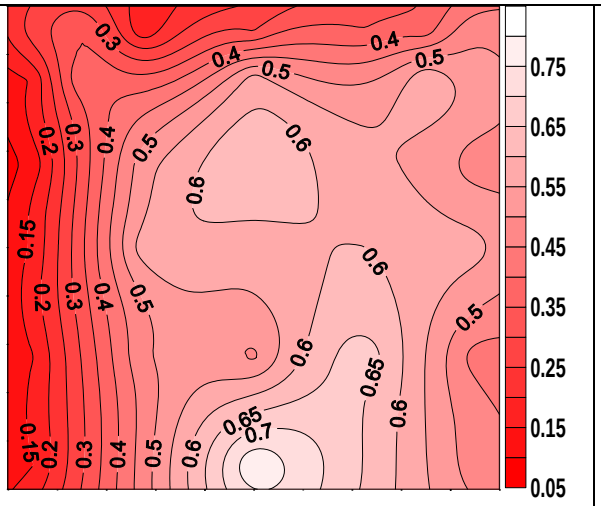

Figure 1B.11 Pressure coefficient contours on the windward face of the SEB when θ=+15^o

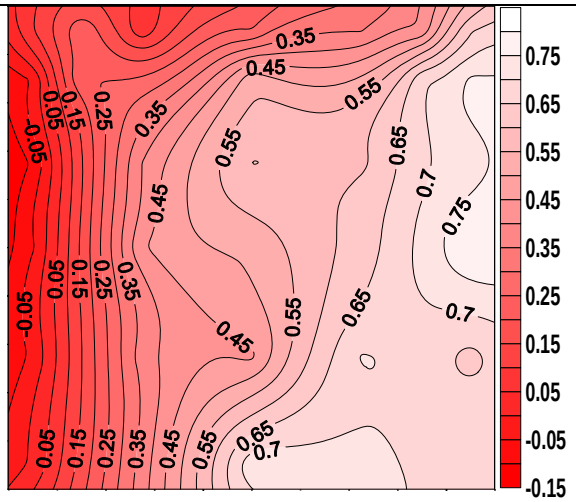

Figure 1B.12 Pressure coefficient contours on the windward face of the SEB when θ=+30^o

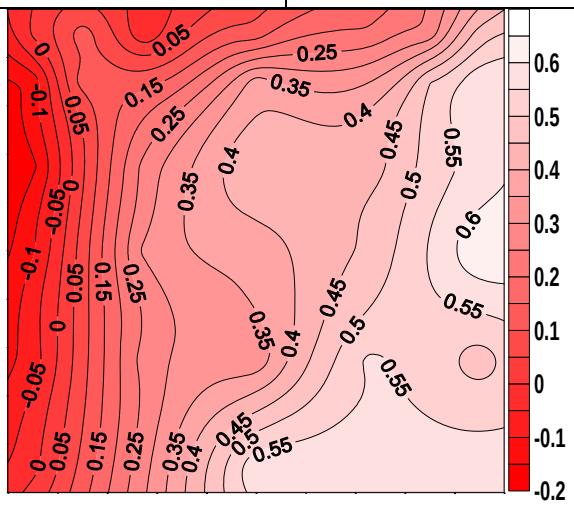

Figure 1B.13 Pressure coefficient contours on the windward face of the SEB when θ=+45^o

Pressure Coefficient Contours on Side Face of SEB for Type B Terrain

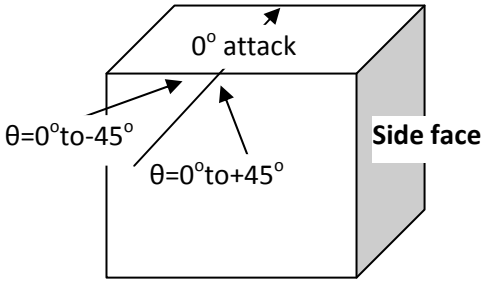

Figure 1B.14 Angle of attack of wind on windward wall of SEB, direction of which varies from -45^o to +45^o

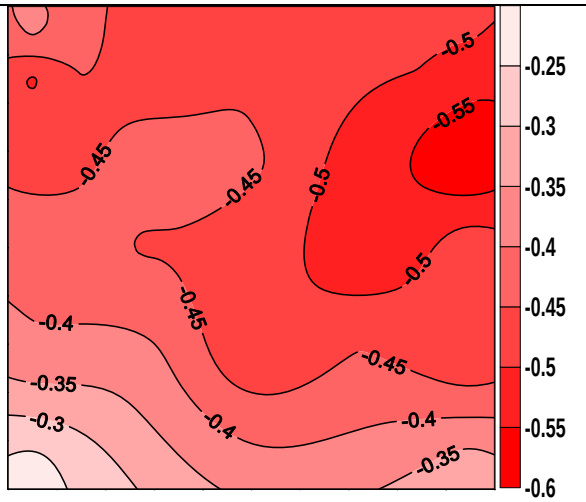

Figure 1B.15 Pressure coefficient contours on the side face of the SEB when θ= -45°

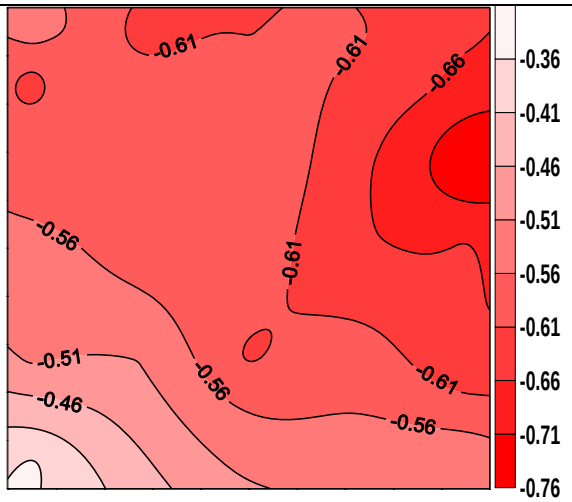

Figure 1B.16 Pressure coefficient contours on the side face of the SEB when θ= -30°

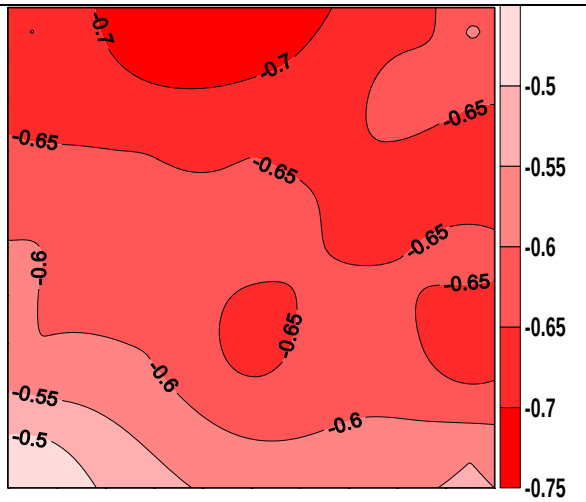

Figure 1B.17 Pressure coefficient contours on the side face of the SEB when θ= -15°

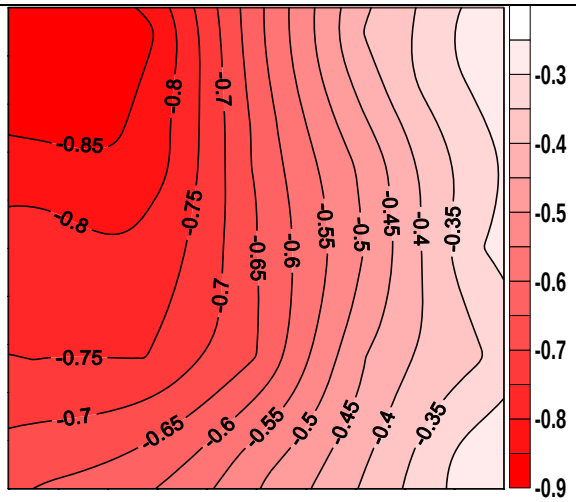

Figure 1B.18 Pressure coefficient contours on the side face of the building when θ= 0°

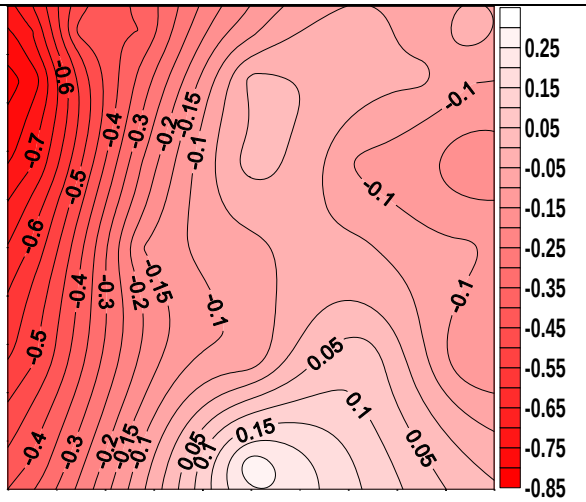

Figure 1B.19 Pressure coefficient contours on the side face of the SEB when θ=+15°

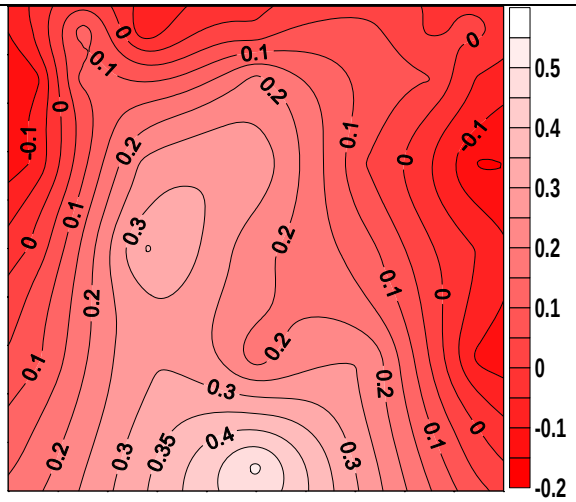

Figure 1B.20 Pressure coefficient contours on the side face of the SEB when θ=+30°

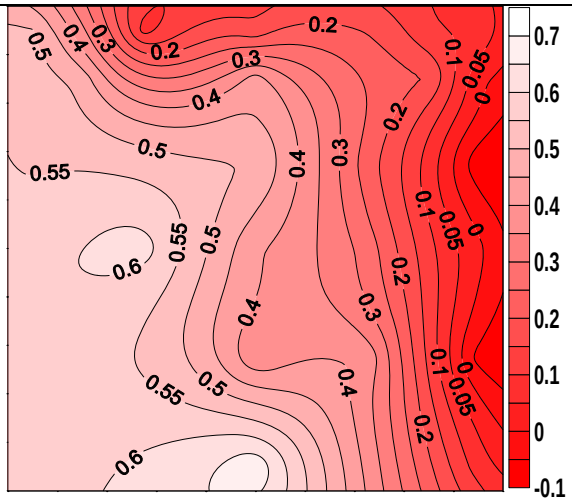

Figure 1B.21 Pressure coefficient contours on the side face of the SEB when θ=+45^o

Pressure Coefficient Contours on Leeward Face of SEB for Type B Terrain

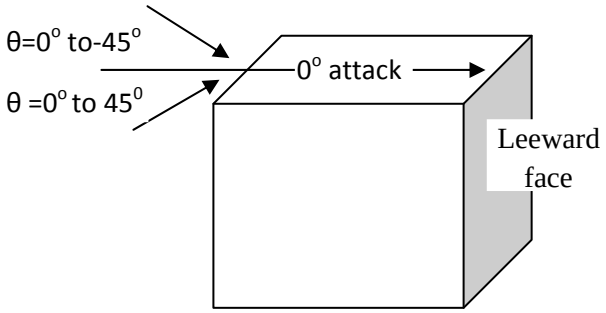

Figure 1B.22 Angle of attack of wind on windward wall of SEB, direction of which varies from -45^o to +45^o

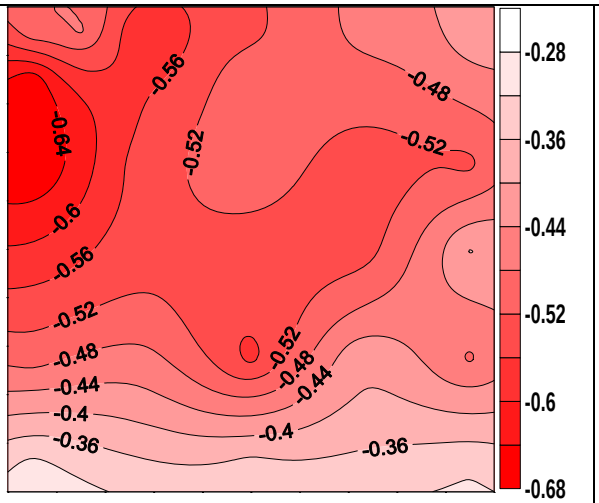

Figure 1B.23 Pressure coefficient contours on the leeward face of the SEB when θ= -45^o

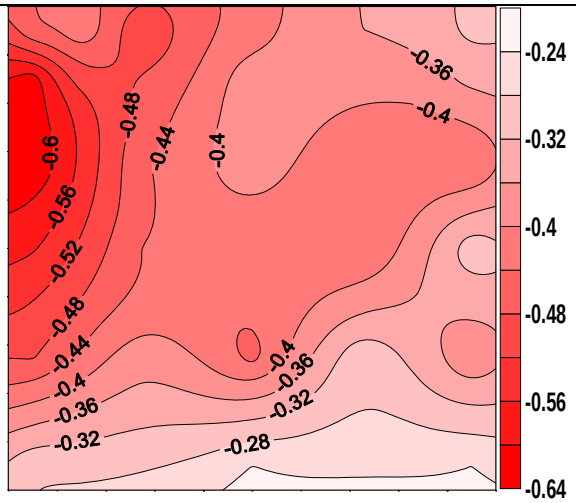

Figure 1B.24 Pressure coefficient contours on the leeward face of the SEB when θ= -30^o

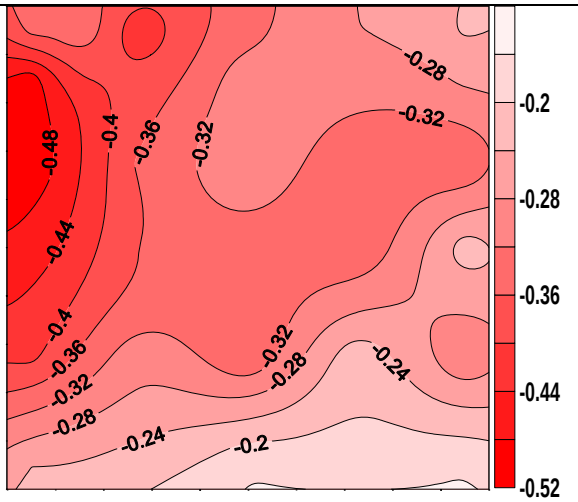

Figure 1B.25 Pressure coefficient contours on the leeward face of the SEB when θ= -15°

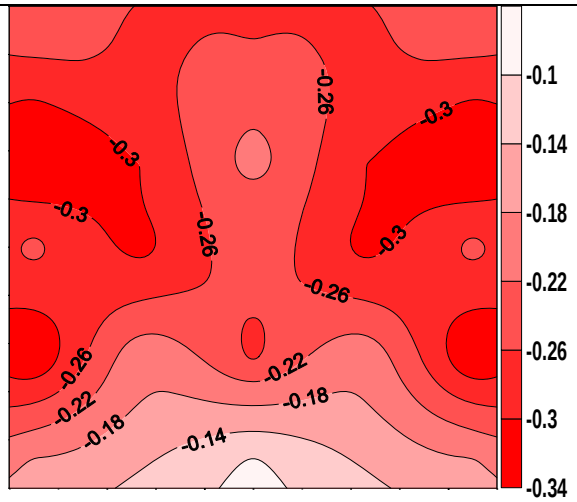

Figure 1B.26 Pressure coefficient contours on the leeward face of the SEB when θ= 0°

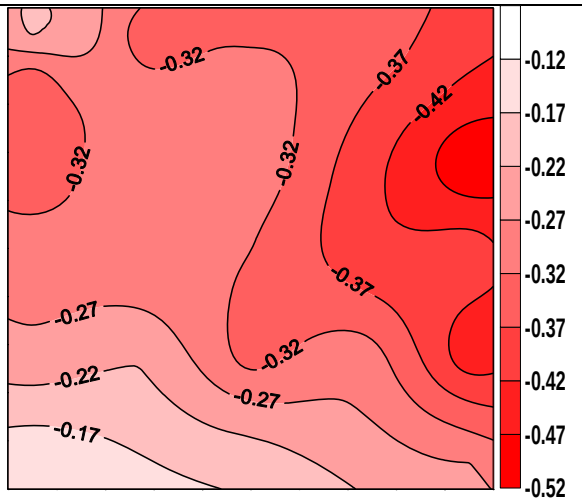

Figure 1B.27 Pressure coefficient contours on the leeward face of the SEB when θ= +15°

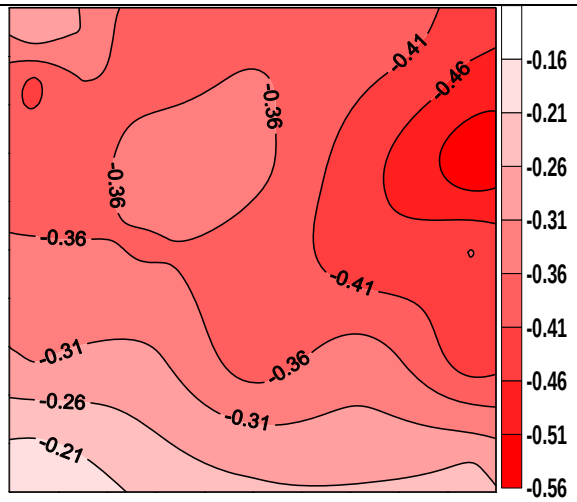

Figure 1B.28 Pressure coefficient contours on the leeward face of the SEB when θ= +30°

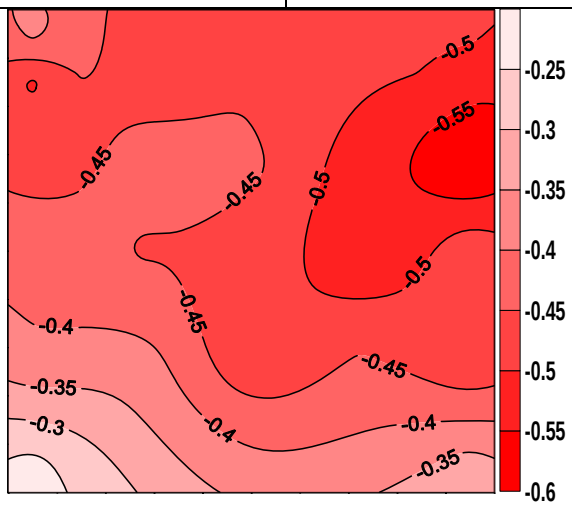

Figure 1B.29 Pressure coefficient contours on the leeward face of the SEB when θ= +45°

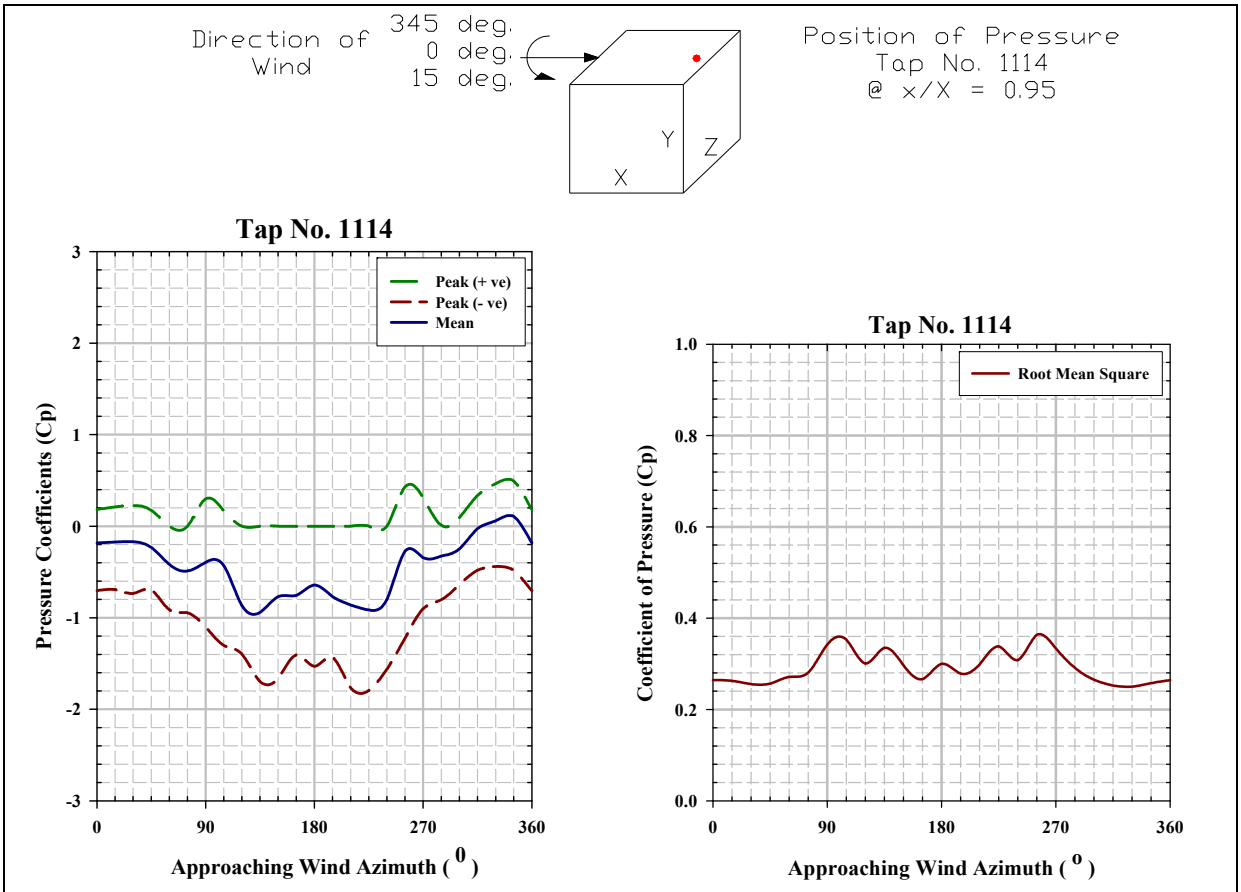

Figure 1B.30 Mean, peak and rms pressure coefficients for tap number 1114

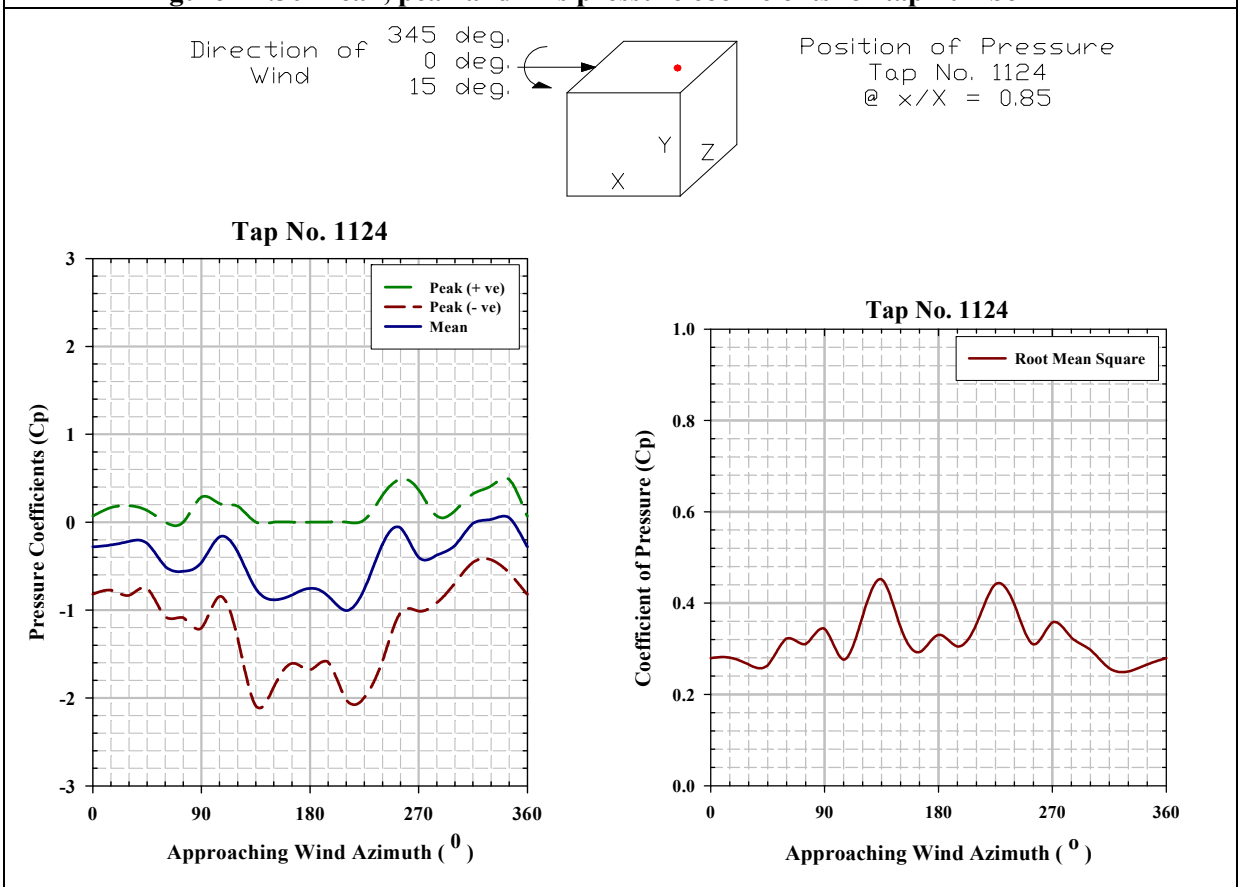

Figure 1B.31 Mean, peak and rms pressure coefficients for tap number 1124

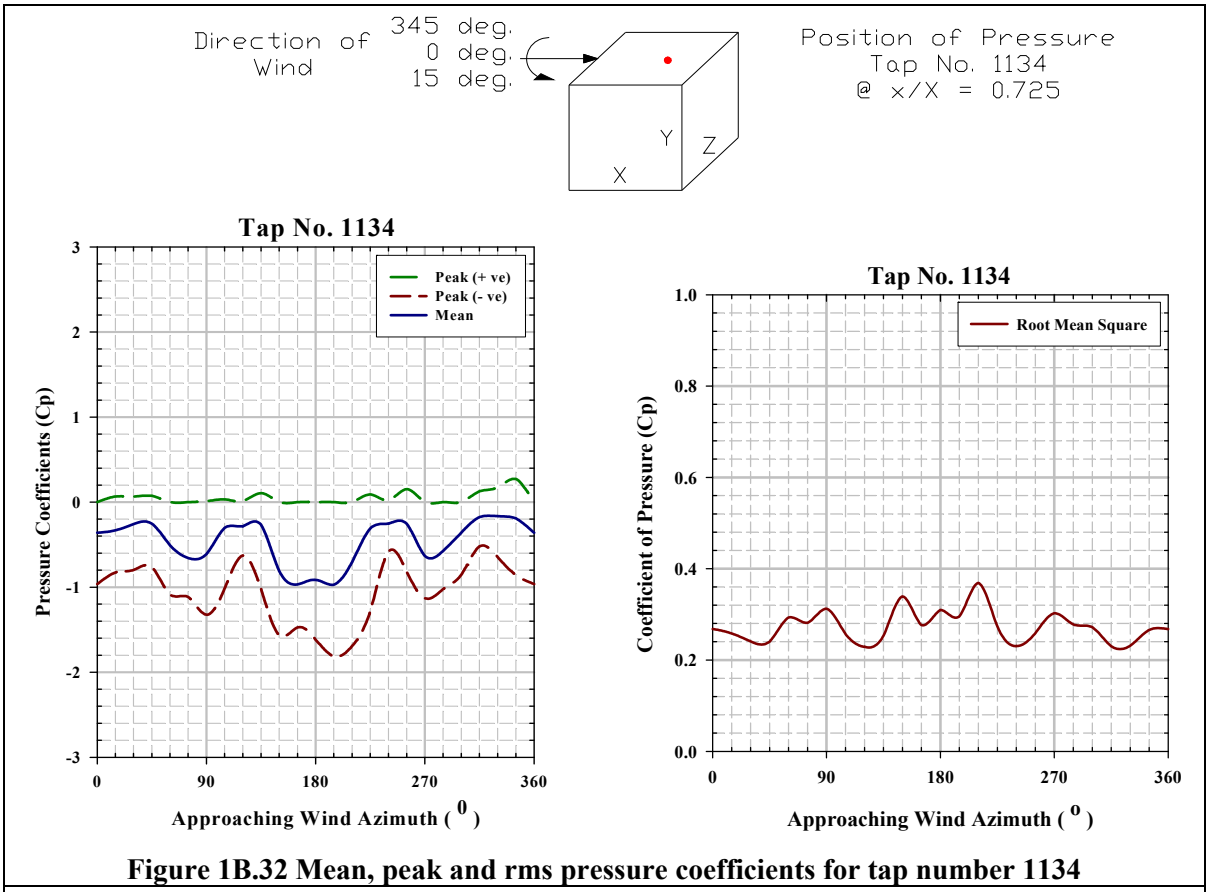

Figure 1B.32 Mean, peak and rms pressure coefficients for tap number 1134

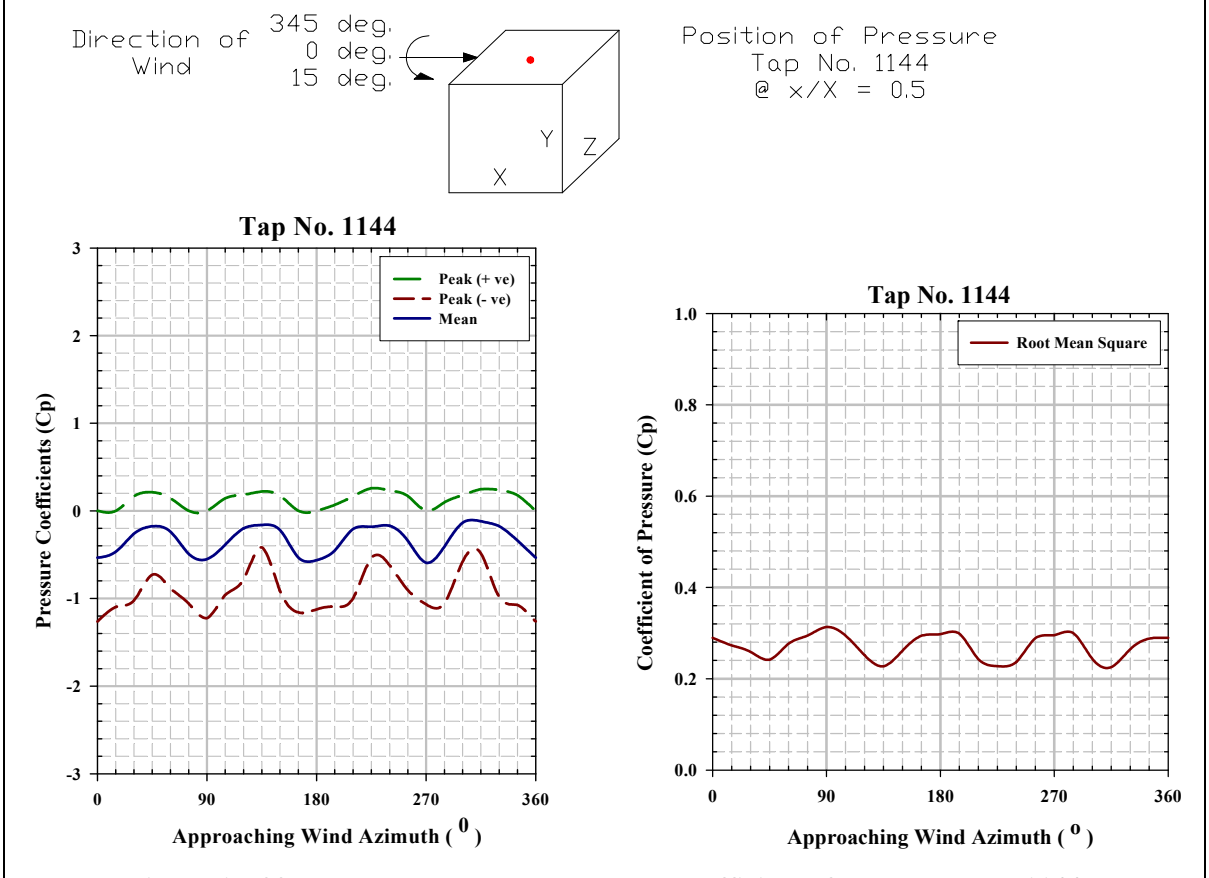

Figure 1B.33 Mean, peak and rms pressure coefficients for tap number 1144

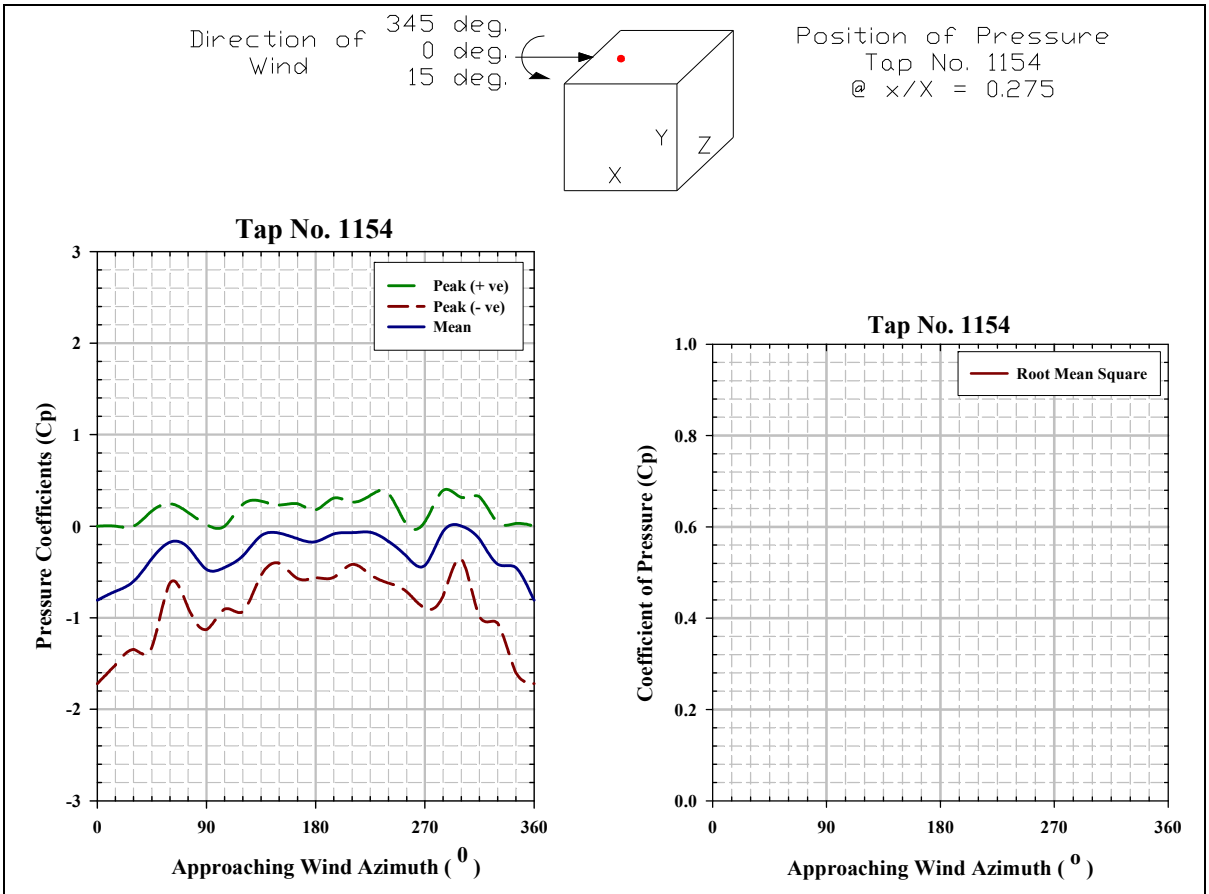

Figure 1B.34 Mean, peak and rms pressure coefficients for tap number 1154

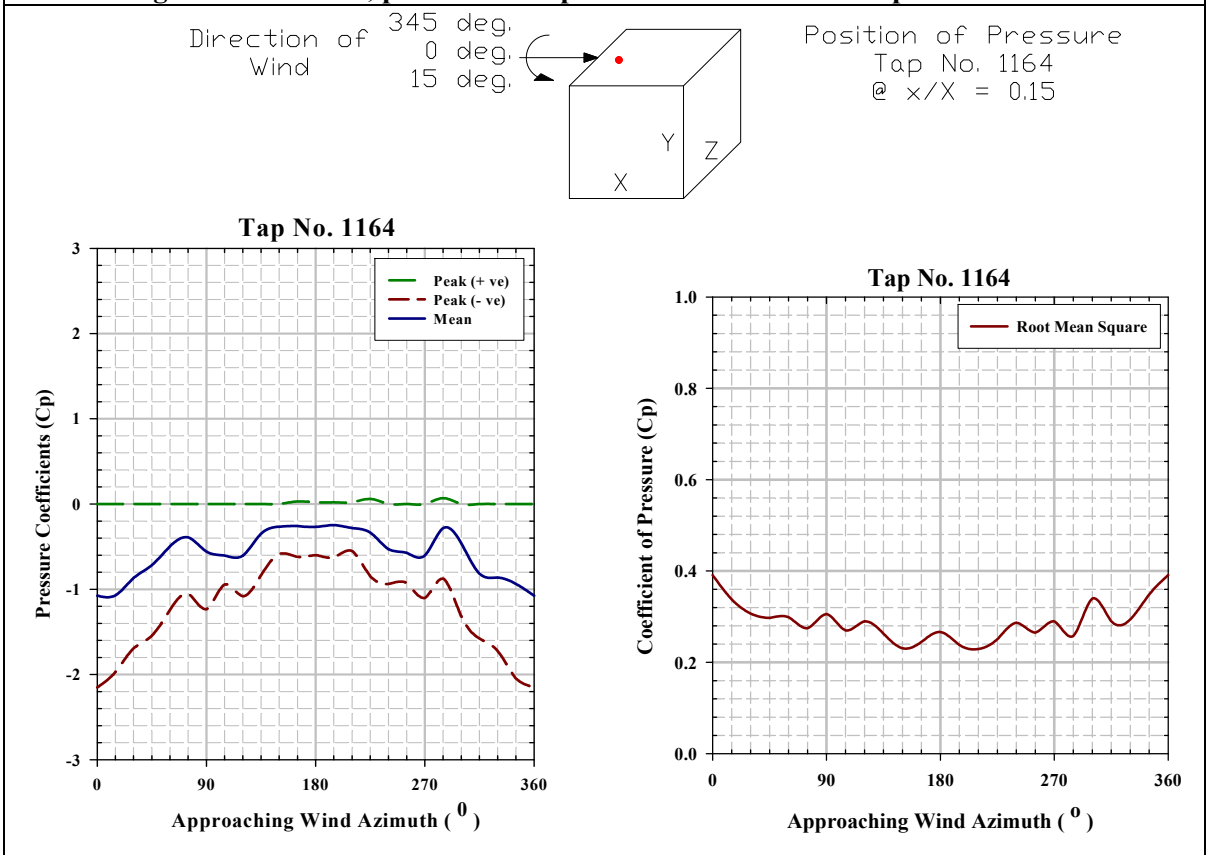

Figure 1B.35 Mean, peak and rms pressure coefficients for tap number 1164

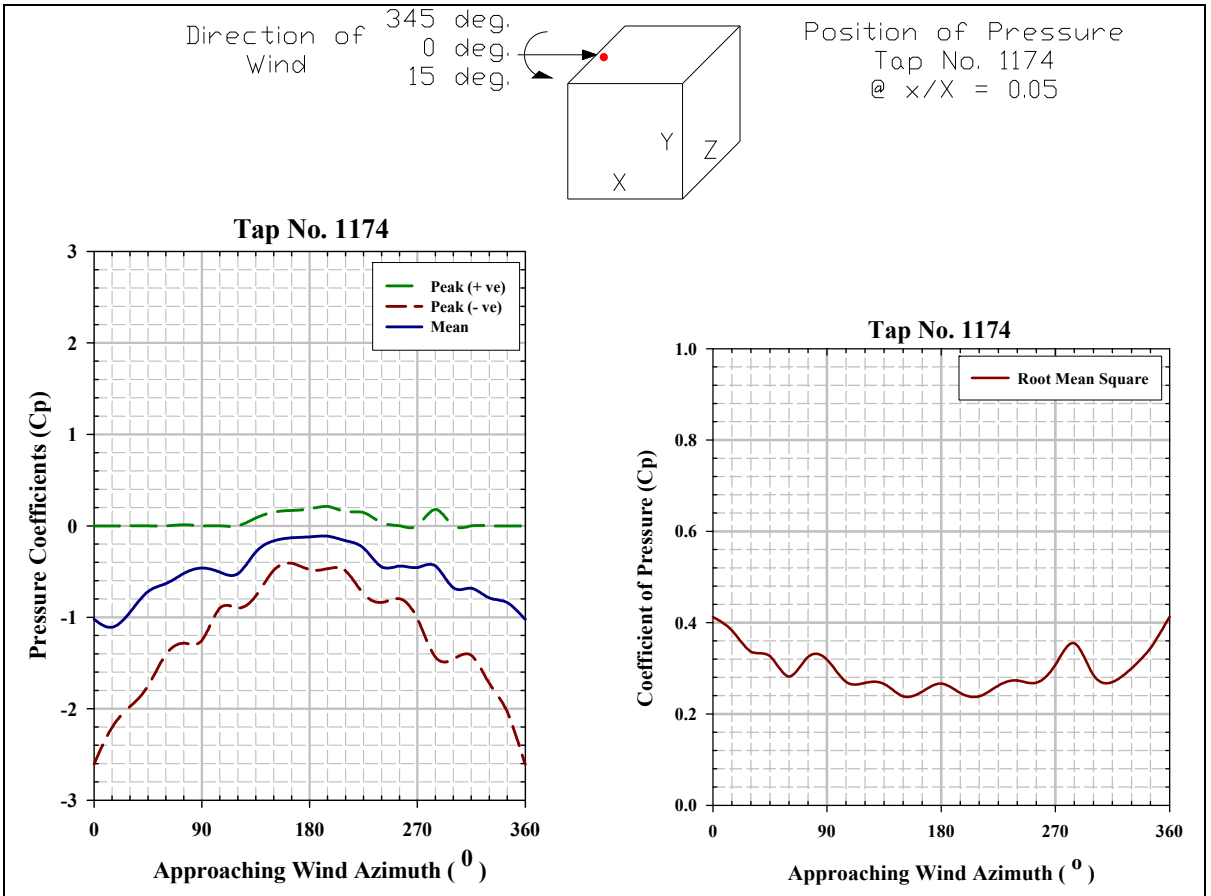

Figure 1B.36 Mean, peak and rms pressure coefficients for tap number 1174

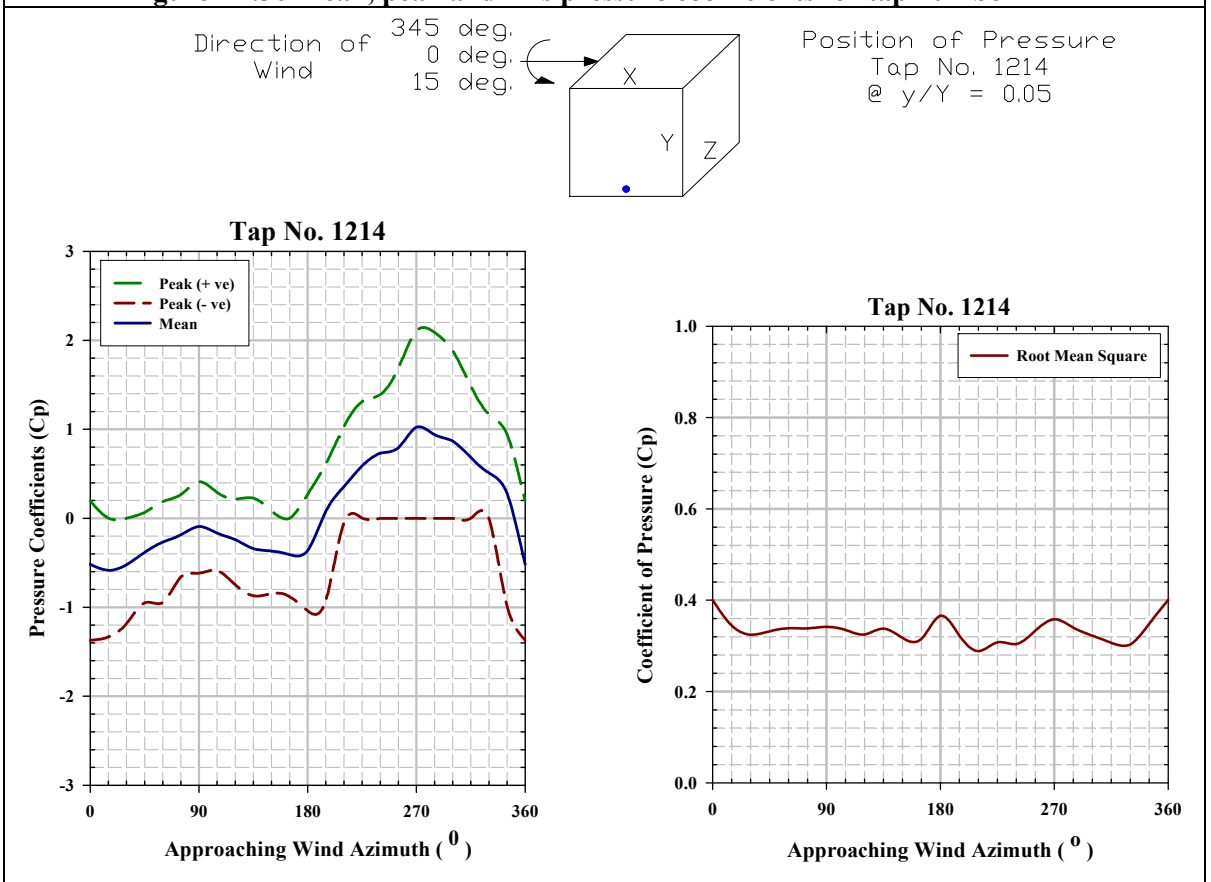

Figure 1B.37 Mean, peak and rms pressure coefficients for tap number 1214

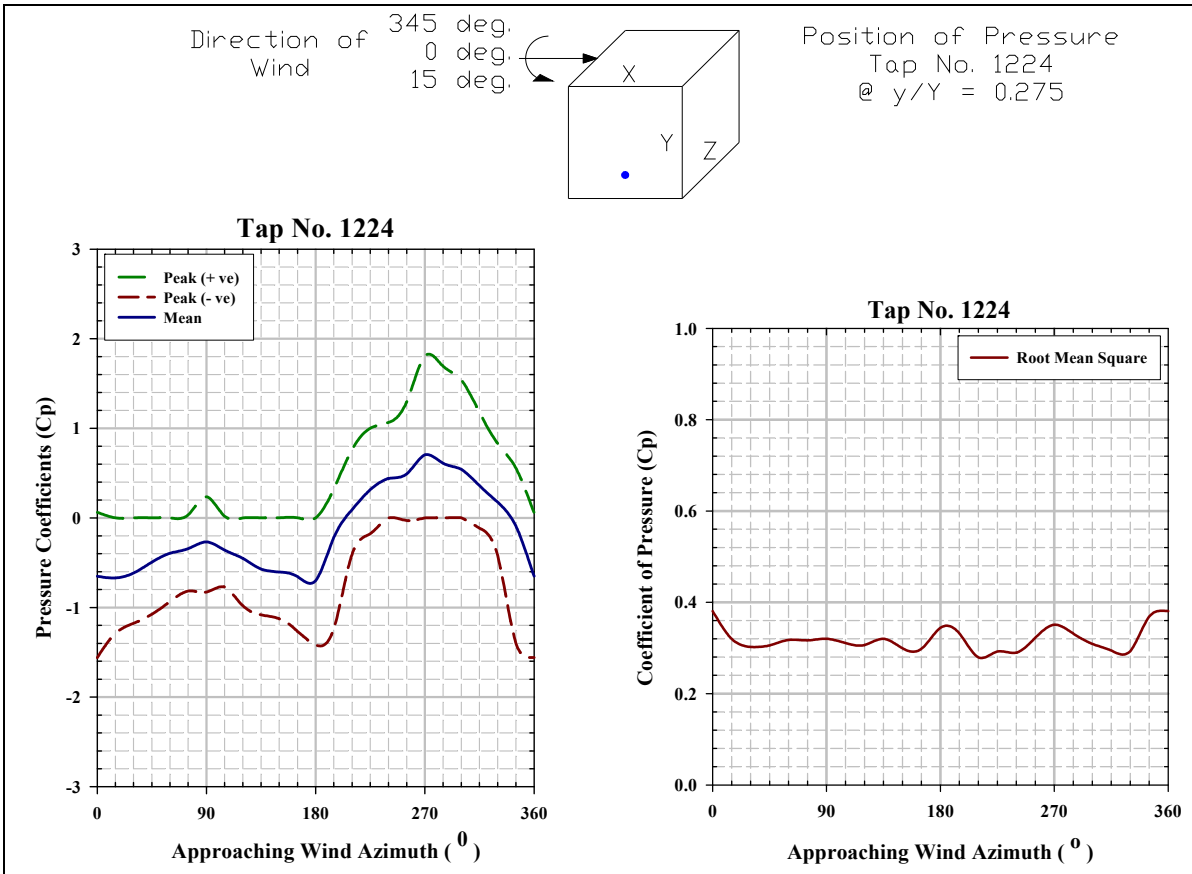

Figure 1B.38 Mean, peak and rms pressure coefficients for tap number 1224

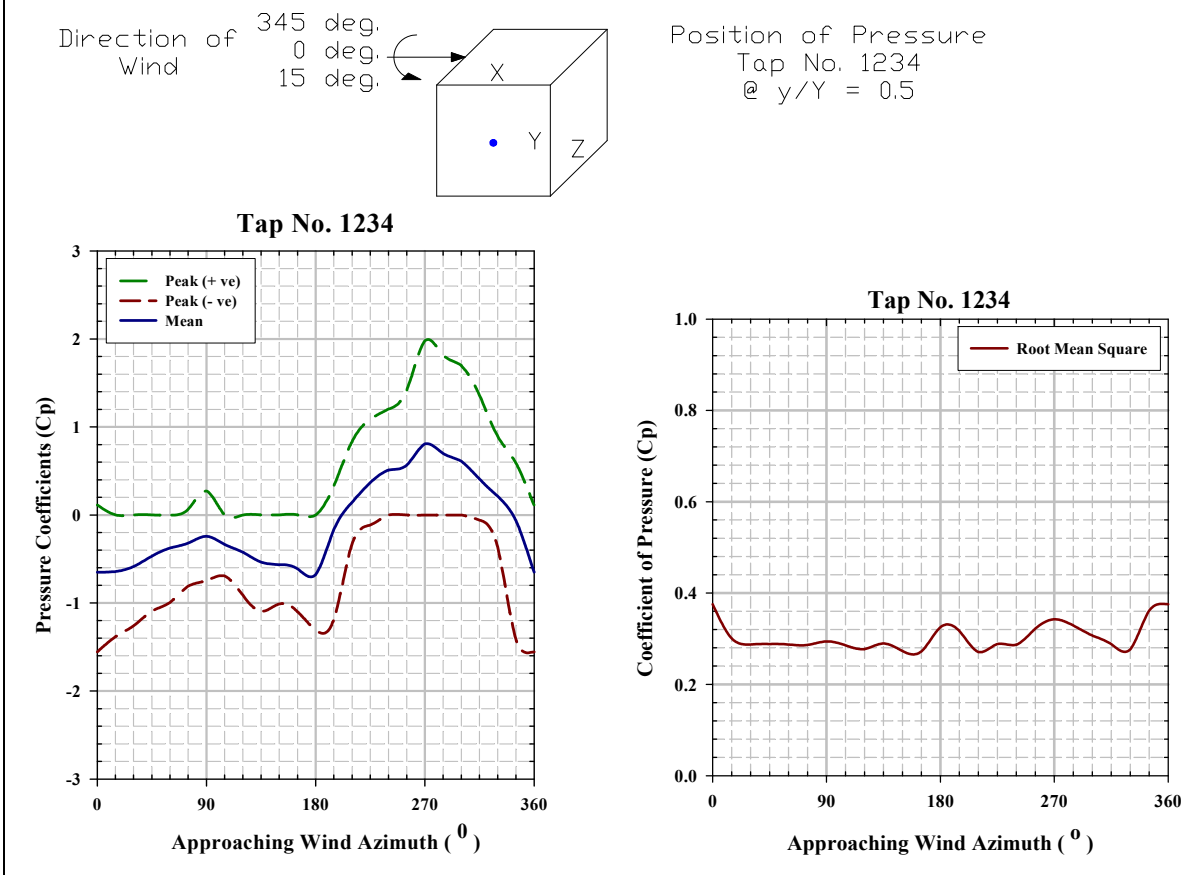

Figure 1B.39 Mean, peak and rms pressure coefficients for tap number 1234

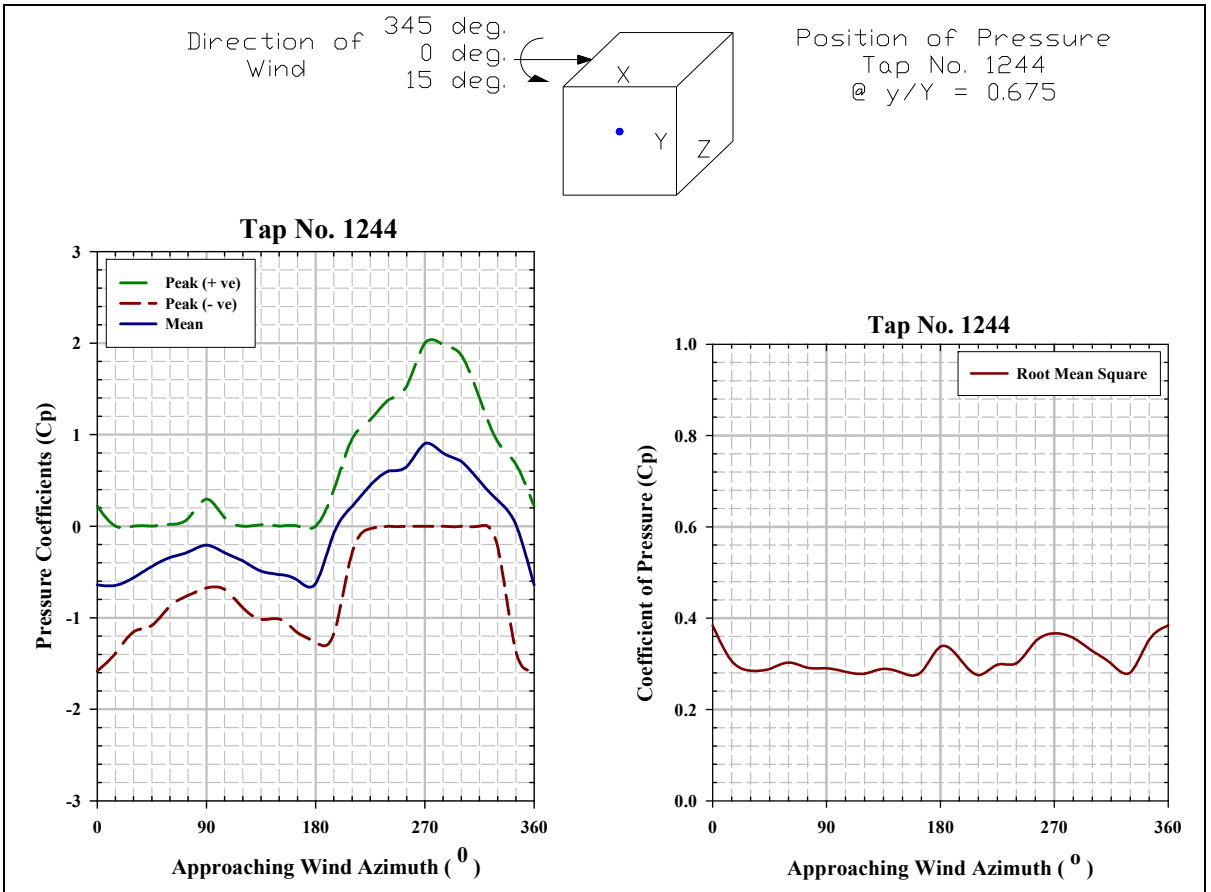

Figure 1B.40 Mean, peak and rms pressure coefficients for tap number 1244

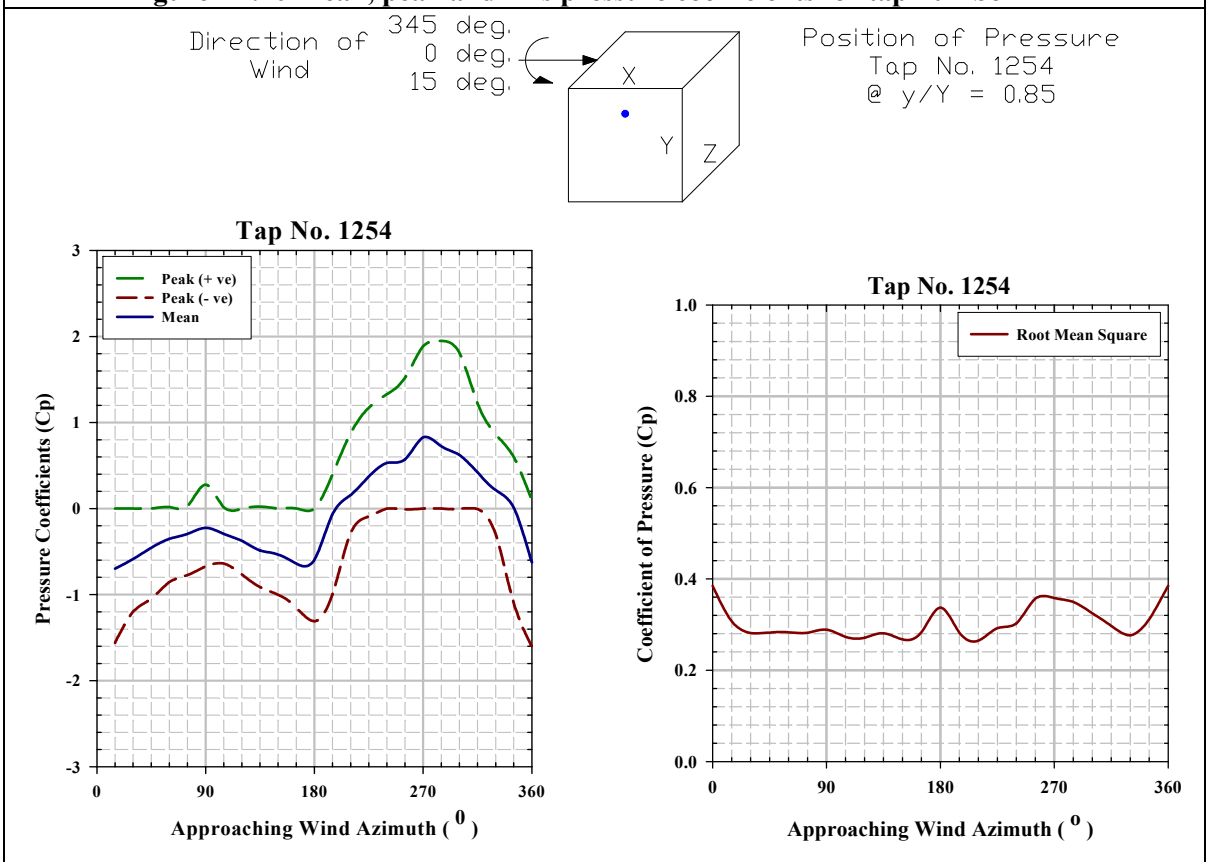

Figure 1B.41 Mean, peak and rms pressure coefficients for tap number 1254

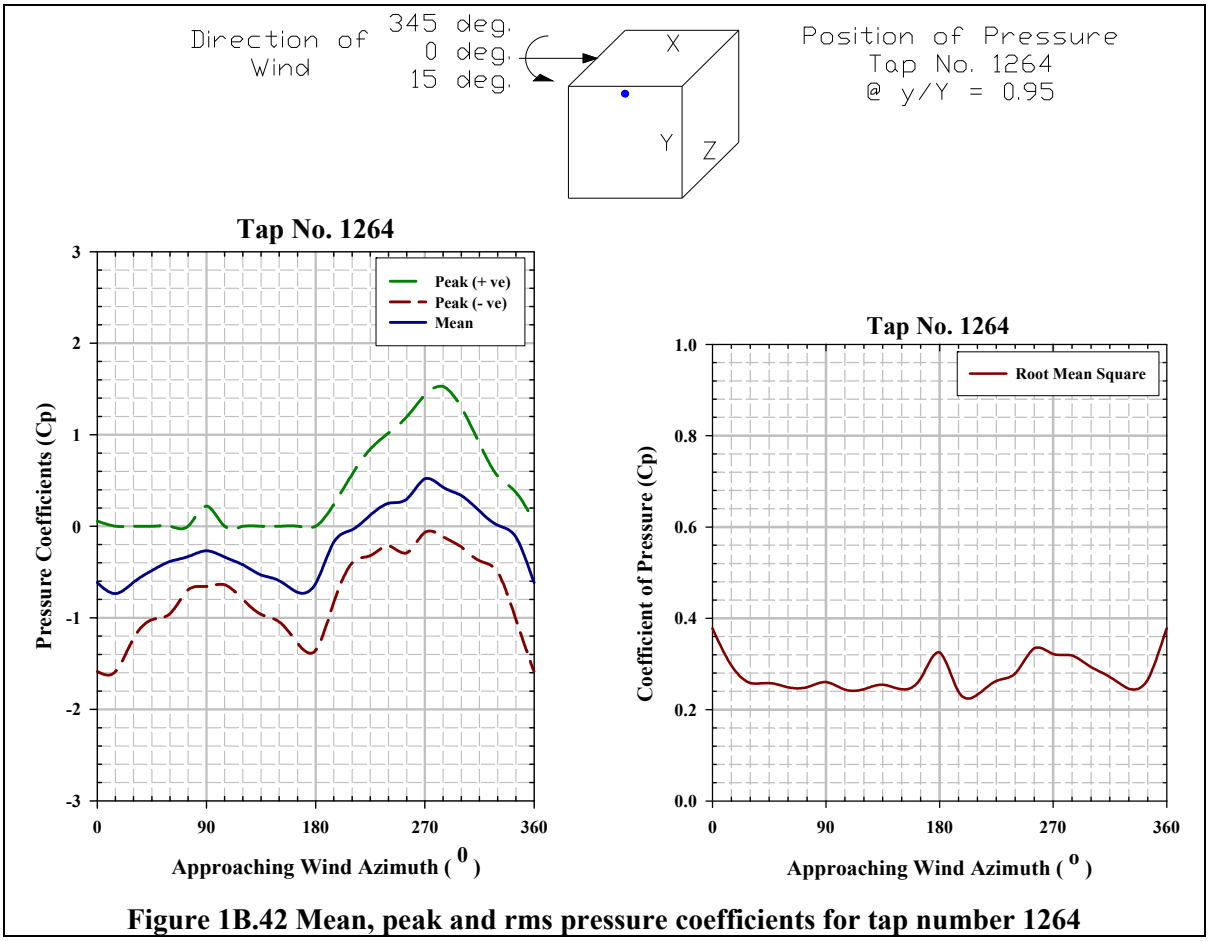

Figure 1B.42 Mean, peak and rms pressure coefficients for tap number 1264

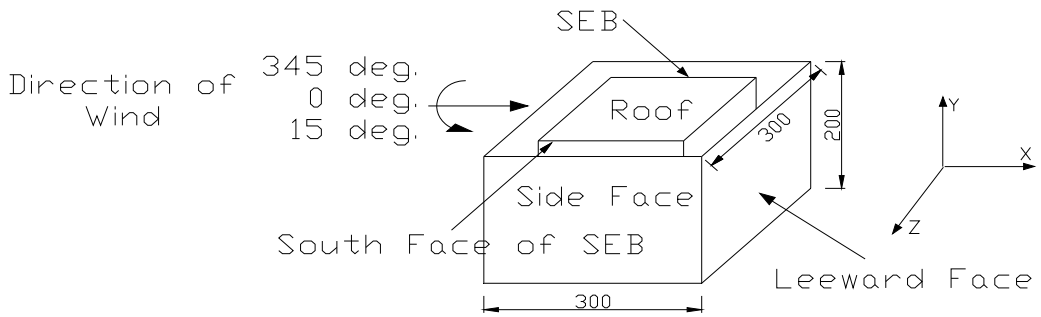

Figure 2.1 Scaled SEB surrounded by impermeable sheet all around

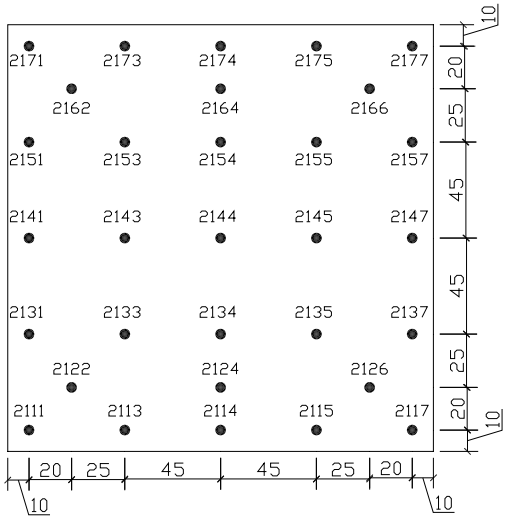

Figure 2.2 Pressure tap locations on roof

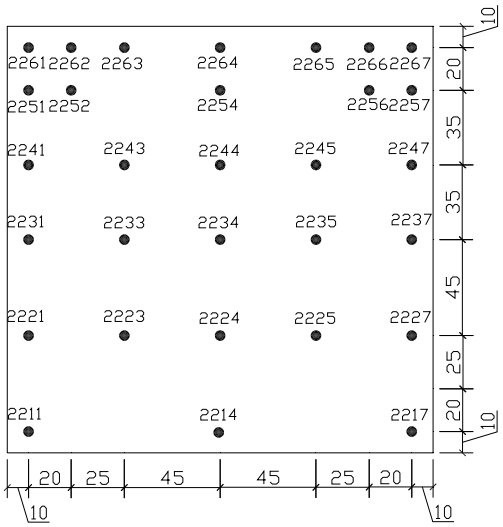

Figure 2.3 Pressure tap locations on the south wall face

Pressure Coefficient Contours on Roof of SEB for Type A Terrain

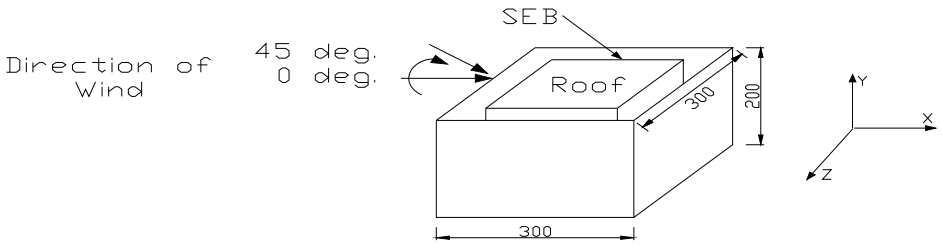

Figure 2A.1 Angle of attack of wind on roof of the SEB , direction of which varies from 0° to +45°

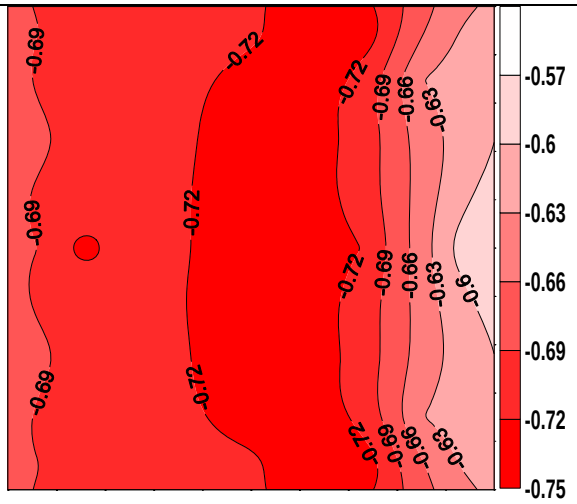

Figure 2A.2 Pressure coefficient contours on the roof of the SEB surrounded by impermeable sheet all around when θ= 0°

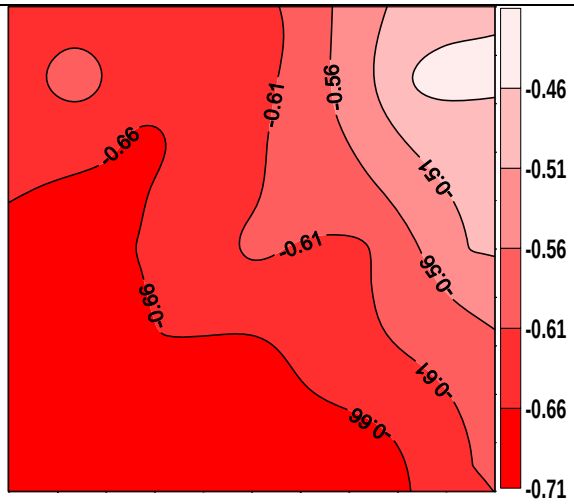

Figure 2A.3 Pressure coefficient contours on the roof of the SEB surrounded by impermeable sheet all around when θ= 15°

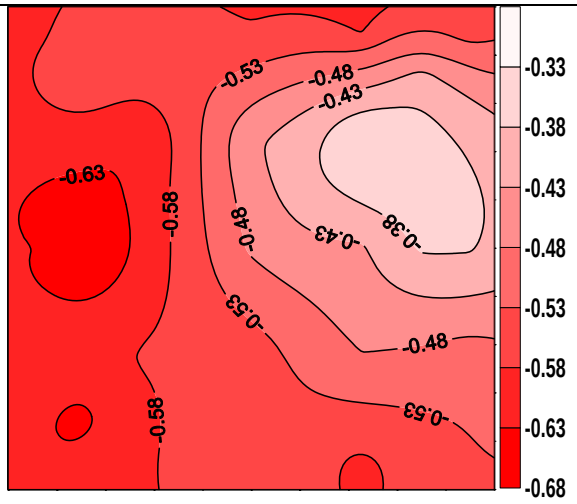

Figure 2A.4 Pressure coefficient contours on the roof of the SEB surrounded by impermeable sheet all around when θ= 30°

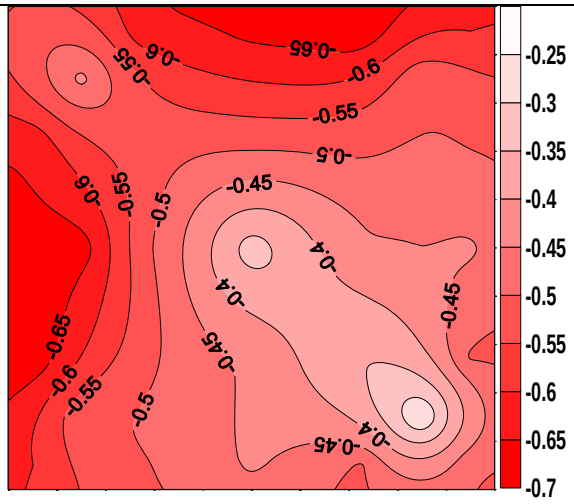

Figure 2A.5 Pressure coefficient contours on the roof of the SEB surrounded by impermeable sheet all around when θ= 45°

Pressure Coefficient Contours on Windward Face of SEB for Type A Terrain

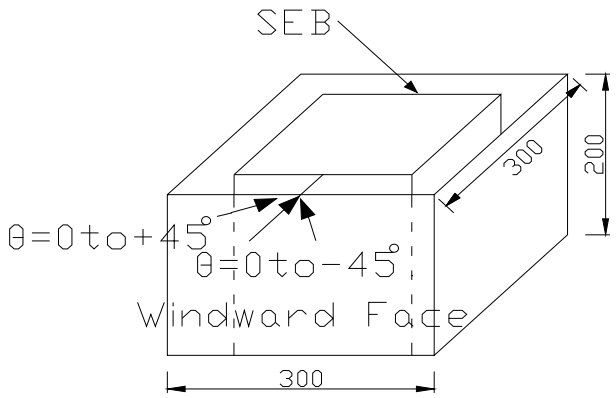

Figure 2A.6 Angle of attack of wind on windward wall of SEB, direction of which varies from -45° to +45°

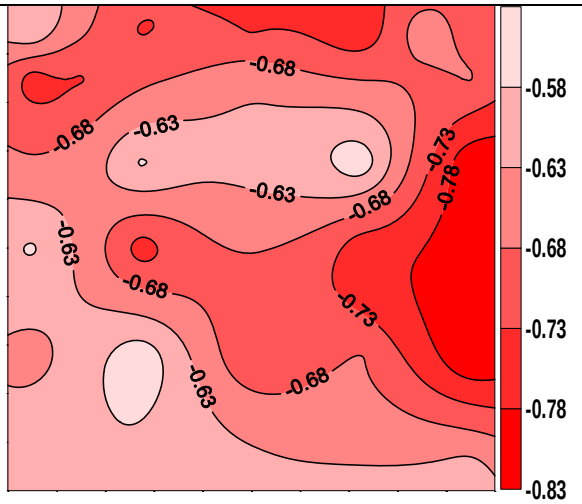

Figure 2A.7 Pressure coefficient contours on the windward face of the SEB surrounded by impermeable sheet all around when θ= -45°

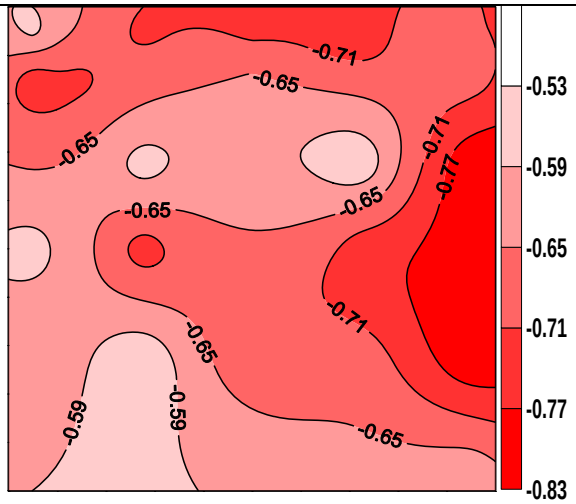

Figure 2A.8 Pressure coefficient contours on the windward face of the SEB surrounded by impermeable sheet all around when θ= -30°

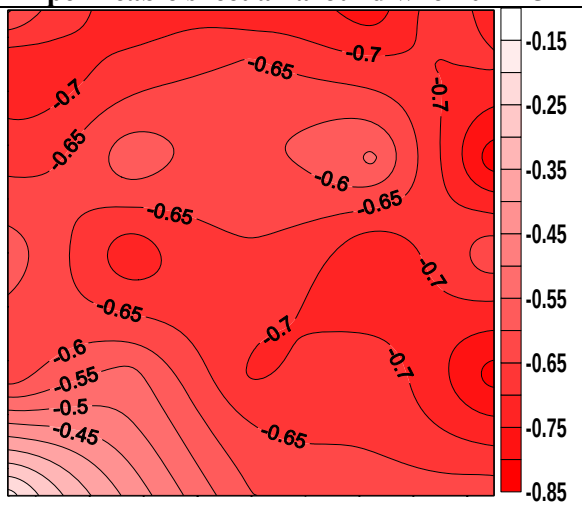

Figure 2A.9 Pressure coefficient contours on the windward face of the SEB surrounded by impermeable sheet all around when θ= -15°

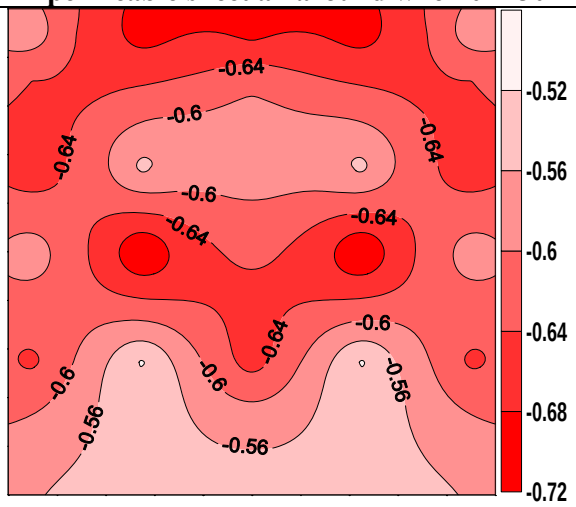

Figure 2A.10 Pressure coefficient contours on the windward face of the SEB surrounded by impermeable sheet all around when θ=0°

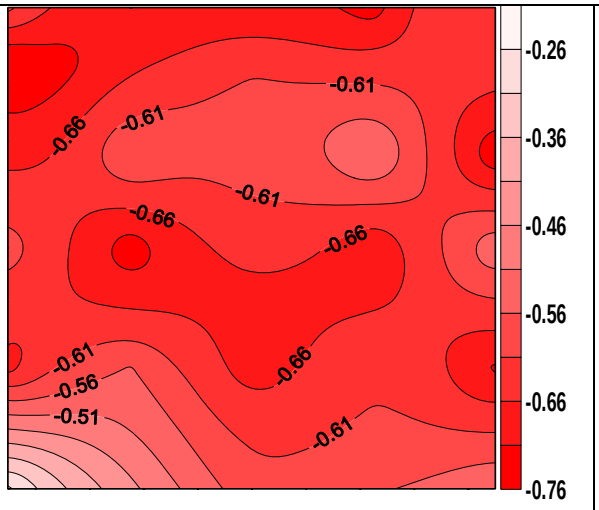

Figure 2A.11 Pressure coefficient contours on the windward face of the SEB surrounded by impermeable sheet all around when θ=+15°

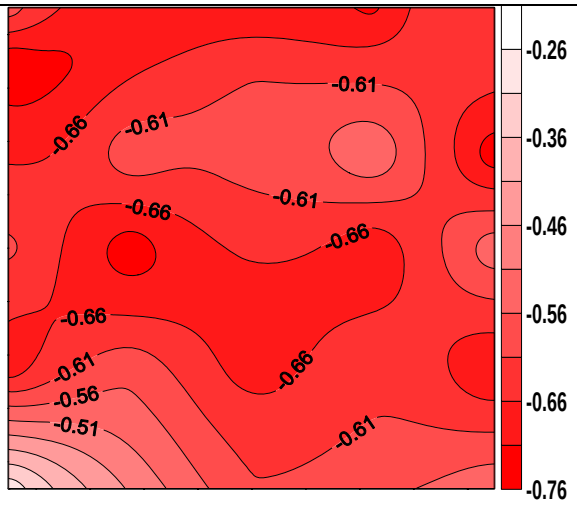

Figure 2A.12 Pressure coefficient contours on the windward face of the SEB surrounded by impermeable sheet all around when θ=+30°

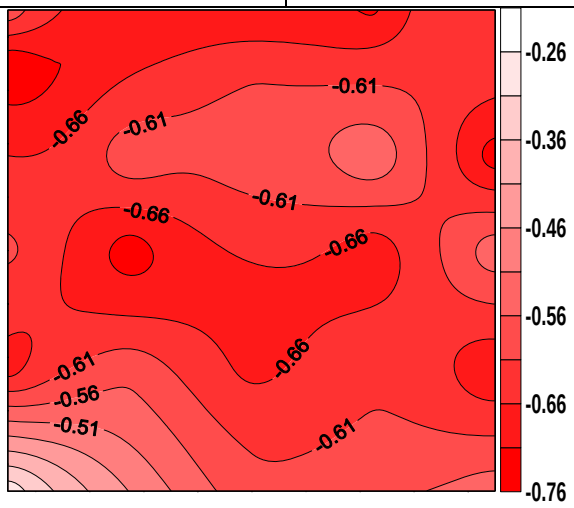

Figure 2A.13 Pressure coefficient contours on the windward face of the SEB surrounded by impermeable sheet all around when θ=+45°

Pressure Coefficient Contours on Side Face of SEB for Type A Terrain

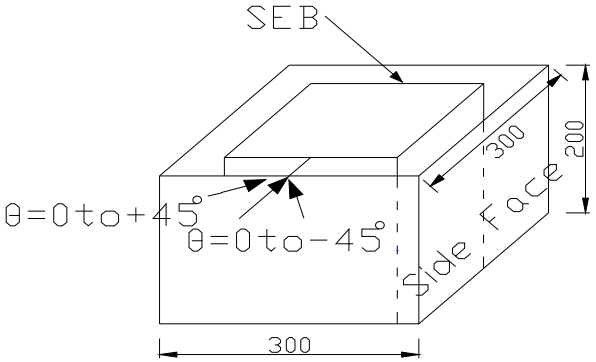

Figure 2A.14 Angle of attack of wind on windward wall of SEB, direction of which varies from -45° to +45°

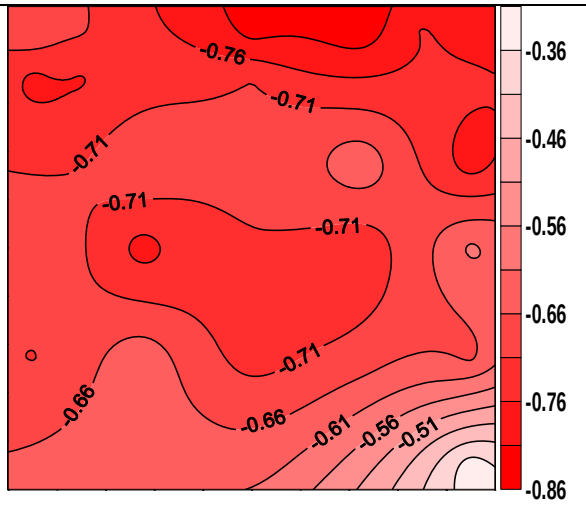

Figure 2A.15 Pressure coefficient contours on the side face of the SEB surrounded by impermeable sheet all around when θ= -45°

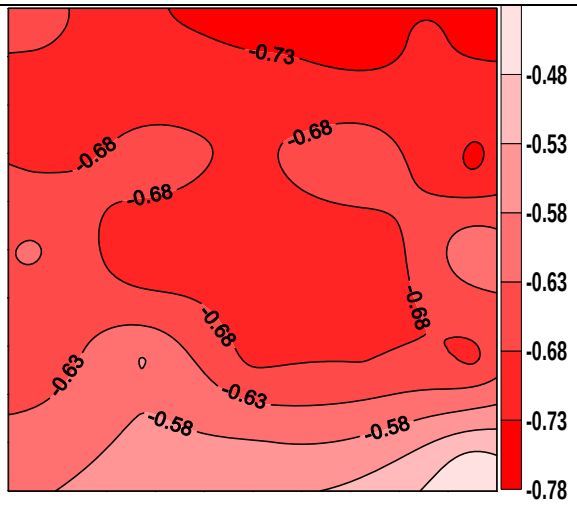

Figure 2A.16 Pressure coefficient contours on the side face of the SEB surrounded by impermeable sheet all around when θ= -30°

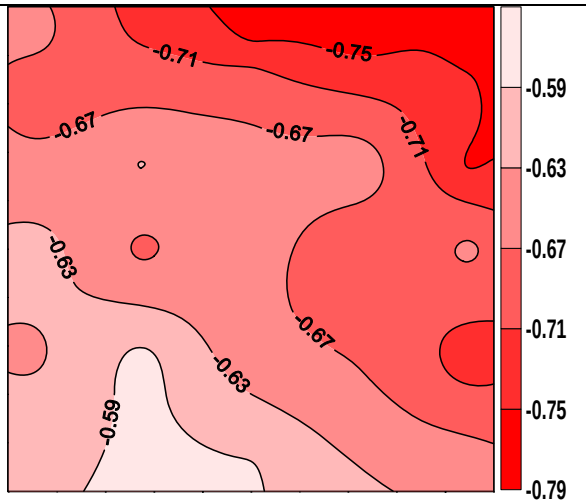

Figure 2A.17 Pressure coefficient contours on the side face of the SEB surrounded by impermeable sheet all around when θ= -15°

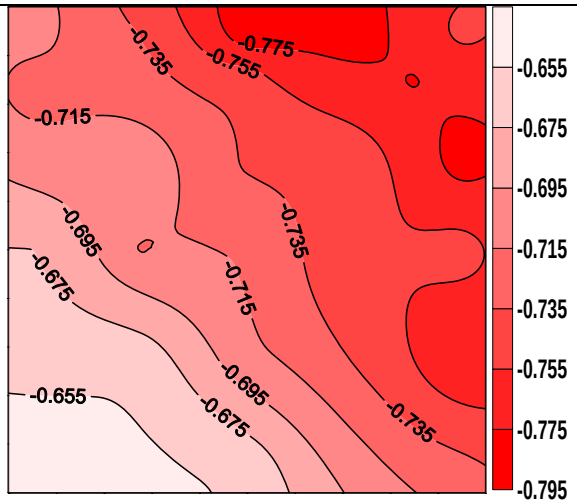

Figure 2A.18 Pressure coefficient contours on the side face of the building surrounded by impermeable sheet all around when θ= 0°

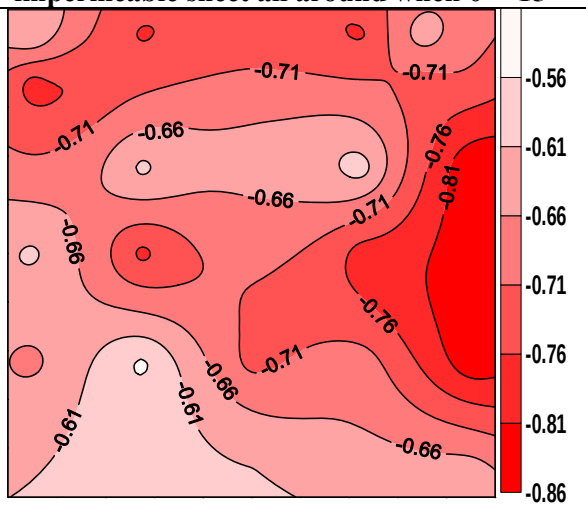

Figure 2A.19 Pressure coefficient contours on the side face of the SEB surrounded by impermeable sheet all around when θ=+15°

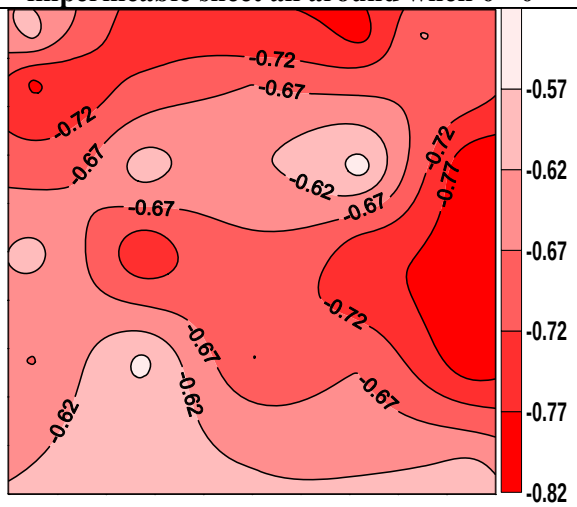

Figure 2A.20 Pressure coefficient contours on the side face of the SEB surrounded by impermeable sheet all around when θ=+30°

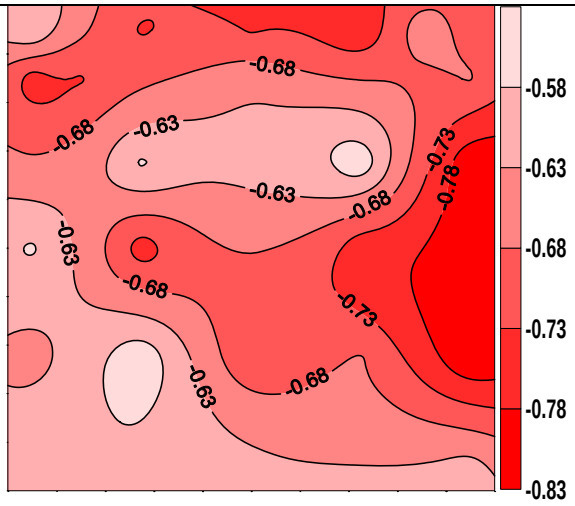

Figure 2A.21 Pressure coefficient contours on the side face of the SEB surrounded by impermeable sheet all around when θ=+45°

Pressure Coefficient Contours on Leeward Face of SEB for Type A Terrain

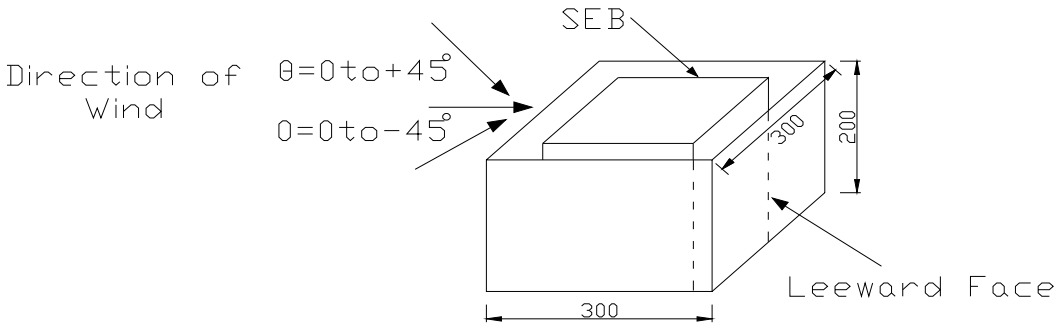

Figure 2A.22 Angle of attack of wind on windward wall of SEB, direction of which varies from -45° to +45°

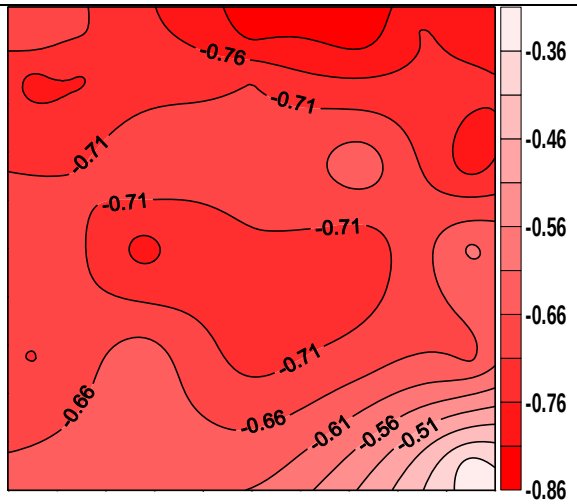

Figure 2A.23 Pressure coefficient contours on the leeward face of the SEB surrounded by impermeable sheet all around when θ= -45°

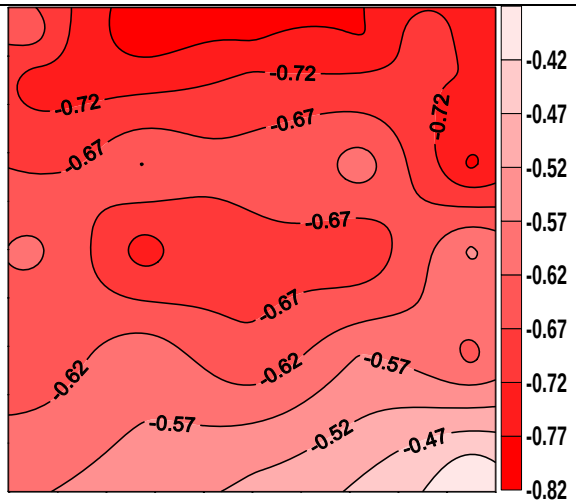

Figure 2A.24 Pressure coefficient contours on the leeward face of the SEB surrounded by impermeable sheet all around when θ= -30°

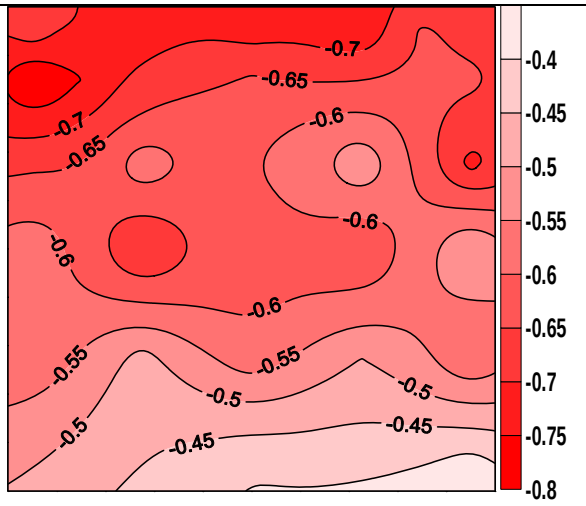

Figure 2A.25 Pressure coefficient contours on the leeward face of the SEB surrounded by impermeable sheet all around when θ= -15°

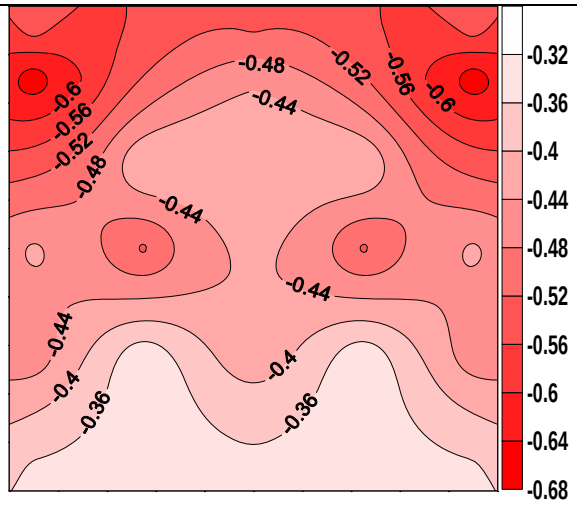

Figure 2A.26 Pressure coefficient contours on the leeward face of the SEB surrounded by impermeable sheet all around when θ= 0°

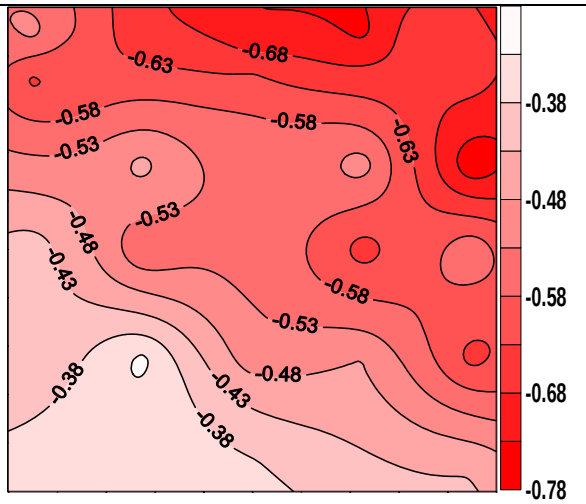

Figure 2A.27 Pressure coefficient contours on the leeward face of the SEB surrounded by impermeable sheet all around when θ= +15°

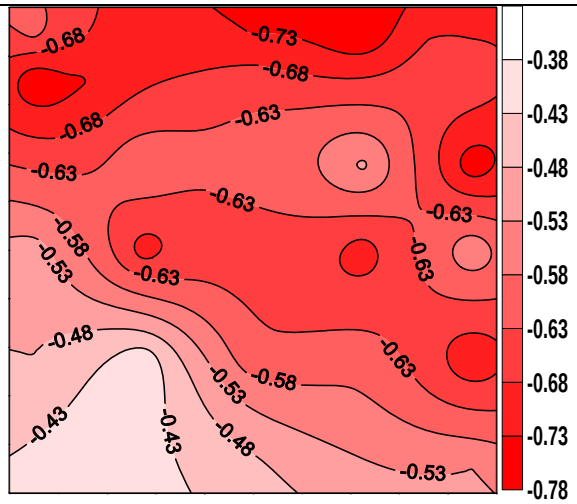

Figure 2A.28 Pressure coefficient contours on the leeward face of the SEB surrounded by impermeable sheet all around when θ= +30°

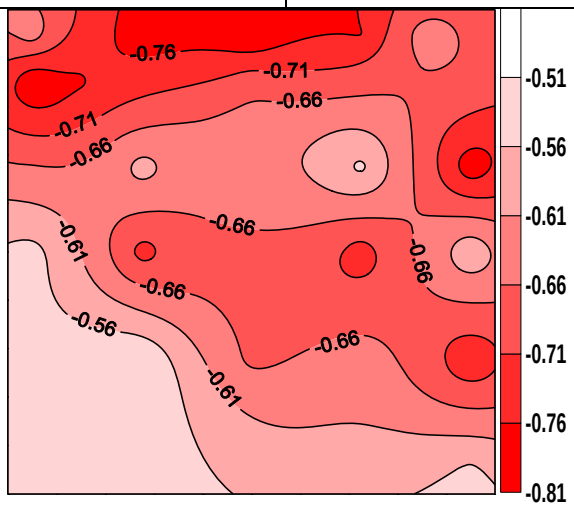

Figure 2A.29 Pressure coefficient contours on the leeward face of the SEB surrounded by impermeable sheet all around when θ= +45°

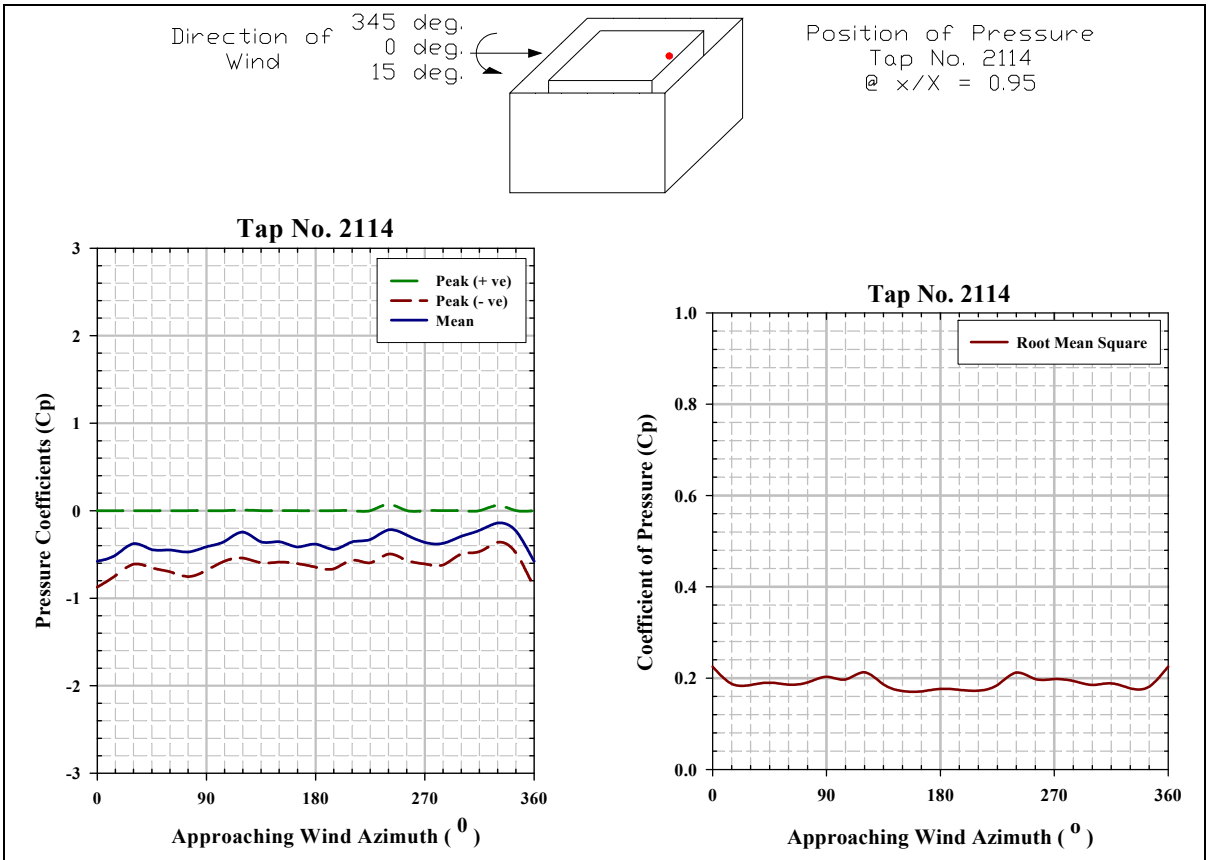

Figure 2A.30 Mean, peak and rms pressure coefficients for the tap number 2114

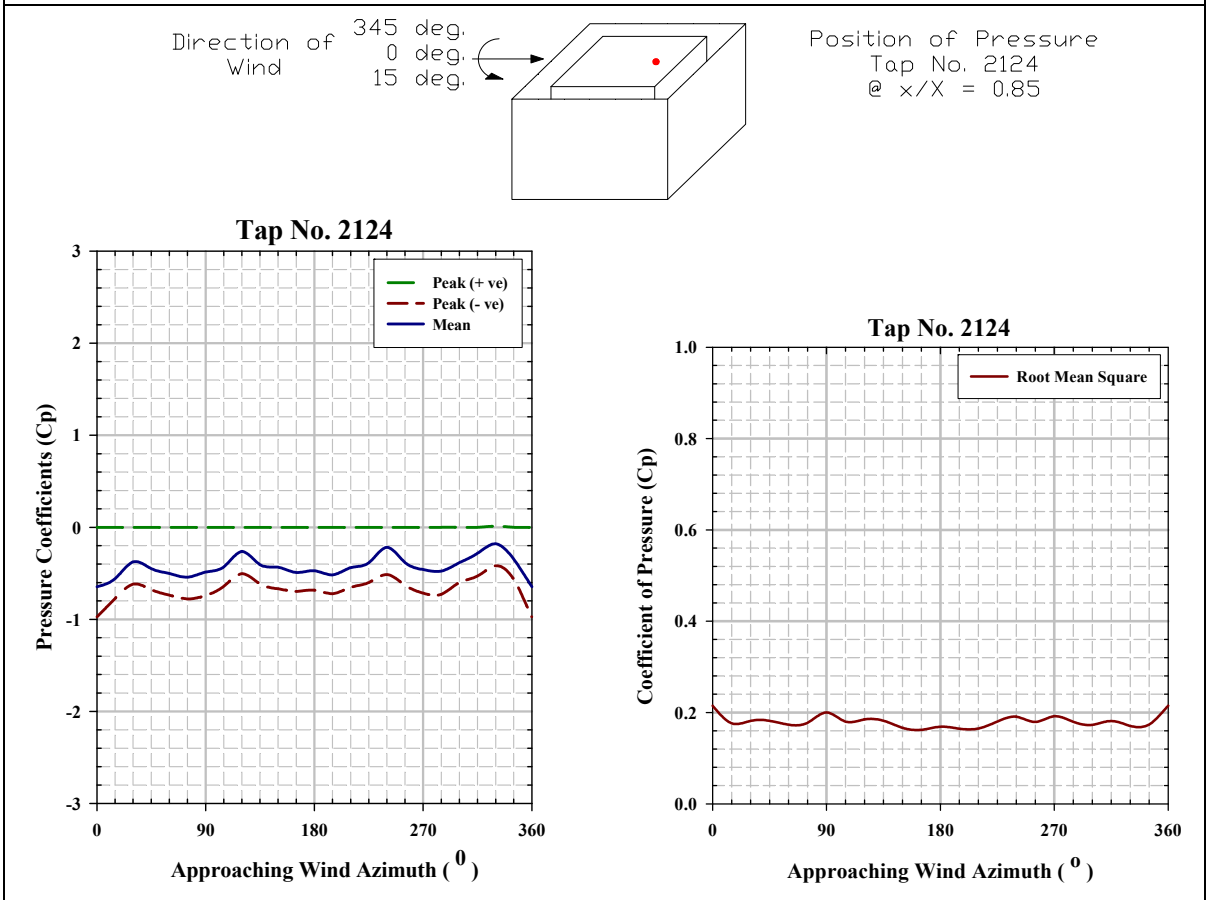

Figure 2A.31 Mean, peak and rms pressure coefficients for the tap number 2124

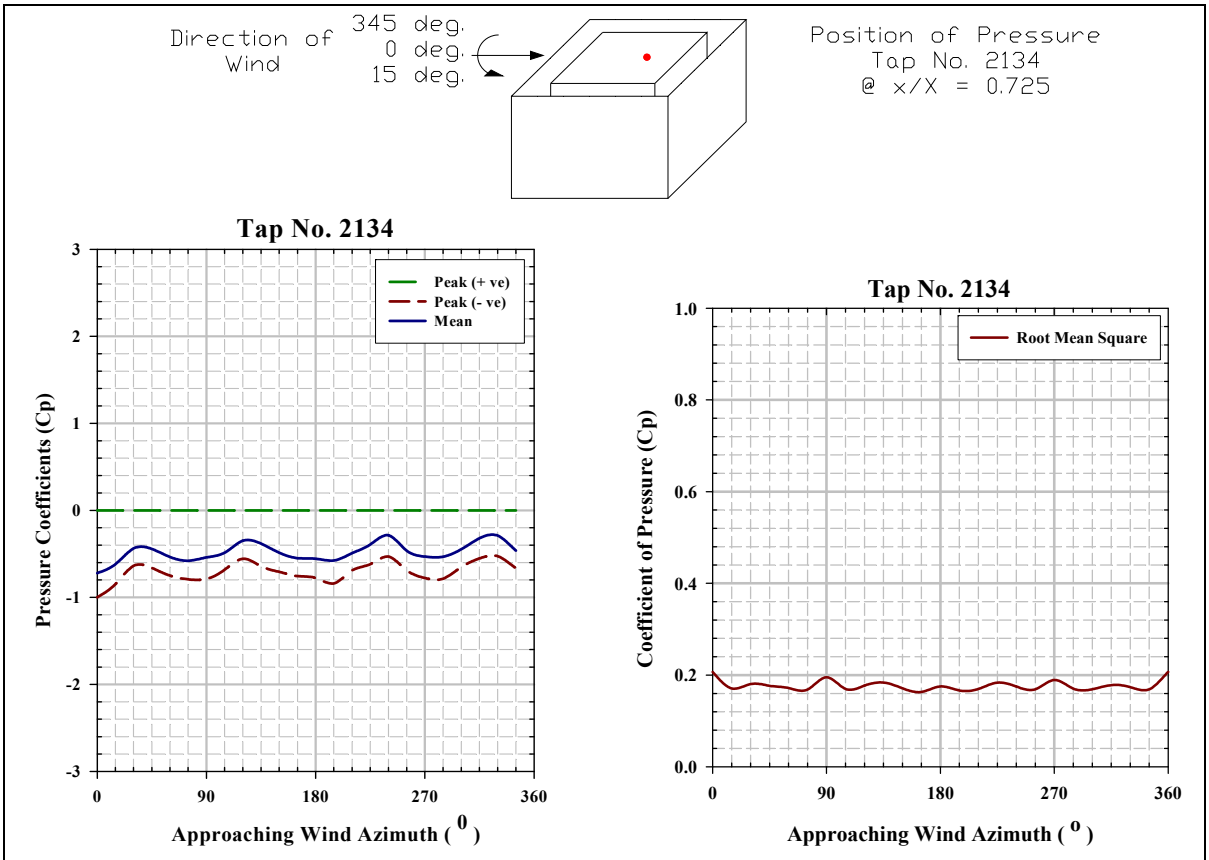

Figure 2A.32 Mean, peak and rms pressure coefficients for the tap number 2134

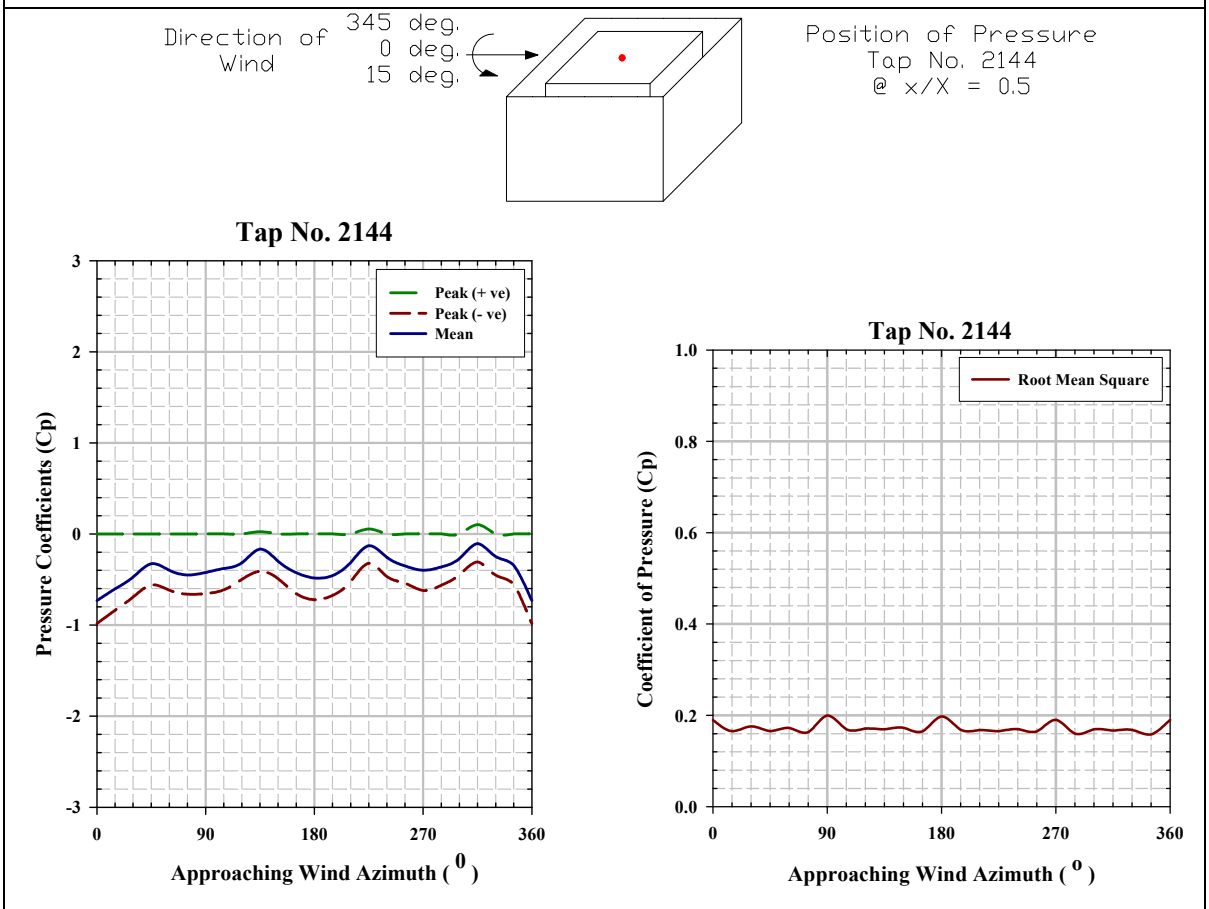

Figure 2A.33 Mean, peak and rms pressure coefficients for the tap number 2144

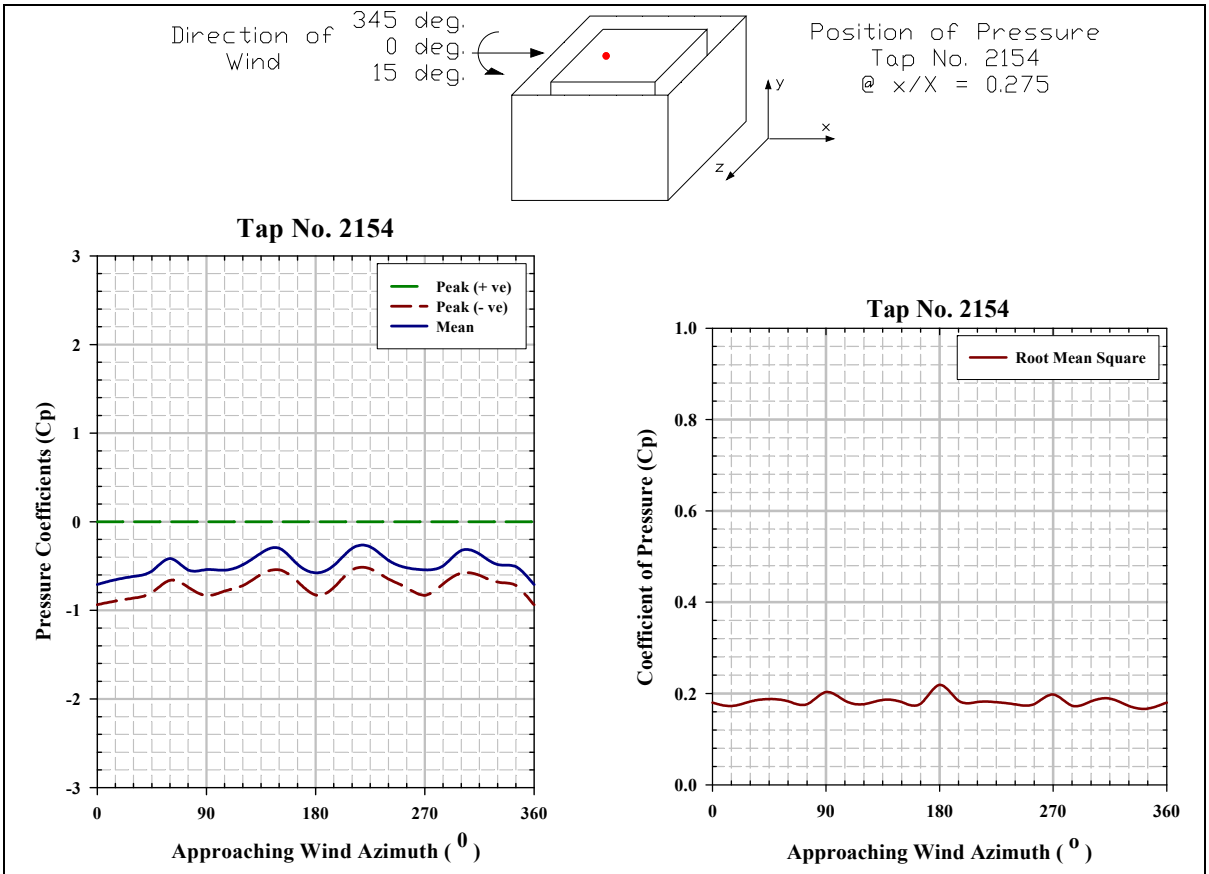

Figure 2A.34 Mean, peak and rms pressure coefficients for the tap number 2154

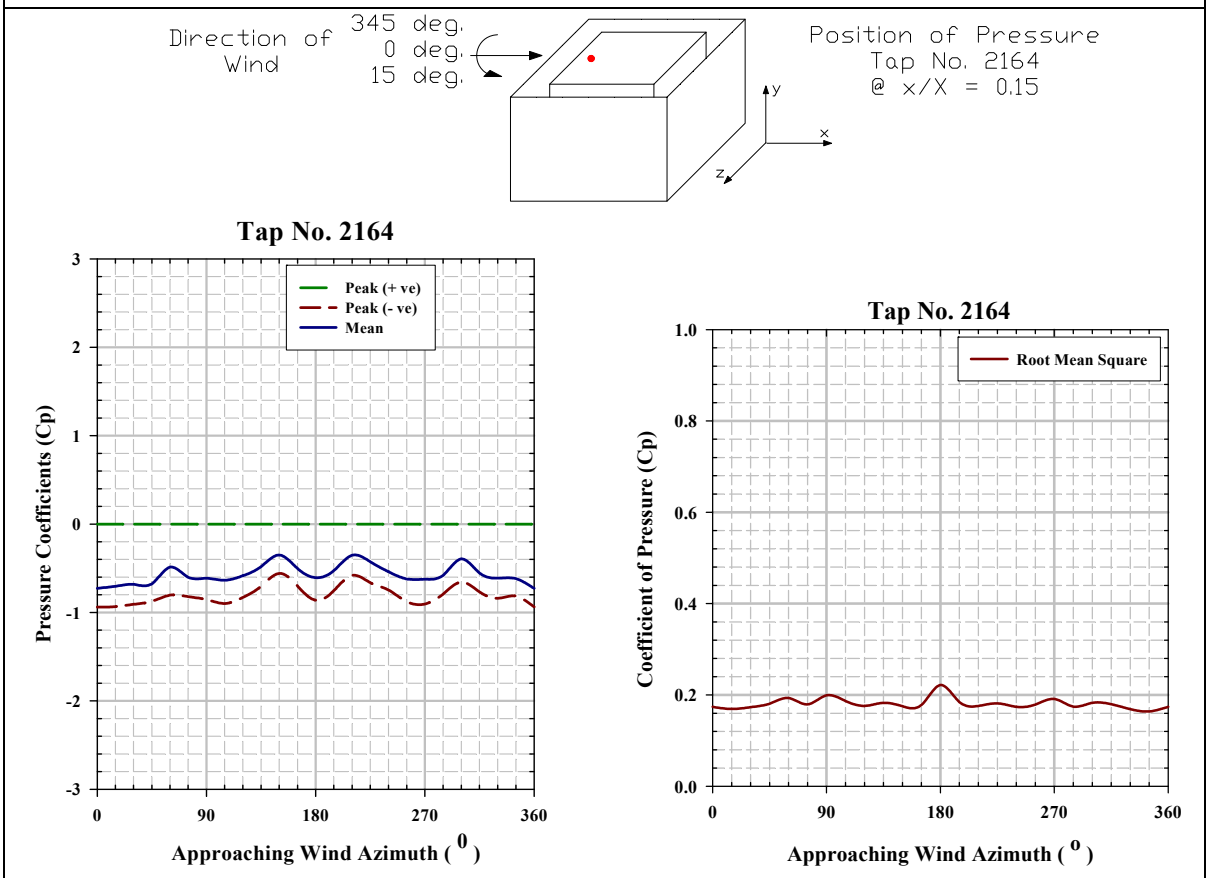

Figure 2A.35 Mean, peak and rms pressure coefficients for the tap number 2164

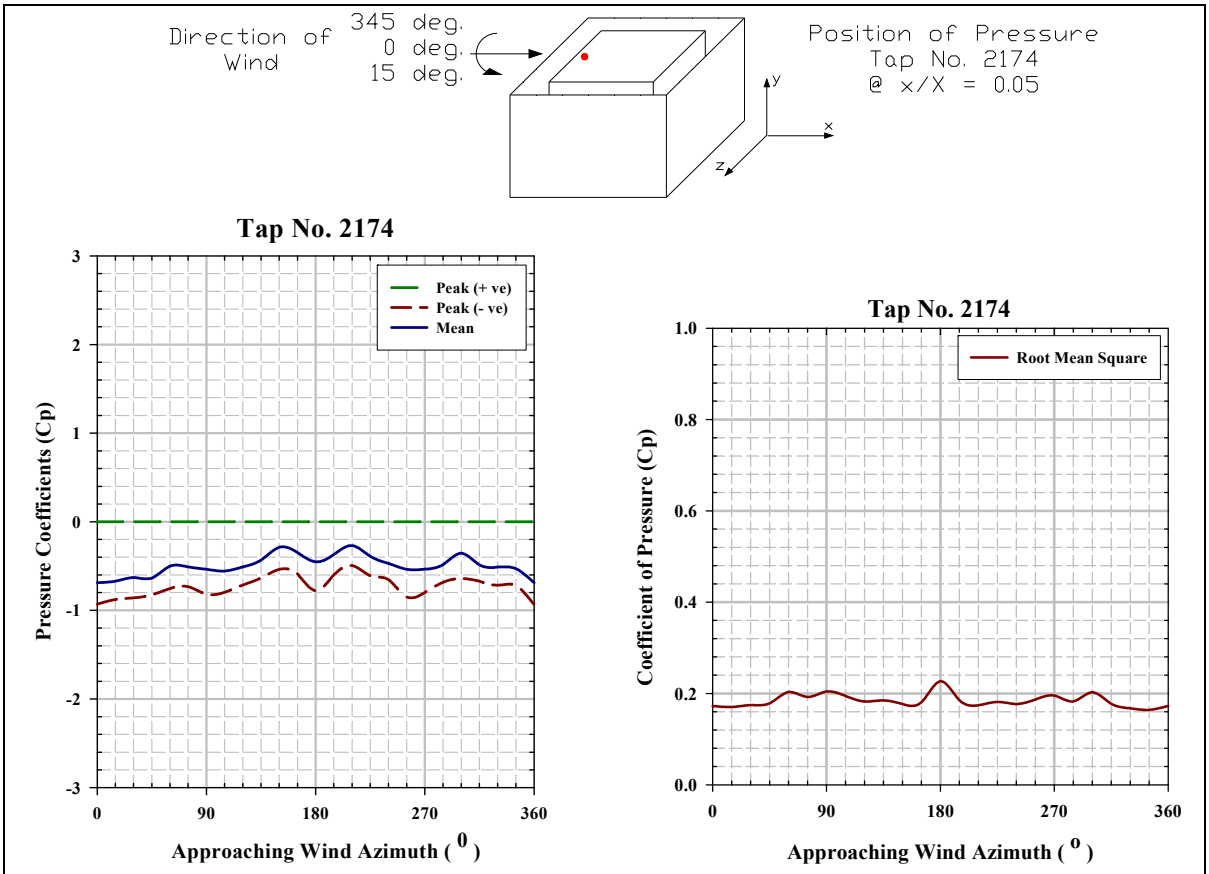

Figure 2A.36 Mean, peak and rms pressure coefficients for the tap number 2174

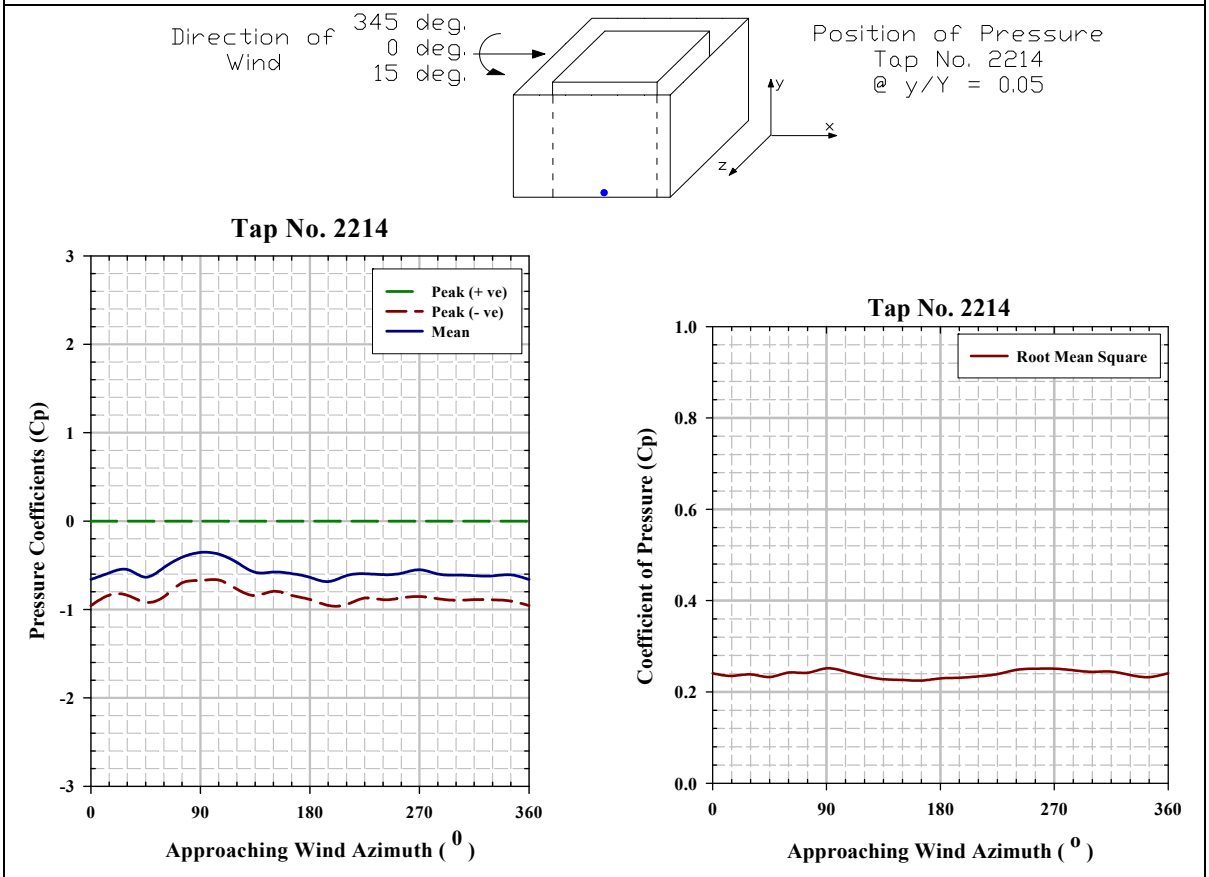

Figure 2A.37 Mean, peak and rms pressure coefficients for the tap number 2214

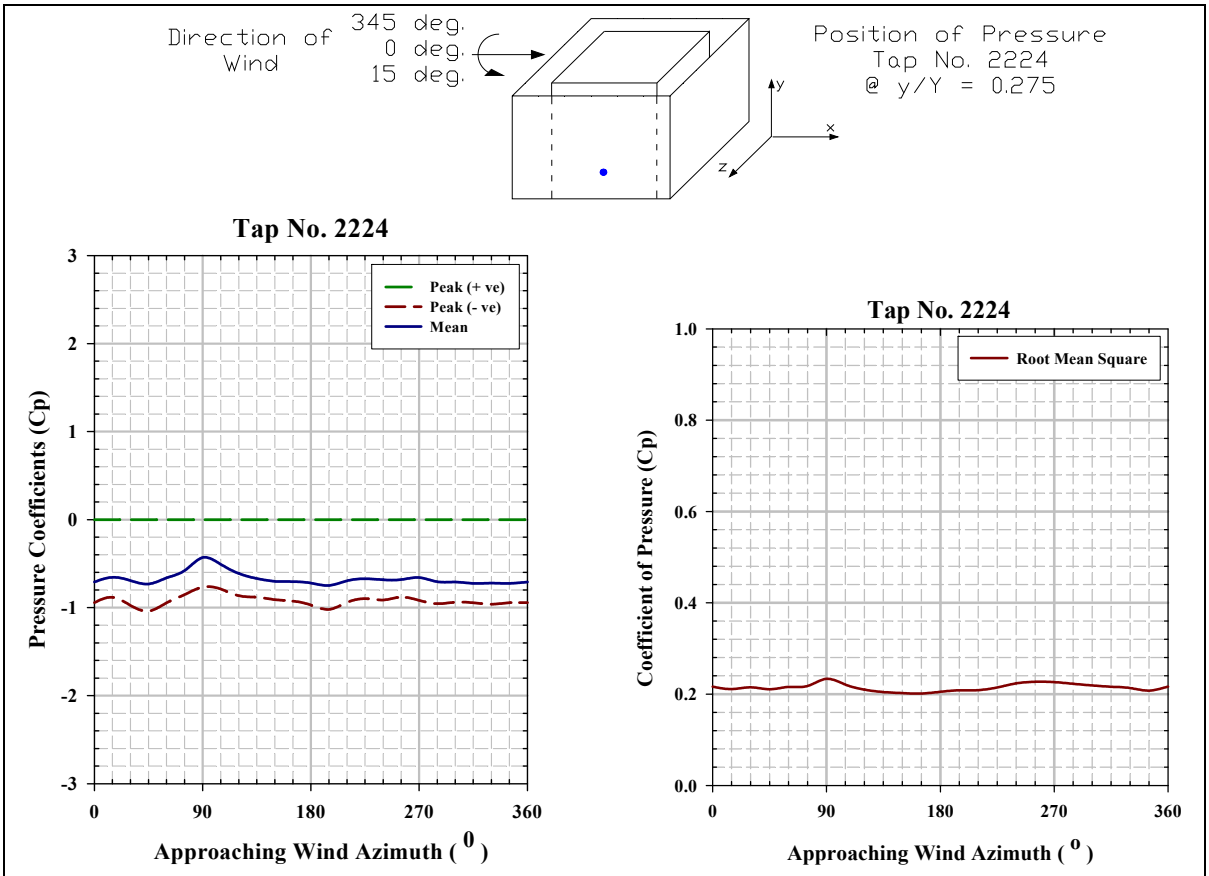

Figure 2A.38 Mean, peak and rms pressure coefficients for the tap number 2224

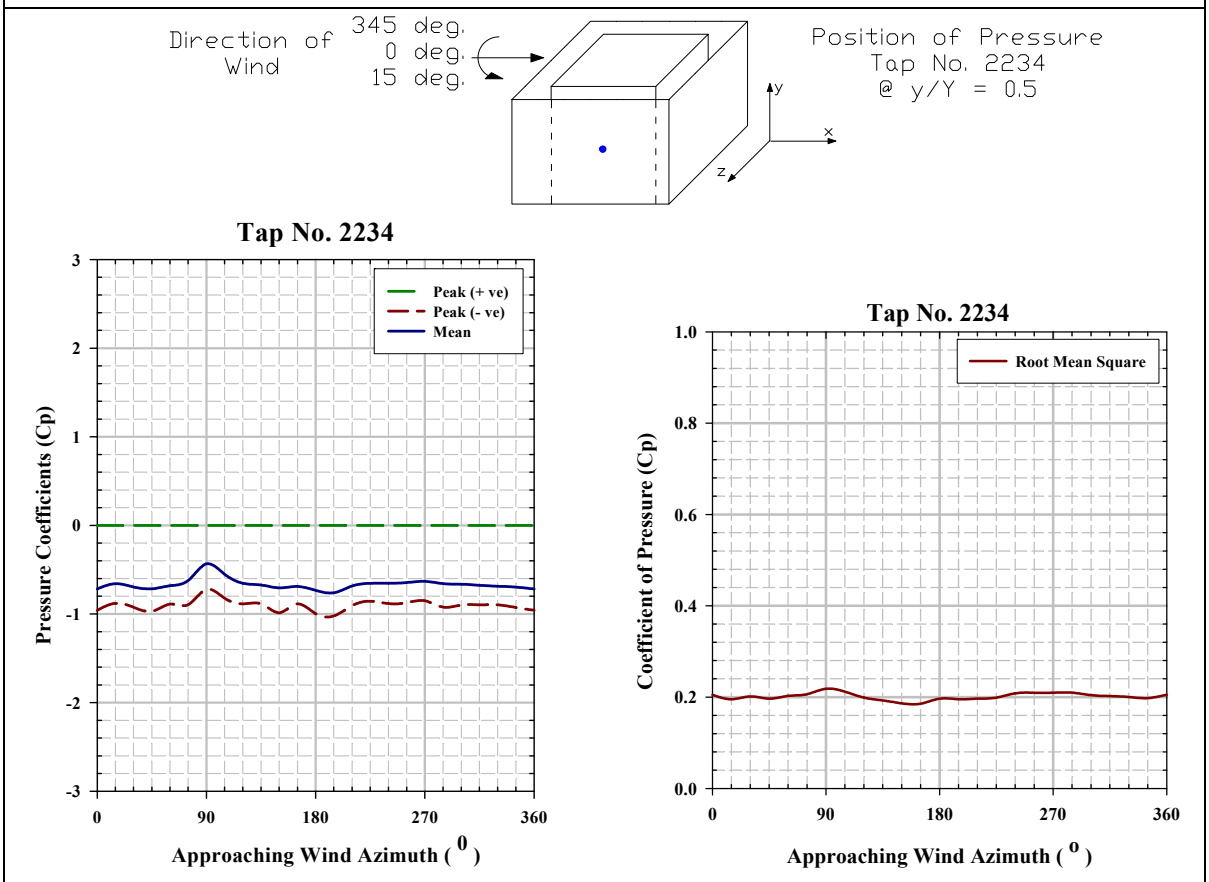

Figure 2A.39 Mean, peak and rms pressure coefficients for the tap number 2234

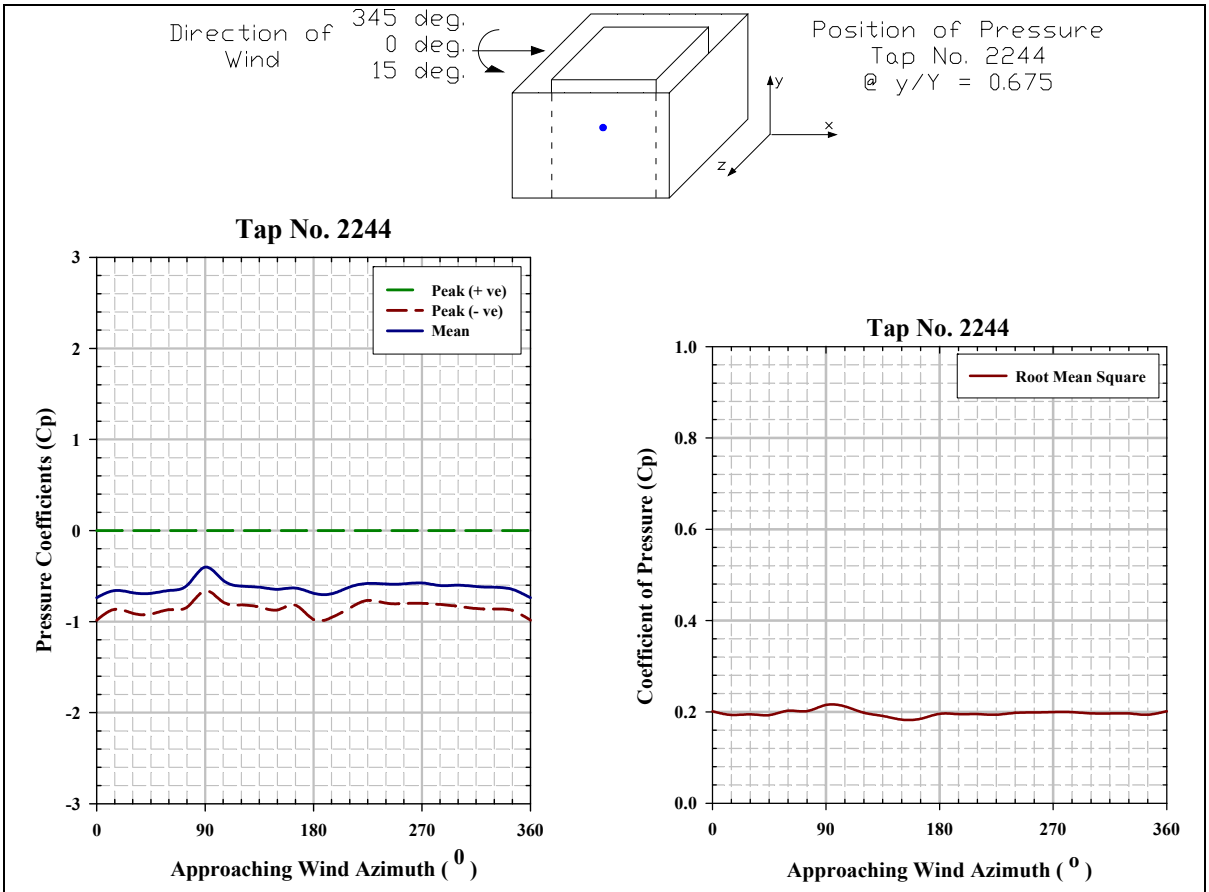

Figure 2A.40 Mean, peak and rms pressure coefficients for the tap number 2244

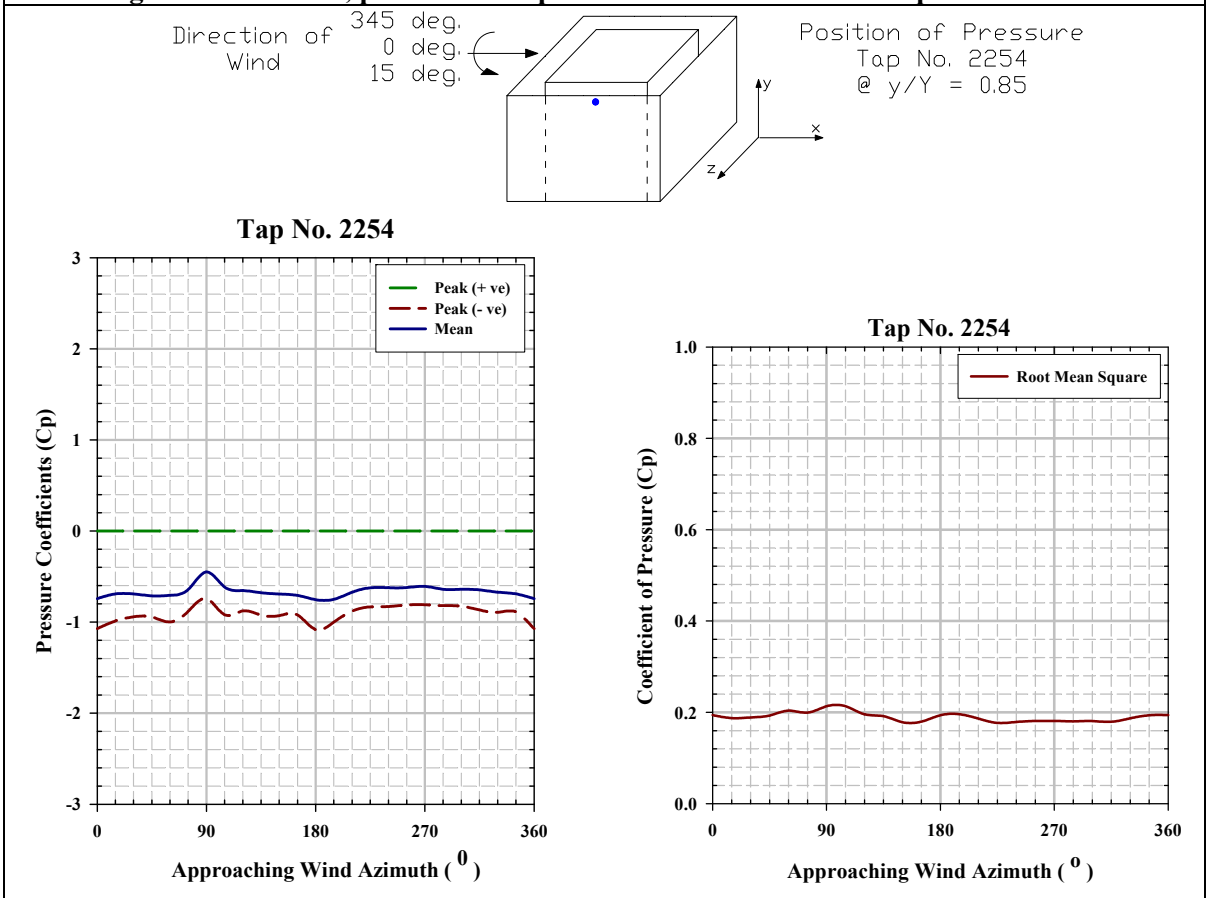

Figure 2A.41 Mean, peak and rms pressure coefficients for the tap number 2254

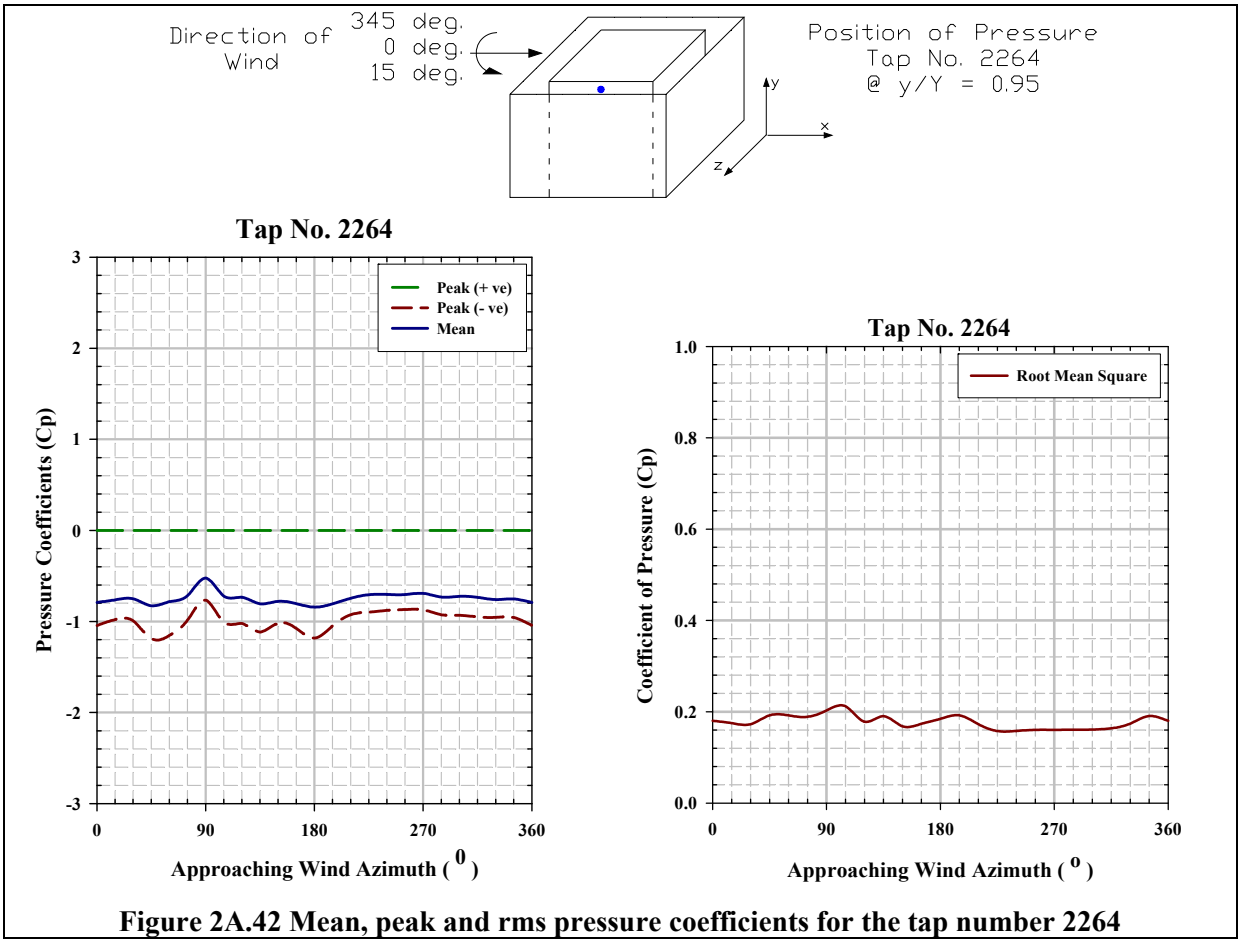

Figure 2A.42 Mean, peak and rms pressure coefficients for the tap number 2264

Pressure Coefficient Contours on Roof of SEB for Type B Terrain

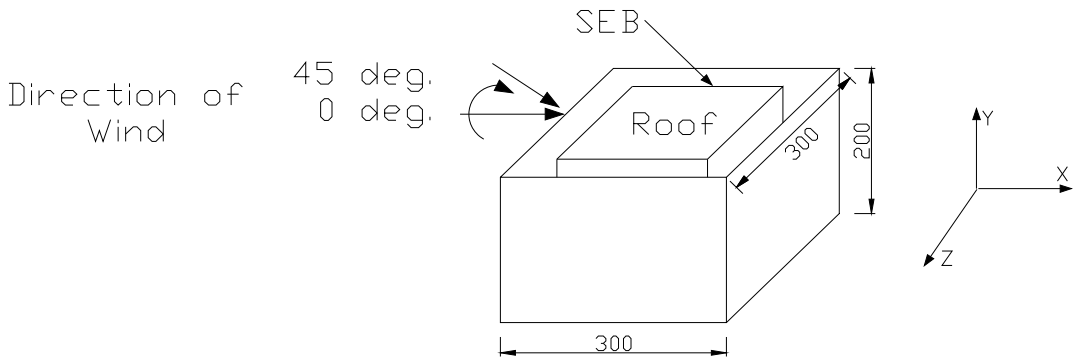

Figure 2B.1 Angle of attack of wind on roof of the SEB , direction of which varies from 0° to +45°

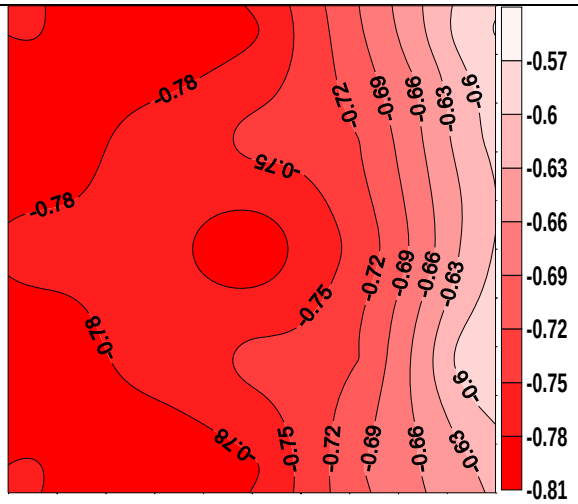

Figure 2B.2 Pressure coefficient contours on the roof of the SEB surrounded by impermeable sheet all around when θ= 0°

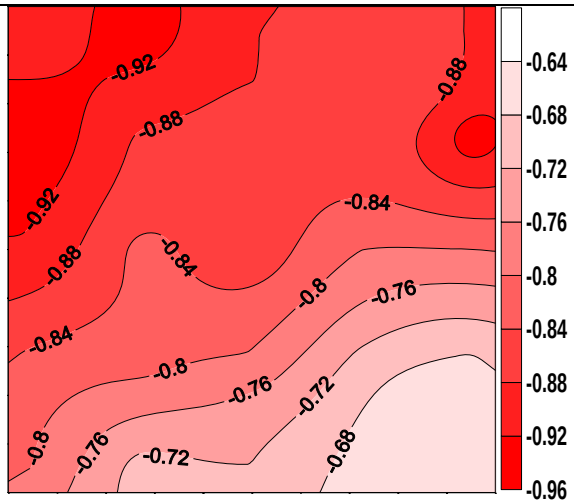

Figure 2B.3 Pressure coefficient contours on the roof of the SEB surrounded by impermeable sheet all around when θ= 15°

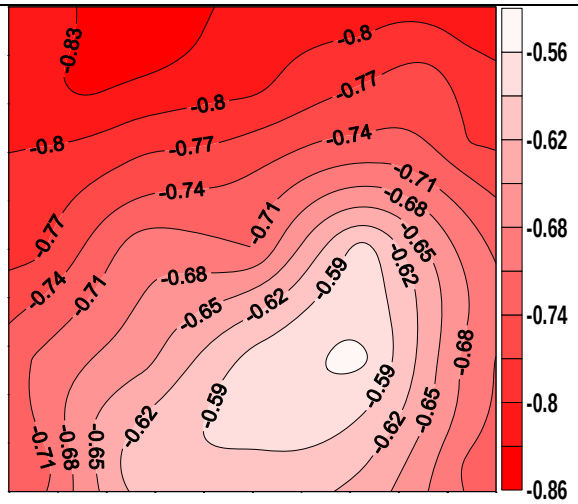

Figure 2B.4 Pressure coefficient contours on the roof of the SEB surrounded by impermeable sheet all around when θ= 30°

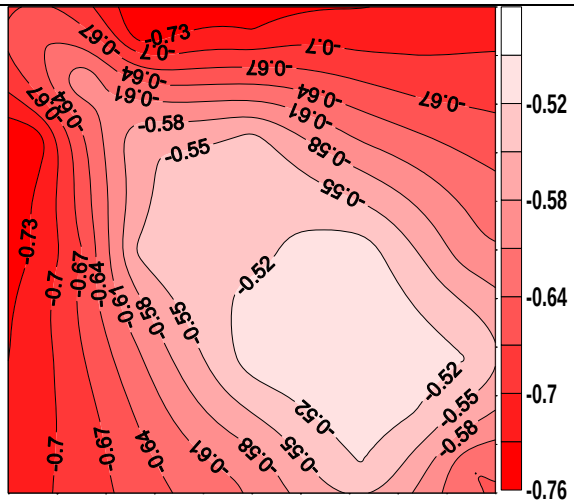

Figure 2B.5 Pressure coefficient contours on the roof of the SEB surrounded by impermeable sheet all around when θ= 45°

Pressure Coefficient Contours on Windward Face of SEB for Type B Terrain

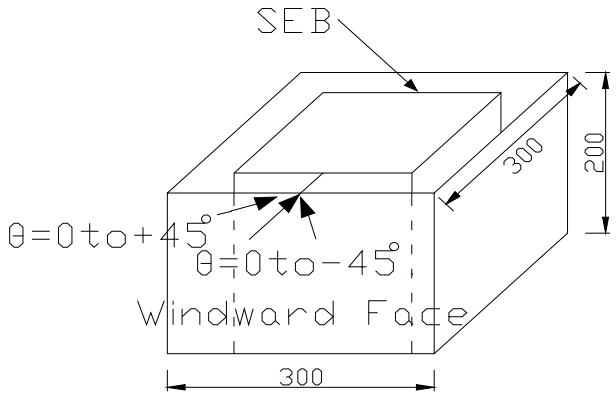

Figure 2B.6 Angle of attack of wind on windward wall of SEB, direction of which varies from -45° to +45°

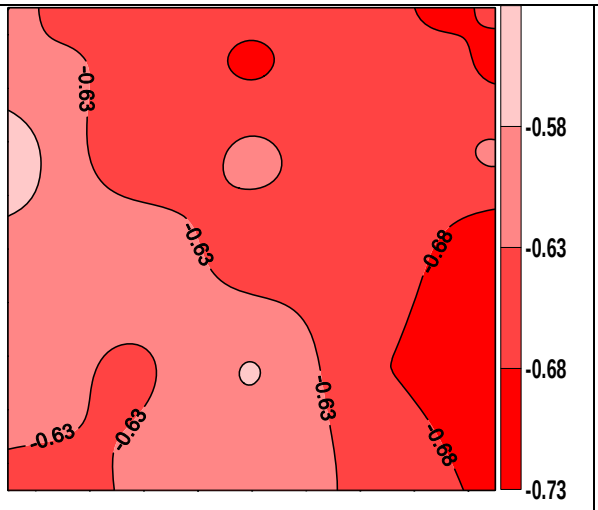

Figure 2B.7 Pressure coefficient contours on the windward face of the SEB surrounded by impermeable sheet all around when θ= -45°

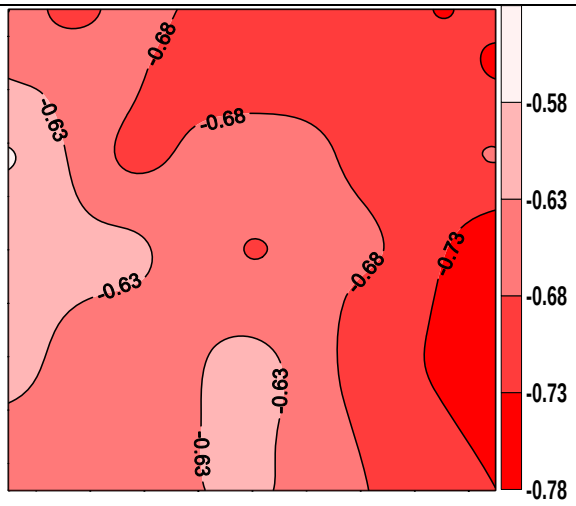

Figure 2B.8 Pressure coefficient contours on the windward face of the SEB surrounded by impermeable sheet all around when θ= -30°

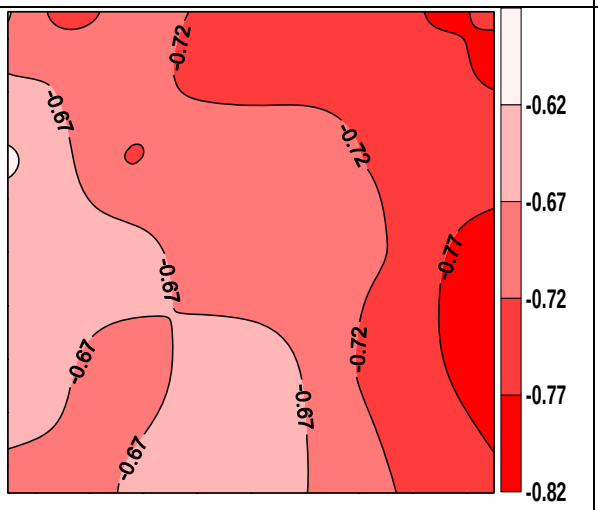

Figure 2B.9 Pressure coefficient contours on the windward face of the SEB surrounded by impermeable sheet all around when θ= -15°

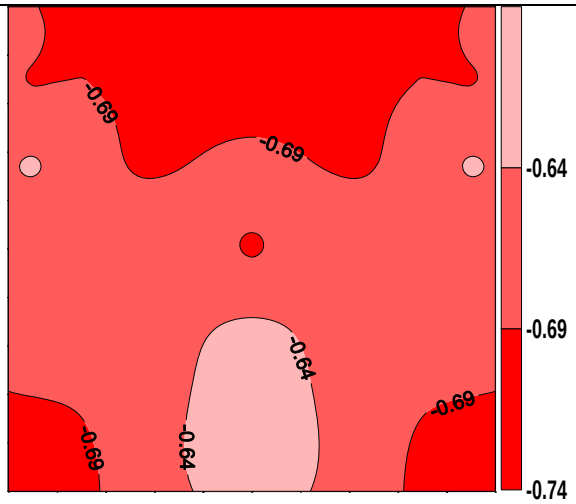

Figure 2B.10 Pressure coefficient contours on the windward face of the SEB surrounded by impermeable sheet all around when θ=0°

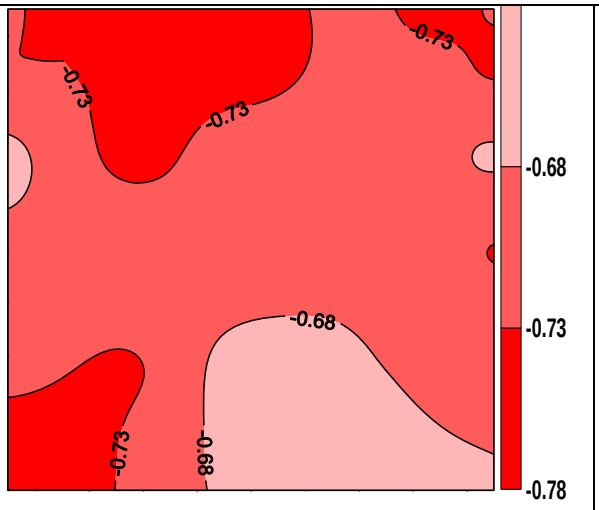

Figure 2B.11 Pressure coefficient contours on the windward face of the SEB surrounded by impermeable sheet all around when θ=+15°

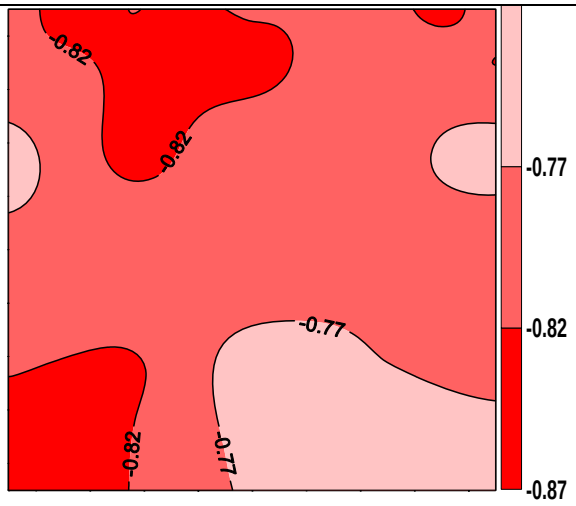

Figure 2B.12 Pressure coefficient contours on the windward face of the SEB surrounded by impermeable sheet all around when θ=+30°

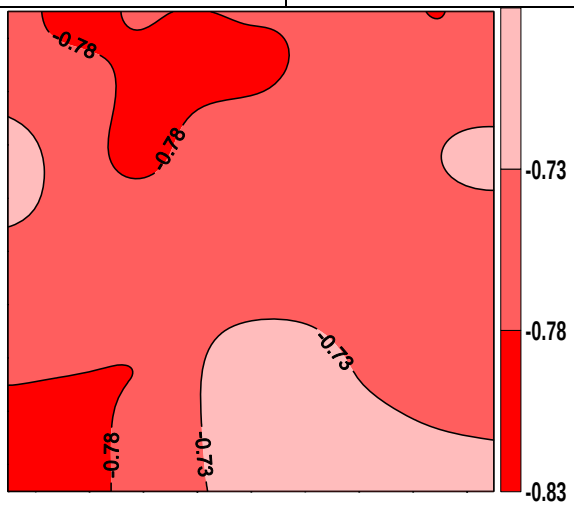

Figure 2B.13 Pressure coefficient contours on the windward face of the SEB surrounded by impermeable sheet all around when θ=+45°

Pressure Coefficient Contours on Side Face of SEB for Type B Terrain

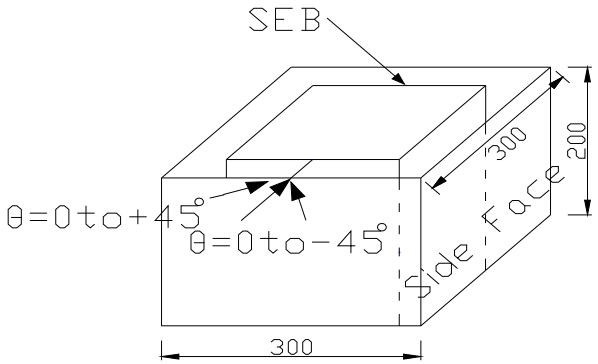

Figure 2B.14 Angle of attack of wind on windward wall of SEB, direction of which varies from -45° to +45°

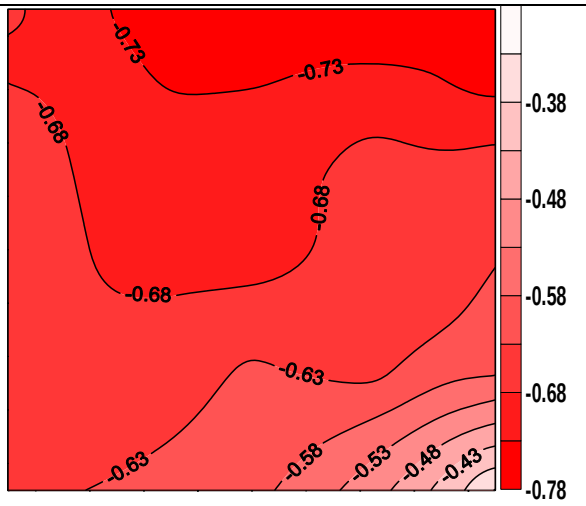

Figure 2B.15 Pressure coefficient contours on the side face of the SEB surrounded by impermeable sheet all around when θ= -45°

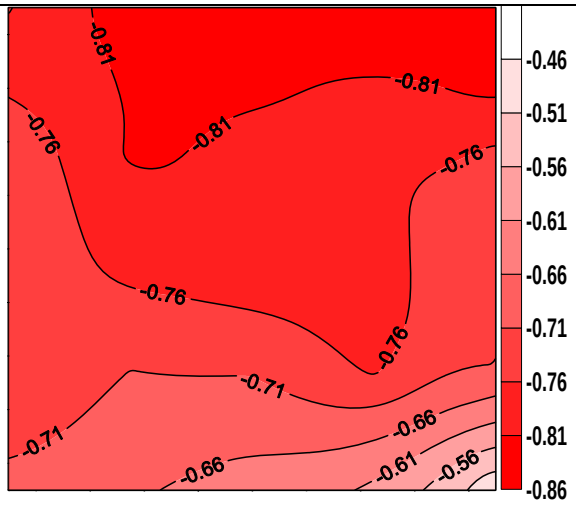

Figure 2B.16 Pressure coefficient contours on the side face of the SEB surrounded by impermeable sheet all around when θ= -30°

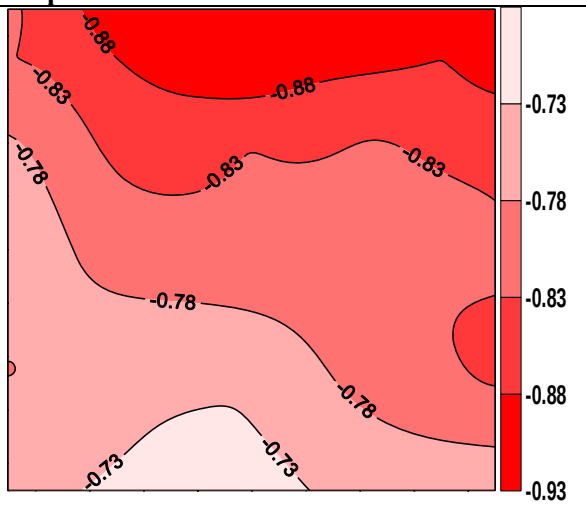

Figure 2B.17 Pressure coefficient contours on the side face of the SEB surrounded by impermeable sheet all around when θ= -15°

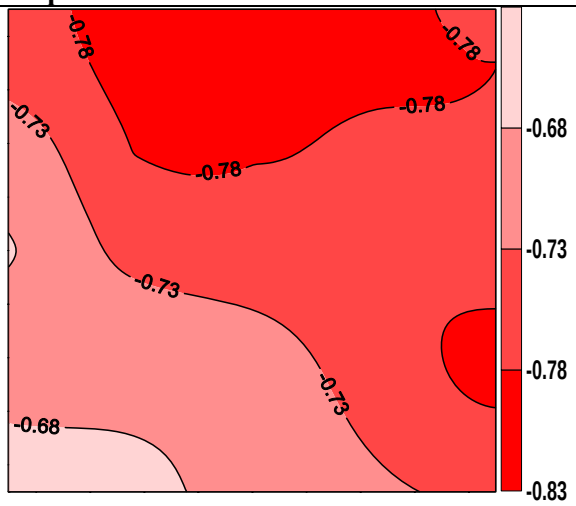

Figure 2B.18 Pressure coefficient contours on the side face of the SEB surrounded by impermeable sheet all around when θ= 0°

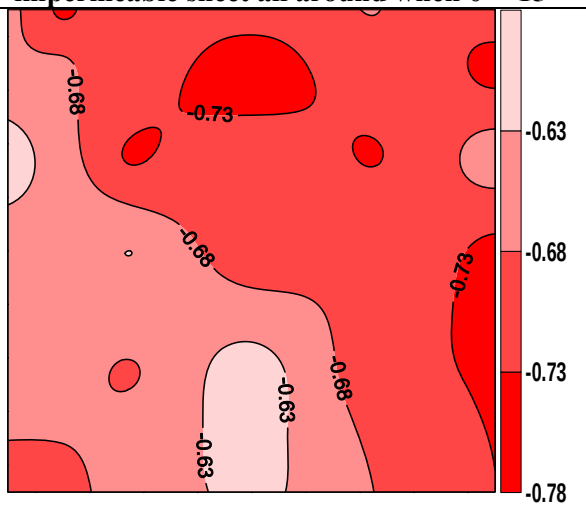

Figure 2B.19 Pressure coefficient contours on the side face of the SEB surrounded by impermeable sheet all around when θ=+15°

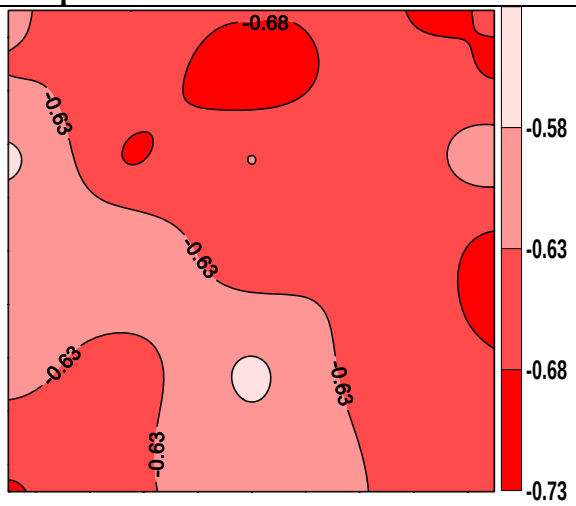

Figure 2B.20 Pressure coefficient contours on the side face of the SEB surrounded by impermeable sheet all around when θ=+30°

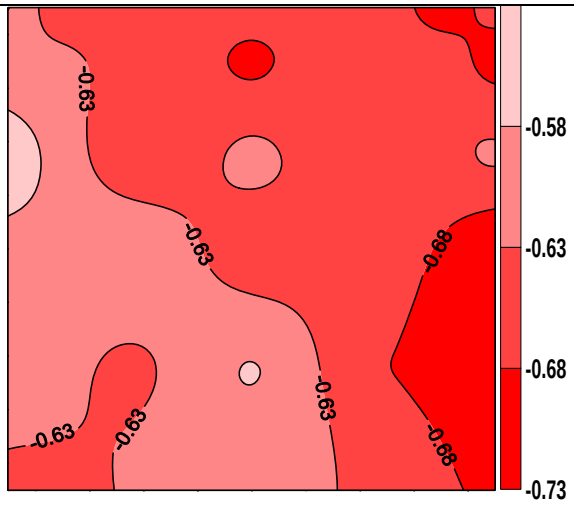

Figure 2B.21 Pressure coefficient contours on the side face of the SEB surrounded by impermeable sheet all around when θ=+45°

Pressure Coefficient Contours on Leeward Face of SEB for Type B Terrain

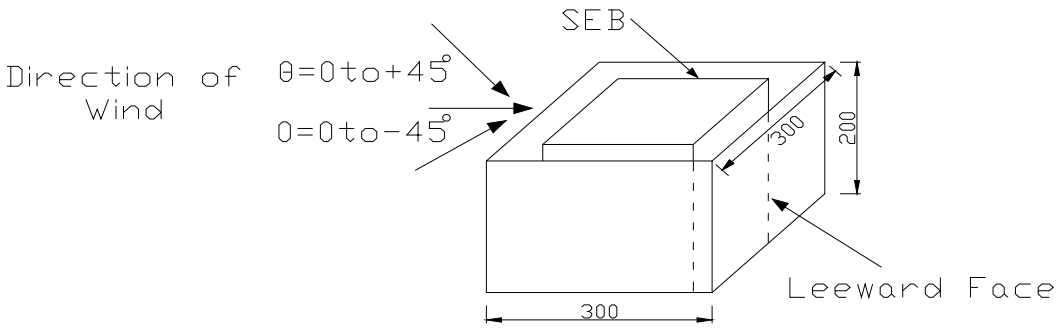

Figure 2B.22 Angle of attack of wind on windward wall of SEB, direction of which varies from -45° to +45°

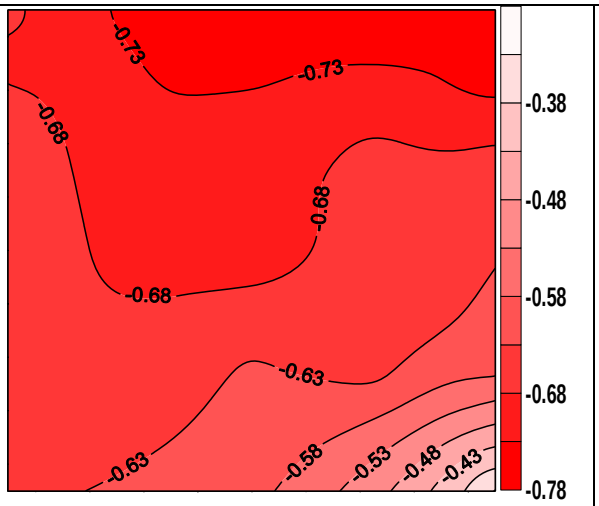

Figure 2B.23 Pressure coefficient contours on the leeward face of the SEB surrounded by impermeable sheet all around when θ= -45°

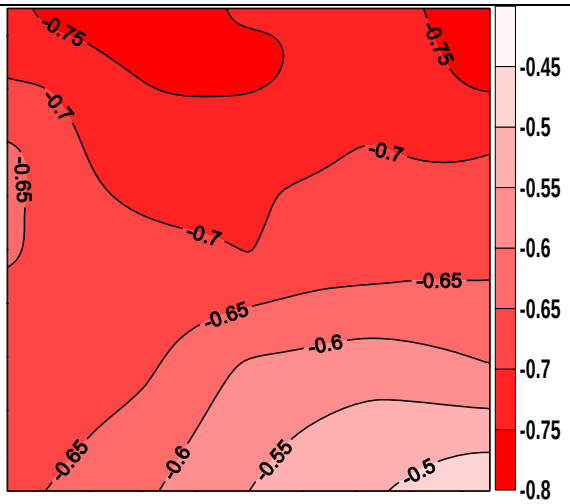

Figure 2B.24 Pressure coefficient contours on the leeward face of the SEB surrounded by impermeable sheet all around when θ= -30°

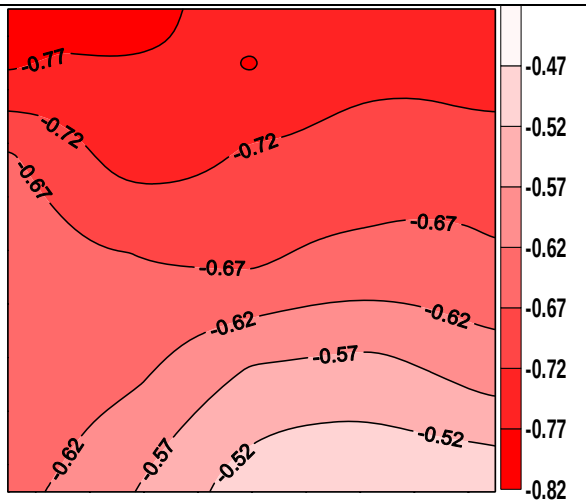

Figure 2B.25 Pressure coefficient contours on the leeward face of the SEB surrounded by impermeable sheet all around when θ= -15°

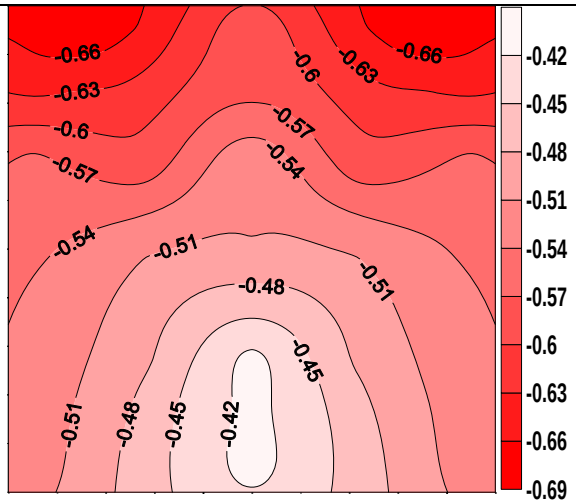

Figure 2B.26 Pressure coefficient contours on the leeward face of the SEB surrounded by impermeable sheet all around when θ= 0°

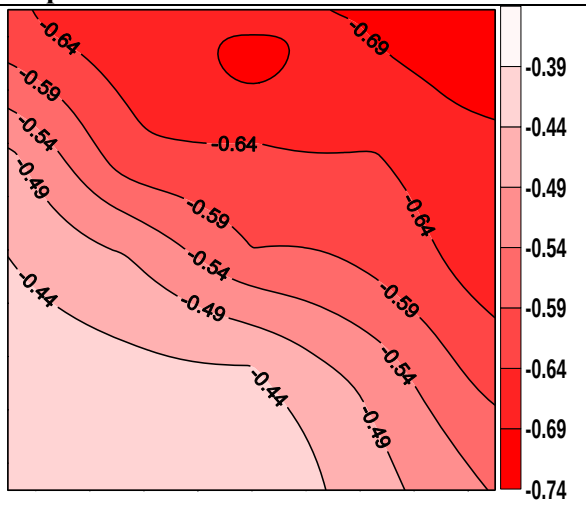

Figure 2B.27 Pressure coefficient contours on the leeward face of the SEB surrounded by impermeable sheet all around when θ= +15°

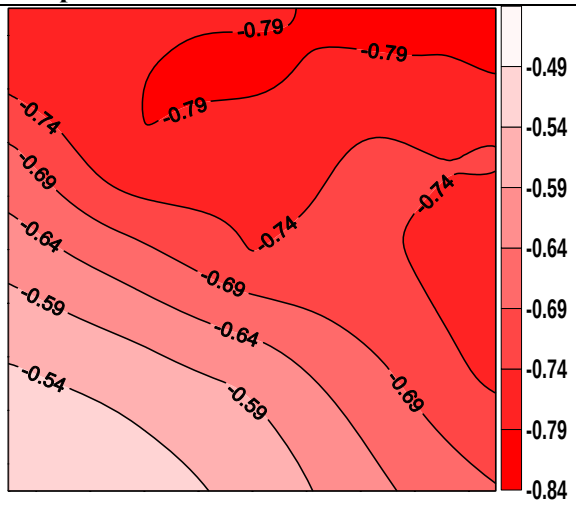

Figure 2B.28 Pressure coefficient contours on the leeward face of the SEB surrounded by impermeable sheet all around when θ= +30°

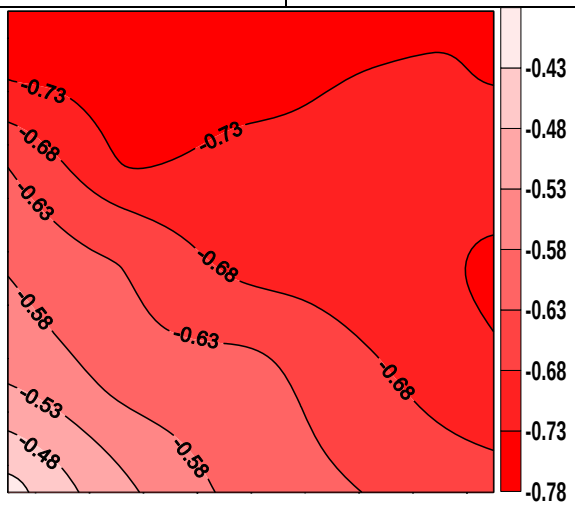

Figure 2B.29 Pressure coefficient contours on the leeward face of the SEB surrounded by impermeable sheet all around when θ= +45°

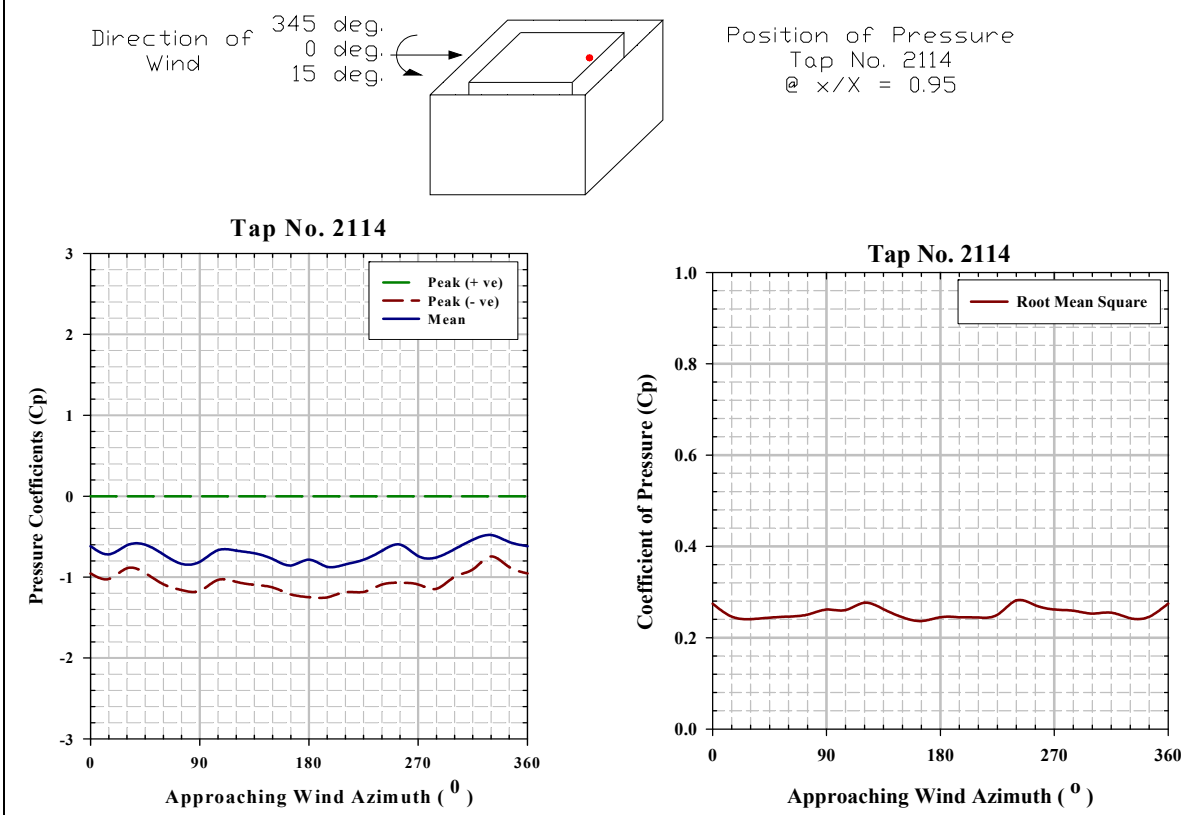

Figure 2B.30 Mean, peak and rms pressure coefficients for the tap number 2114

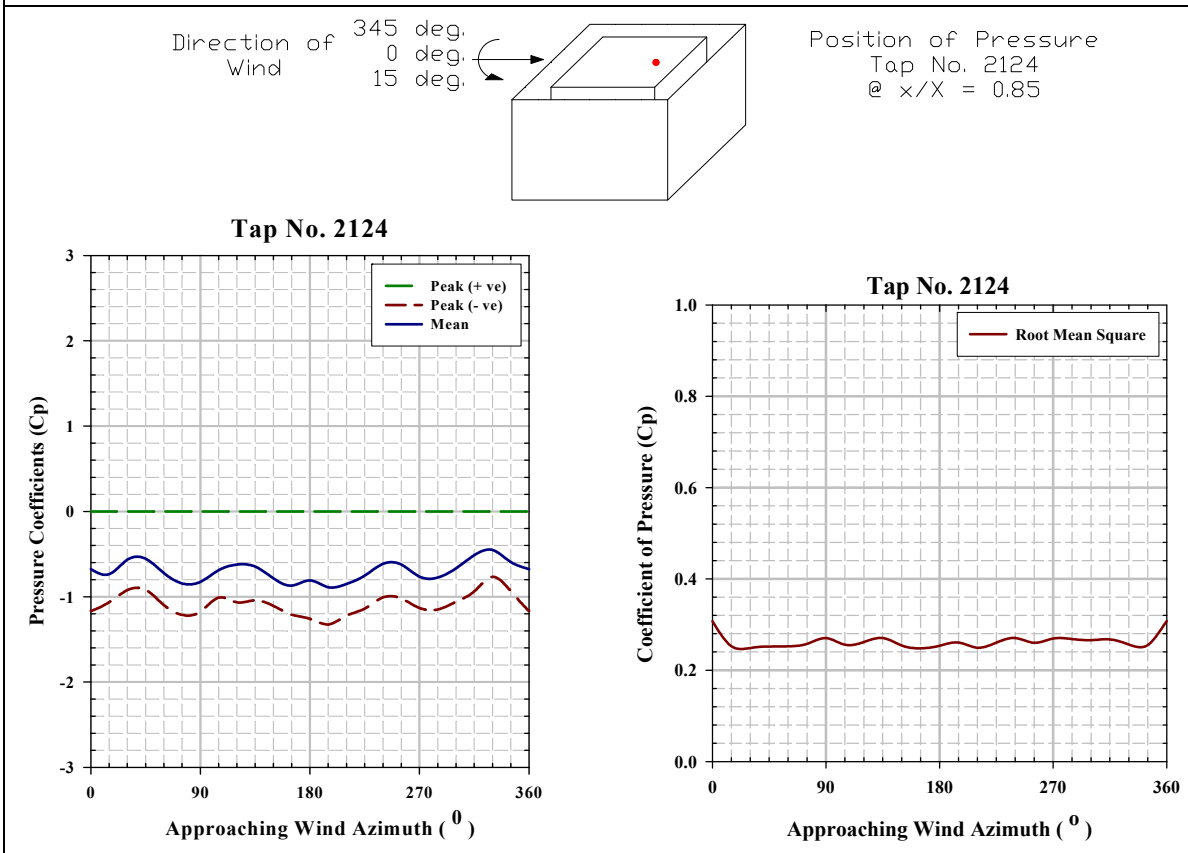

Figure 2B.31 Mean, peak and rms pressure coefficients for the tap number 2124

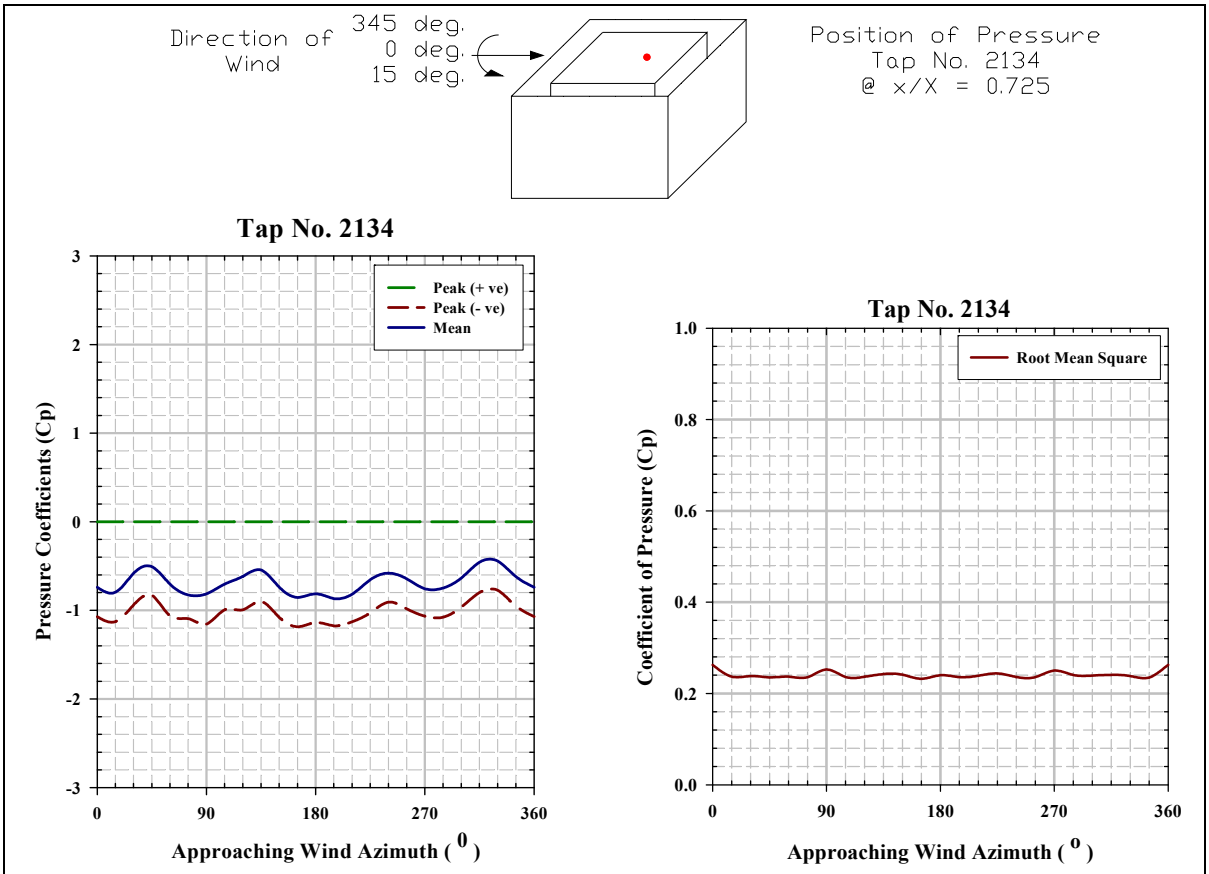

Figure 2B.32 Mean, peak and rms pressure coefficients for the tap number 2134

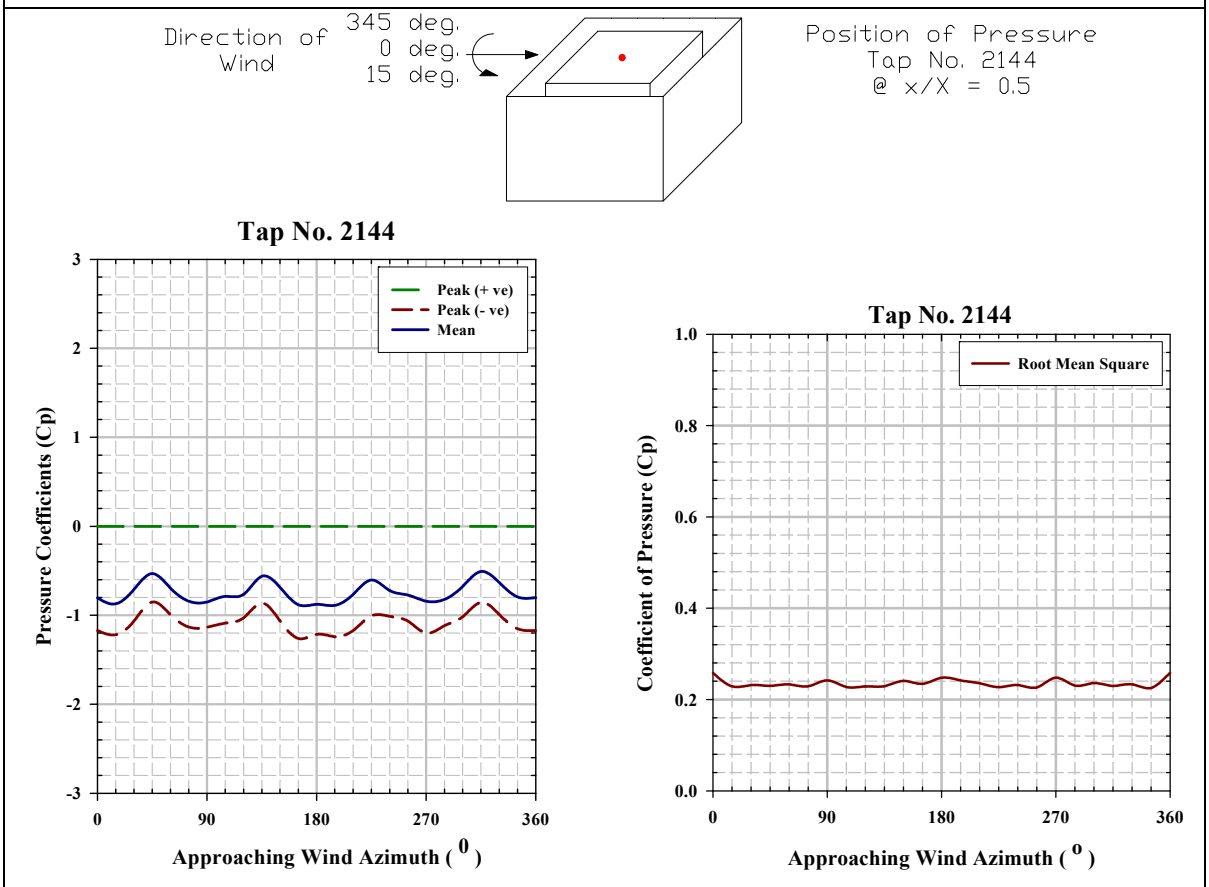

Figure 2B.33 Mean, peak and rms pressure coefficients for the tap number 2144

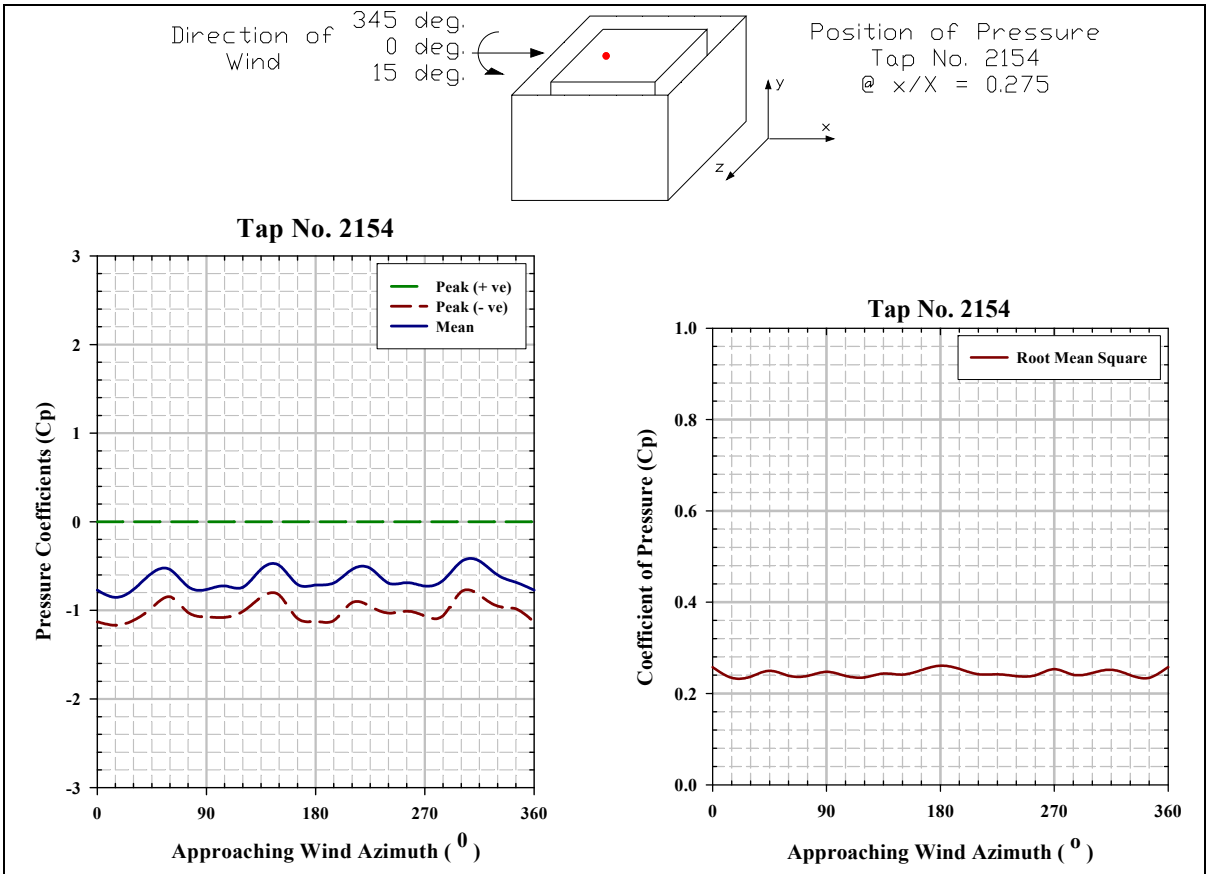

Figure 2B.34 Mean, peak and rms pressure coefficients for the tap number 2154

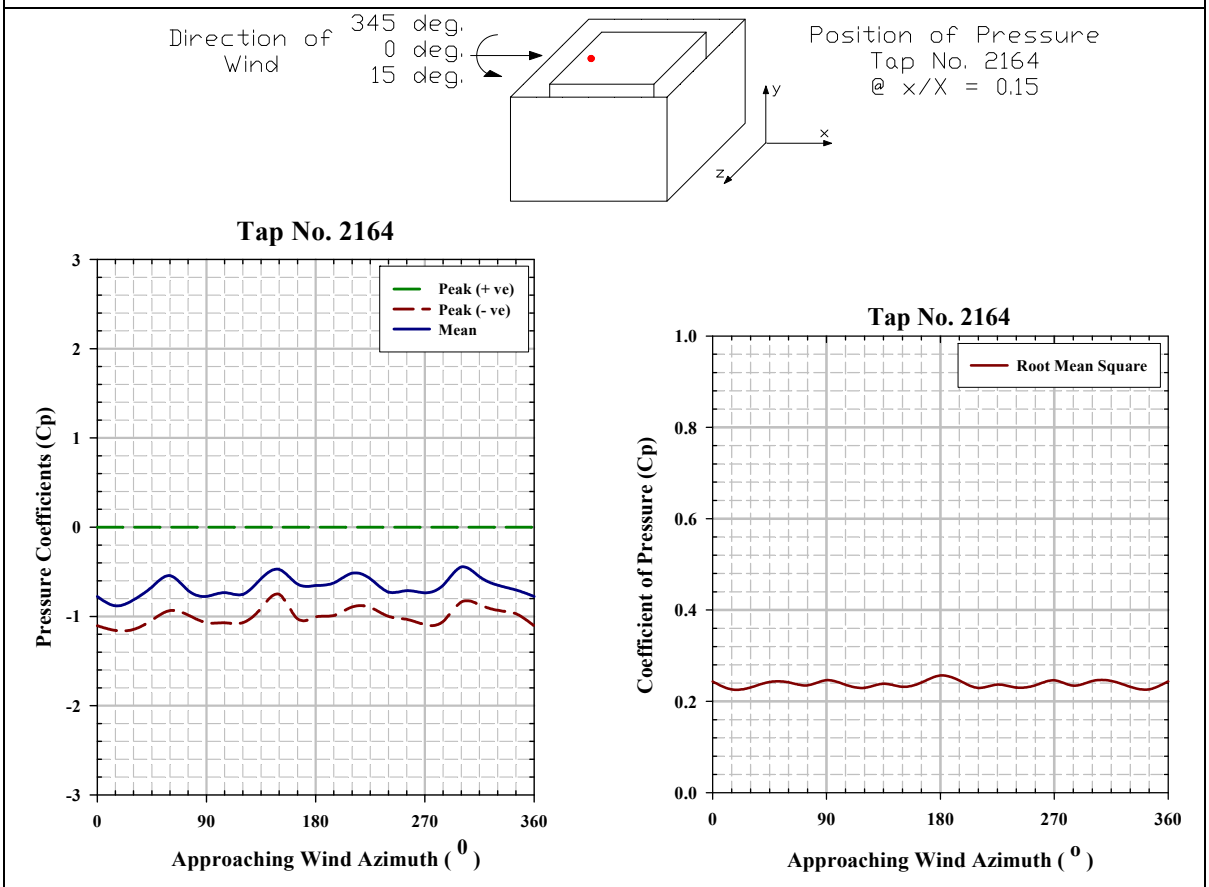

Figure 2B.35 Mean, peak and rms pressure coefficients for the tap number 2164

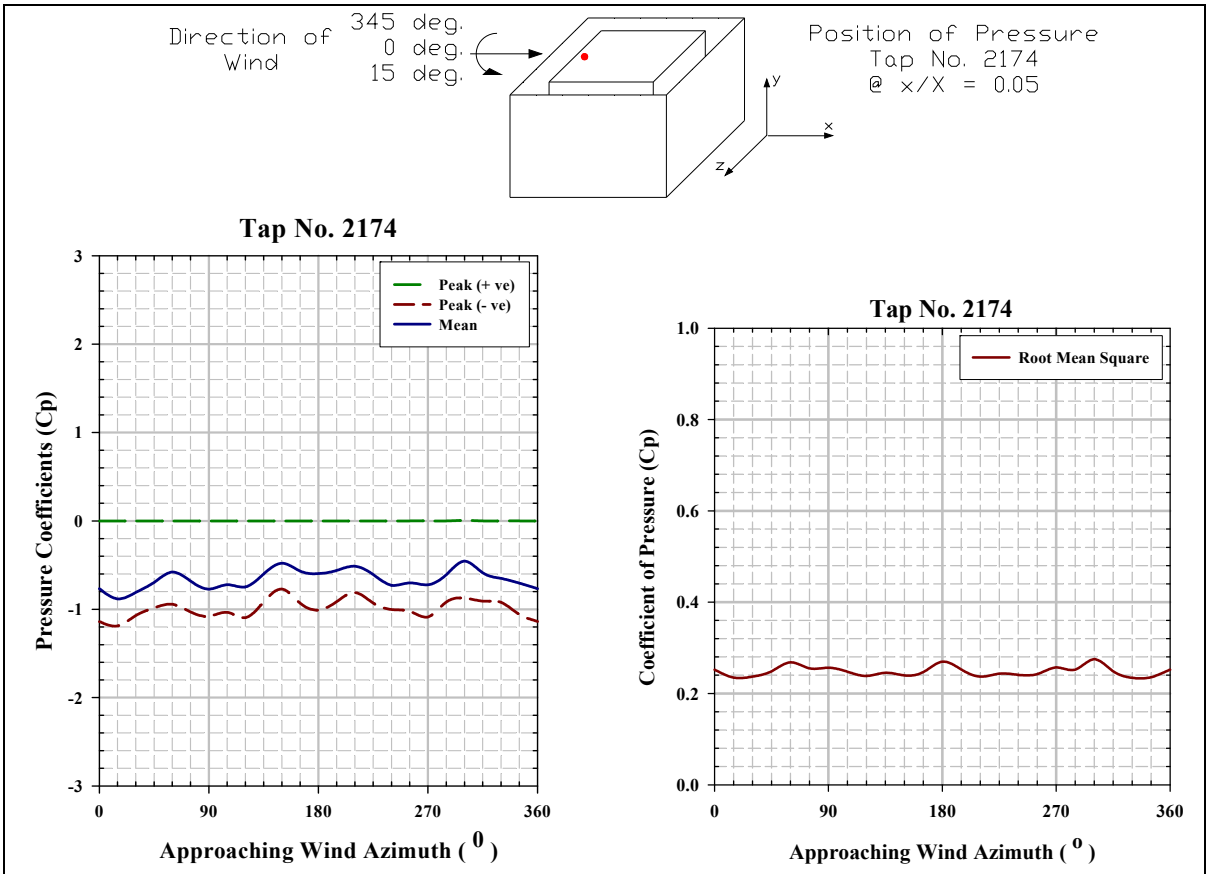

Figure 2B.36 Mean, peak and rms pressure coefficients for the tap number 2174

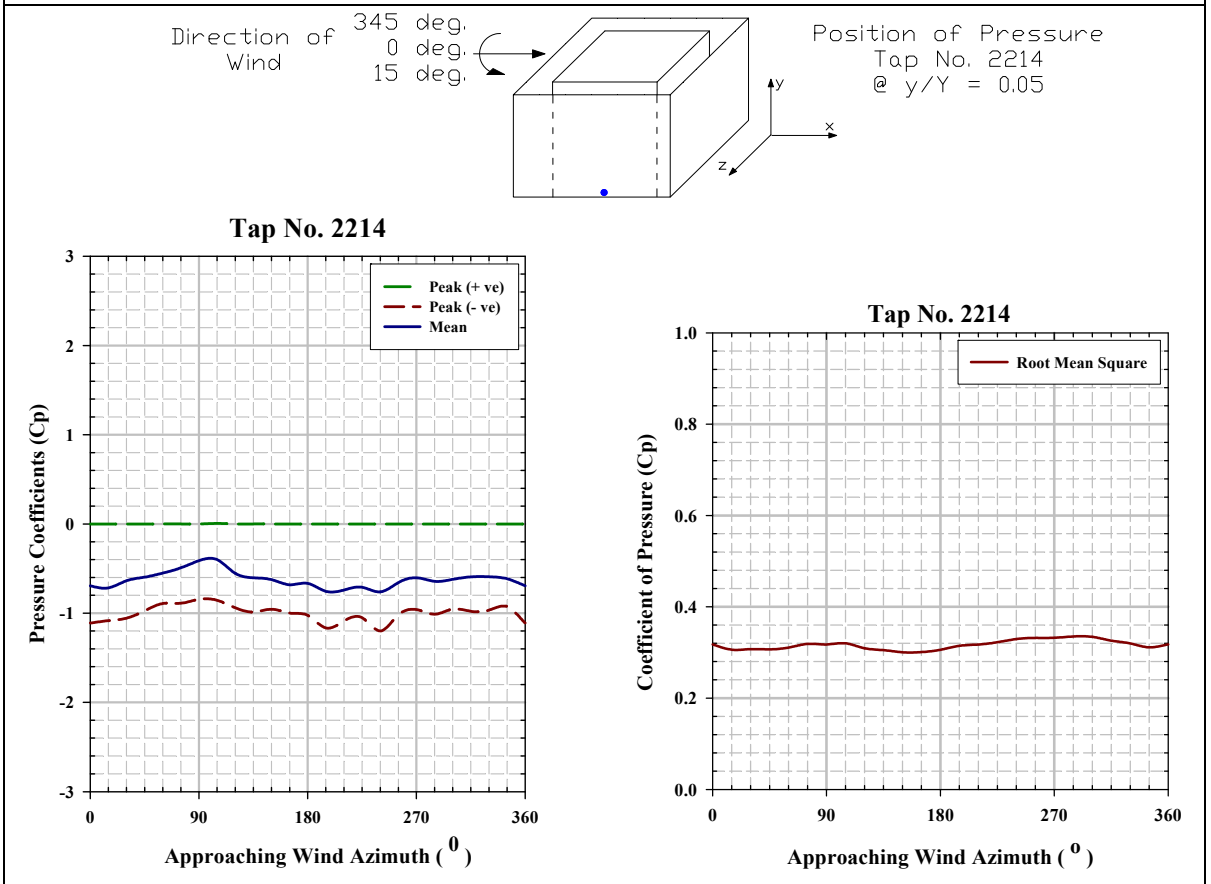

Figure 2B.37 Mean, peak and rms pressure coefficients for the tap number 2214

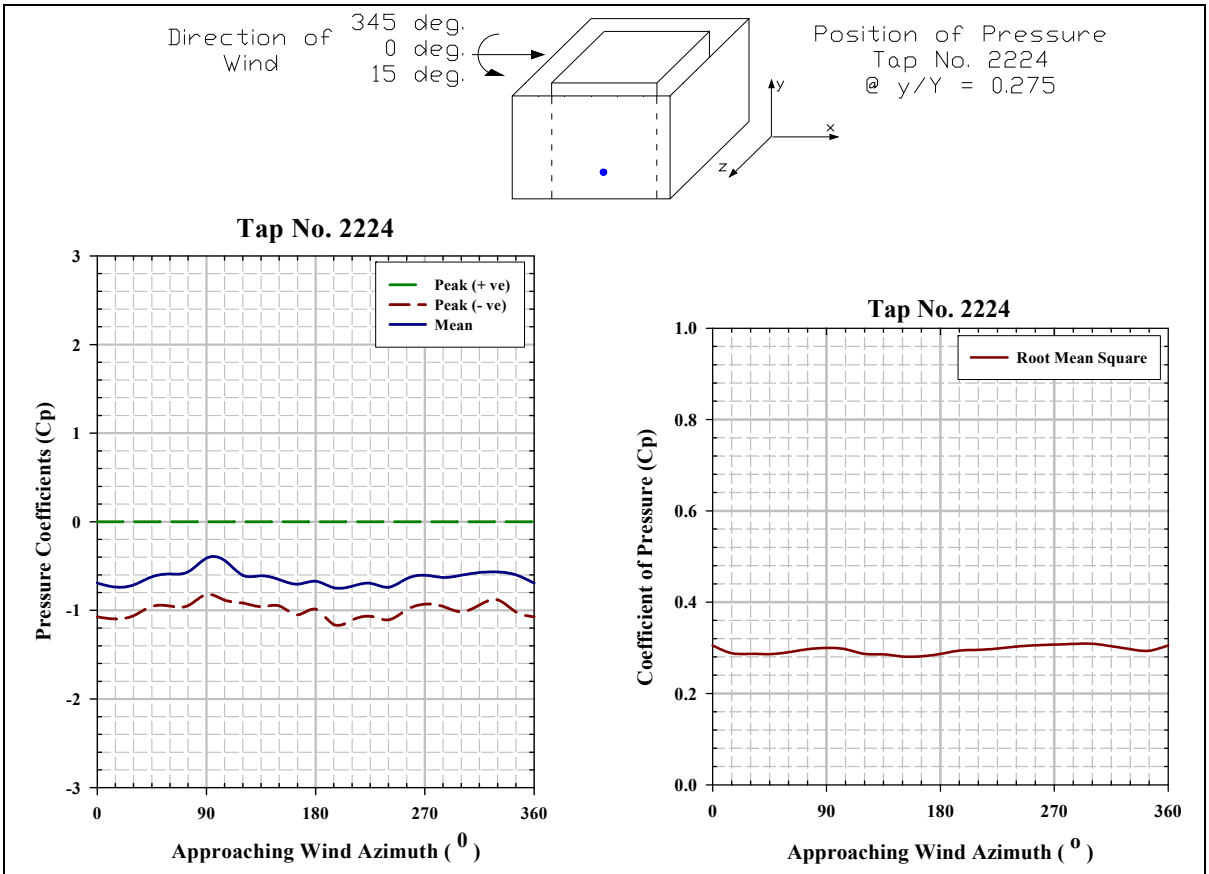

Figure 2B.38 Mean, peak and rms pressure coefficients for the tap number 2224

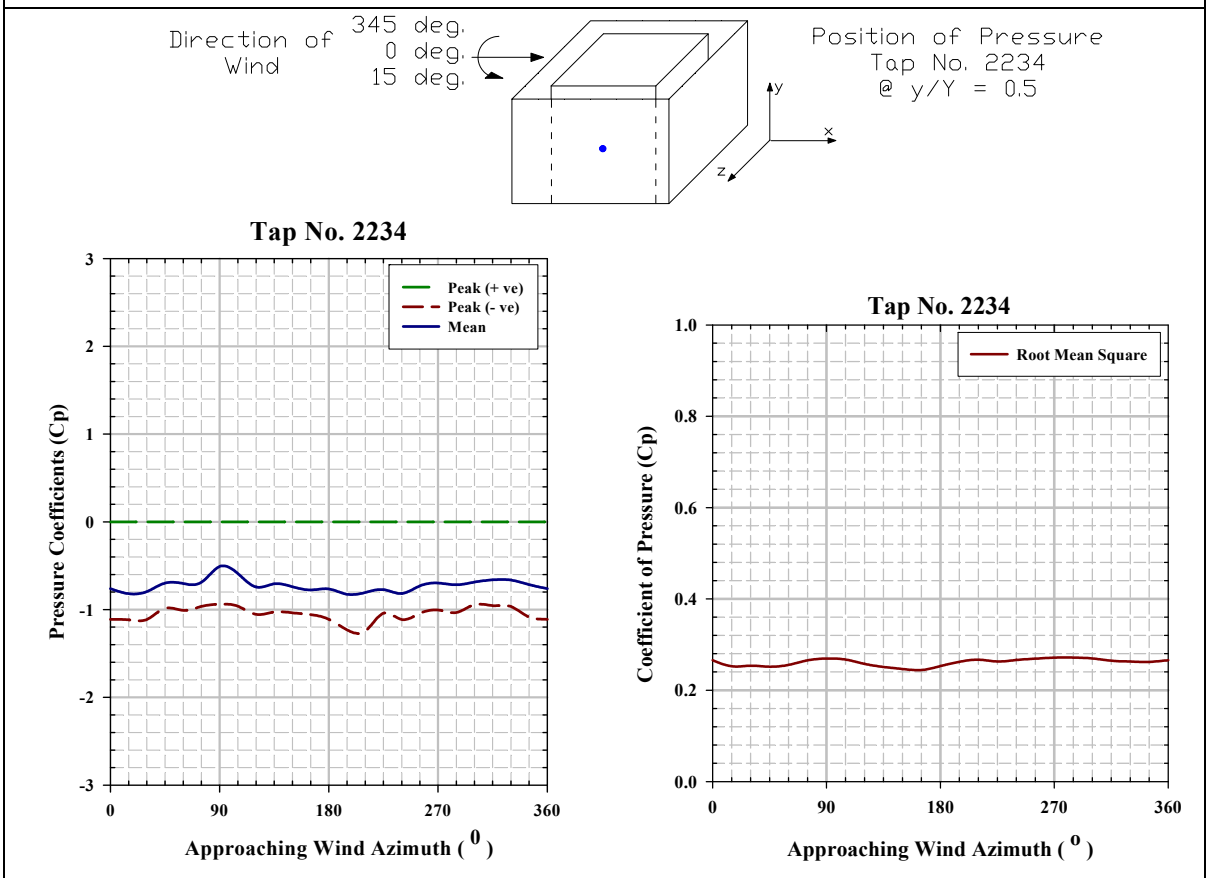

Figure 2B.39 Mean, peak and rms pressure coefficients for the tap number 2234

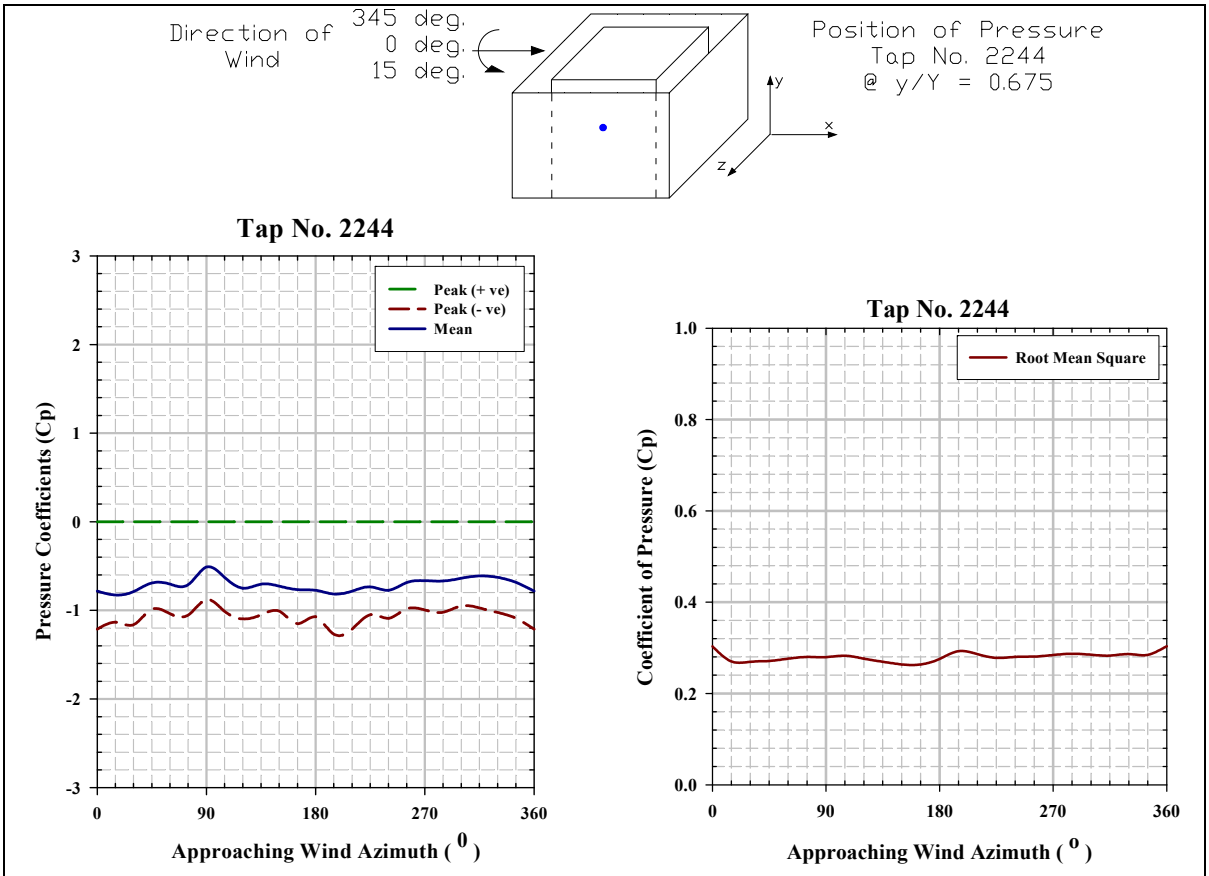

Figure 2B.40 Mean, peak and rms pressure coefficients for the tap number 2244

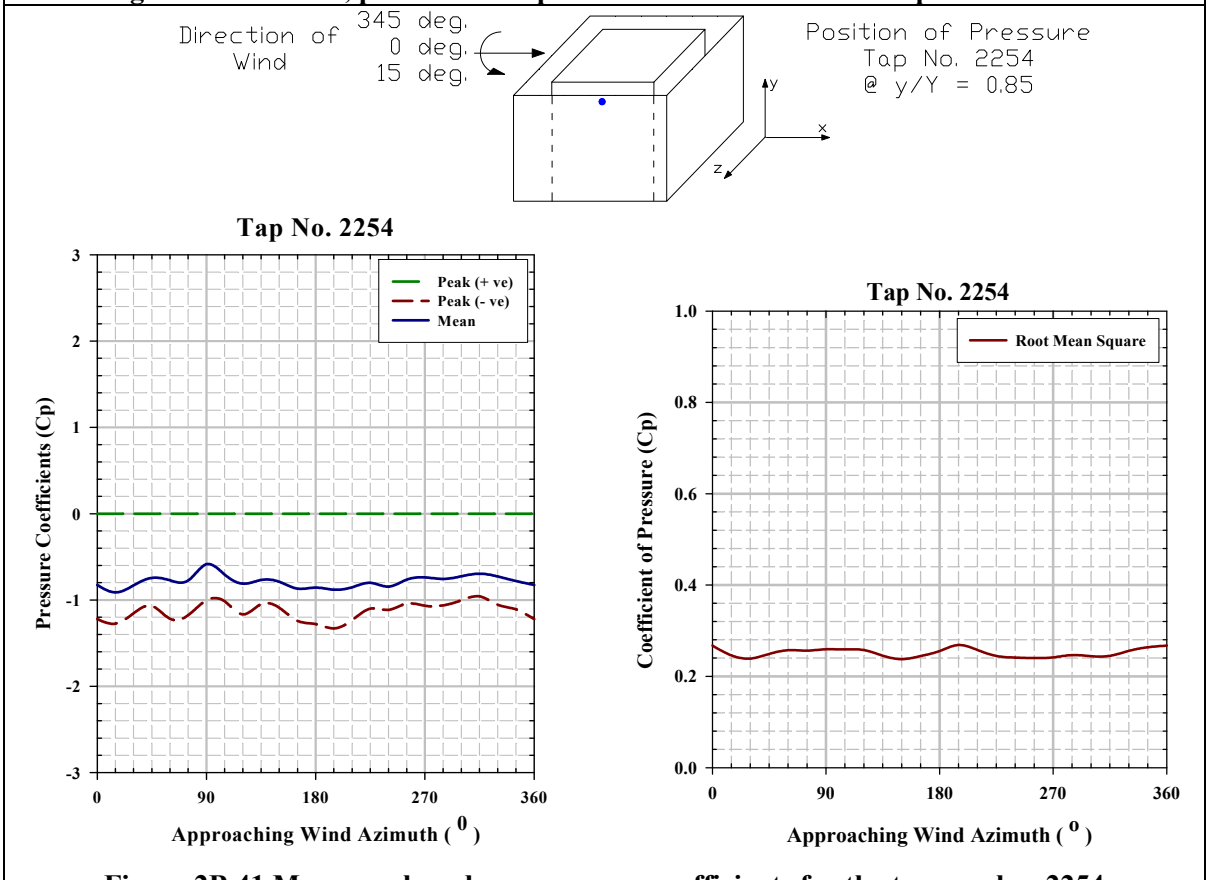

Figure 2B.41 Mean, peak and rms pressure coefficients for the tap number 2254

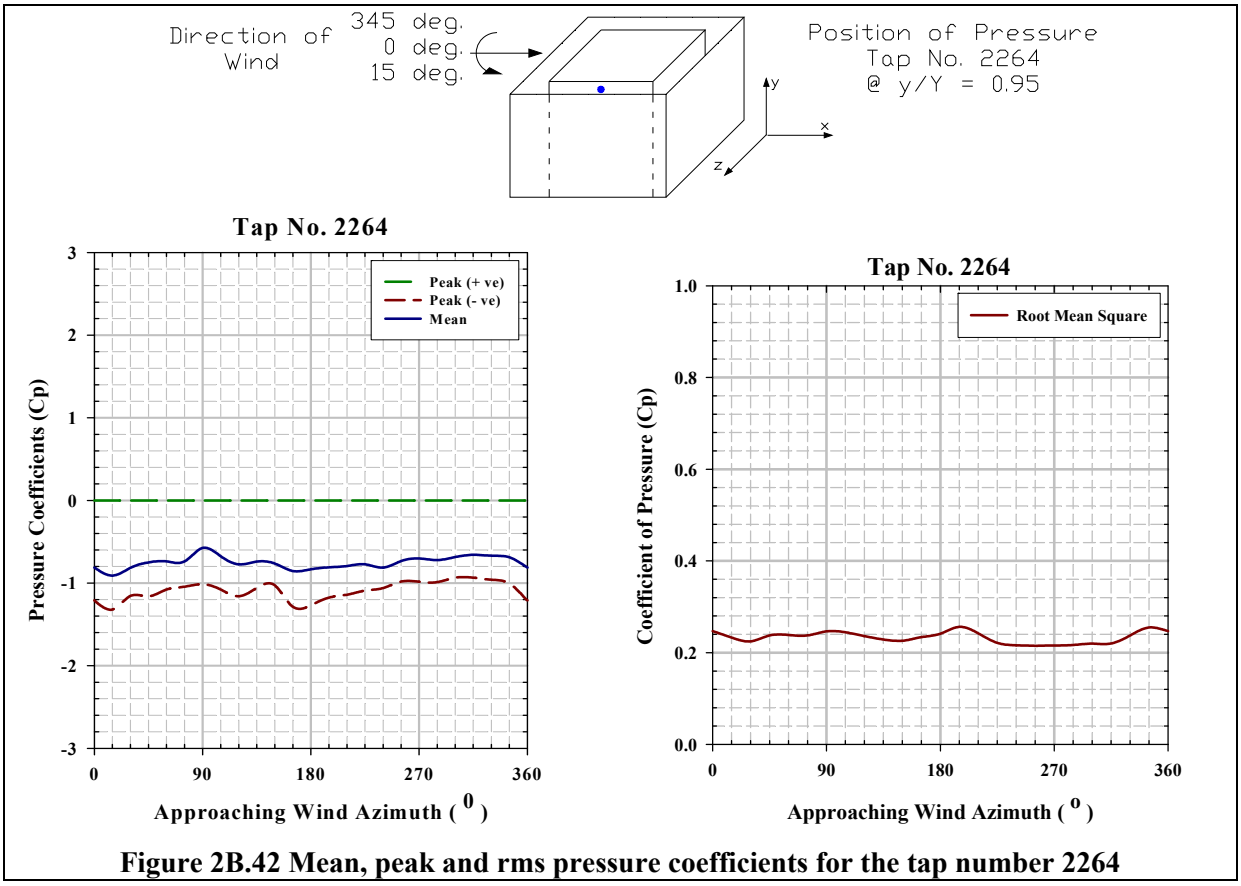

Figure 2B.42 Mean, peak and rms pressure coefficients for the tap number 2264

EXPERIMENT-3

Pressure Coefficients on SEB Surrounded by Elevated Sheet Clad Scaffold

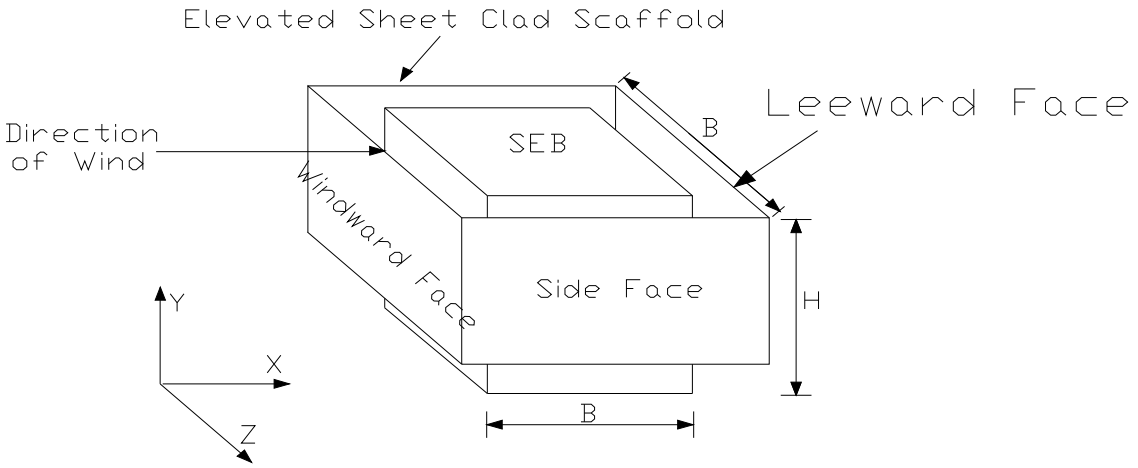

Figure 3.1 Scaled SEB surrounded by elevated impermeable sheet all around

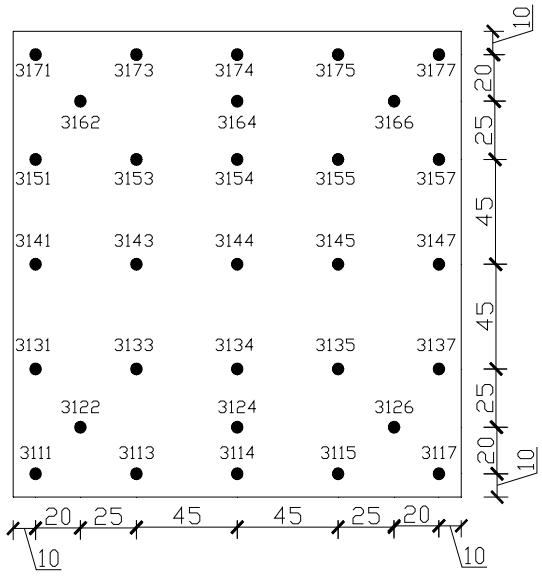

Figure 3.2 Pressure tap locations on roof

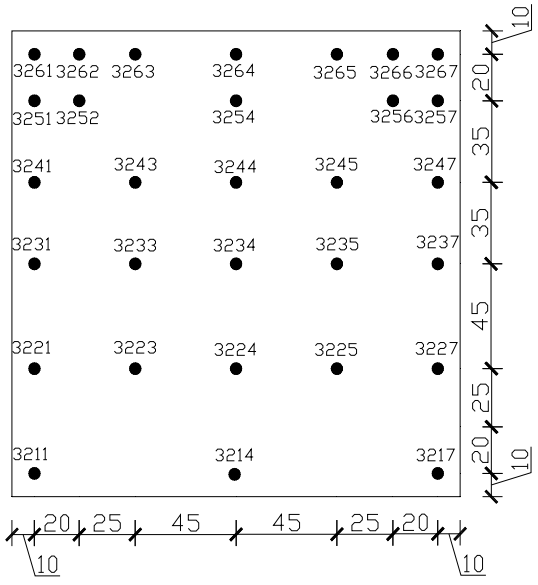

Figure 3.3 Pressure tap locations on the south wall face

Pressure Coefficient Contours on the Roof of SEB for Type A Terrain

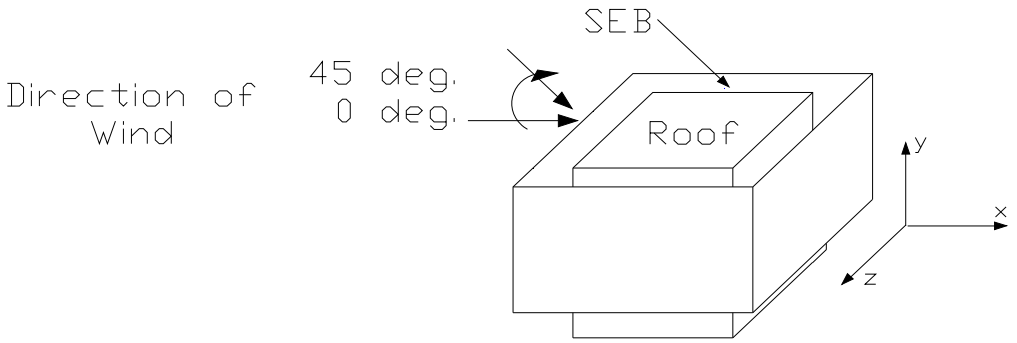

Figure 3A.1 Angle of attack of wind on roof of the SEB , direction of which varies from 0° to +45°

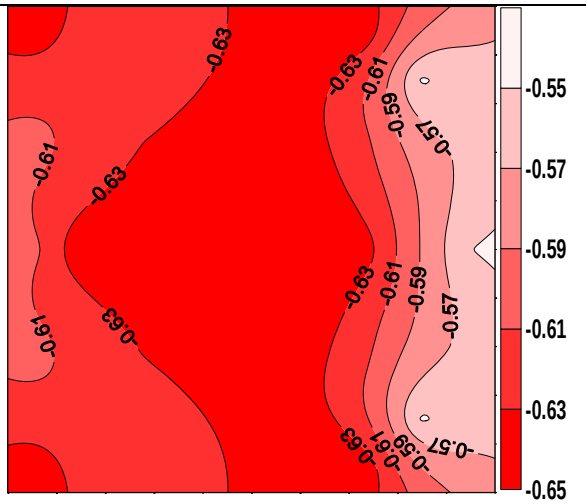

Figure 3A.2 Pressure coefficient contours on the roof of the SEB when θ= 0°

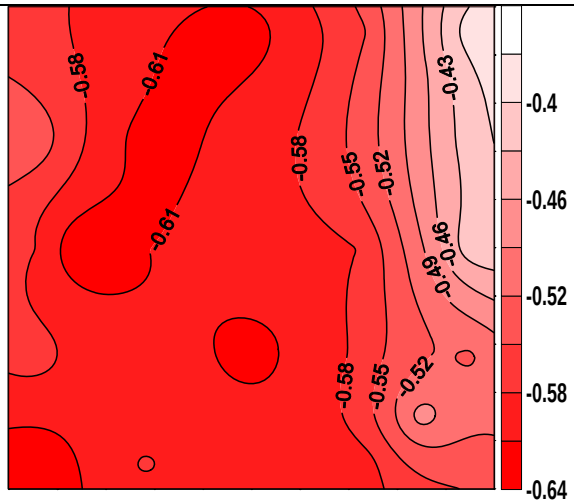

Figure 3A.3 Pressure coefficient contours on the roof of the SEB when θ= 15°

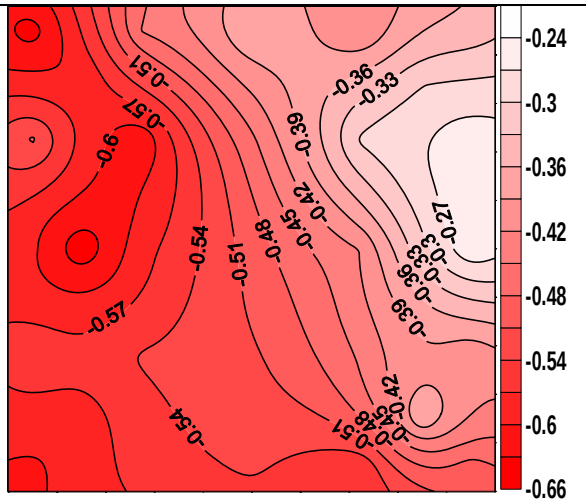

Figure 3A.4 Pressure coefficient contours on the roof of the SEB when θ= 30°

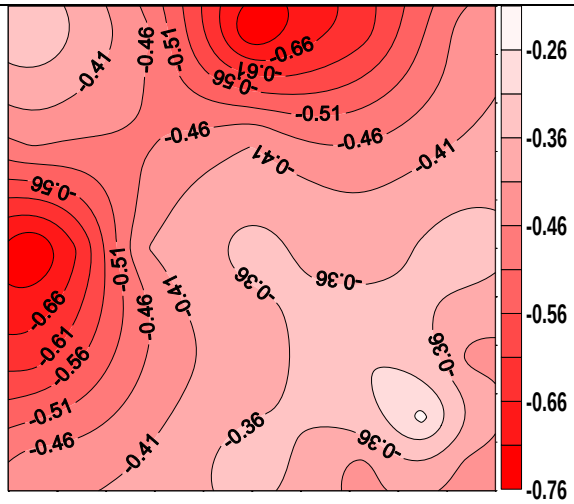

Figure 3A.5 Pressure coefficient contours on the roof of the SEB when θ= 45°

Pressure Coefficient Contours on Windward Face of SEB for Type A Terrain

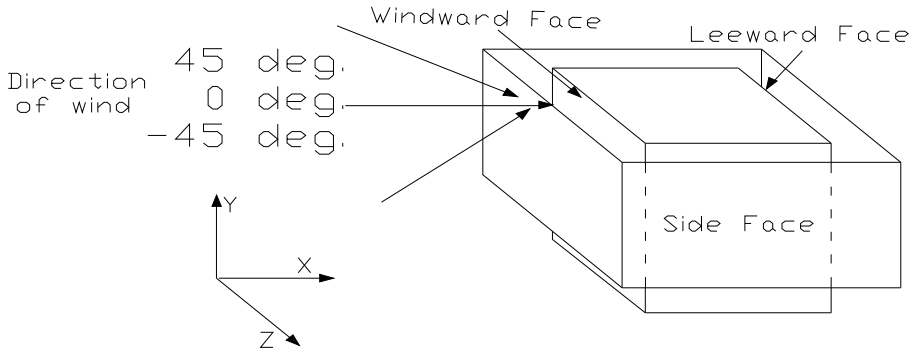

Figure 3A.6 Angle of attack of wind on windward wall of SEB, direction of which varies from -45° to +45°

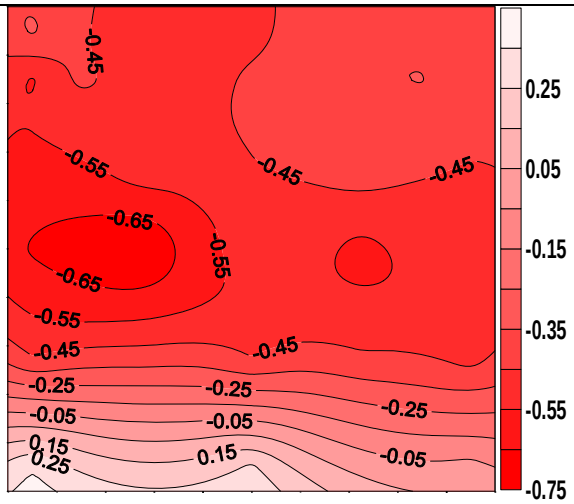

Figure 3A.7 Pressure coefficient contours on the windward face of the SEB surrounded by elevated sheeting all around when θ= -45°

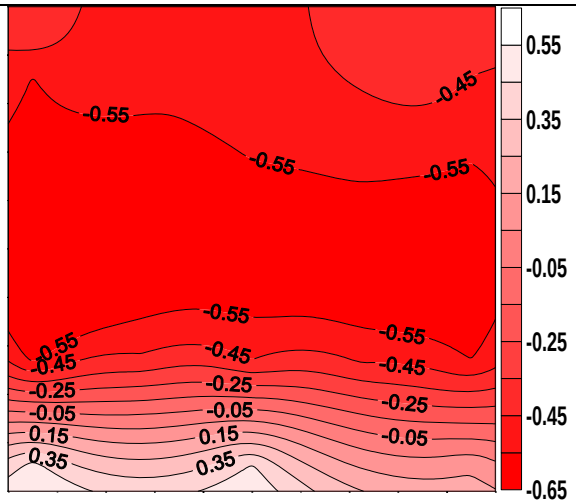

Figure 3A.8 Pressure coefficient contours on the windward face of the SEB surrounded by elevated sheeting all around when θ= -30°

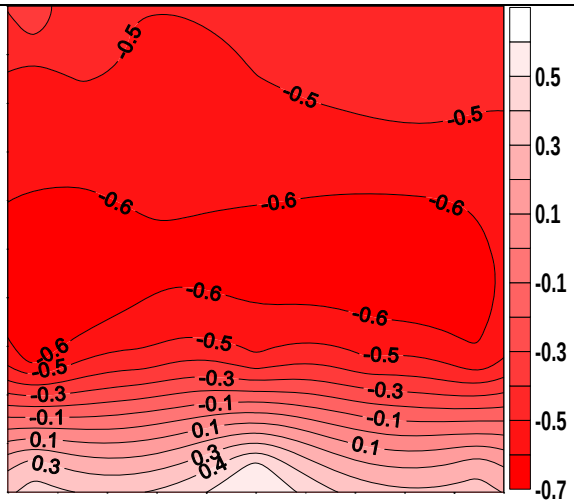

Figure 3A.9 Pressure coefficient contours on the windward face of the SEB surrounded by elevated sheeting all around when θ= -15°

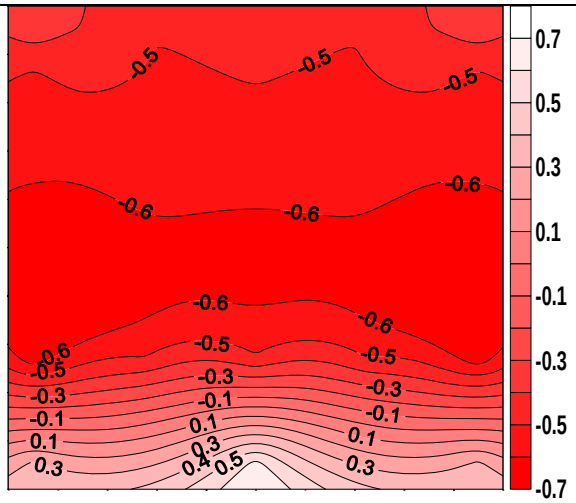

Figure 3A.10 Pressure coefficient contours on the windward face of the SEB surrounded by elevated sheeting all around when θ=0°

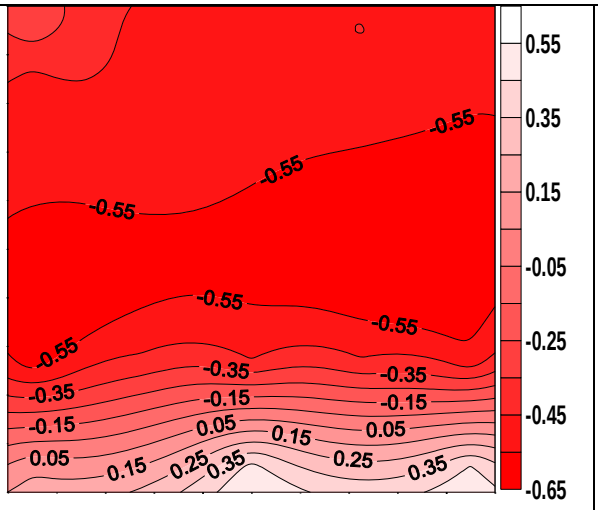

Figure 3A.11 Pressure coefficient contours on the windward face of the SEB surrounded by elevated sheeting all around when θ=+15°

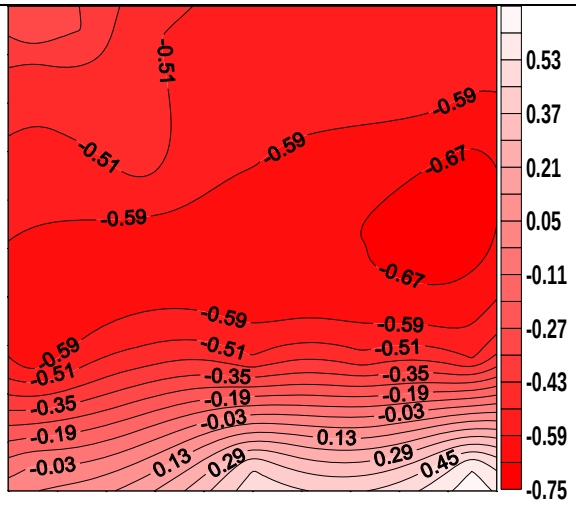

Figure 3A.12 Pressure coefficient contours on the windward face of the SEB surrounded by elevated sheeting all around when θ=+30°

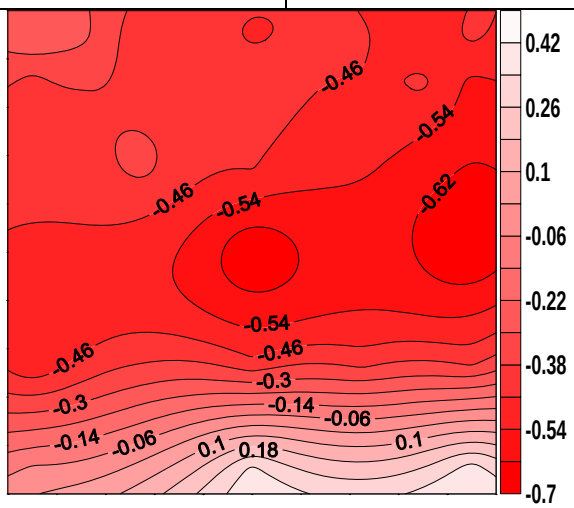

Figure 3A.13 Pressure coefficient contours on the windward face of the SEB surrounded by elevated sheeting all around when θ=+45°

Pressure Coefficient Contours on Side Face of SEB for Type A Terrain

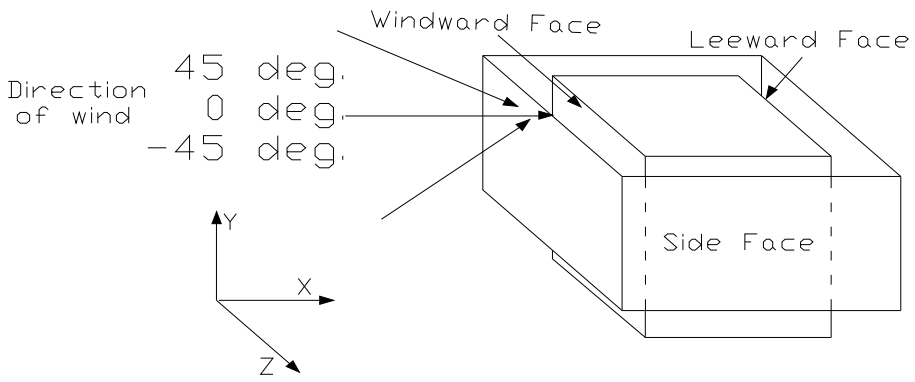

Figure 3A.14 Angle of attack of wind on windward wall of SEB, direction of which varies from -45° to +45°

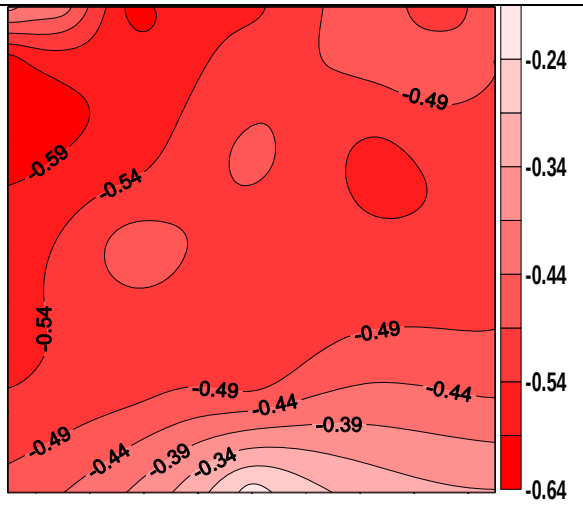

Figure 3A.15 Pressure coefficient contours on the side face of the SEB surrounded by elevated sheeting all around when θ= -45°

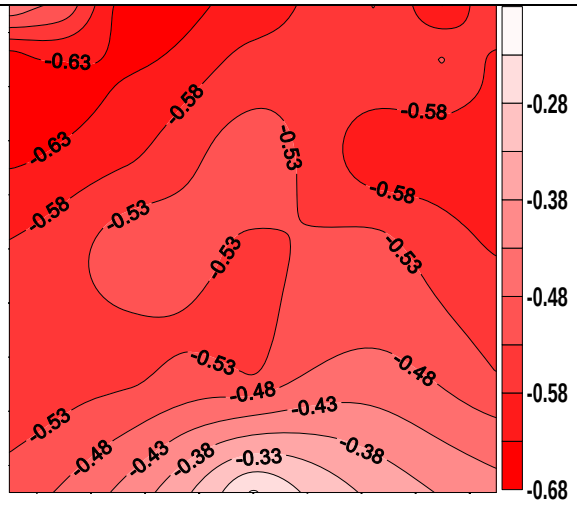

Figure 3A.16 Pressu re coefficient contours on the side face of the SEB surrounded by elevated sheeting all around when θ= -30°

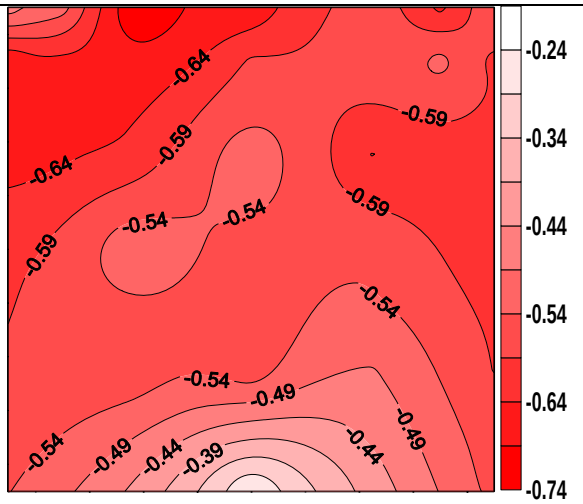

Figure 3A.17 Pressure coefficient contours on the side face of the SEB surrounded by elevated sheeting all around when θ= -15°

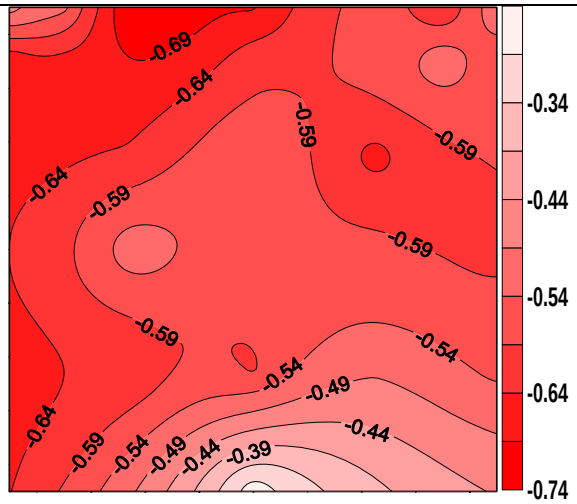

Figure 3A.18 Pressure coefficient contours on the side face of the building surrounded by elevated sheeting all around when θ= 0°

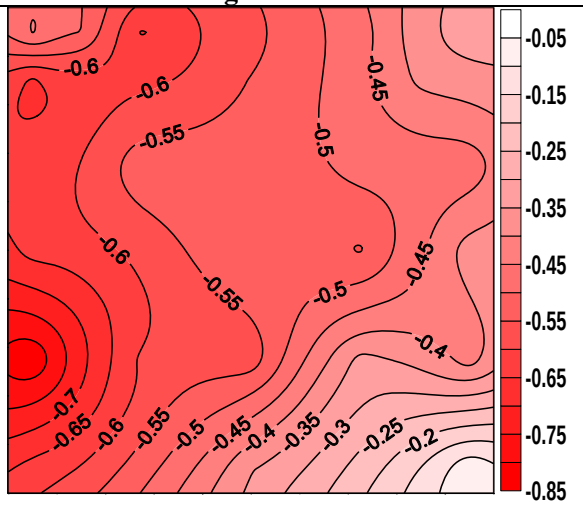

Figure 3A.19 Pressure coefficient contours on the side face of the SEB surrounded by elevated sheeting all around when θ=+15°

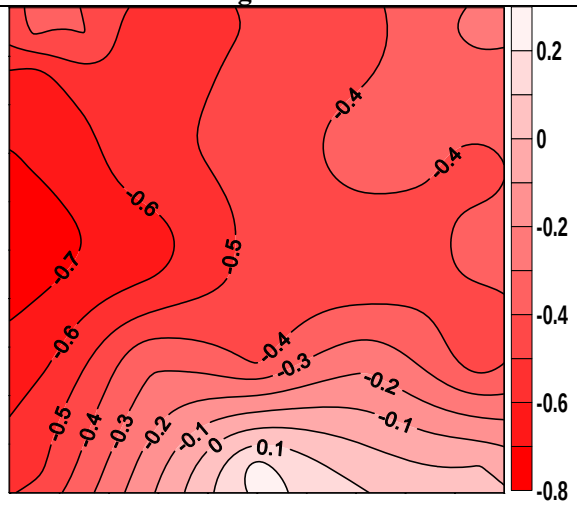

Figure 3A.20 Pressure coefficient contours on the side face of the SEB surrounded by elevated sheeting all around when θ=+30°

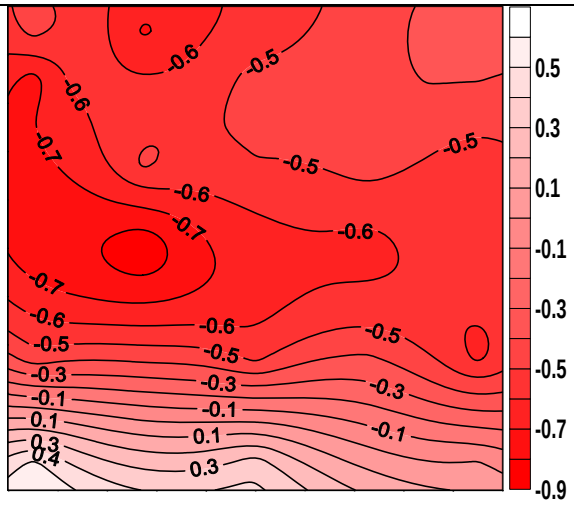

Figure 3A.21 Pressure coefficient contours on the side face of the SEB surrounded by elevated sheeting all around when θ=+45°

Pressure Coefficient Contours on Leeward Face of SEB for Type A Terrain

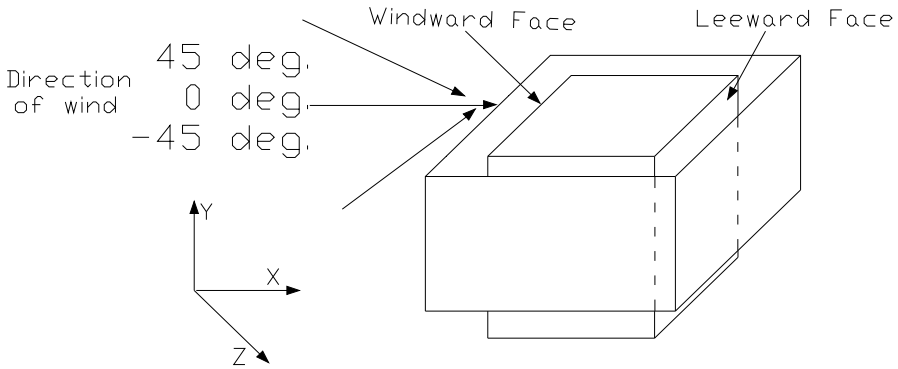

Figure 3A.22 Angle of attack of wind on windward wall of SEB, direction of which varies from -45° to +45°

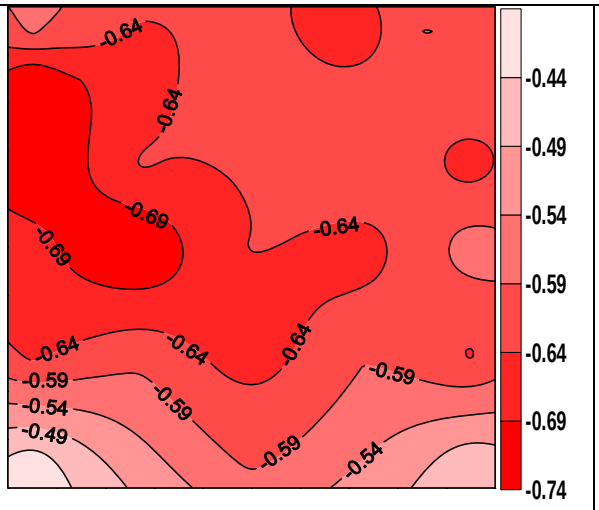

Figure 3A.23 Pressure coefficient contours on the leeward face of the SEB surrounded by elevated sheeting all around when θ= -45°

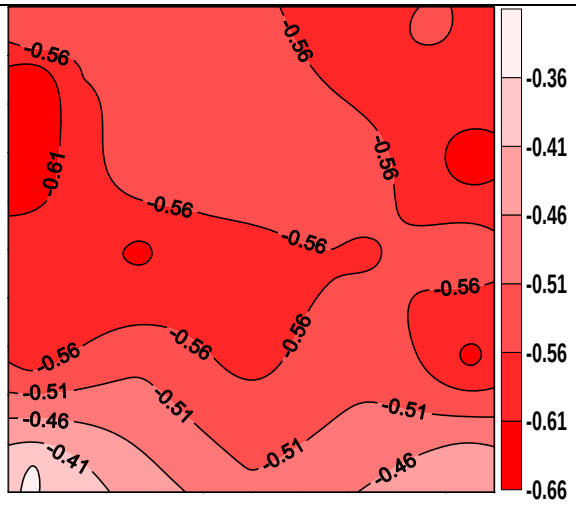

Figure 3A.24 Pressure coefficient contours on the leeward face of the SEB surrounded by elevated sheeting all around when θ= -30°

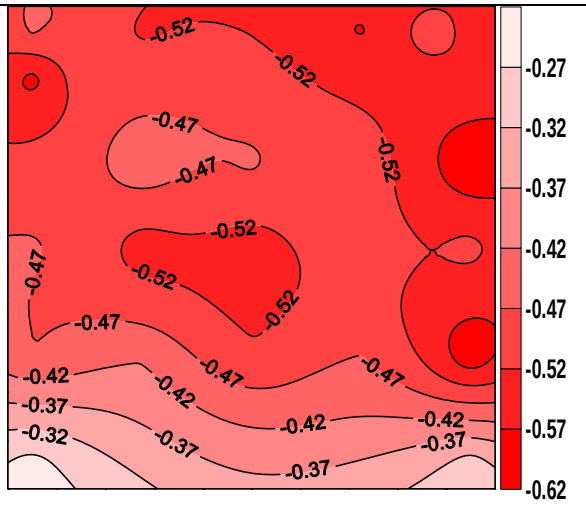

Figure 3A.25 Pressure coefficient contours on the leeward face of the SEB surrounded by elevated sheeting all around when θ= -15°

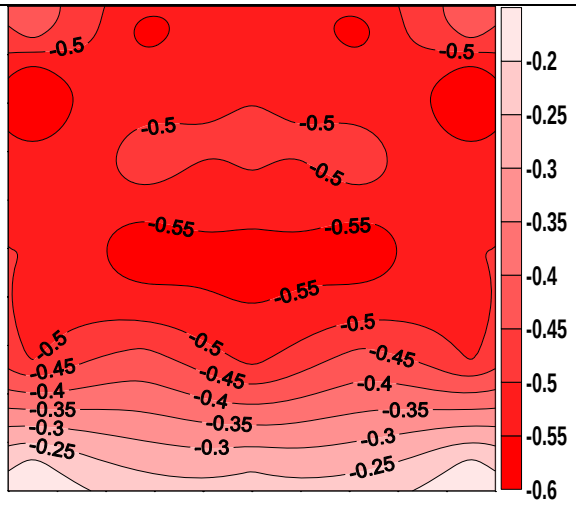

Figure 3A.26 Pressure coefficient contours on the leeward face of the SEB surrounded by elevated sheeting all around when θ= 0°

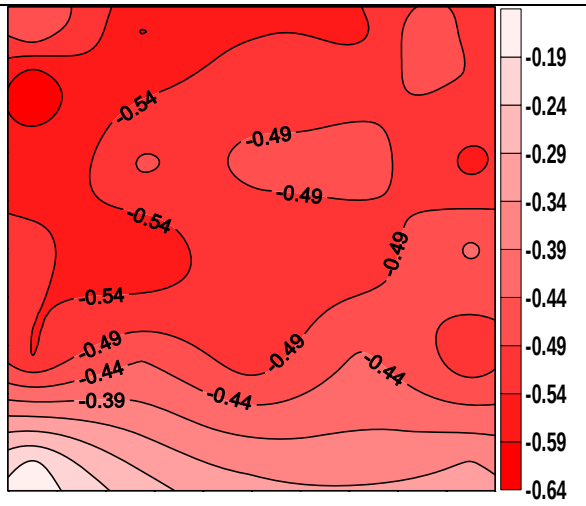

Figure 3A.27 Pressure coefficient contours on the leeward face of the SEB surrounded by elevated sheeting all around when θ= +15°

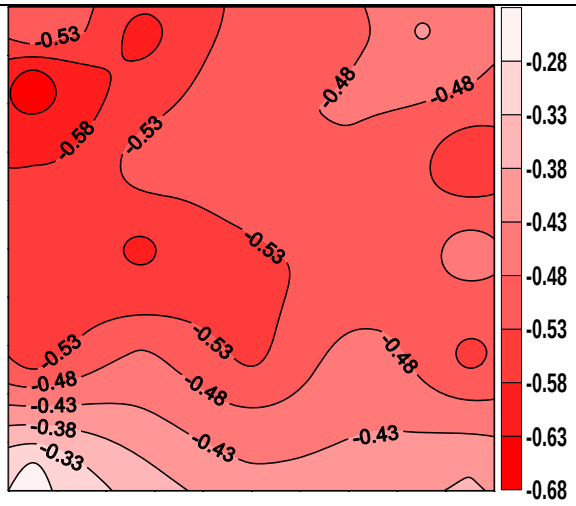

Figure 3A.28 Pressure coefficient contours on the leeward face of the SEB surrounded by elevated sheeting all around when θ= +30°

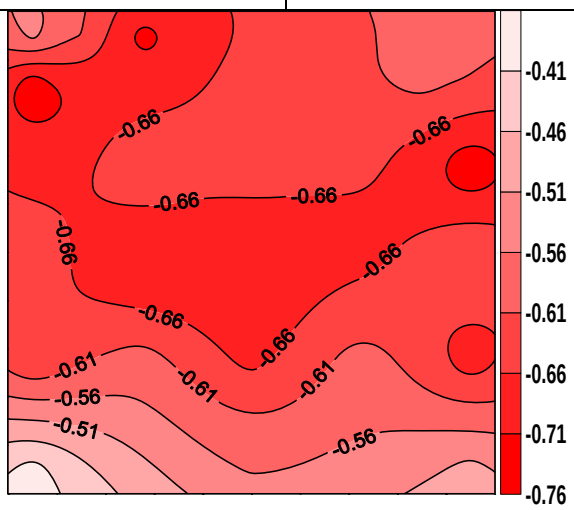

Figure 3A.29 Pressure coefficient contours on the leeward face of the SEB surrounded by elevated sheeting all around when θ= +45°

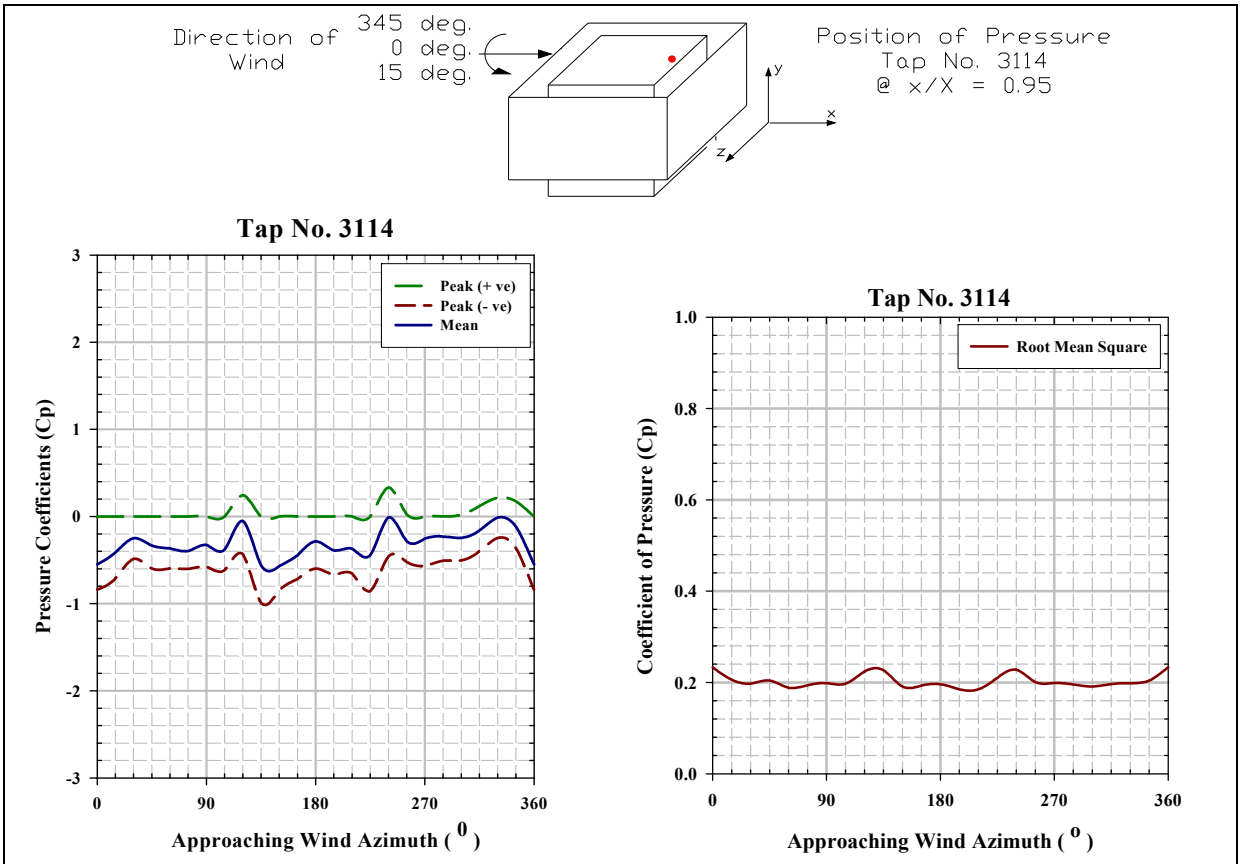

Figure 3A.30 Mean, peak and rms pressure coefficients for tap number 3114

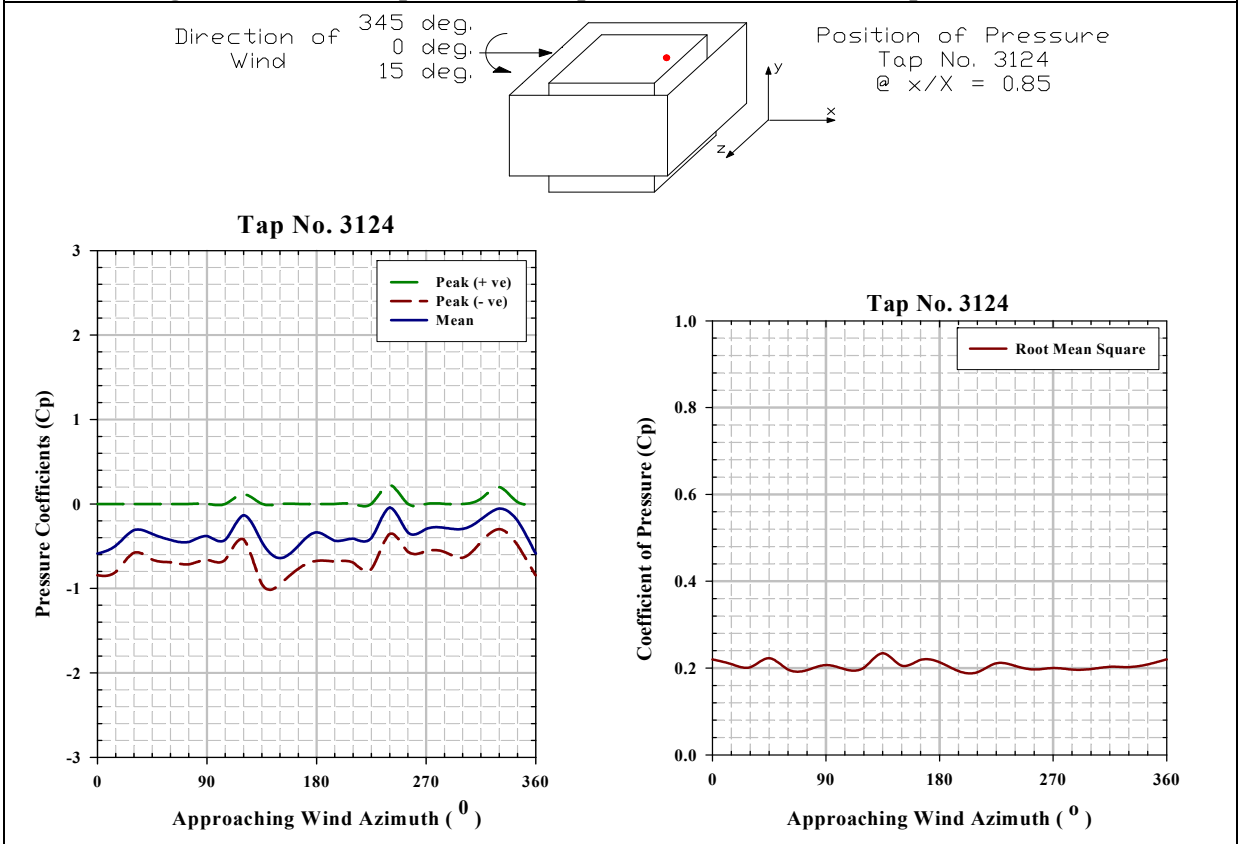

Figure 3A.31 Mean, peak and rms pressure coefficients for tap number 3124

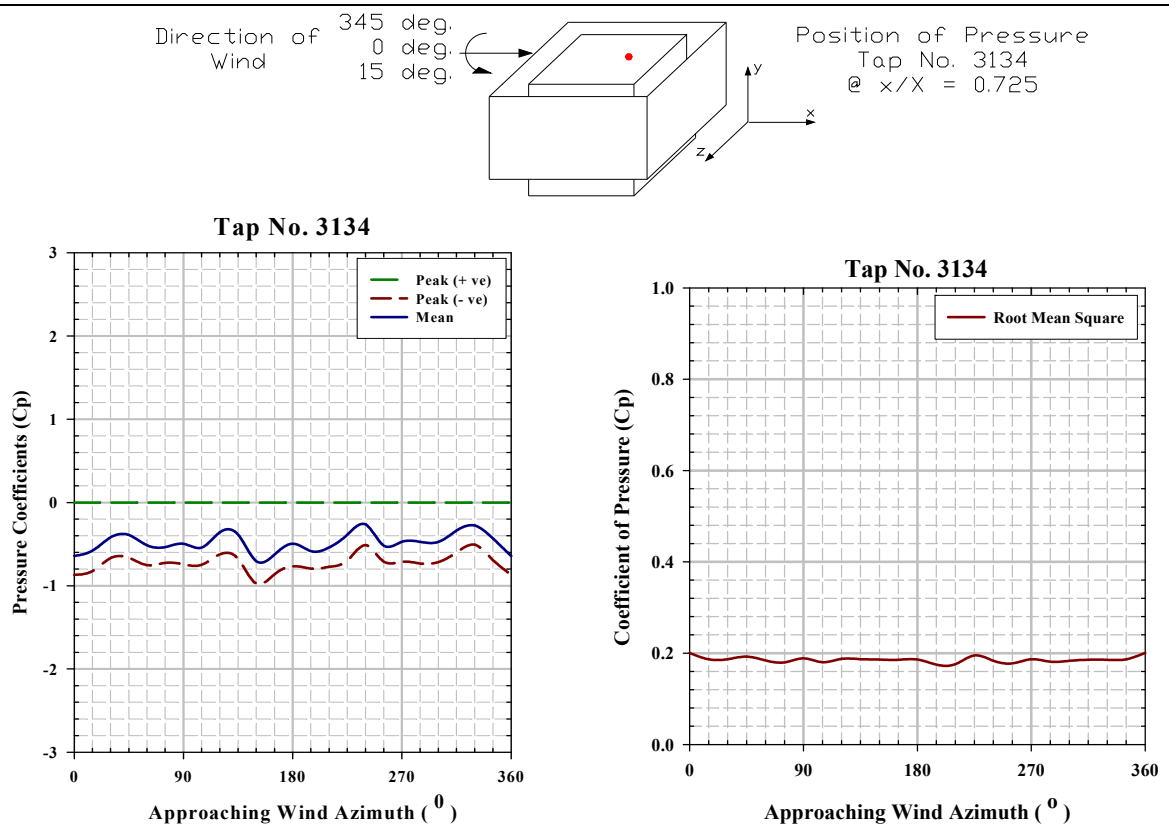

Figure 3A.32 Mean, peak and rms pressure coefficients for tap number 3134

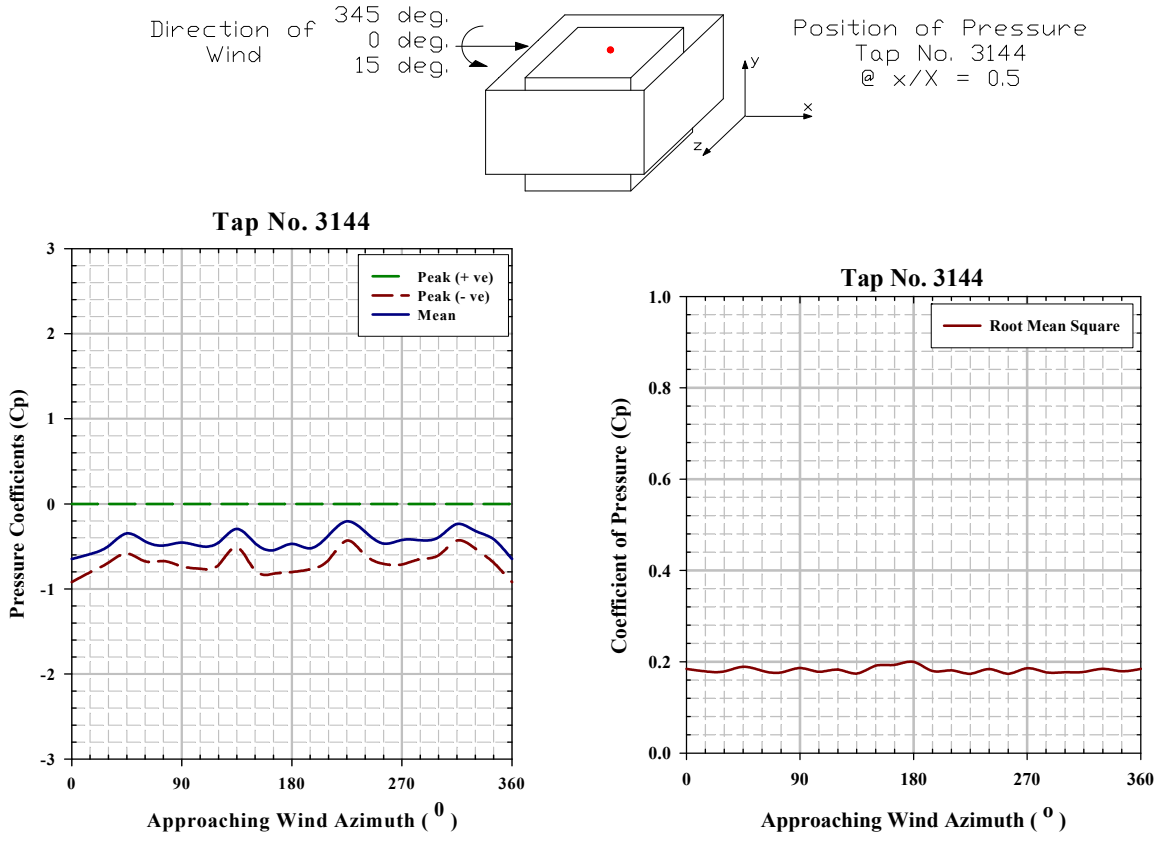

Figure 3A.33 Mean, peak and rms pressure coefficients for tap number 3144

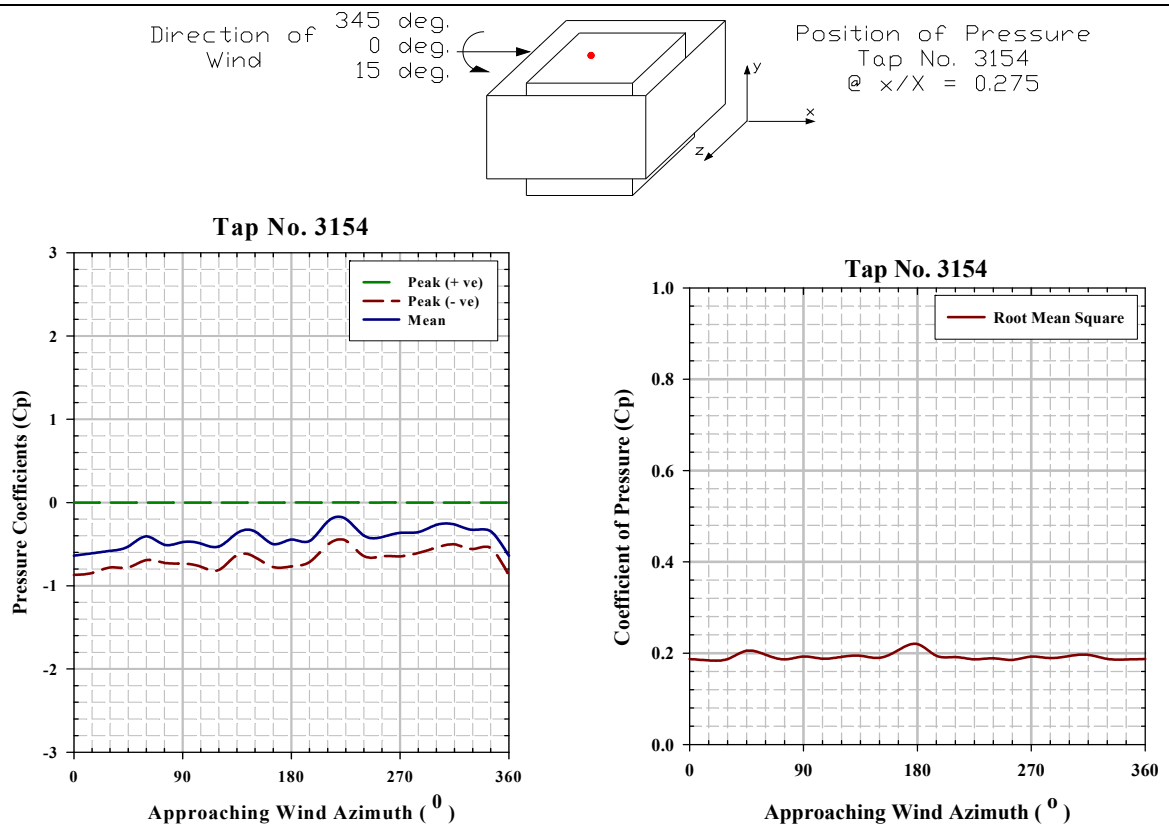

Figure 3A.34 Mean, peak and rms pressure coefficients for tap number 3154

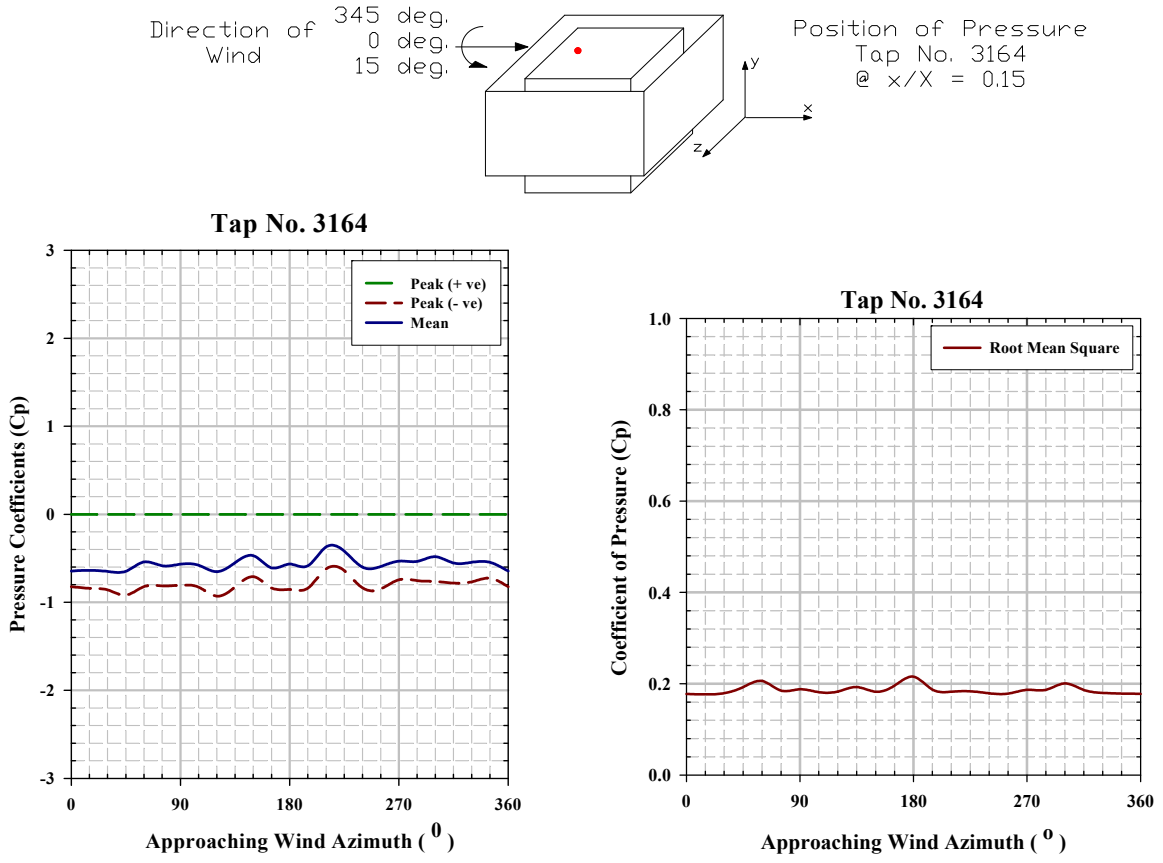

Figure 3A.35 Mean, peak and rms pressure coefficients for tap number 3164

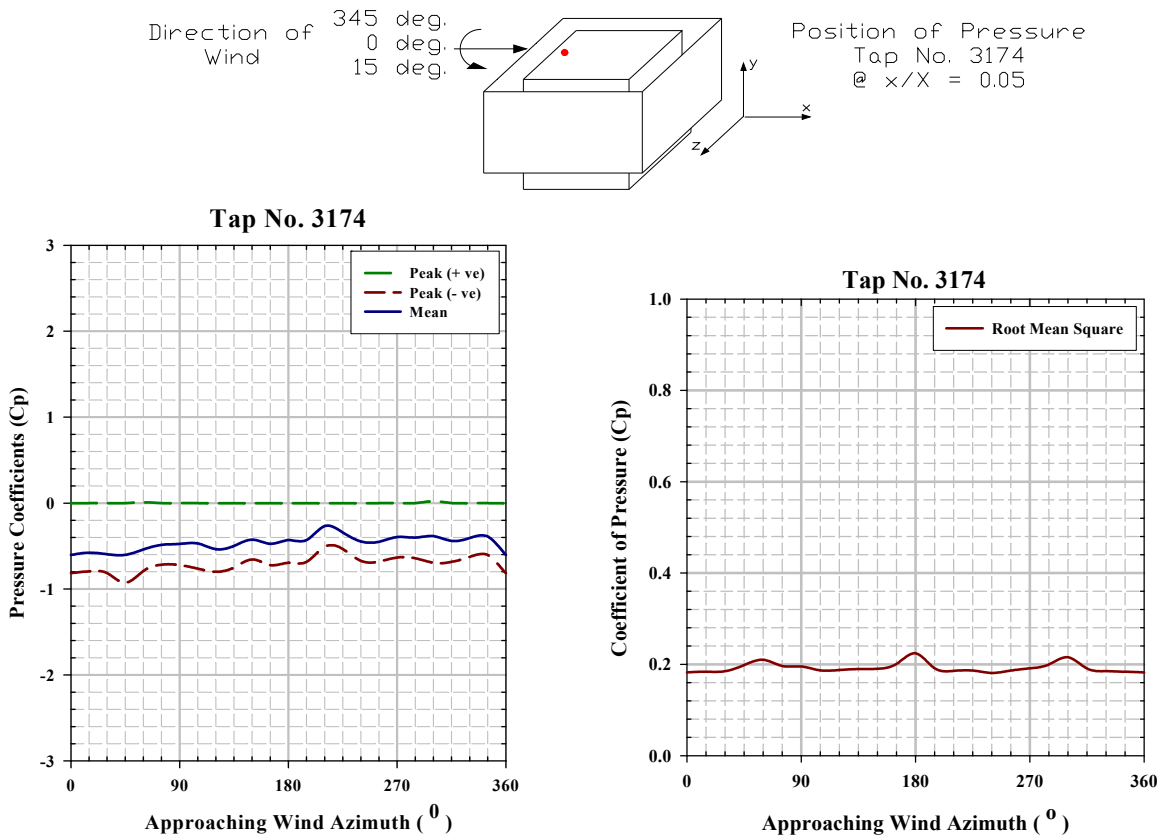

Figure 3A.36 Mean, peak and rms pressure coefficients for tap number 3174

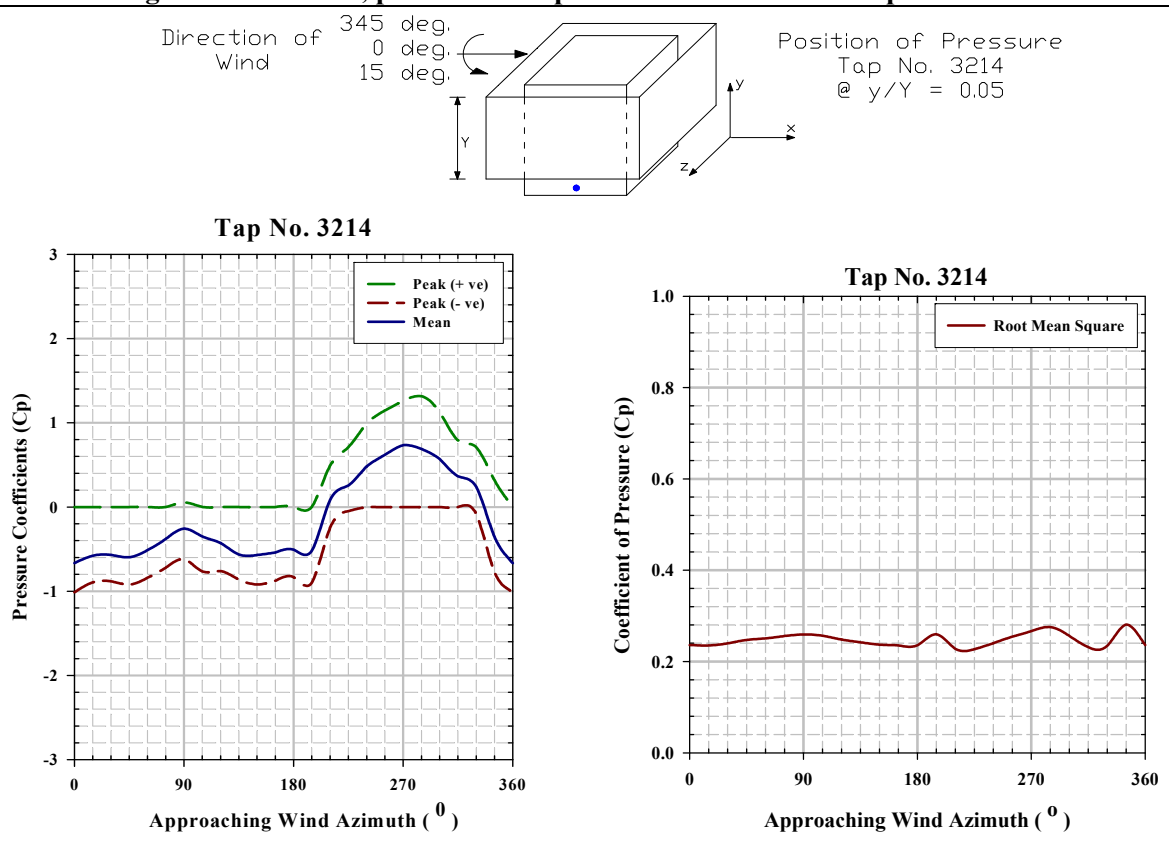

Figure 3A.37 Mean, peak and rms pressure coefficients for tap number 3214

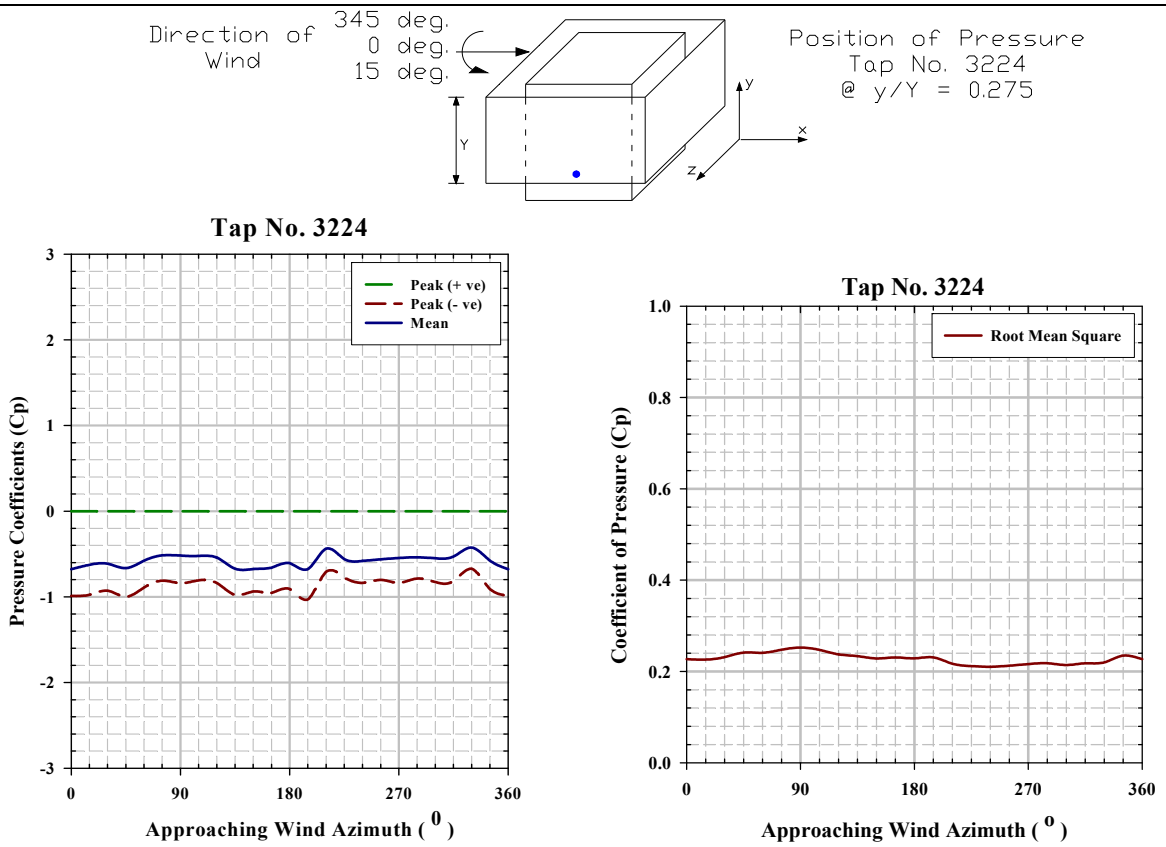

Figure 3A.38 Mean, peak and rms pressure coefficients for tap number 3224

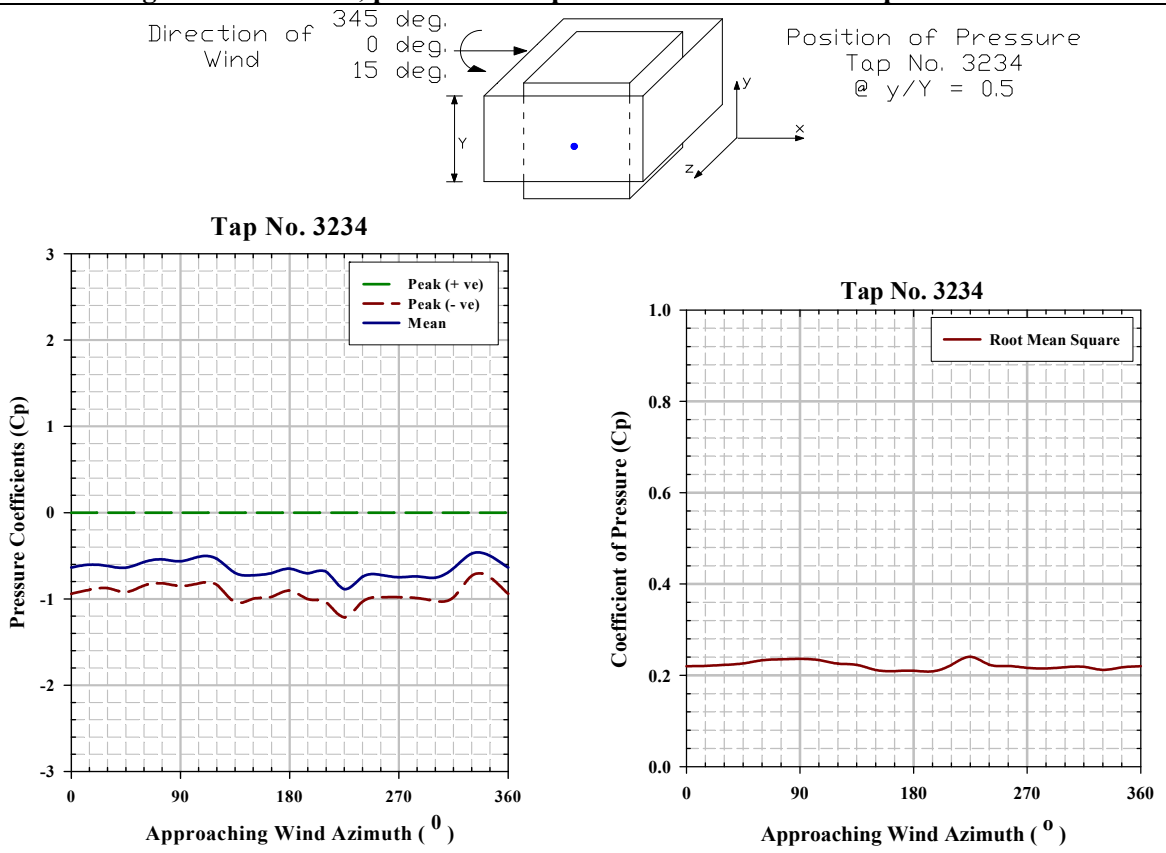

Figure 3A.39 Mean, peak and rms pressure coefficients for tap number 3234

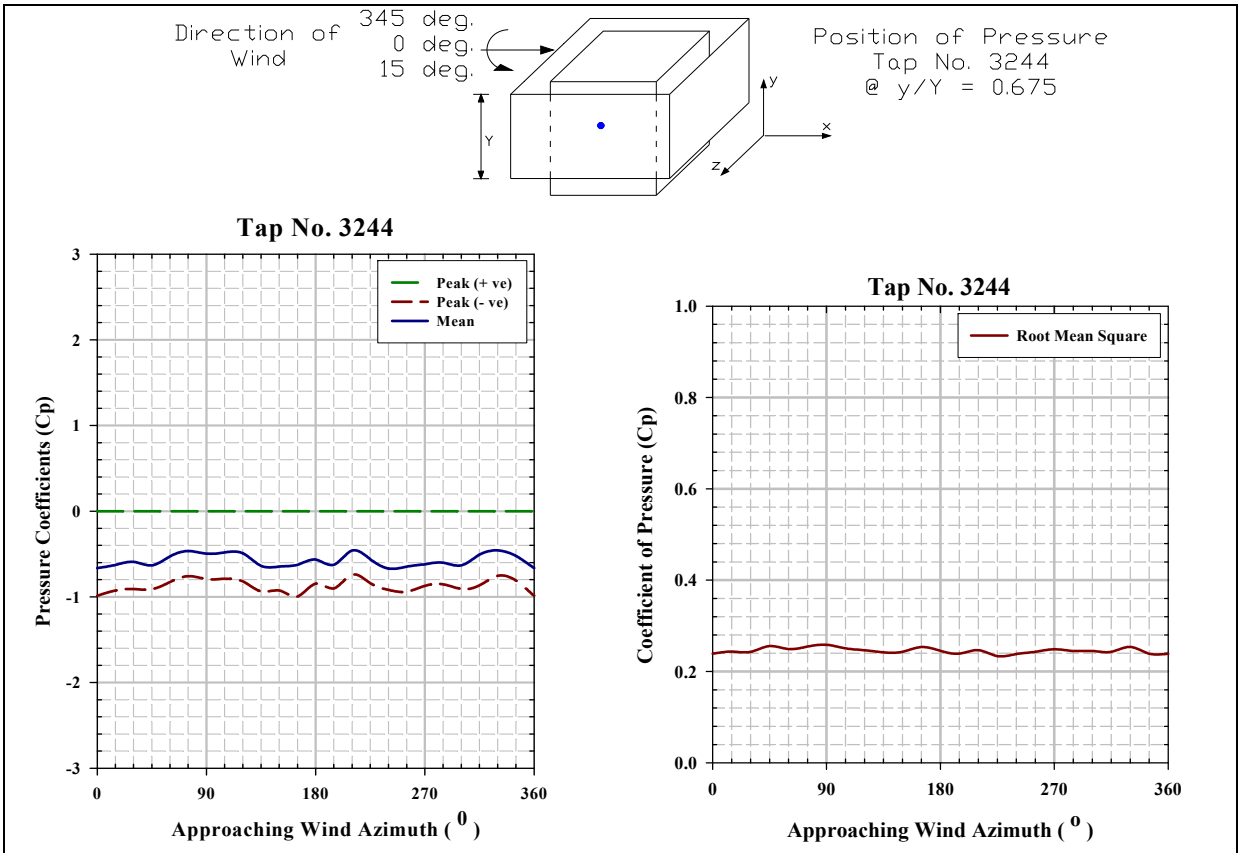

Figure 3A.40 Mean, peak and rms pressure coefficients for tap number 3244

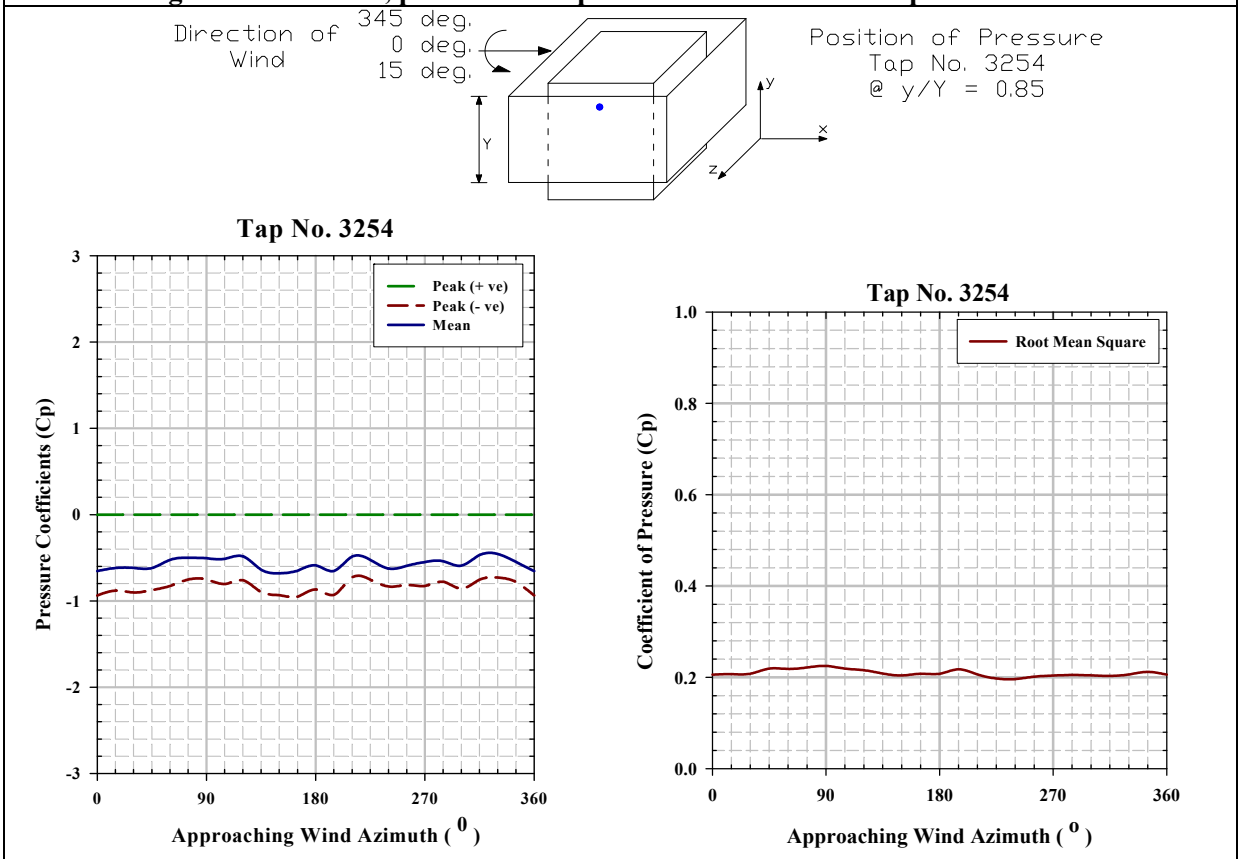

Figure 3A.41 Mean, peak and rms pressure coefficients for tap number 3254

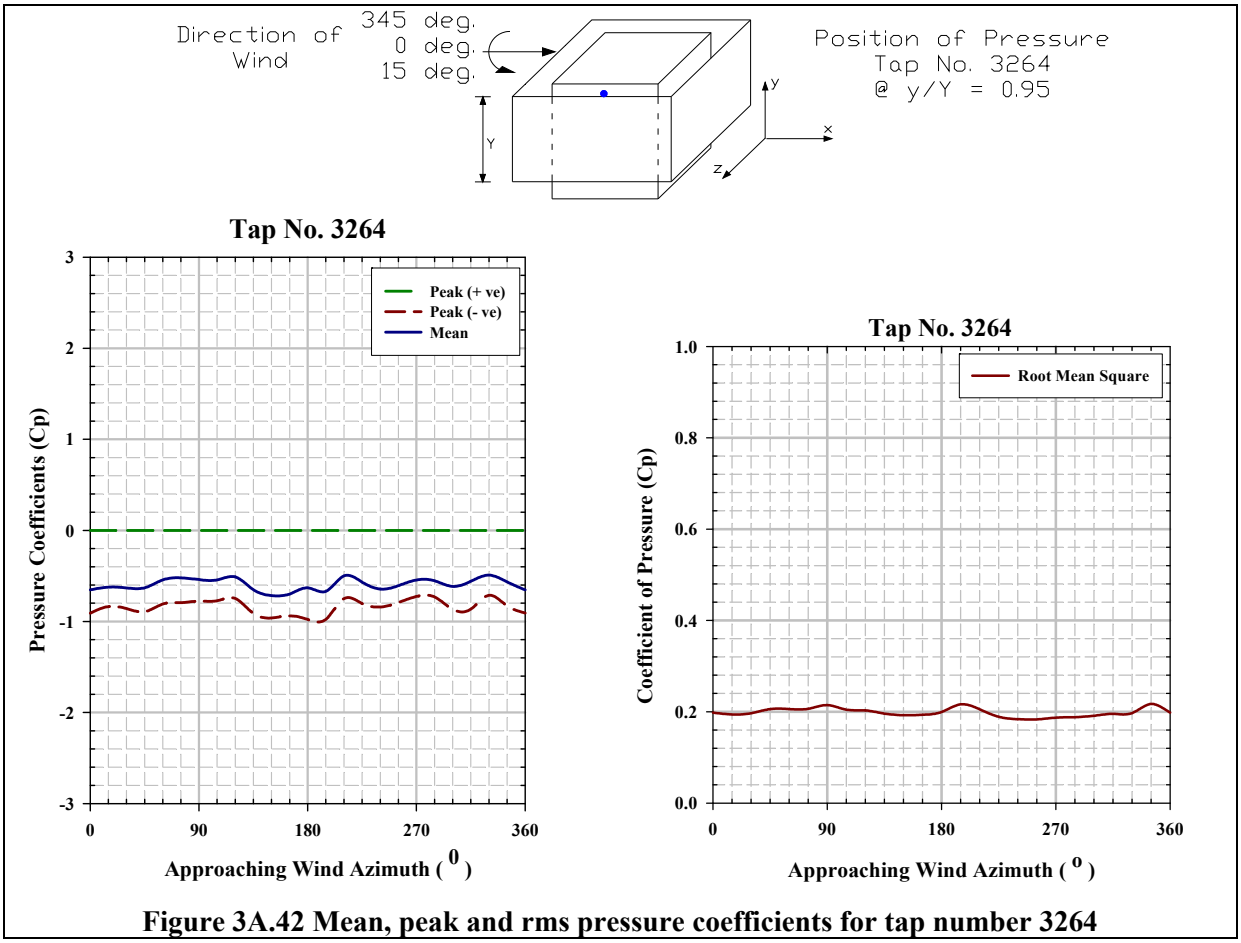

Figure 3A.42 Mean, peak and rms pressure coefficients for tap number 3264

Pressure Coefficient Contours on Roof of SEB for Type B Terrain

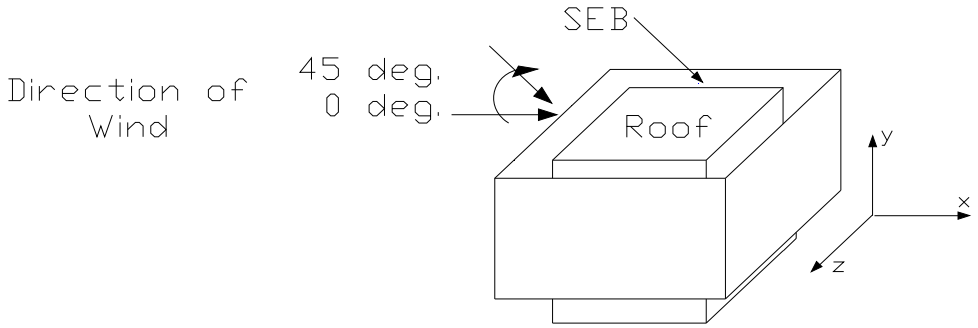

Figure 3B.1 Angle of attack of wind on roof of the SEB , direction of which varies from 0° to +45°

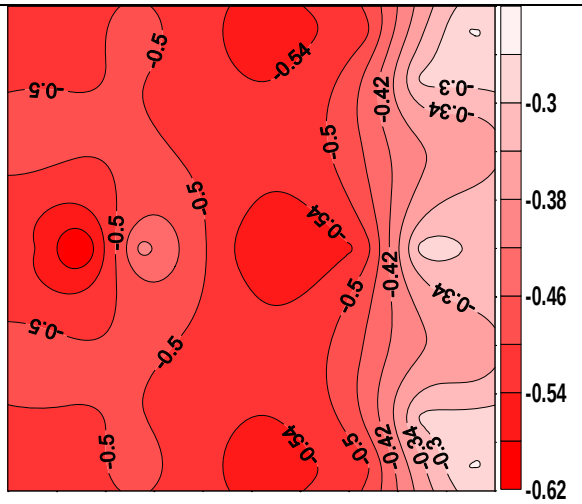

Figure 3B.2 Pressure coefficient contours on the roof of the SEB surrounded by elevated sheet clad scaffold when θ= 0°

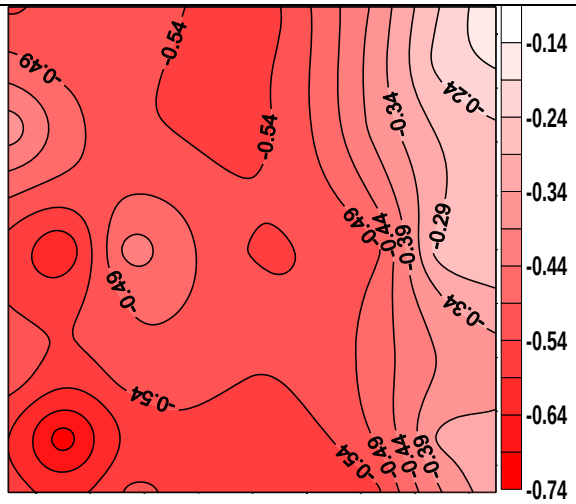

Figure 3B.3 Pressure coefficient contours on the roof of the SEB surrounded by elevated sheet clad scaffold when θ= 15°

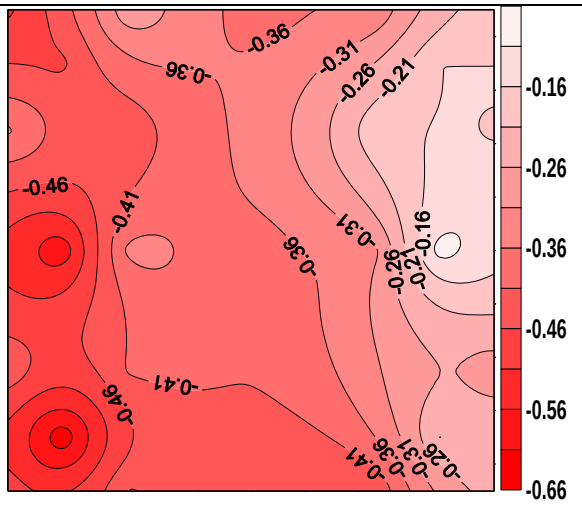

Figure 3B.4 Pressure coefficient contours on the roof of the SEB surrounded by elevated sheet clad scaffold when θ= 30°

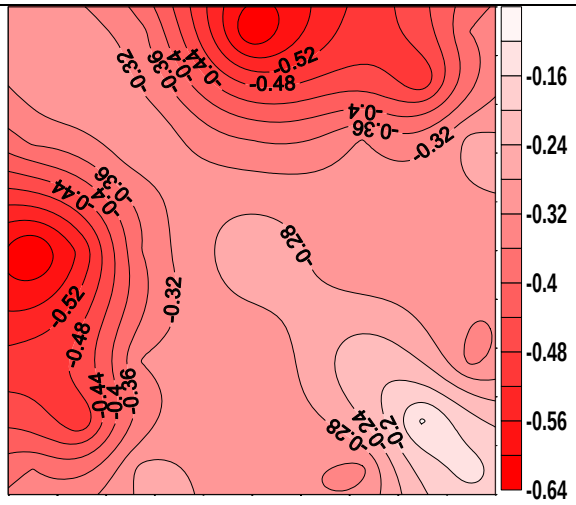

Figure 3B.5 Pressure coefficient contours on the roof of the SEB surrounded by elevated sheet clad scaffold when θ= 45°

Pressure Coefficient Contours on Windward Face of SEB for Type B Terrain

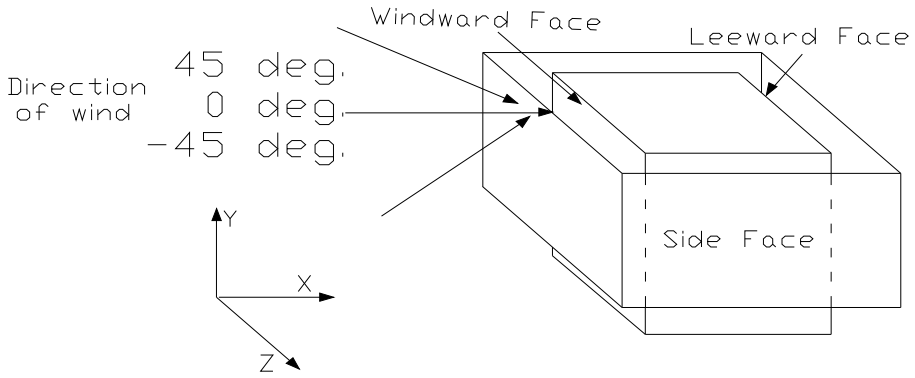

Figure 3B.6 Angle of attack of wind on windward wall of SEB, direction of which varies from -45° to +45°

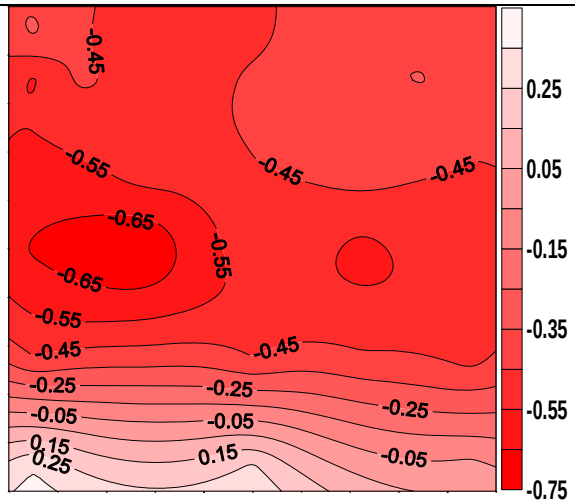

Figure 3B.7 Pressure coefficient contours on the windward face of the SEB surrounded by elevated sheet clad scaffold when θ= -45°

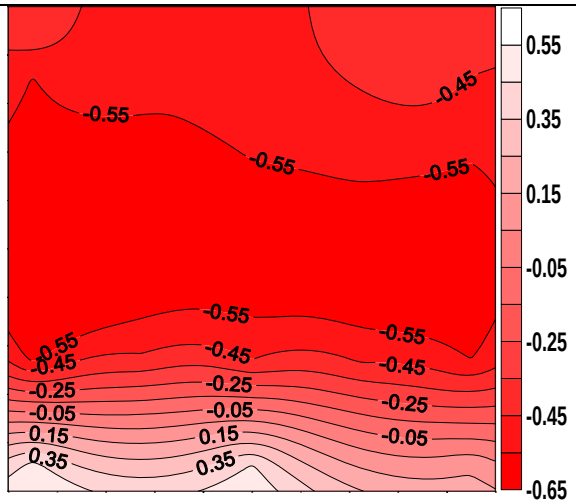

Figure 3B.8 Pressure coefficient contours on the windward face of the SEB surrounded by elevated sheet clad scaffold when θ= -30°

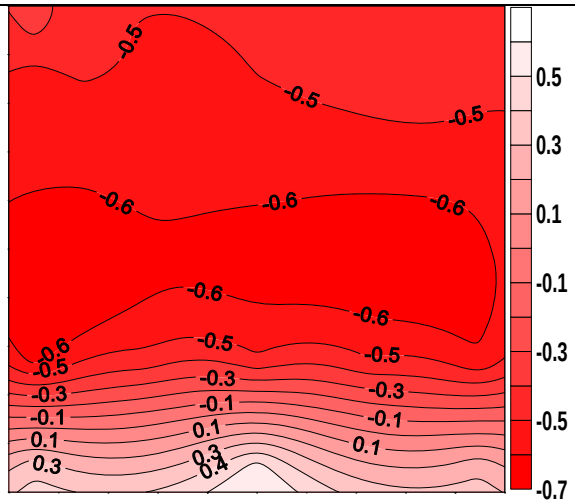

Figure 3B.9 Pressure coefficient contours on the windward face of the SEB surrounded by elevated sheet clad scaffold when θ= -15°

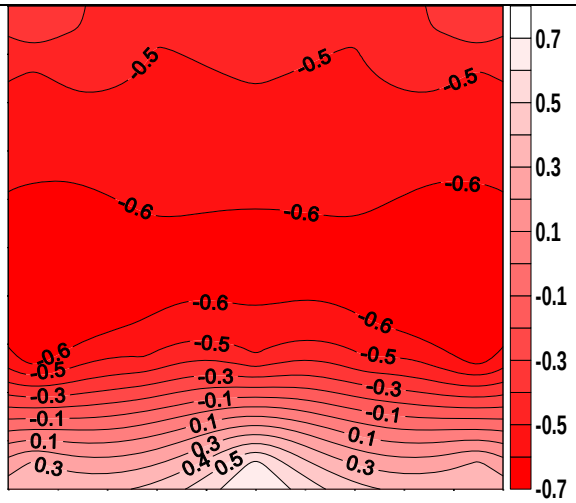

Figure 3B.10 Pressure coefficient contours on the windward face of the SEB surrounded by elevated sheet clad scaffold when θ=0°

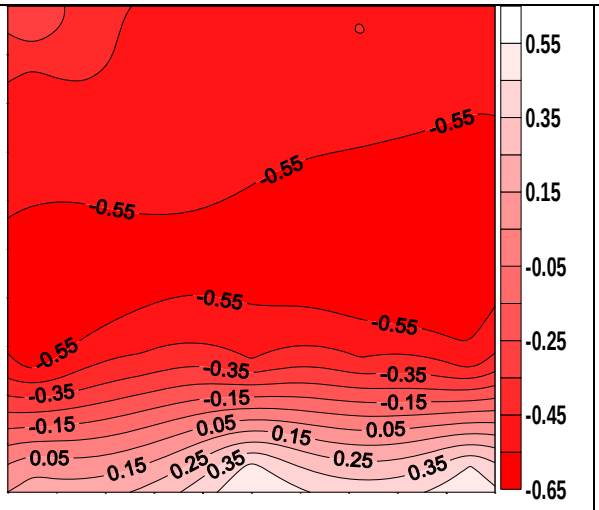

Figure 3B.11 Pressure coefficient contours on the windward face of the SEB surrounded by elevated sheet clad scaffold when θ=+15°

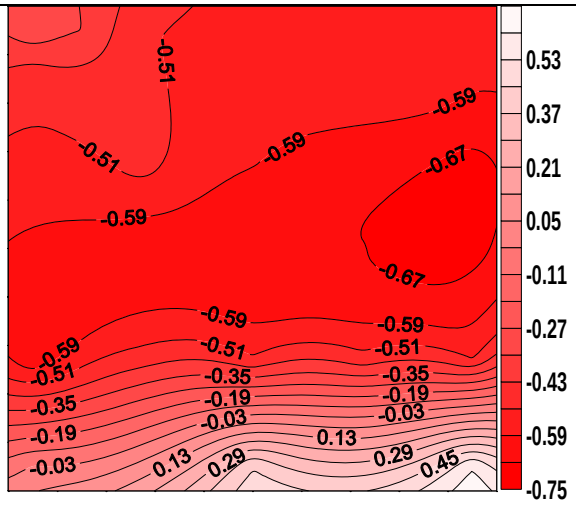

Figure 3B.12 Pressure coefficient contours on the windward face of the SEB surrounded by elevated sheet clad scaffold when θ=+30°

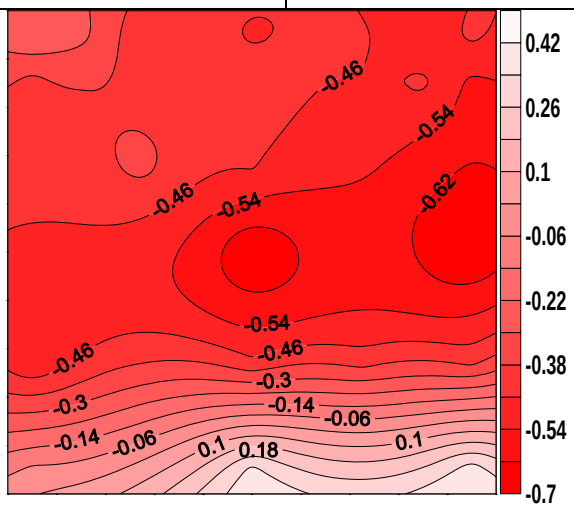

Figure 3B.13 Pressure coefficient contours on the windward face of the SEB surrounded by elevated sheet clad scaffold when θ=+45°

Pressure Coefficient Contours on Side Face of SEB for Type B Terrain

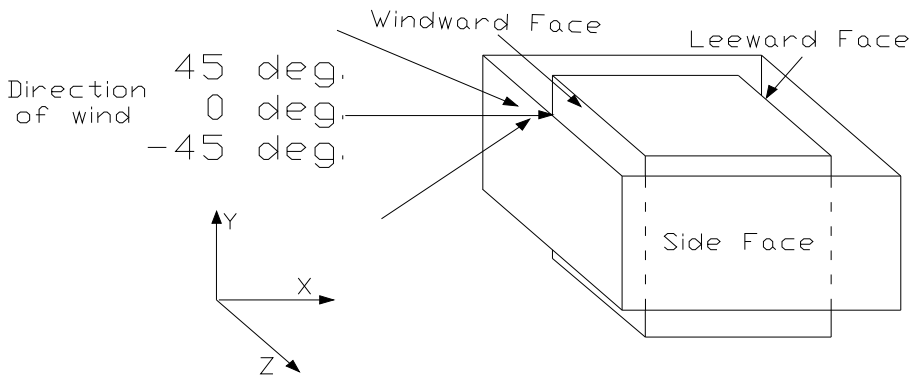

Figure 3B.14 Angle of attack of wind on windward wall of SEB, direction of which varies from -45° to +45°

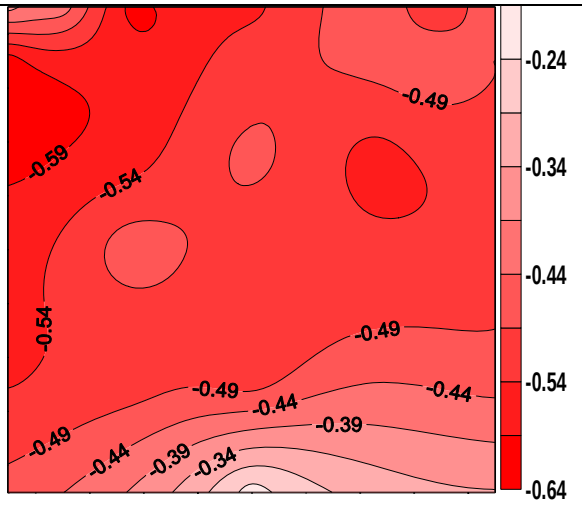

Figure 3B.15 Pressure coefficient contours on the side face of the SEB surrounded by elevated sheet clad scaffold when θ= -45°

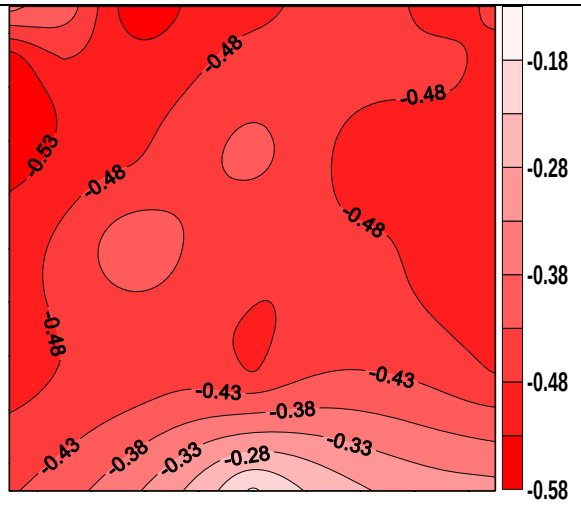

Figure 3B.16 Pressure coefficient contours on the side face of the SEB surrounded by elevated sheet clad scaffold when θ= -30°

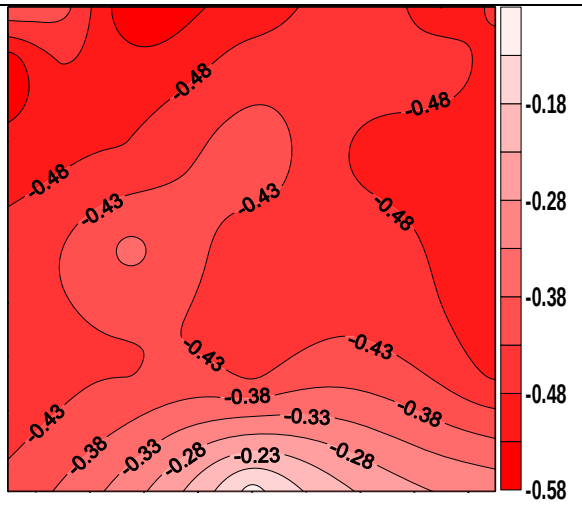

Figure 3B.17 Pressure coefficient contours on the side face of the SEB surrounded by elevated sheet clad scaffold when θ= -15°

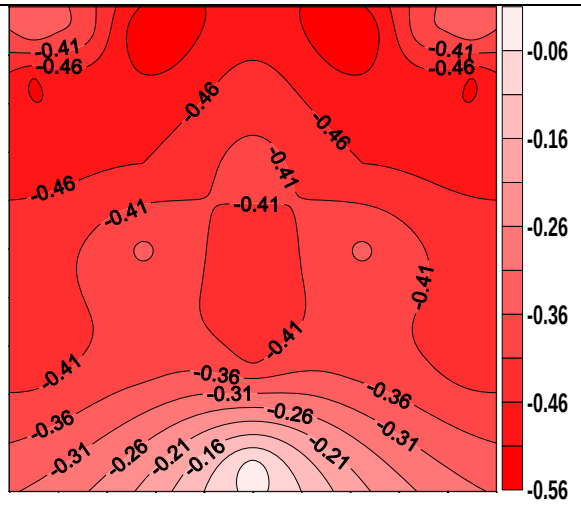

Figure 3B.18 Pressure coefficient contours on the side face of the building surrounded by elevated sheet clad scaffold when θ= 0°

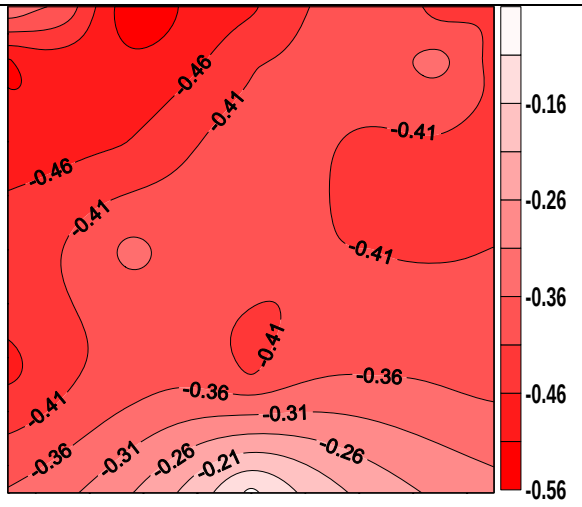

Figure 3B.19 Pressure coefficient contours on the side face of the SEB surrounded by elevated sheet clad scaffold when θ=+15°

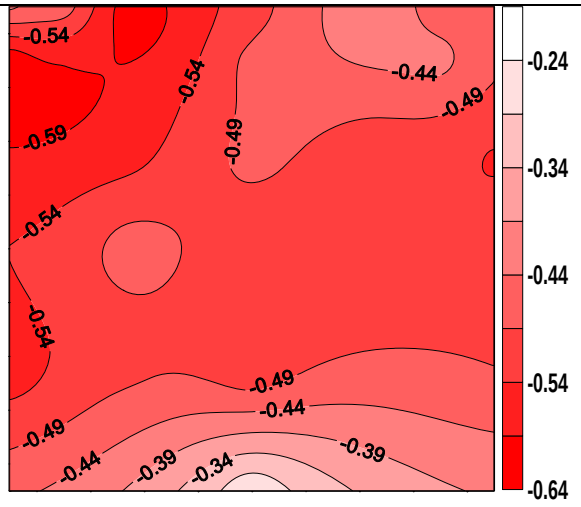

Figure 3B.20 Pressure coefficient contours on the side face of the SEB surrounded by elevated sheet clad scaffold when θ=+30°

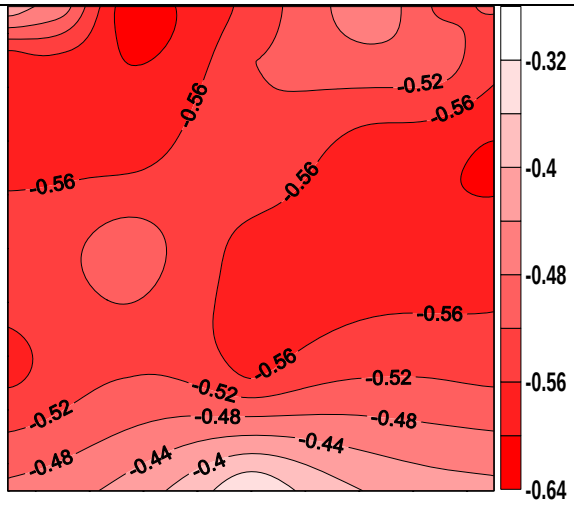

Figure 3B.21 Pressure coefficient contours on the side face of the SEB surrounded by elevated sheet clad scaffold when θ=+45°

Pressure Coefficient Contours on Leeward Face of SEB for Type B Terrain

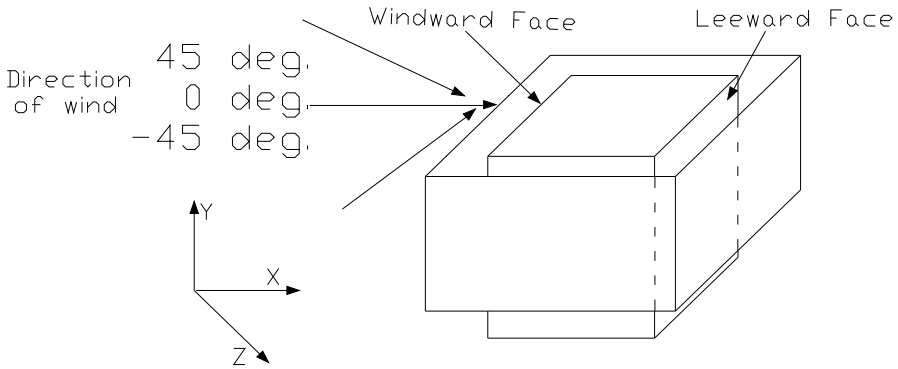

Figure 3B.22 Angle of attack of wind on windward wall of SEB, direction of which varies from -45° to +45°

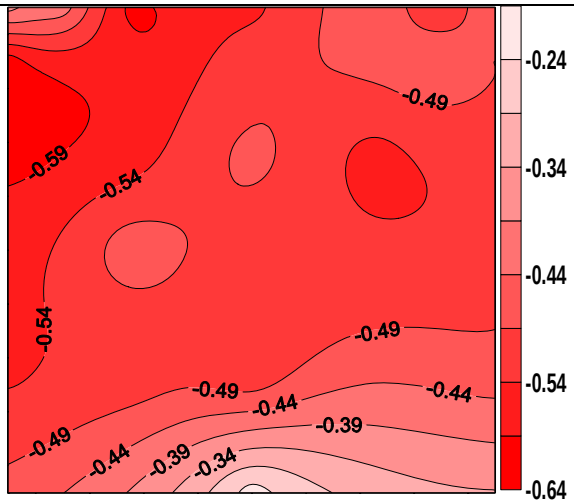

Figure 3B.23 Pressure coefficient contours on the leeward face of the SEB surrounded by elevated sheet clad scaffold when θ= -45°

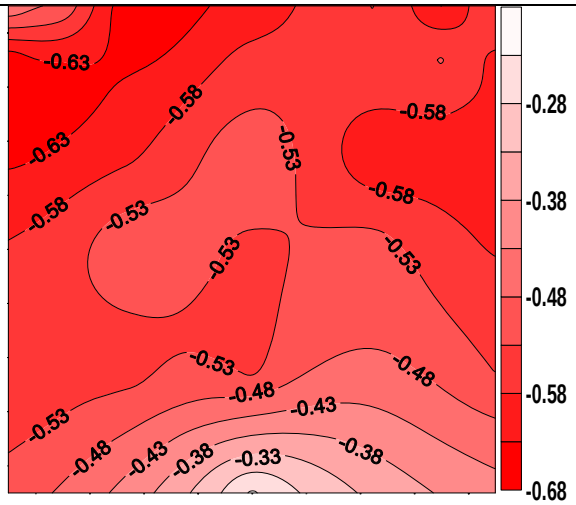

Figure 3B.24 Pressure coefficient contours on the leeward face of the SEB surrounded by elevated sheet clad scaffold when θ= -30°

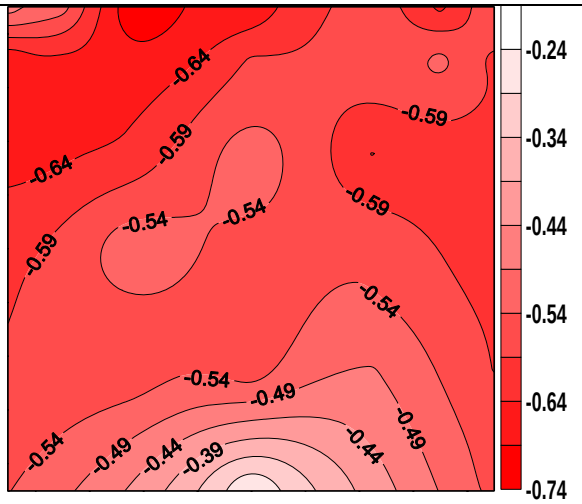

Figure 3B.25 Pressure coefficient contours on the leeward face of the SEB surrounded by elevated sheet clad scaffold when θ= -15°

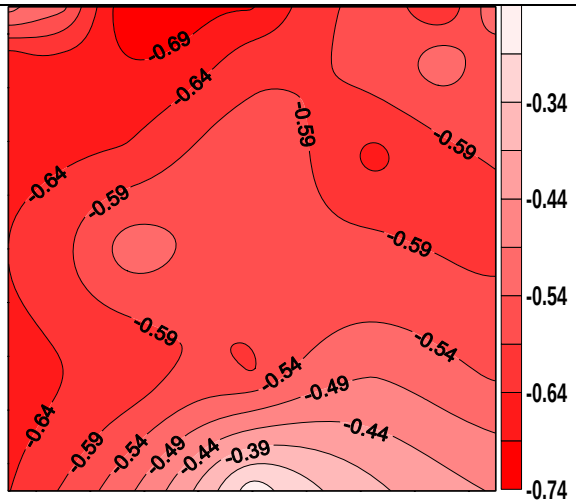

Figure 3B.26 Pressure coefficient contours on the leeward face of the SEB surrounded by elevated sheet clad scaffold when θ= 0°

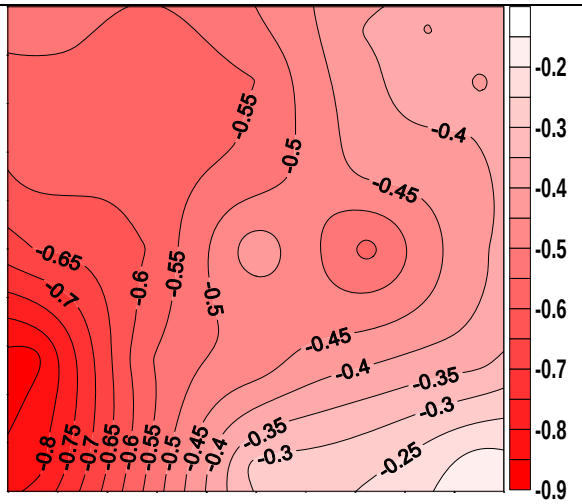

Figure 3B.27 Pressure coefficient contours on the leeward face of the SEB surrounded by elevated sheet clad scaffold when θ= +15°

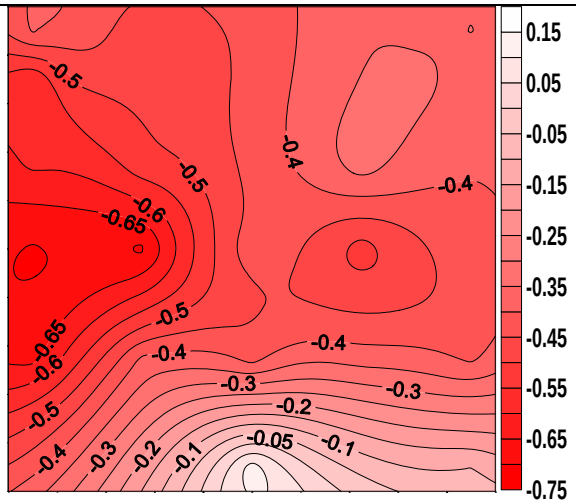

Figure 3B.28 Pressure coefficient contours on the leeward face of the SEB surrounded by elevated sheet clad scaffold when θ= +30°

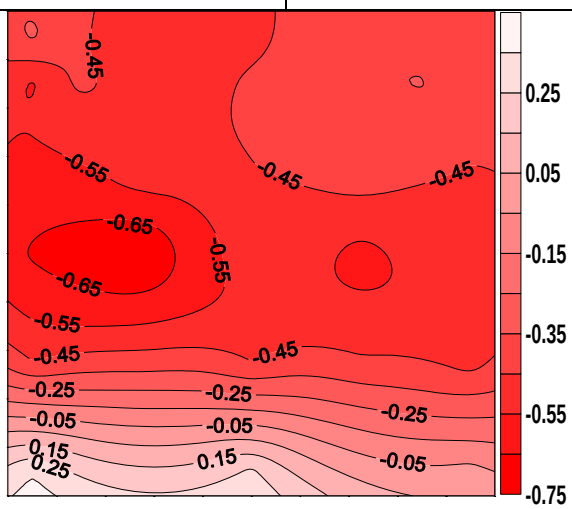

Figure 3B.29 Pressure coefficient contours on the leeward face of the SEB surrounded by elevated sheet clad scaffold when θ= +45°

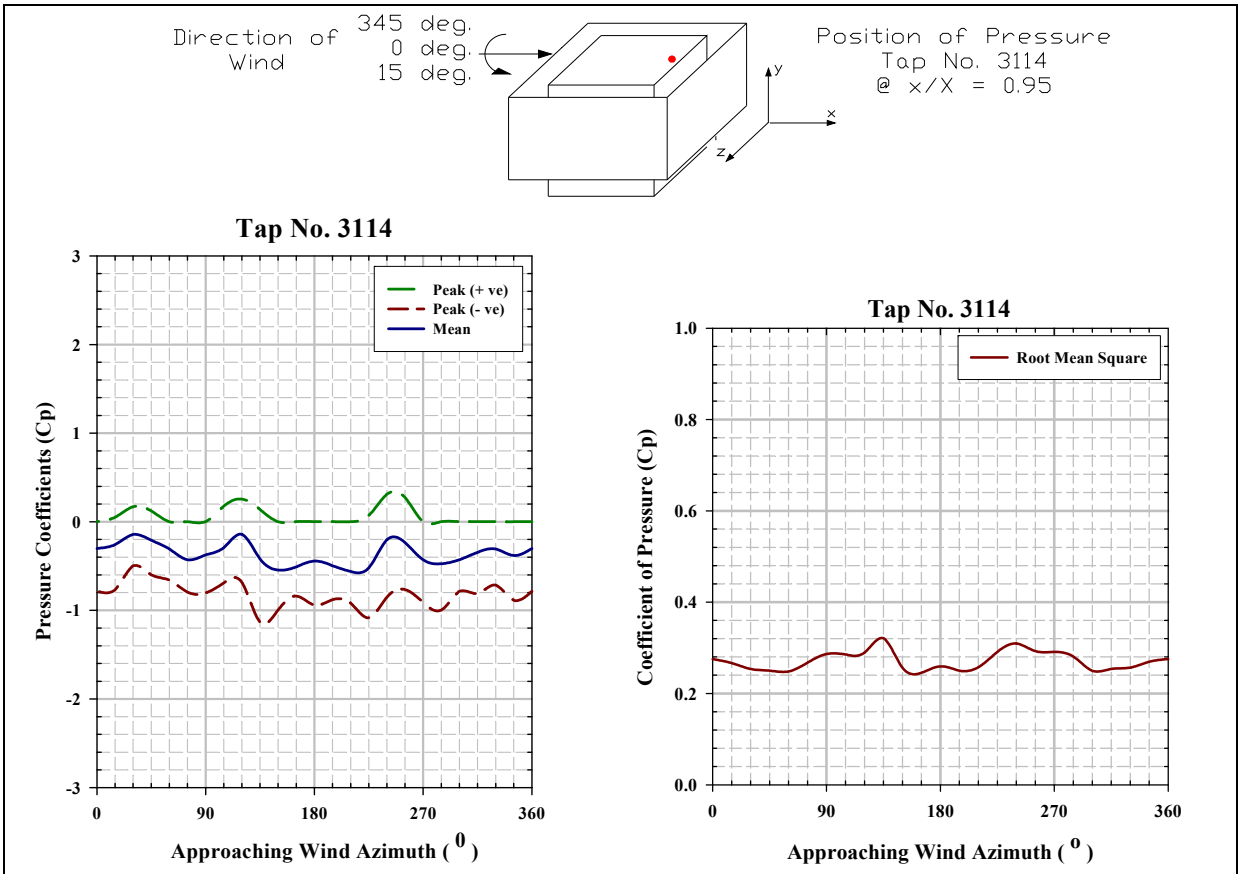

Figure 3B.30 Mean, peak and rms pressure coefficients for tap number 3114

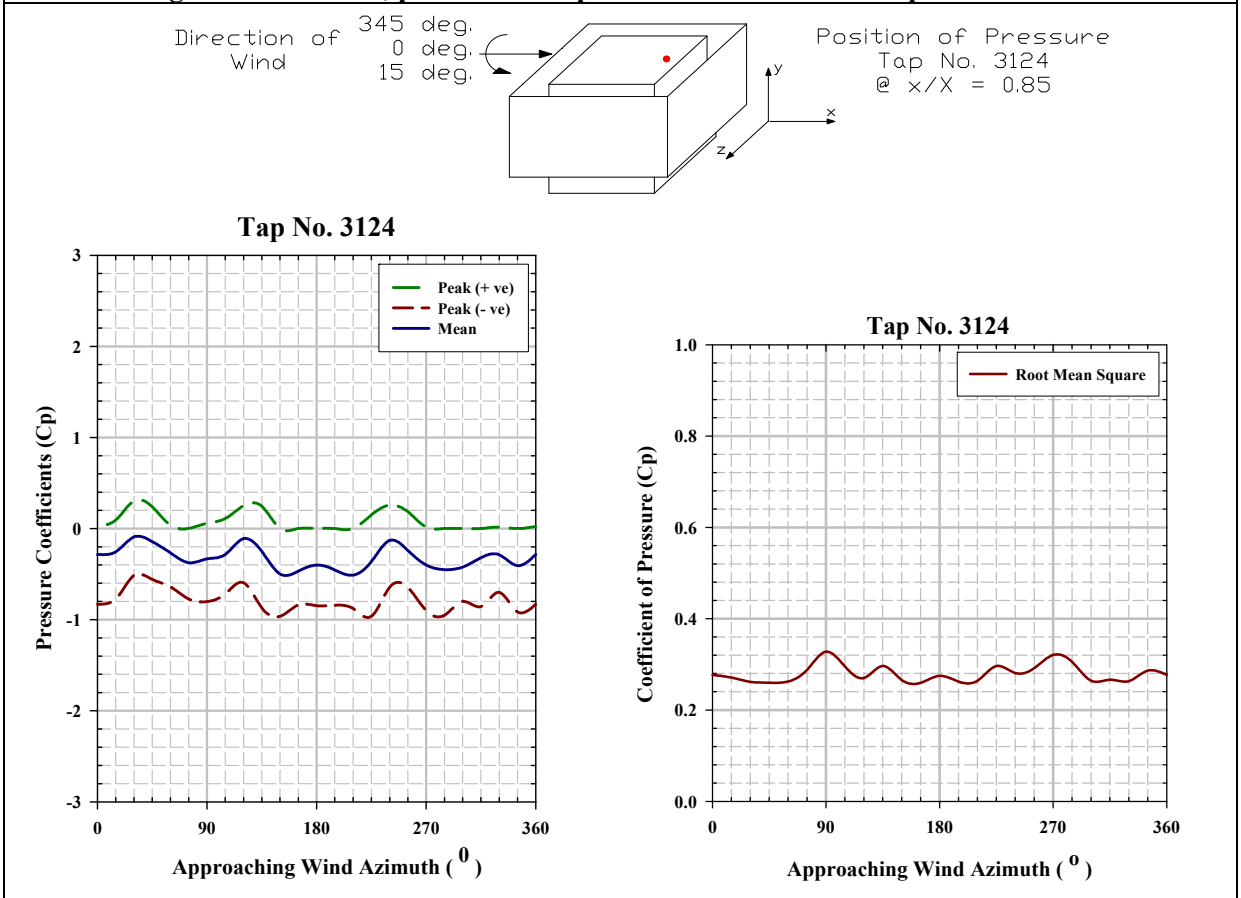

Figure 3B.31 Mean, peak and rms pressure coefficients for tap number 3124

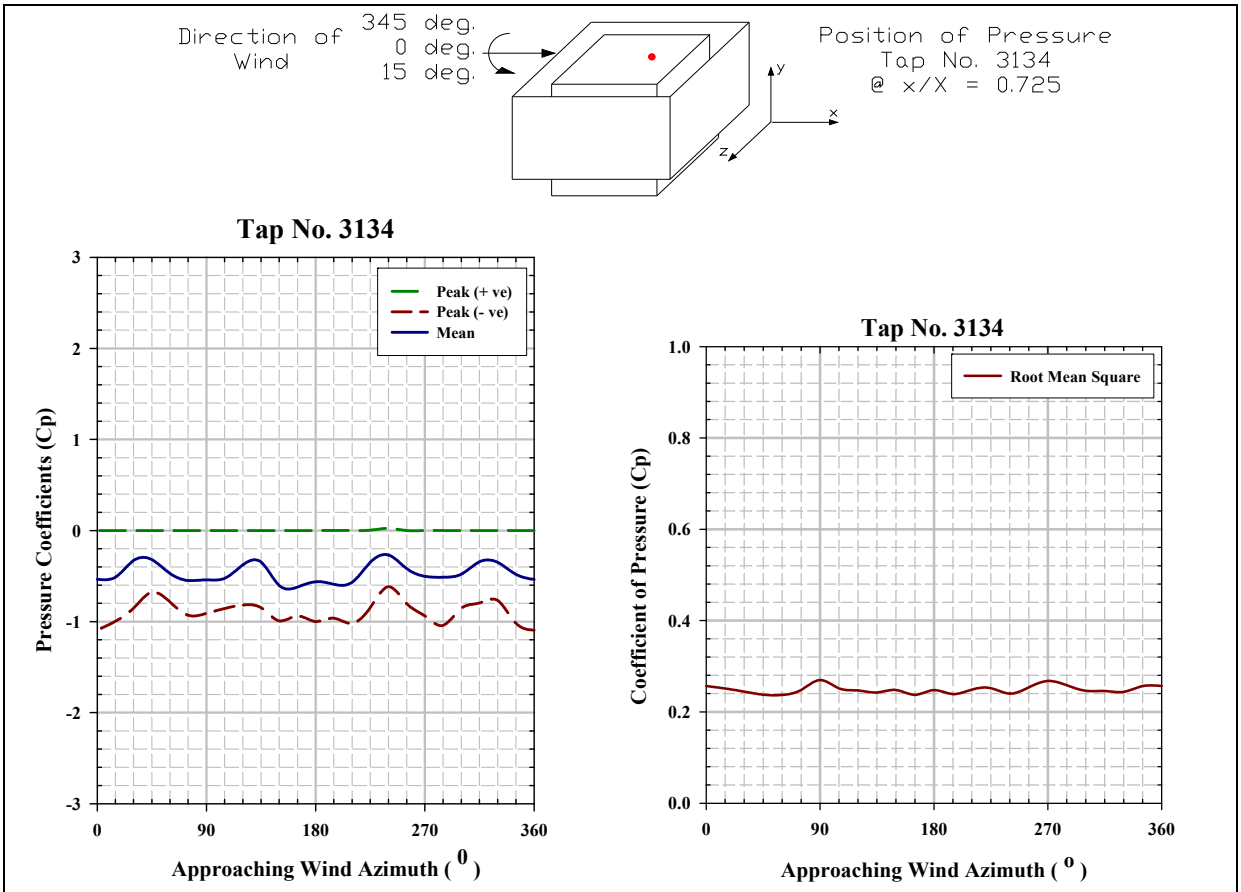

Figure 3B.32 Mean, peak and rms pressure coefficients for tap number 3134

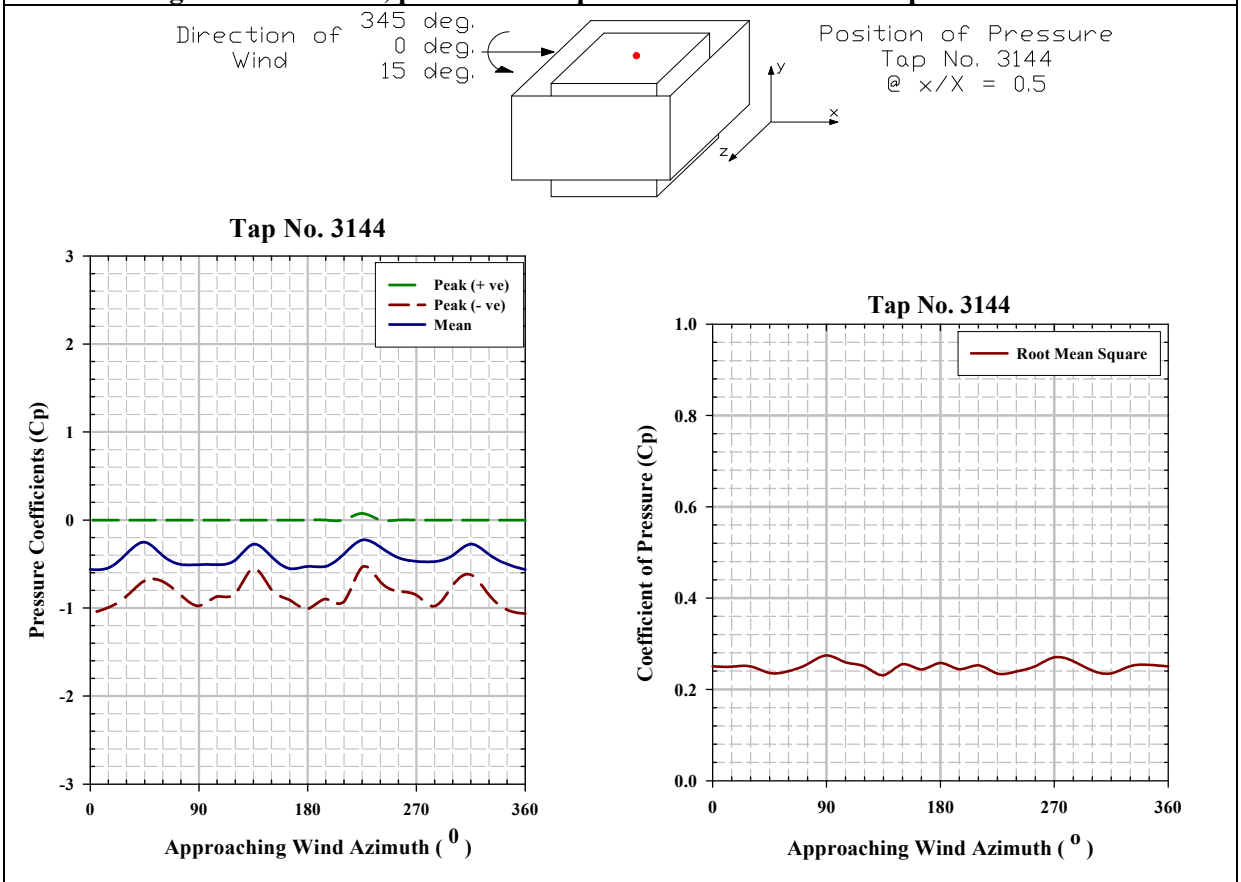

Figure 3B.33 Mean, peak and rms pressure coefficients for tap number 3144

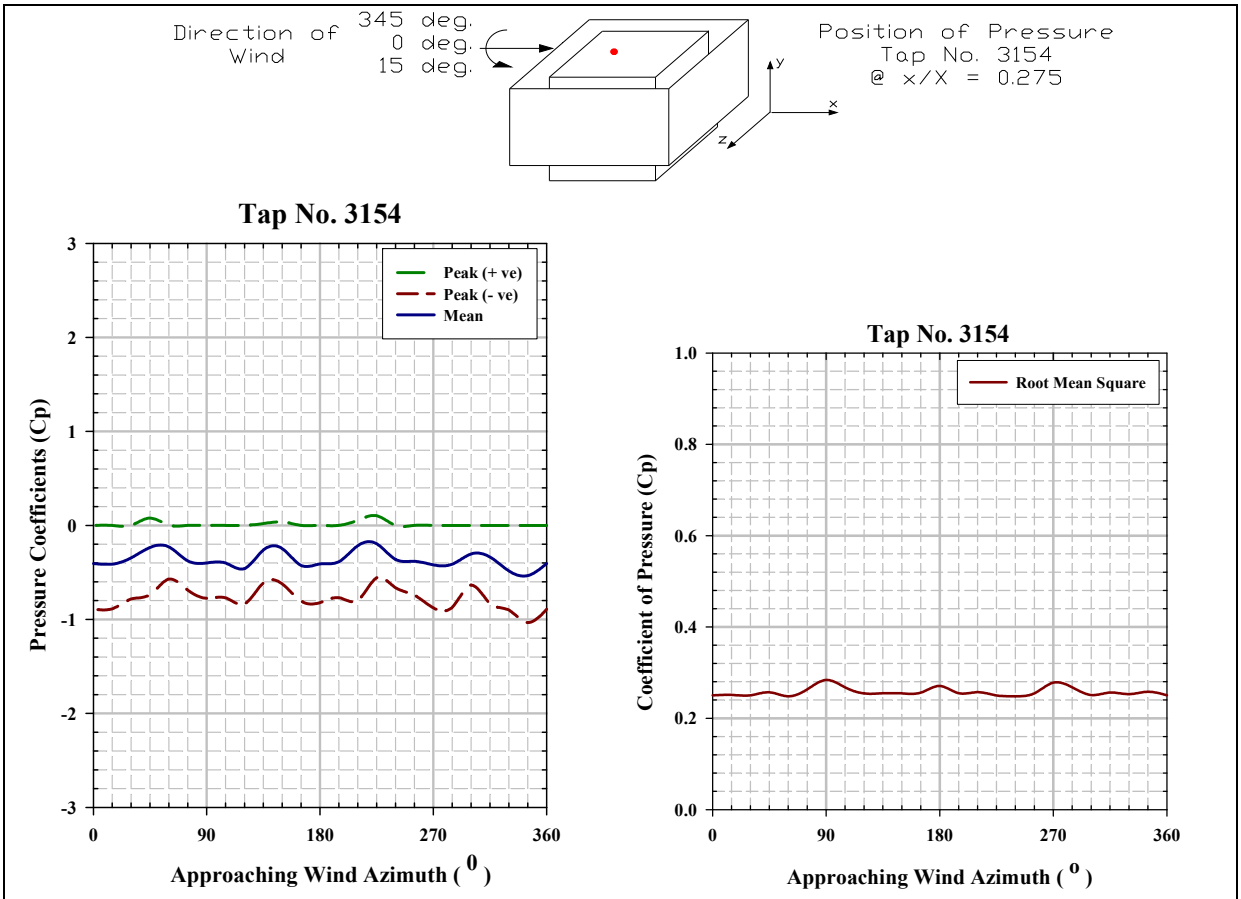

Figure 3B.34 Mean, peak and rms pressure coefficients for tap number 3154

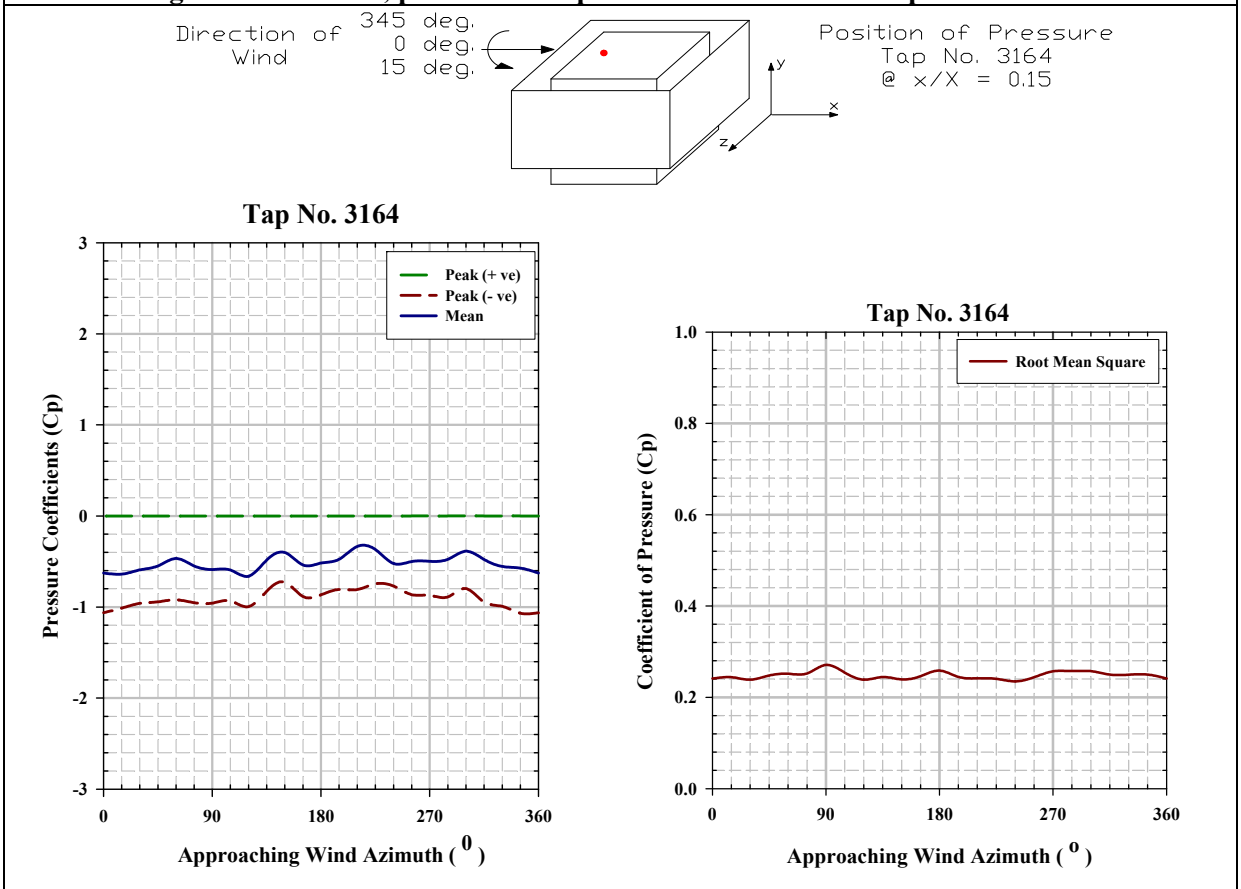

Figure 3B.35 Mean, peak and rms pressure coefficients for tap number 3164

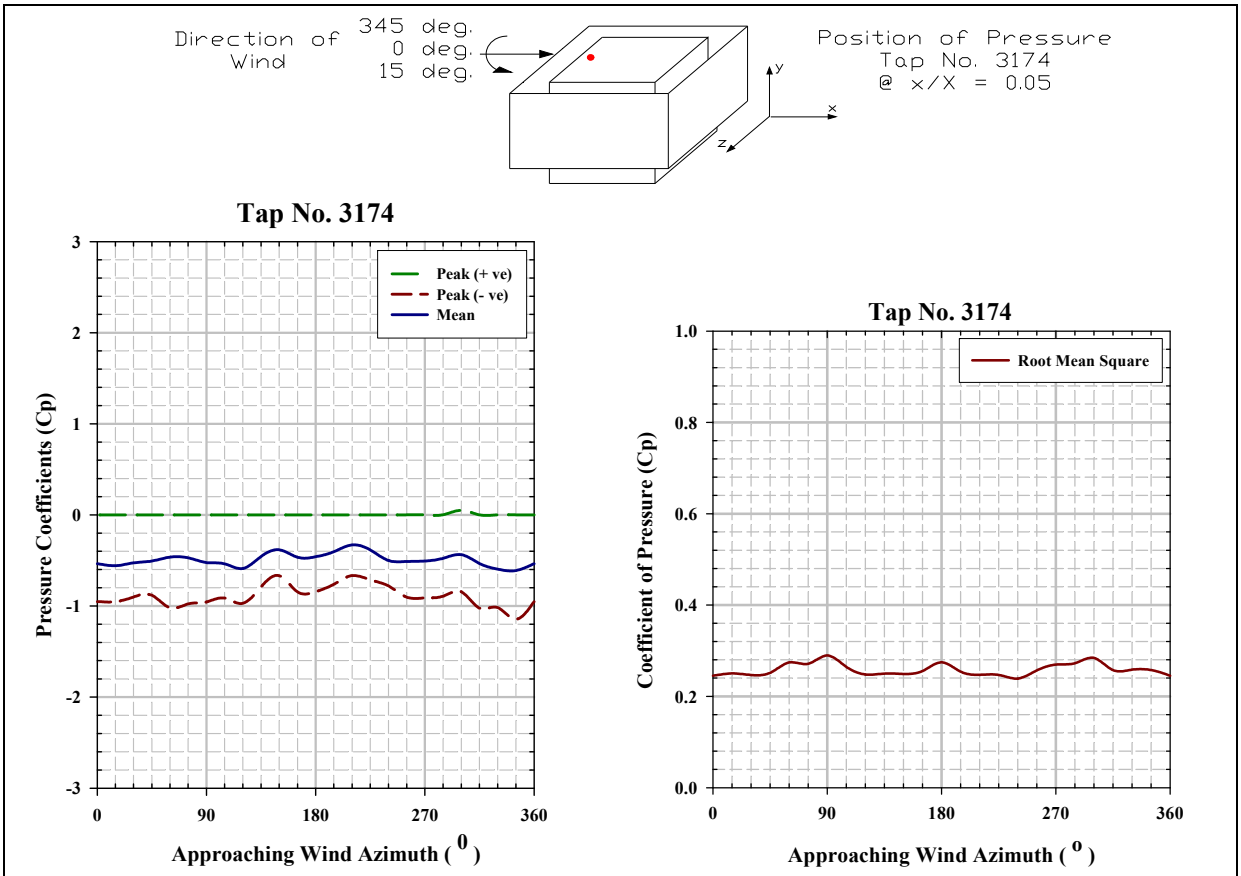

Figure 3B.36 Mean, peak and rms pressure coefficients for tap number 3174

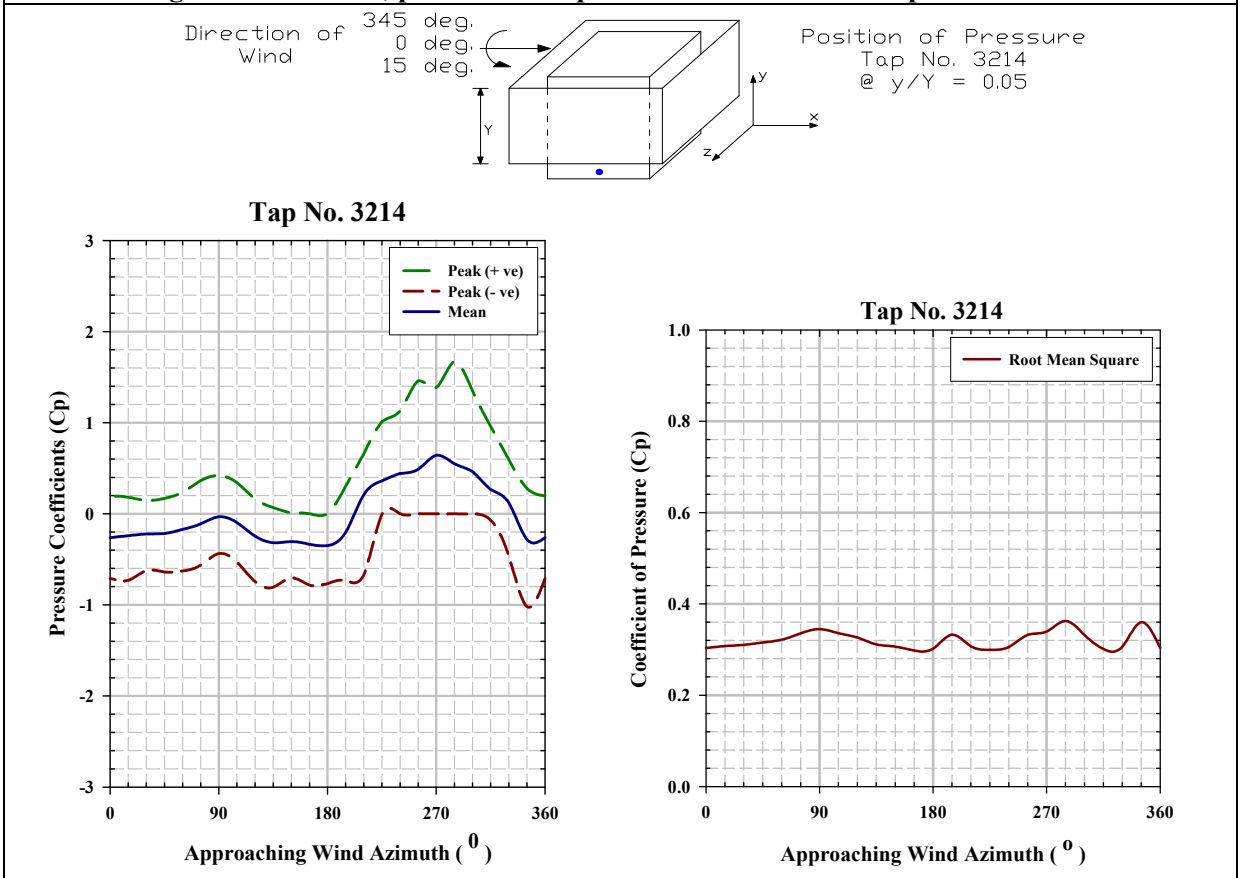

Figure 3B.37 Mean, peak and rms pressure coefficients for tap number 3214

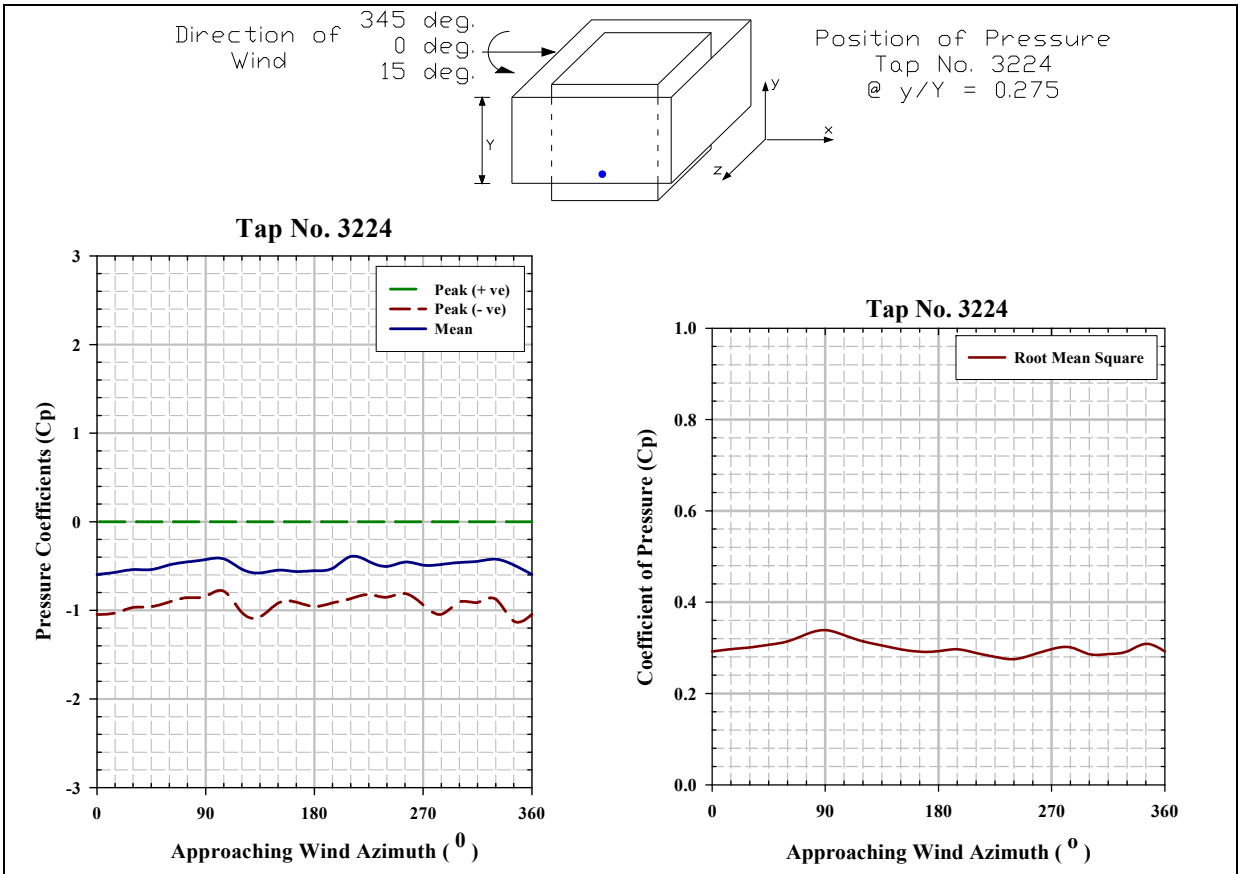

Figure 3B.38 Mean, peak and rms pressure coefficients for tap number 3224

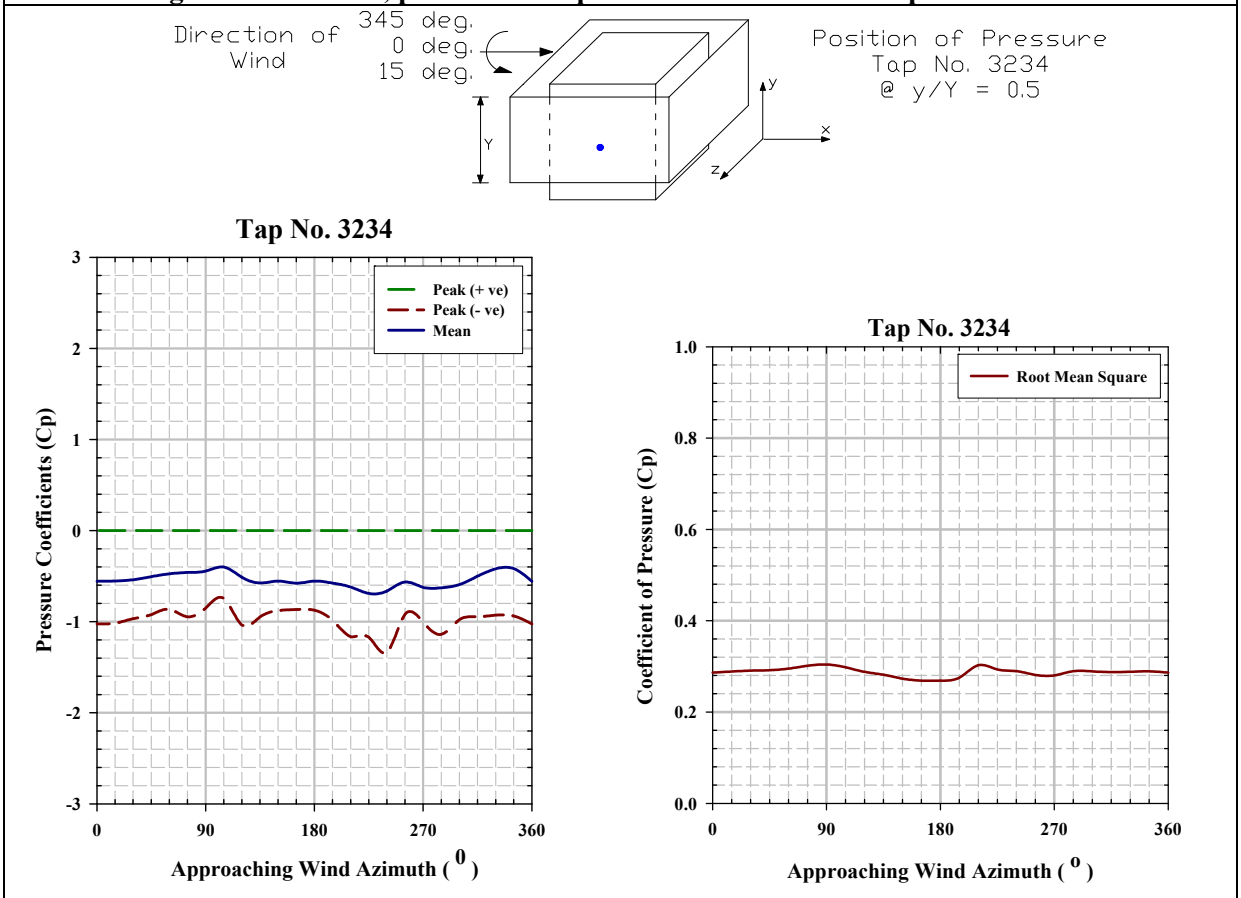

Figure 3B.39 Mean, peak and rms pressure coefficients for tap number 3234

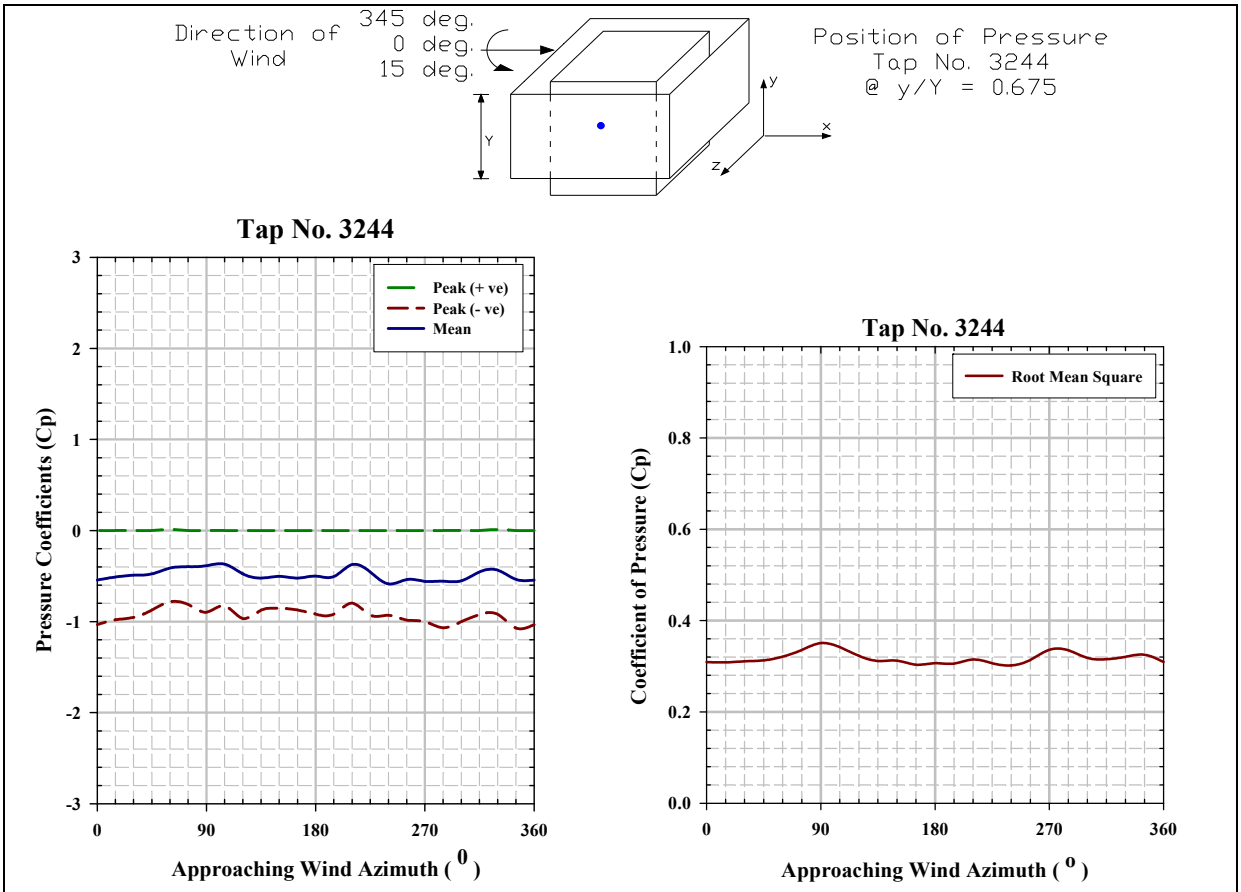

Figure 3B.40 Mean, peak and rms pressure coefficients for tap number 3244

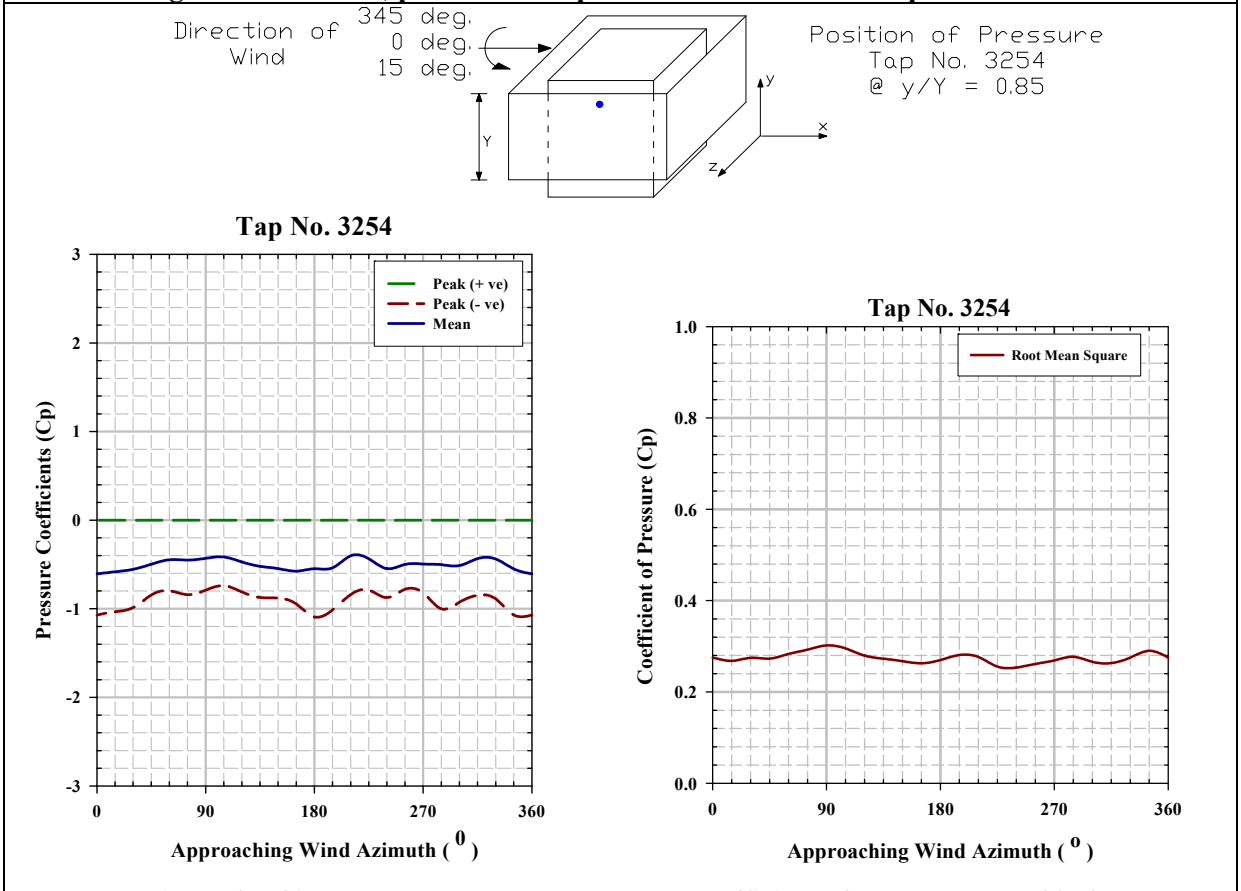

Figure 3B.41 Mean, peak and rms pressure coefficients for tap number 3254

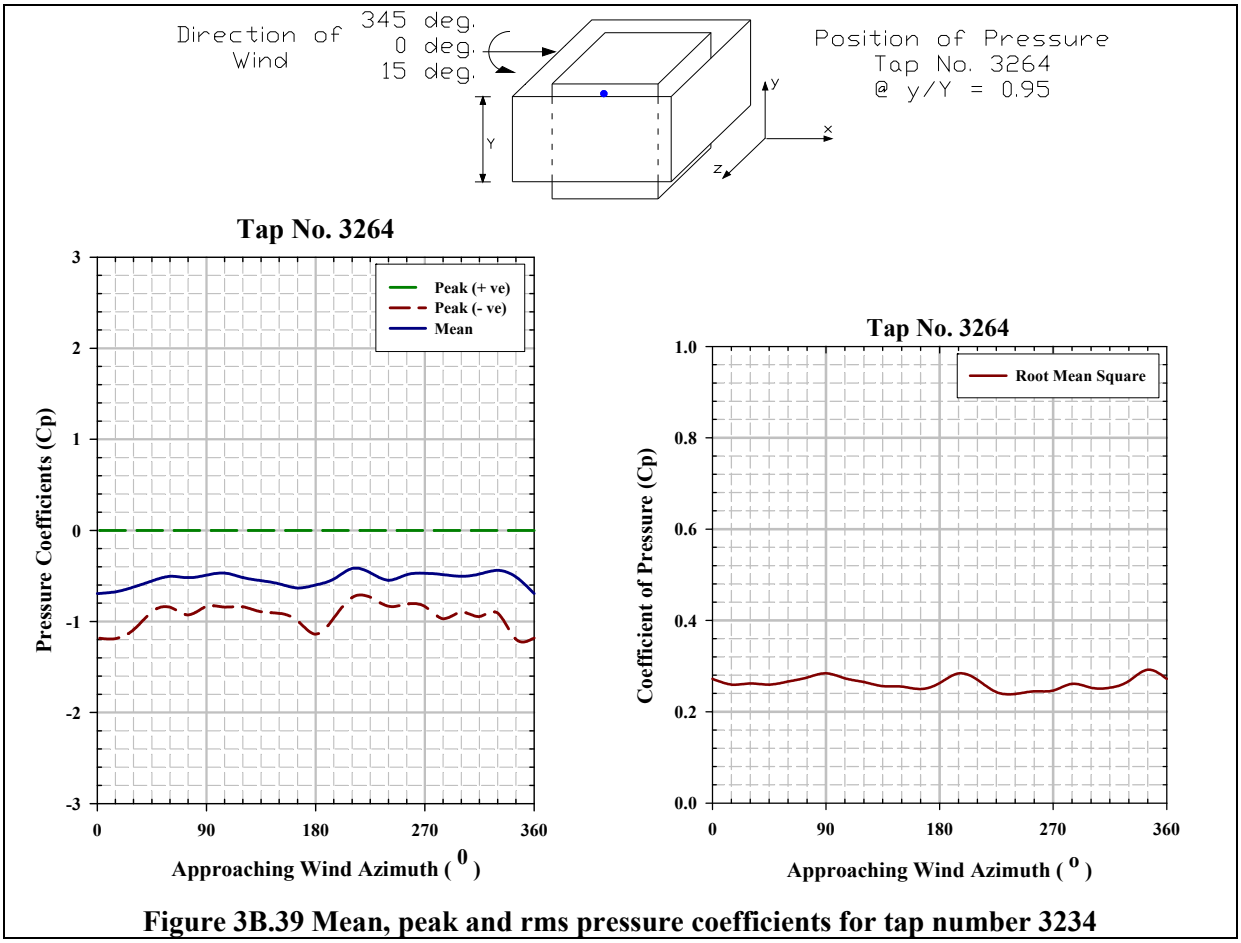

Figure 3B.39 Mean, peak and rms pressure coefficients for tap number 3234

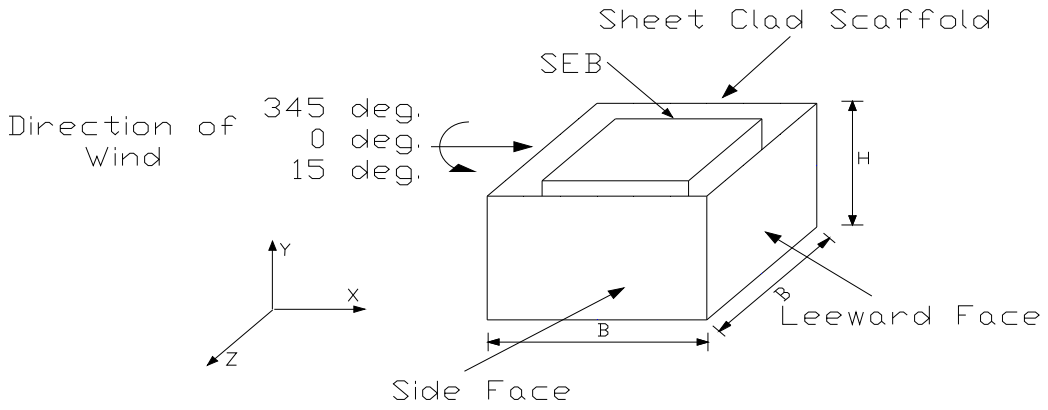

Figure 4.1 Scaled cubical SEB surrounded by sheet clad scaffold

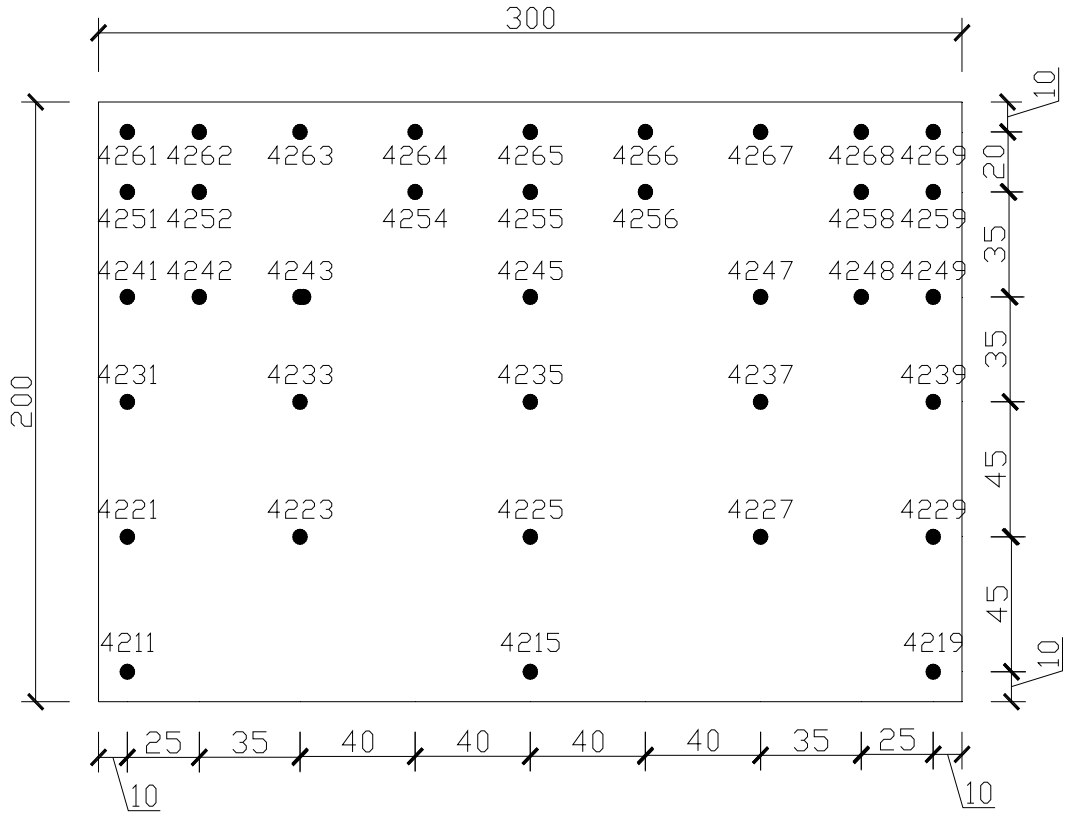

Figure 4.2 Pressure tap locations on the outer face of the sheet clad scaffold

Pressure Coefficient Contours on Windward Outer Face of the Sheet Clad Scaffold for Type A Terrain

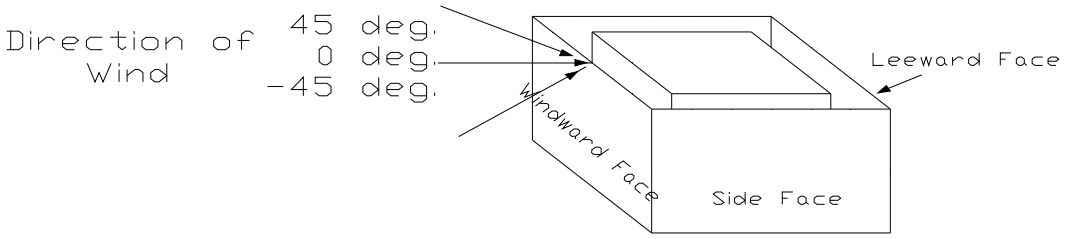

Figure 4A.1 Angle of attack of wind on windward outer face of sheet clad scaffold surrounding SEB, direction of which varies from -45^o to +45^o

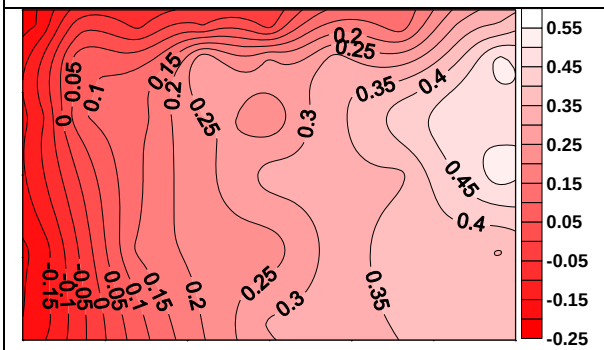

Figure 4A.2 Pressure coefficient contours on the windward outer face of the sheet clad scaffold when θ= 45^o

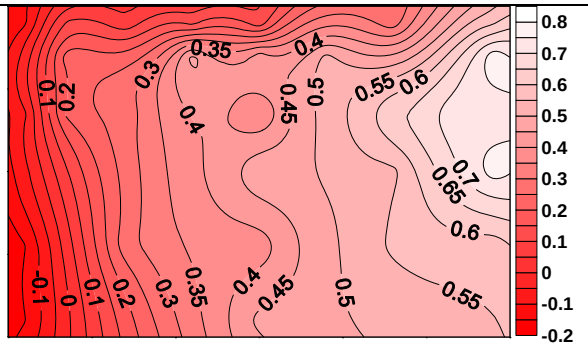

Figure 4A.3 Pressure coefficient contours on the windward outer face of the sheet clad scaffold when θ= 30^o

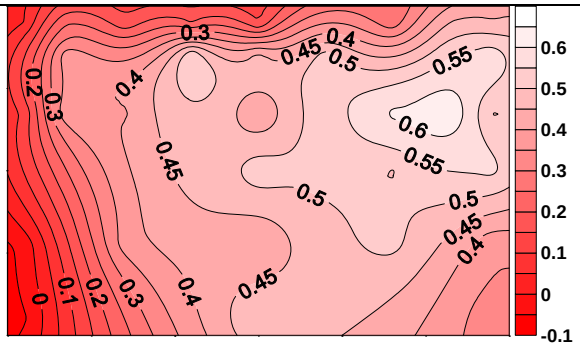

Figure 4A.4 Pressure coefficient contours on the windward outer face of the sheet clad scaffold when θ= 15^o

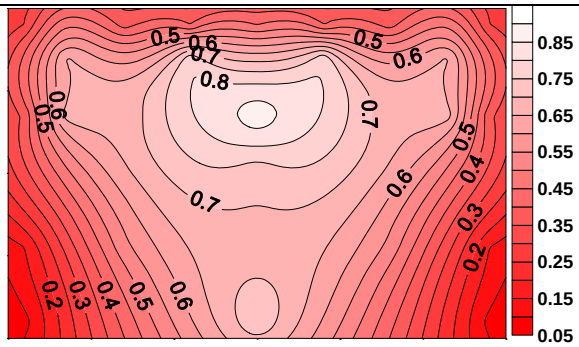

Figure 4A.5 Pressure coefficient contours on the windward outer face of the sheet clad scaffold when θ= 0^o

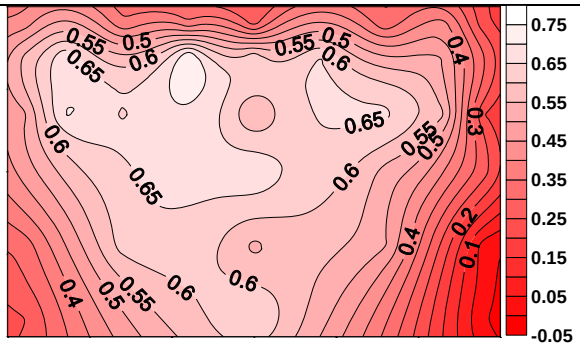

Figure 4A.6 Pressure coefficient contours on the windward outer face of the sheet clad scaffold when θ= -15^o

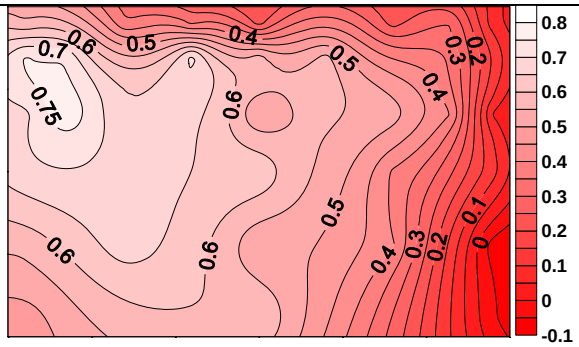

Figure 4A.7 Pressure coefficient contours on the windward outer face of the sheet clad scaffold when θ= -30^o

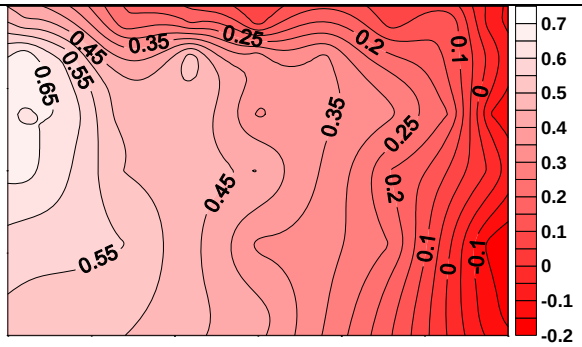

Figure 4A.8 Pressure coefficient contours on the windward outer face of the sheet clad scaffold when θ= -45°

Pressure Coefficient Contours on the Side Outer Face of the Sheet Clad Scaffold for Type A Terrain

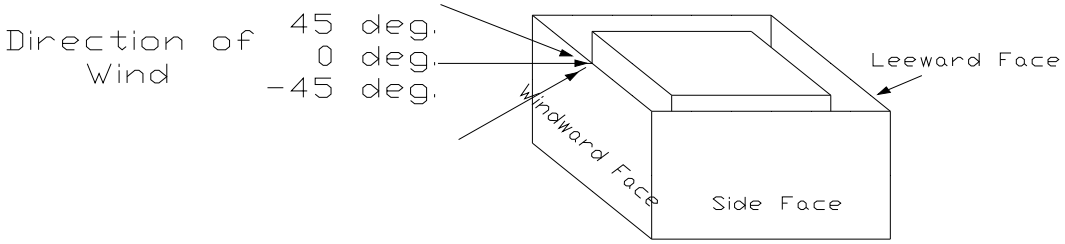

Figure 4A.9 Angle of attack of wind on windward outer face of sheet clad scaffold surrounding SEB, direction of which varies from 45° to -45°

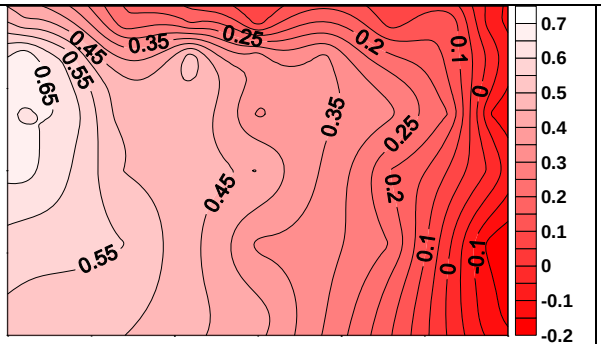

Figure 4A.10 Pressure coefficient contours on the side outer face of the sheet clad scaffold when θ= 45°

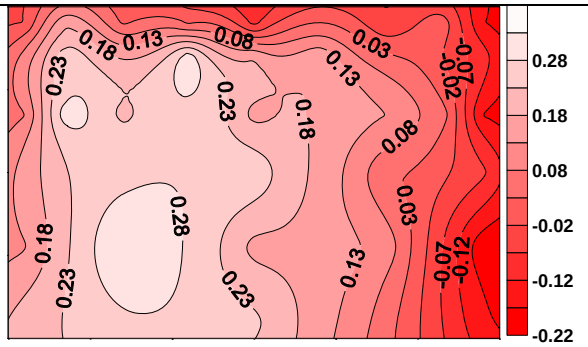

Figure 4A.11 Pressure coefficient contours on the side outer face of the sheet clad scaffold when θ= 30°

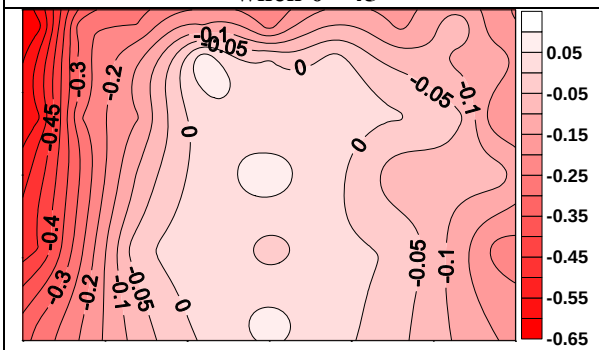

Figure 4A.12 Pressure coefficient contours on the side outer face of the sheet clad scaffold when θ= 15°

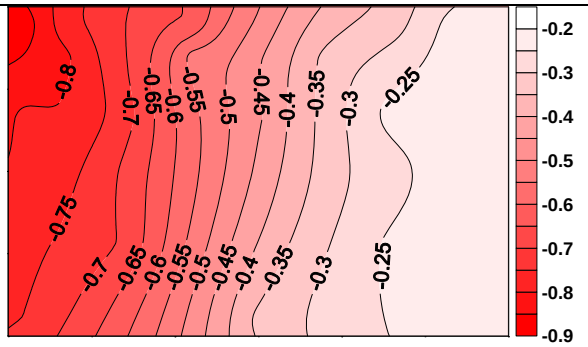

Figure 4A.13 Pressure coefficient contours on the side outer face of the sheet clad scaffold when θ= 0°

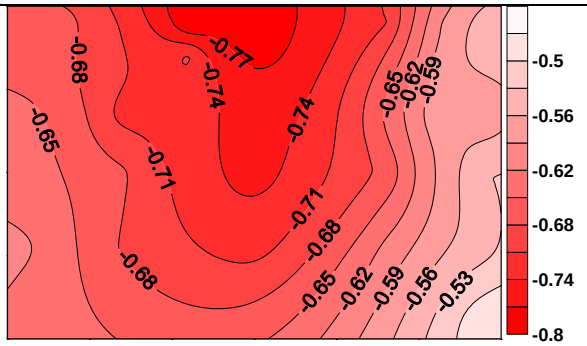

Figure 4A.14 Pressure coefficient contours on the side outer face of the sheet clad scaffold when θ= -15°

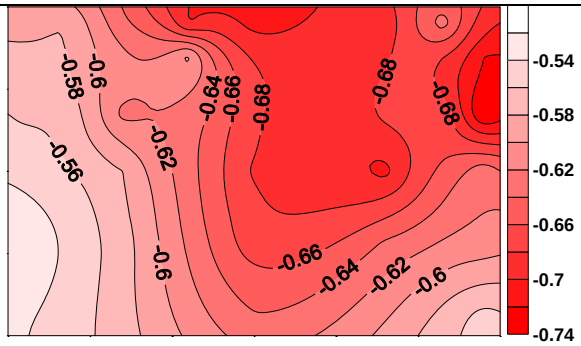

Figure 4A.15 Pressure coefficient contours on the side outer face of the sheet clad scaffold when θ= -30°

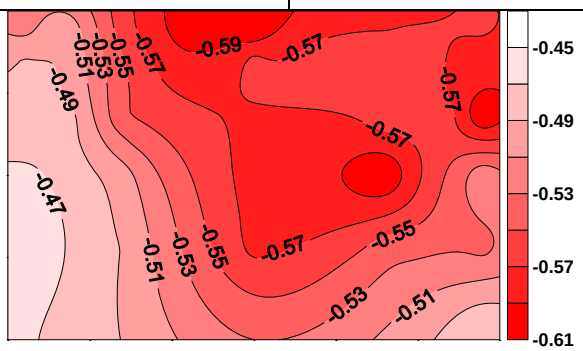

Figure 4A.16 Pressure coefficient contours on the side outer face of the sheet clad scaffold when θ= -45°

Pressure Coefficient Contours on the Leeward Outer Face of the Sheet Clad Scaffold for Type A Terrain

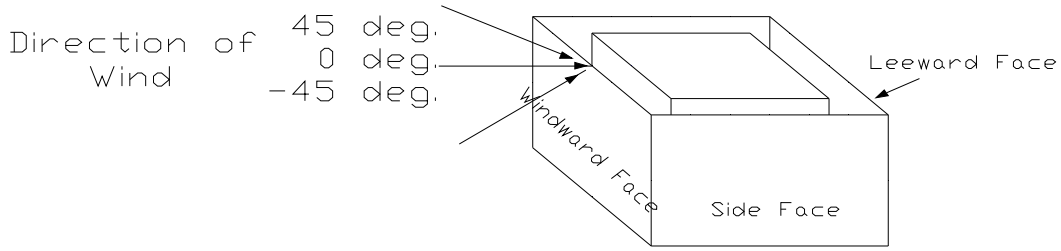

Figure 4A.17 Angle of attack of wind on windward outer face of sheet clad scaffold surrounding SEB, direction of which varies from 45° to -45°

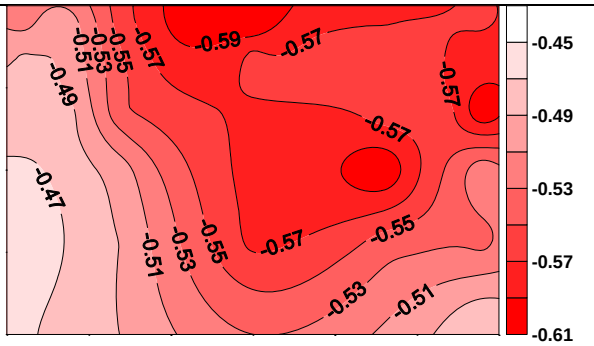

Figure 4A.18 Pressure coefficient contours on the leeward outer face of the sheet clad scaffold when θ= 45°

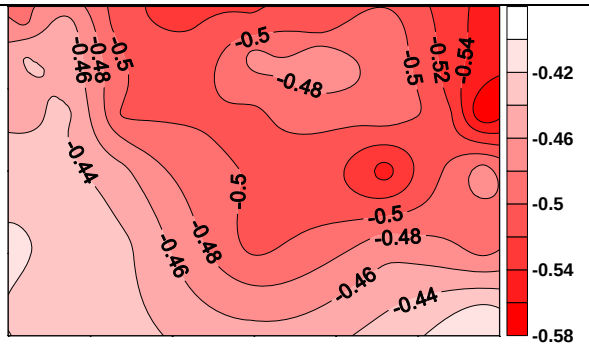

Figure 4A.19 Pressure coefficient contours on the leeward outer face of the sheet clad scaffold when θ= 30°

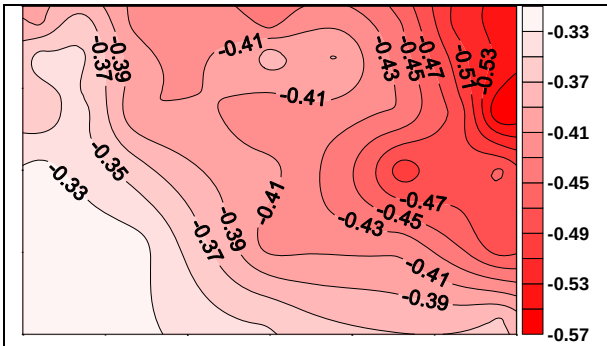

Figure 4A.20 Pressure coefficient contours on the leeward outer face of the sheet clad scaffold when θ= 15°

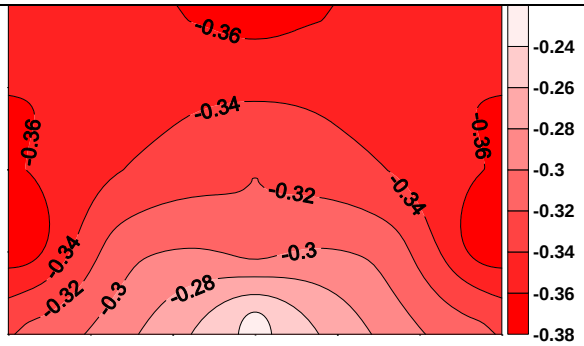

Figure 4A.21 Pressure coefficient contours on the leeward outer face of the sheet clad scaffold when θ= 0°

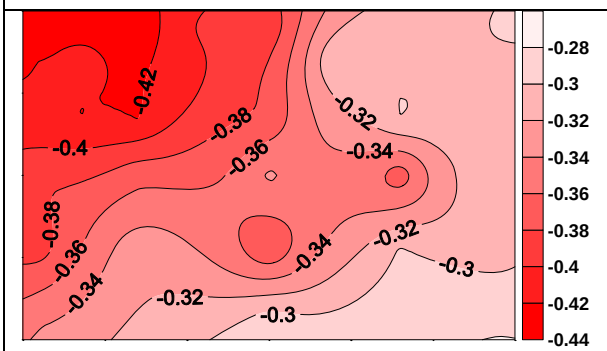

Figure 4A.22 Pressure coefficient contours on the leeward outer face of the sheet clad scaffold when θ= -15°

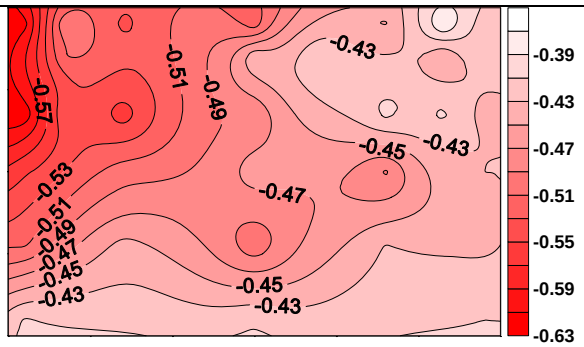

Figure 4A.23 Pressure coefficient contours on the leeward outer face of the sheet clad scaffold when θ= -30°

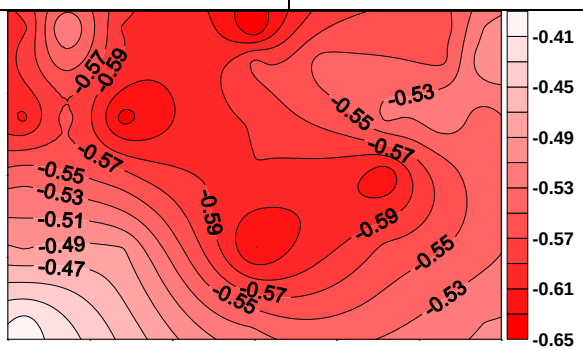

Figure 4A.24 Pressure coefficient contours on the leeward outer face of the sheet clad scaffold when θ= -45°

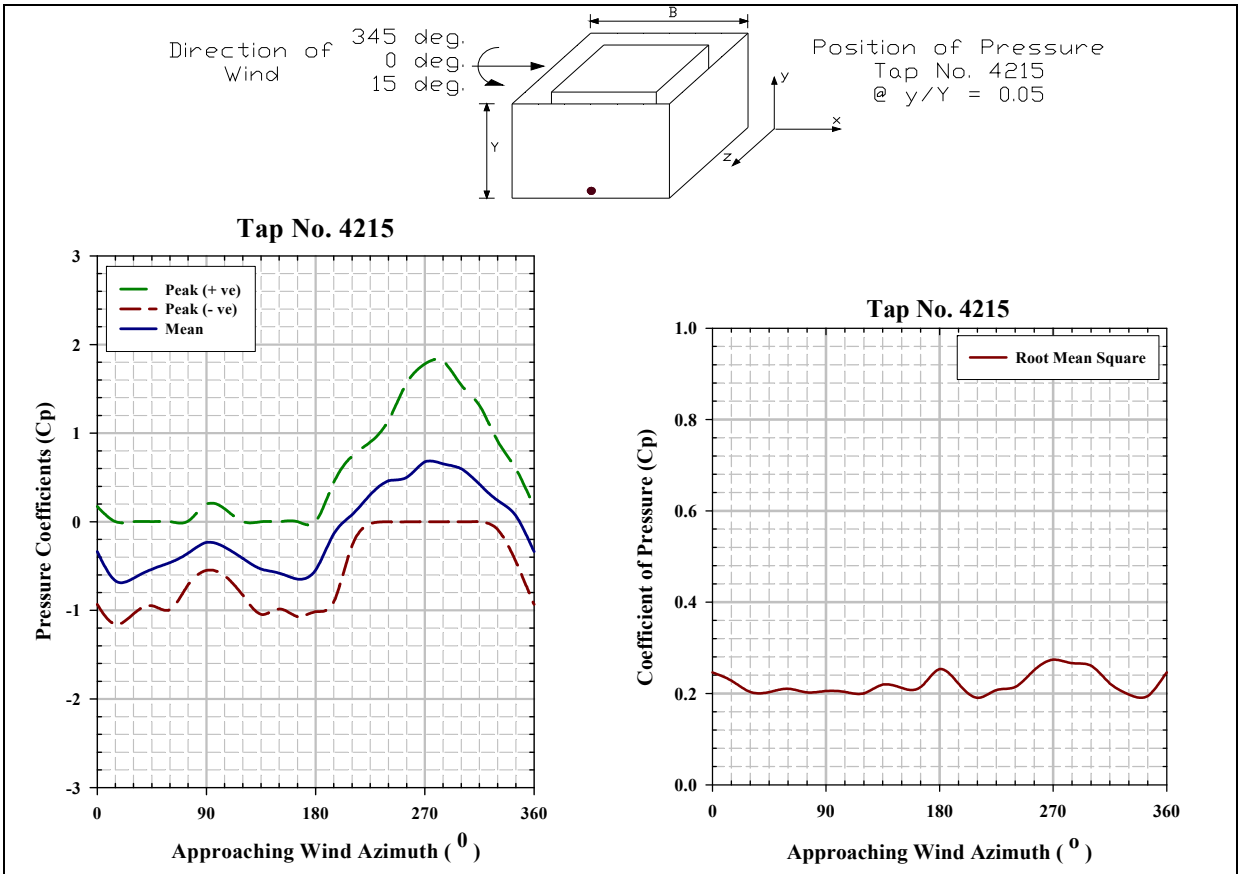

Figure 4A.25 Mean, peak and rms pressure coefficients for tap number 4215

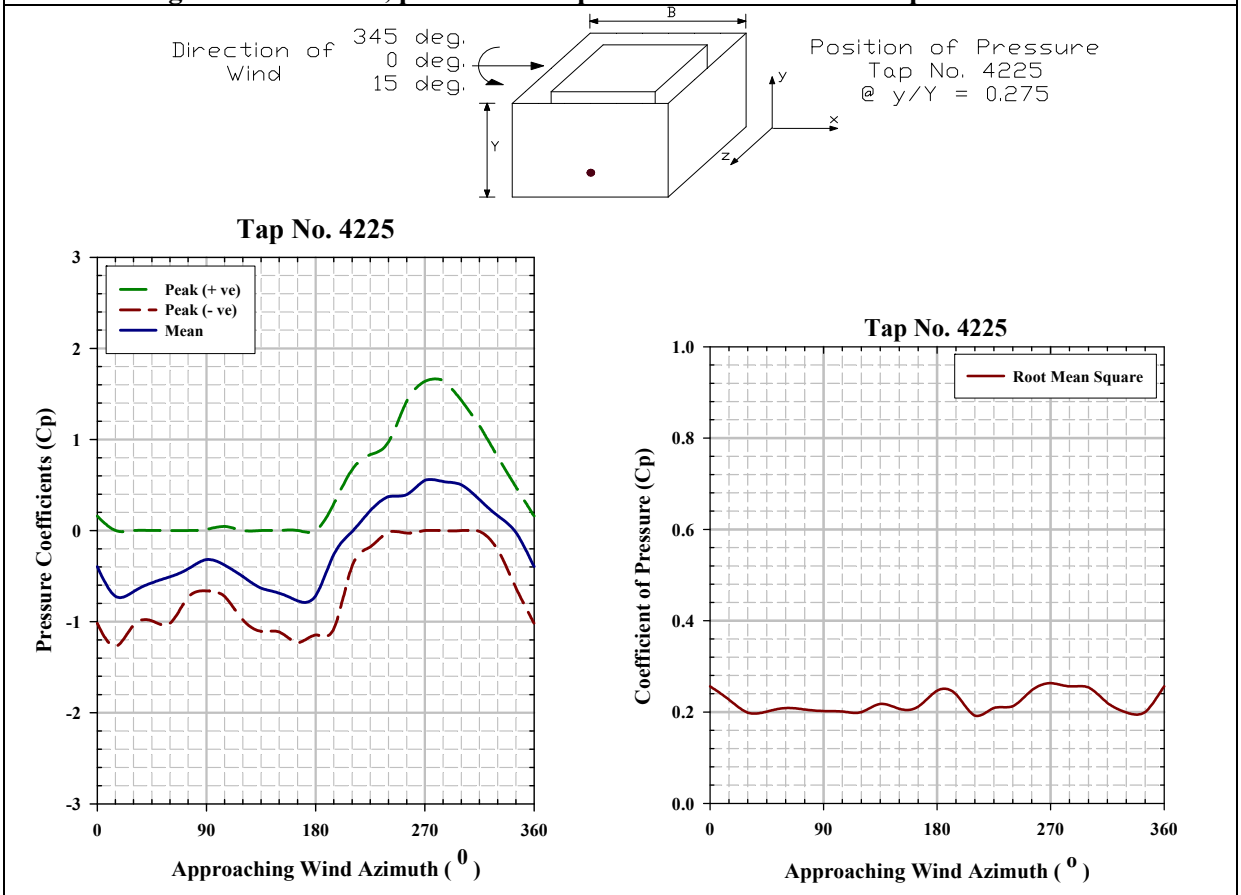

Figure 4A.26 Mean, peak and rms pressure coefficients for tap number 4225

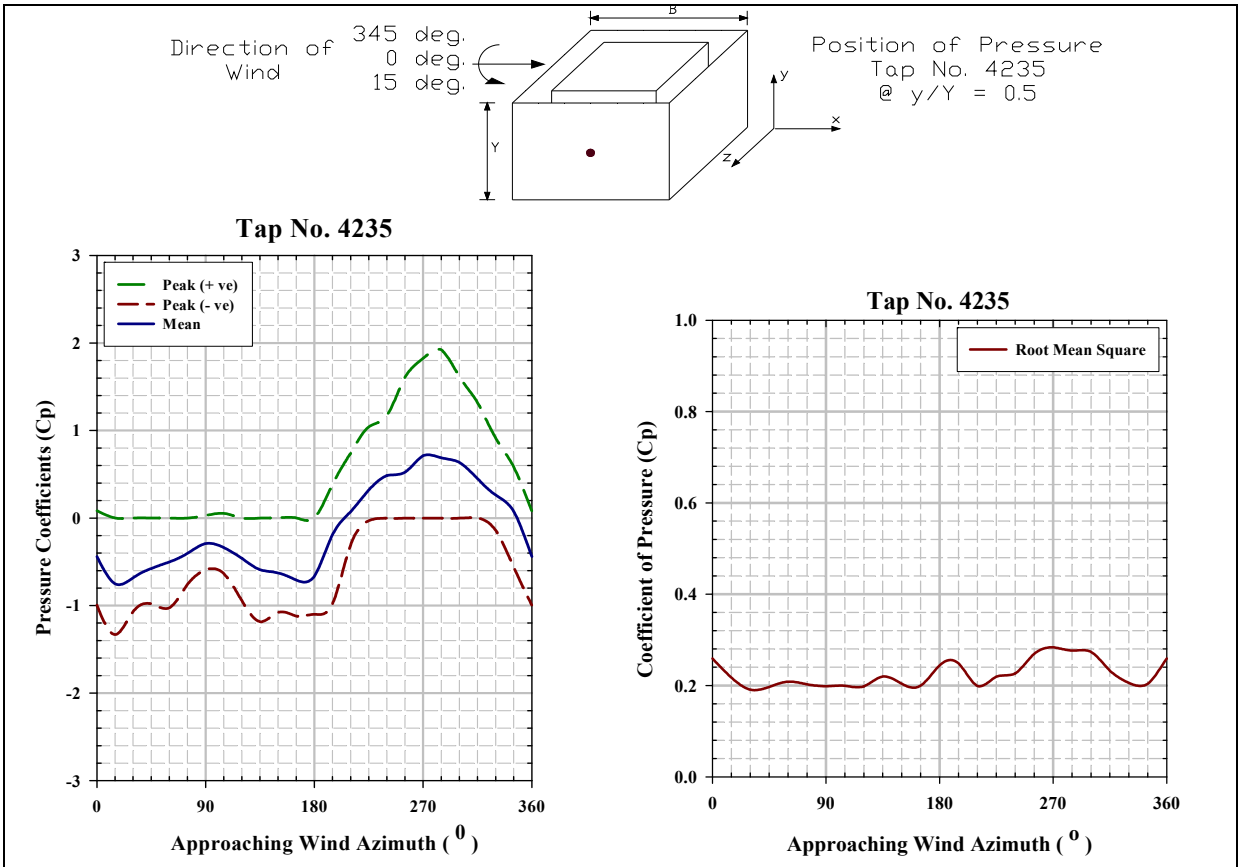

Figure 4A.27 Mean, peak and rms pressure coefficients for tap number 4235

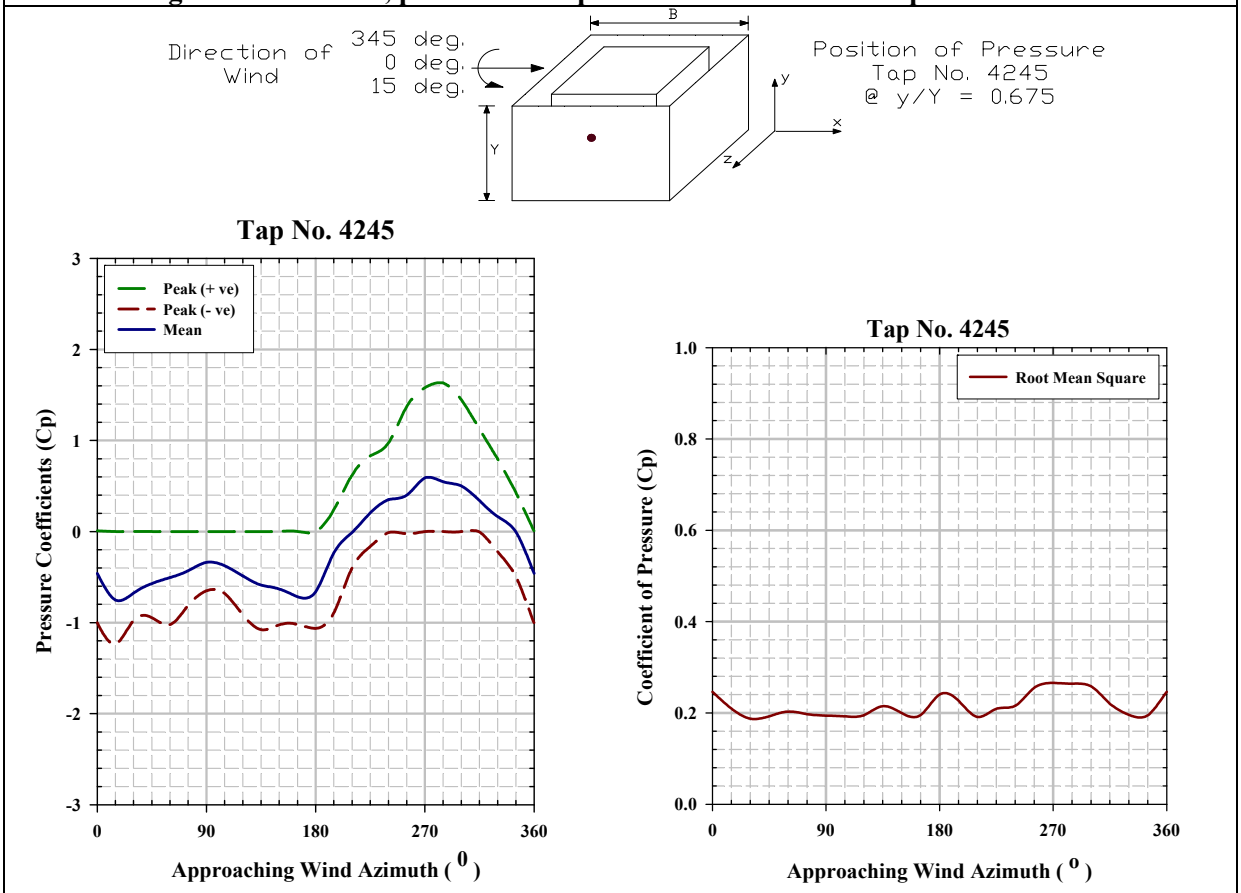

Figure 4A.28 Mean, peak and rms pressure coefficients for tap number 4245

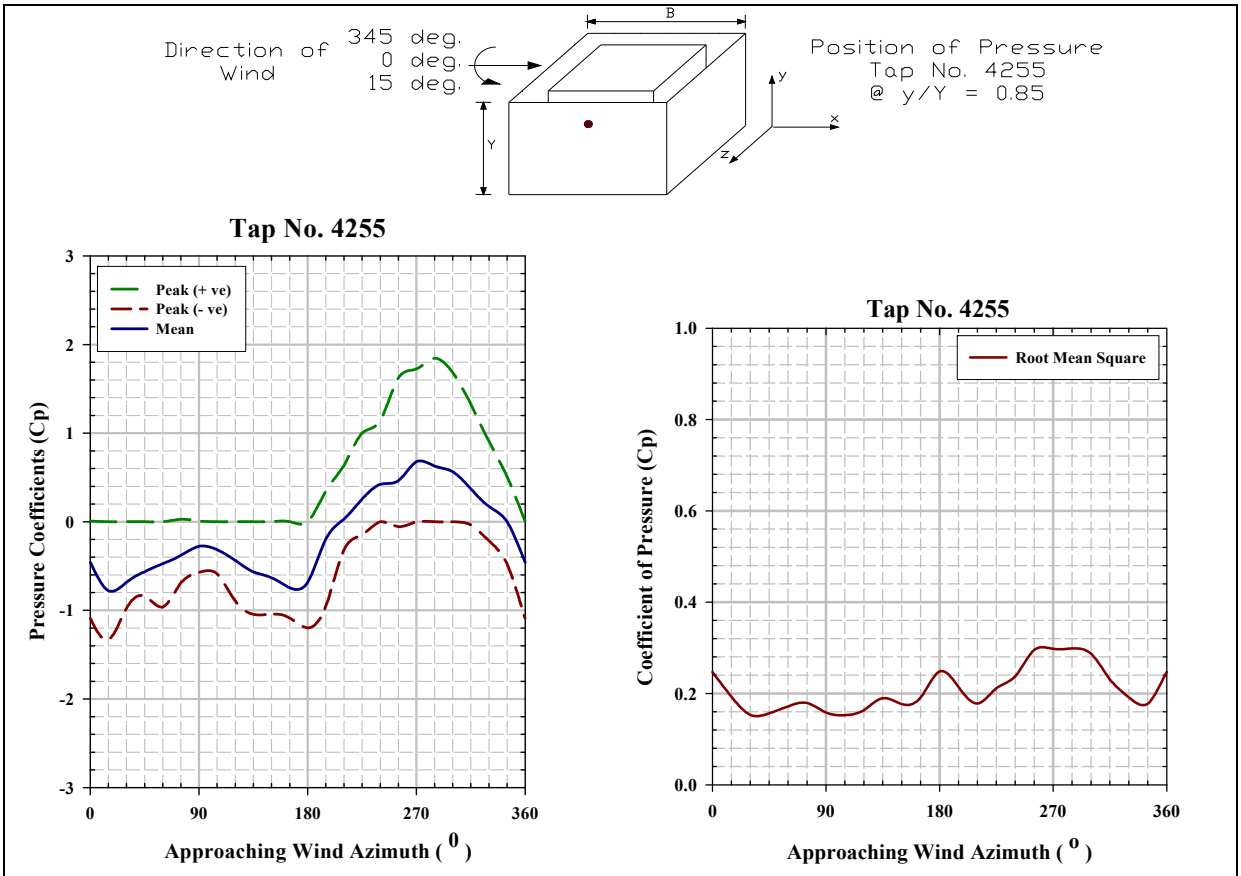

Figure 4A.29 Mean, peak and rms pressure coefficients for tap number 4255

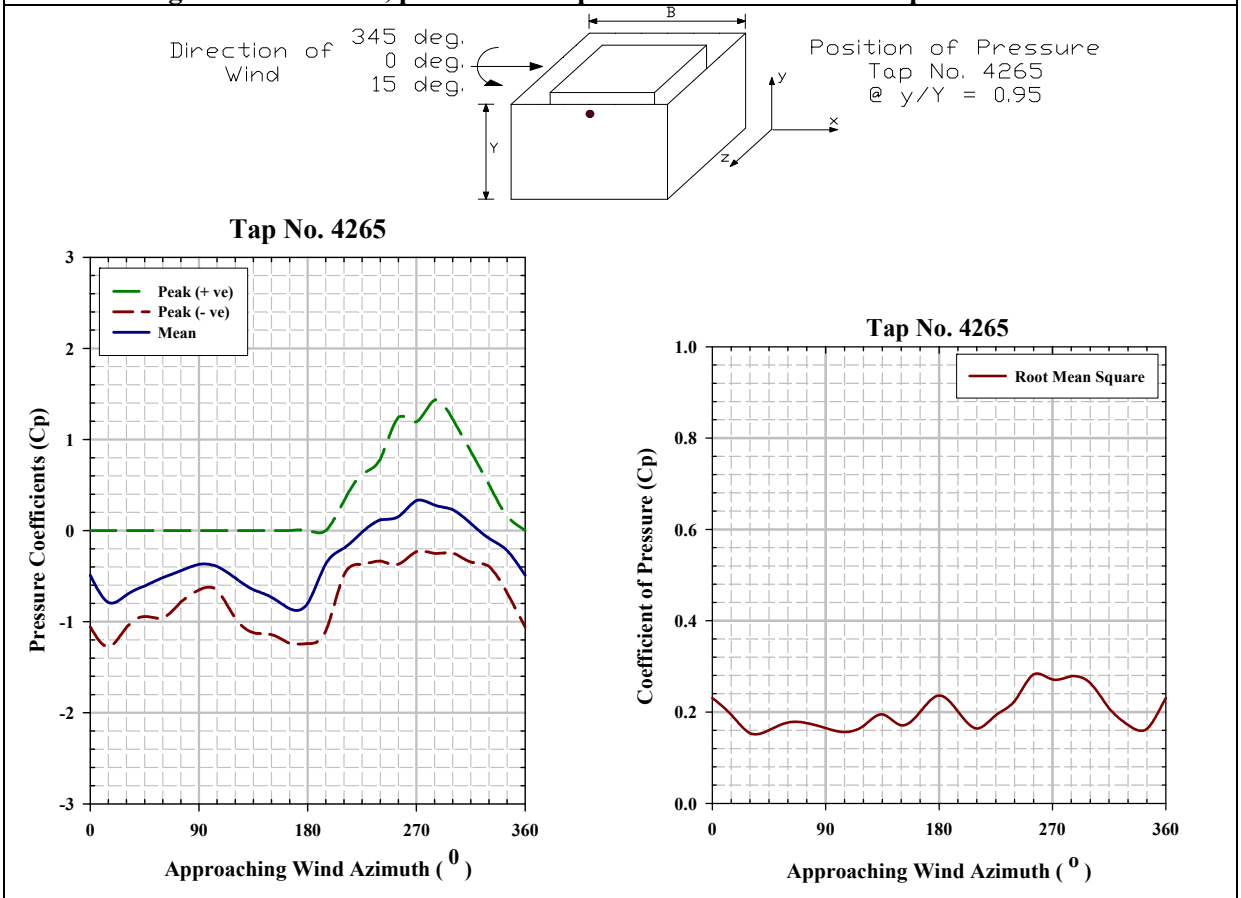

Figure 4A.30 Mean, peak and rms pressure coefficients for tap number 4265

Pressure Coefficient Contours on Windward Outer Face of the Sheet Clad Scaffold for Type B Terrain

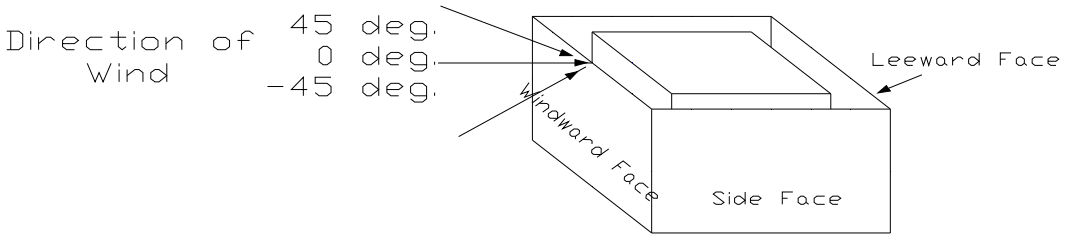

Figure 4B.1 Angle of attack of wind on windward outer face of sheet clad scaffold surrounding SEB, direction of which varies from -45° to +45°

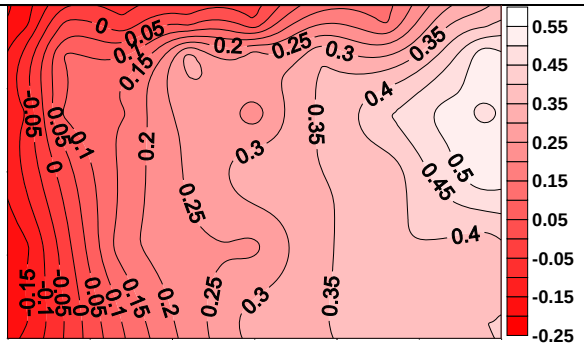

Figure 4B.2 Pressure coefficient contours on the windward outer face of the sheet clad scaffold when θ= 45°

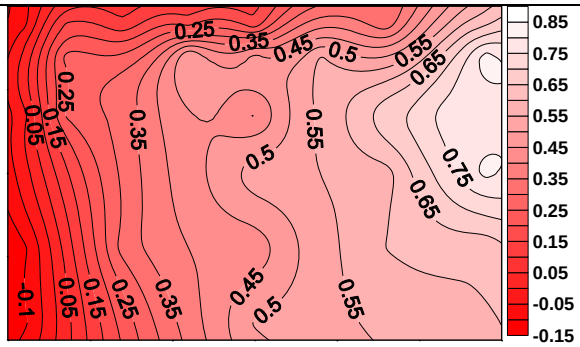

Figure 4B.3 Pressure coefficient contours on the windward outer face of the sheet clad scaffold when θ= 30°

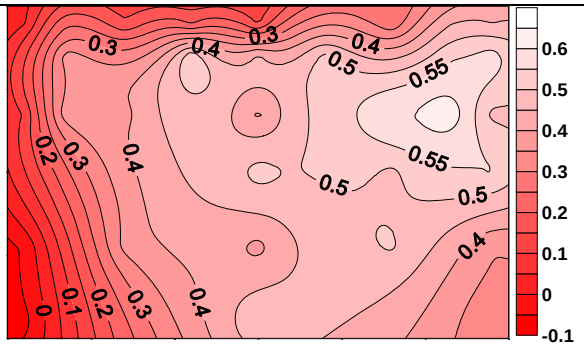

Figure 4B.4 Pressure coefficient contours on the windward outer face of the sheet clad scaffold when θ= 15°

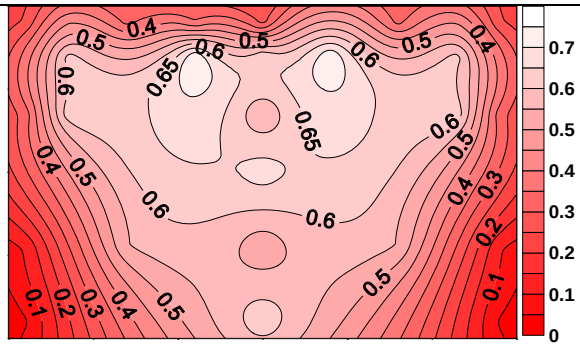

Figure 4B.5 Pressure coefficient contours on the windward outer face of the sheet clad scaffold when θ= 0°

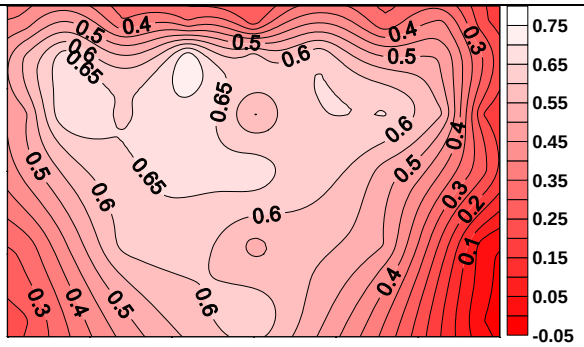

Figure 4B.6 Pressure coefficient contours on the windward outer face of the sheet clad scaffold when θ= -15°

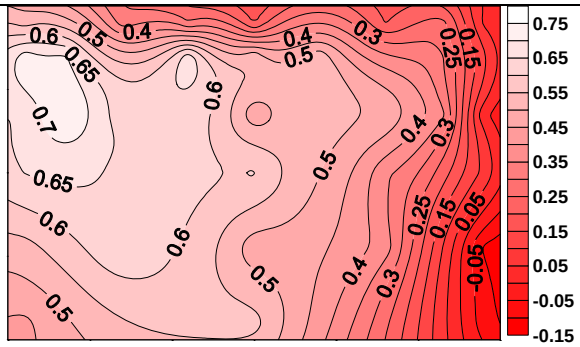

Figure 4B.7 Pressure coefficient contours on the windward outer face of the sheet clad scaffold when θ= -30°

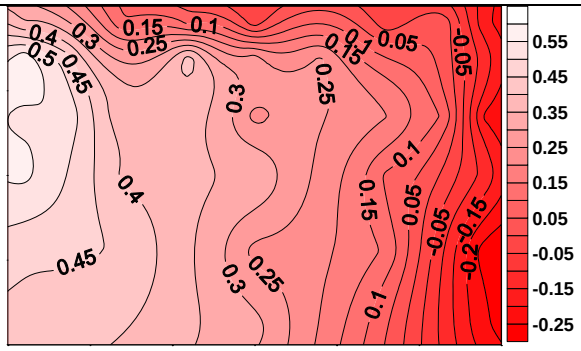

Figure 4B.8 Pressure coefficient contours on the windward outer face of the sheet clad scaffold when θ= -45°

Pressure Coefficient Contours on the Side Outer Face of the Sheet Clad Scaffold for Type B Terrain

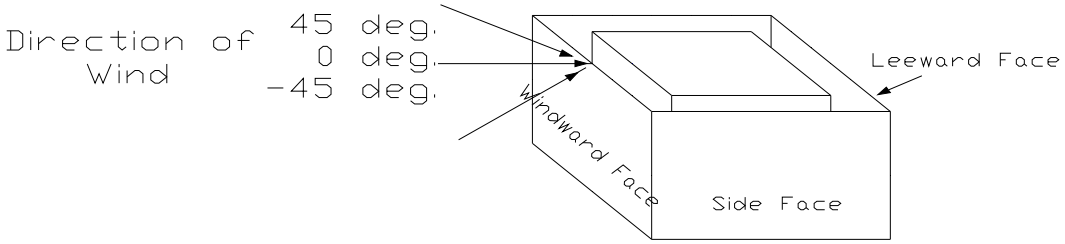

Figure 4B.9 Angle of attack of wind on windward outer face of sheet clad scaffold surrounding SEB, direction of which varies from 45° to -45°

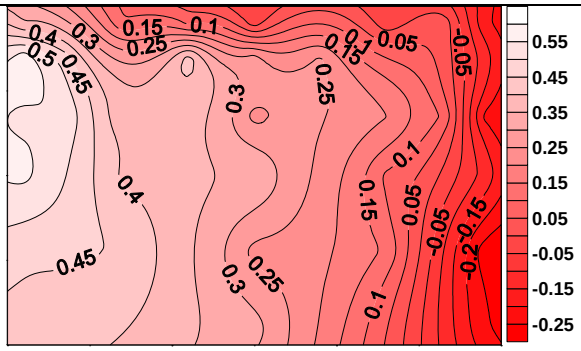

Figure 4B.10 Pressure coefficient contours on the side outer face of the sheet clad scaffold when θ= 45°

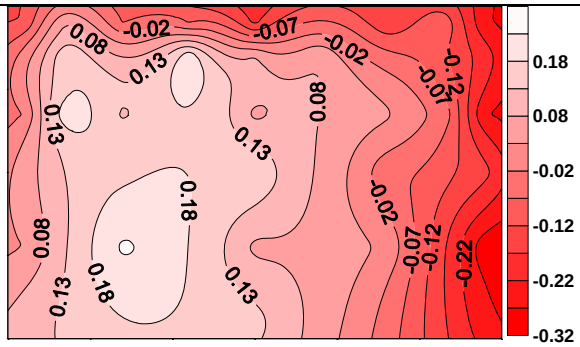

Figure 4B.11 Pressure coefficient contours on the side outer face of the sheet clad scaffold when θ= 30°

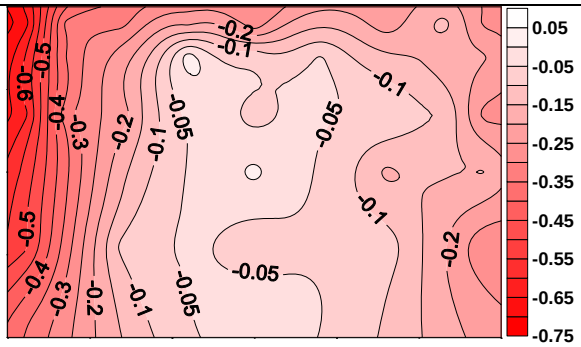

Figure 4B.12 Pressure coefficient contours on the side outer face of the sheet clad scaffold when θ= 15°

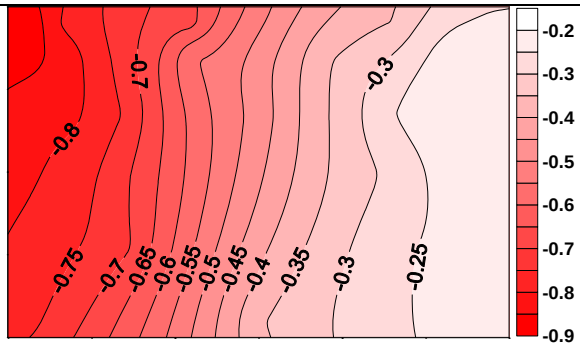

Figure 4B.13 Pressure coefficient contours on the side outer face of the sheet clad scaffold when θ= 0°

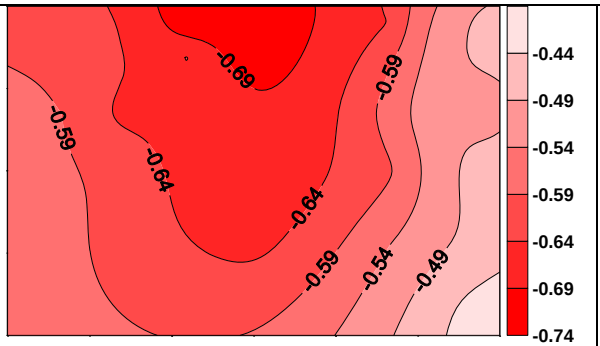

Figure 4B.14 Pressure coefficient contours on the side outer face of the sheet clad scaffold when θ= -15°

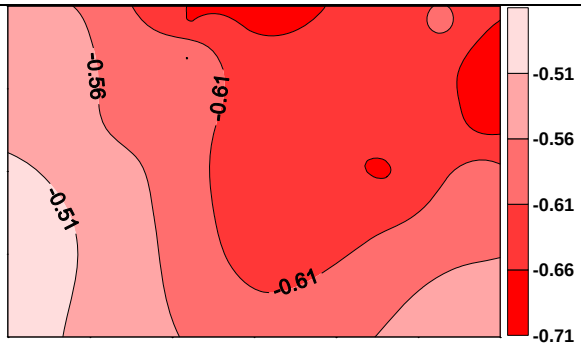

Figure 4B.15 Pressure coefficient contours on the side outer face of the sheet clad scaffold when θ= -30°

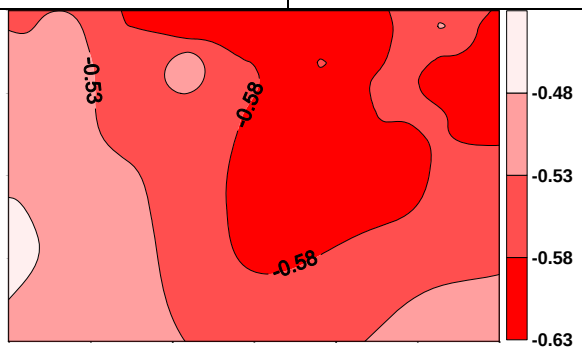

Figure 4B.16 Pressure coefficient contours on the side outer face of the sheet clad scaffold when θ= -45°

Pressure Coefficient Contours on the Leeward Outer Face of the Sheet Clad Scaffold for Type B Terrain

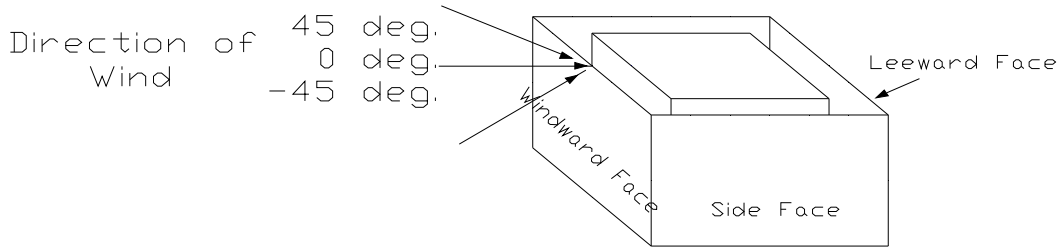

Figure 4B.17 Angle of attack of wind on windward outer face of sheet clad scaffold surrounding SEB, direction of which varies from 45° to -45°

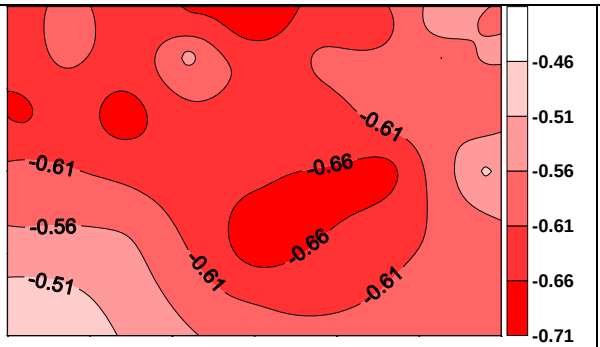

Figure 4B.18 Pressure coefficient contours on the leeward outer face of the sheet clad scaffold when θ= 45°

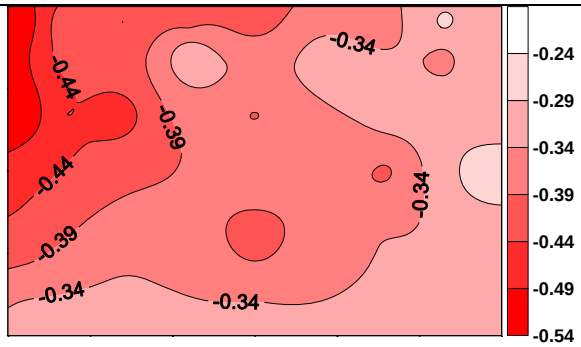

Figure 4B.19 Pressure coefficient contours on the leeward outer face of the sheet clad scaffold when θ= 30°

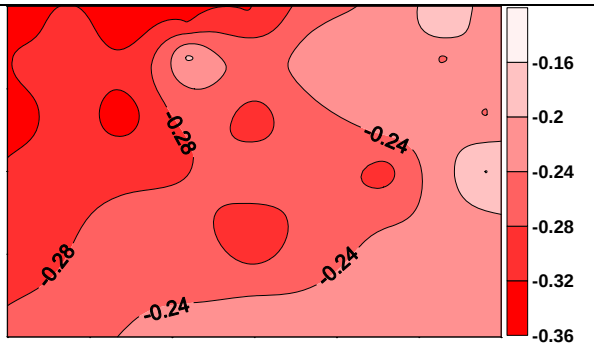

Figure 4B.20 Pressure coefficient contours on the leeward outer face of the sheet clad scaffold when θ= 15^{o}

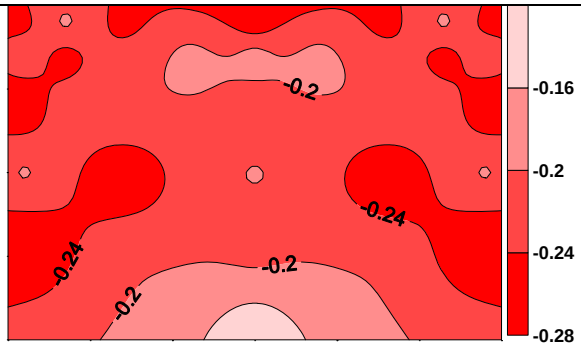

Figure 4B.21 Pressure coefficient contours on the leeward outer face of the sheet clad scaffold when θ= 0^{o}

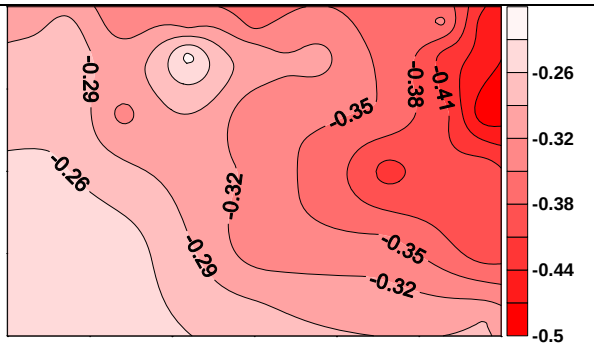

Figure 4B.22 Pressure coefficient contours on the leeward outer face of the sheet clad scaffold when θ= -15^{o}

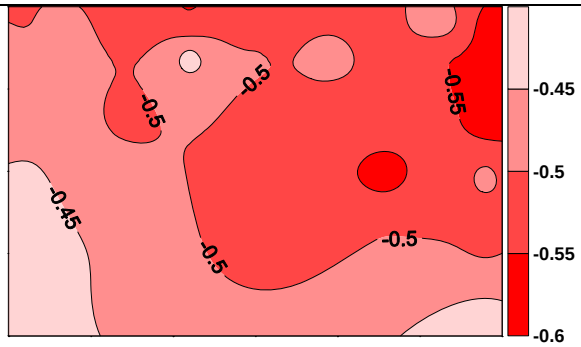

Figure 4B.23 Pressure coefficient contours on the leeward outer face of the sheet clad scaffold when θ= -30^{o}

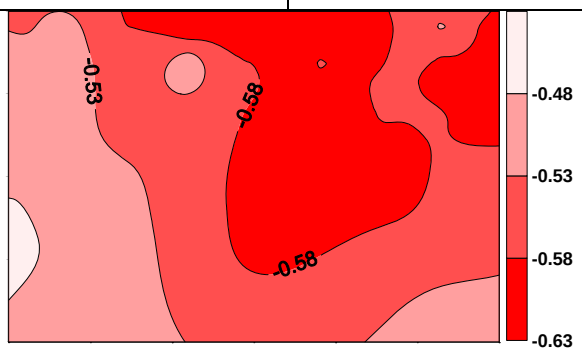

Figure 4B.24 Pressure coefficient contours on the leeward outer face of the sheet clad scaffold when θ= -45^{o}

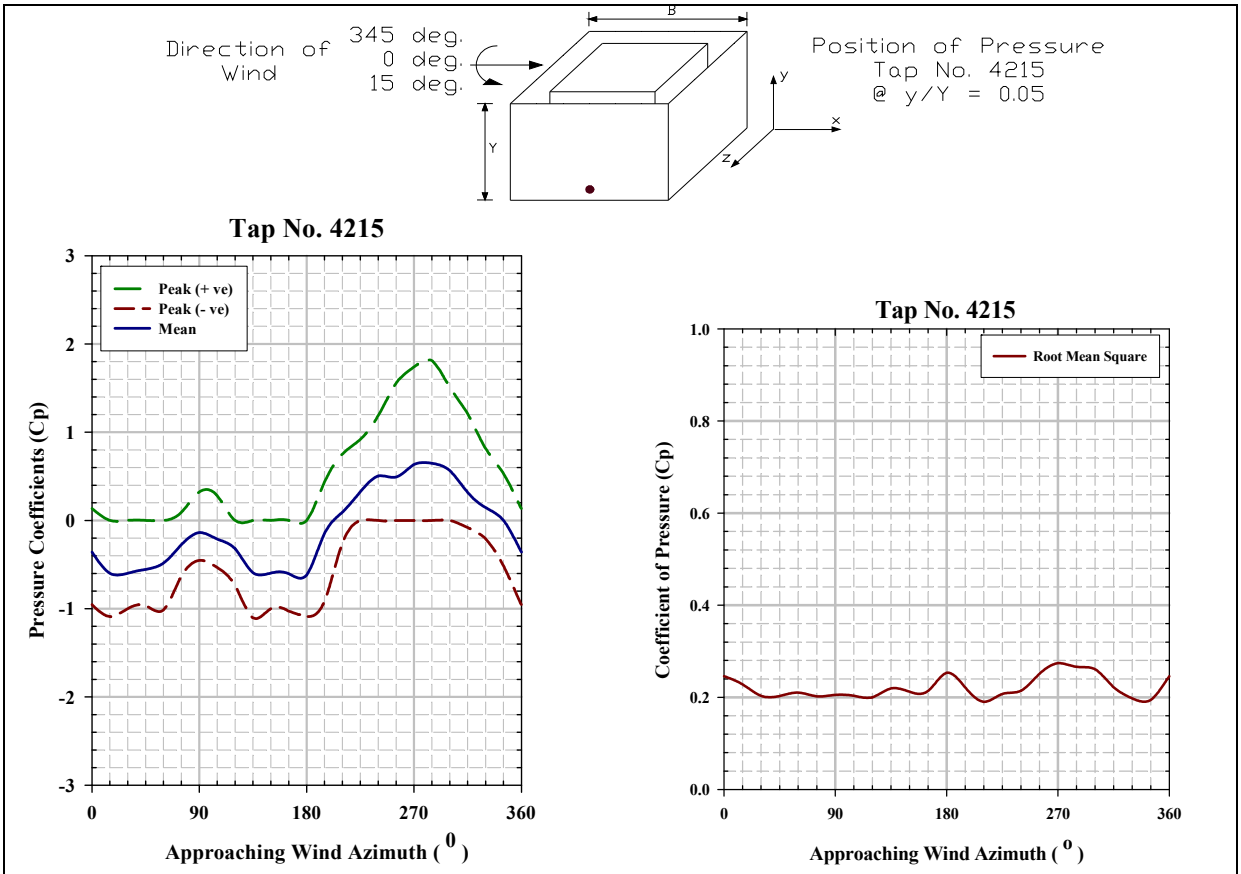

Figure 4B.25 Mean, peak and rms pressure coefficients for tap number 4215

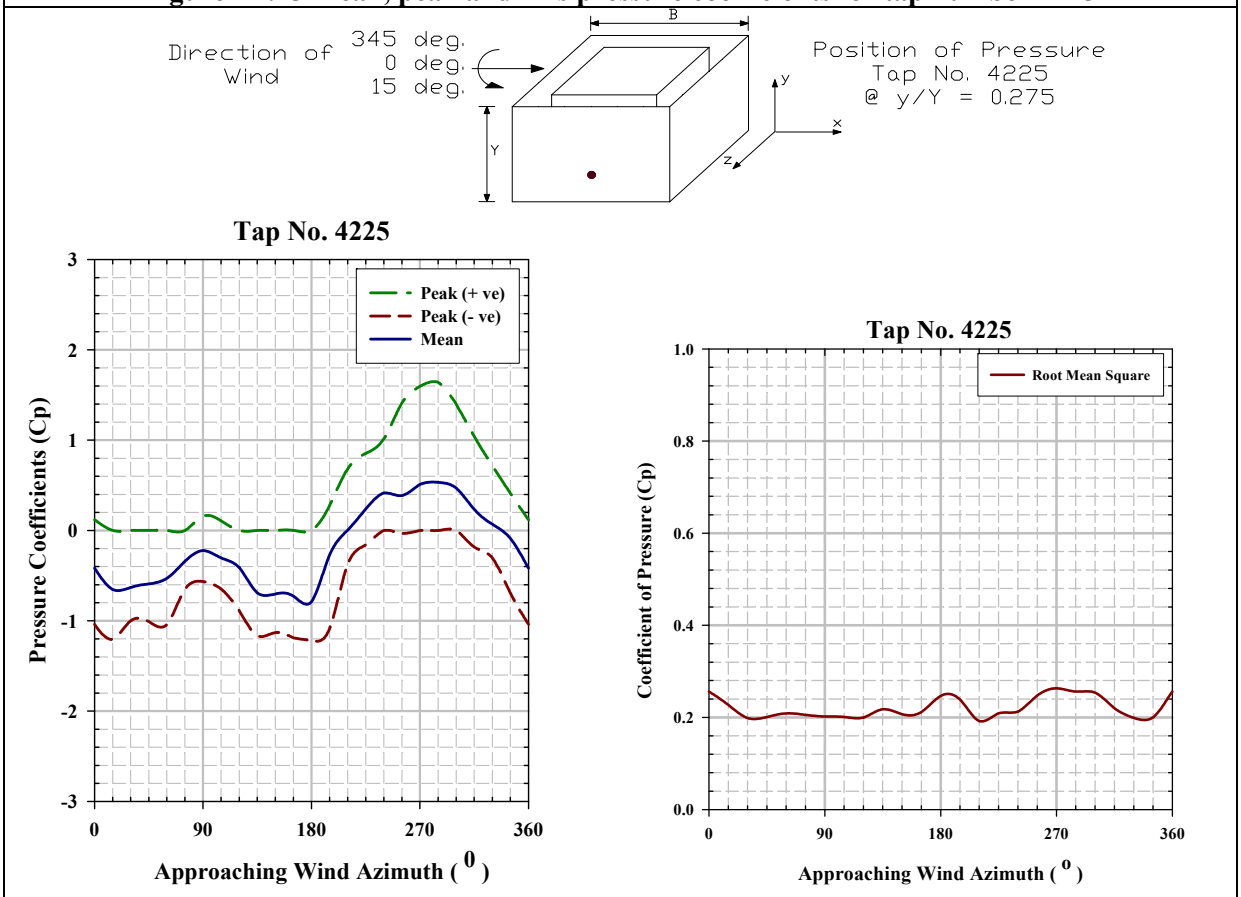

Figure 4B.26 Mean, peak and rms pressure coefficients for tap number 4225

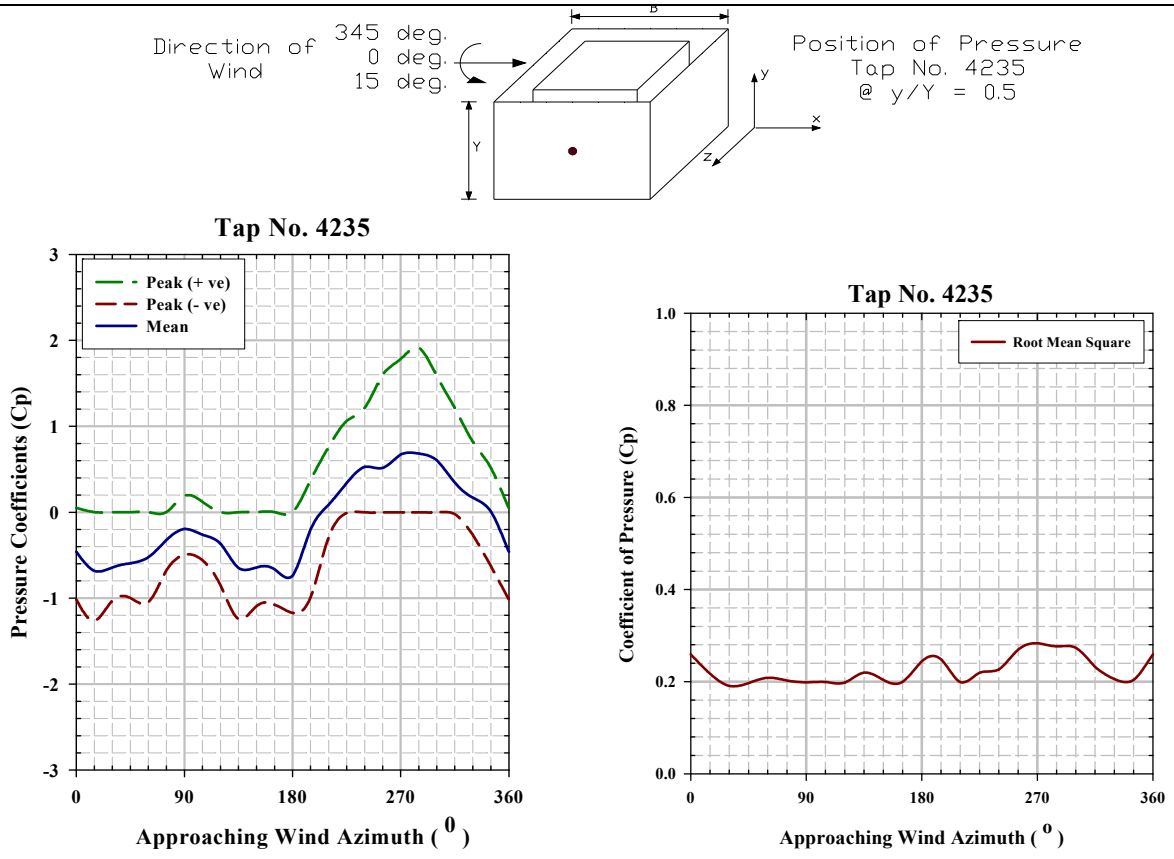

Figure 4B.27 Mean, peak and rms pressure coefficients for tap number 4235

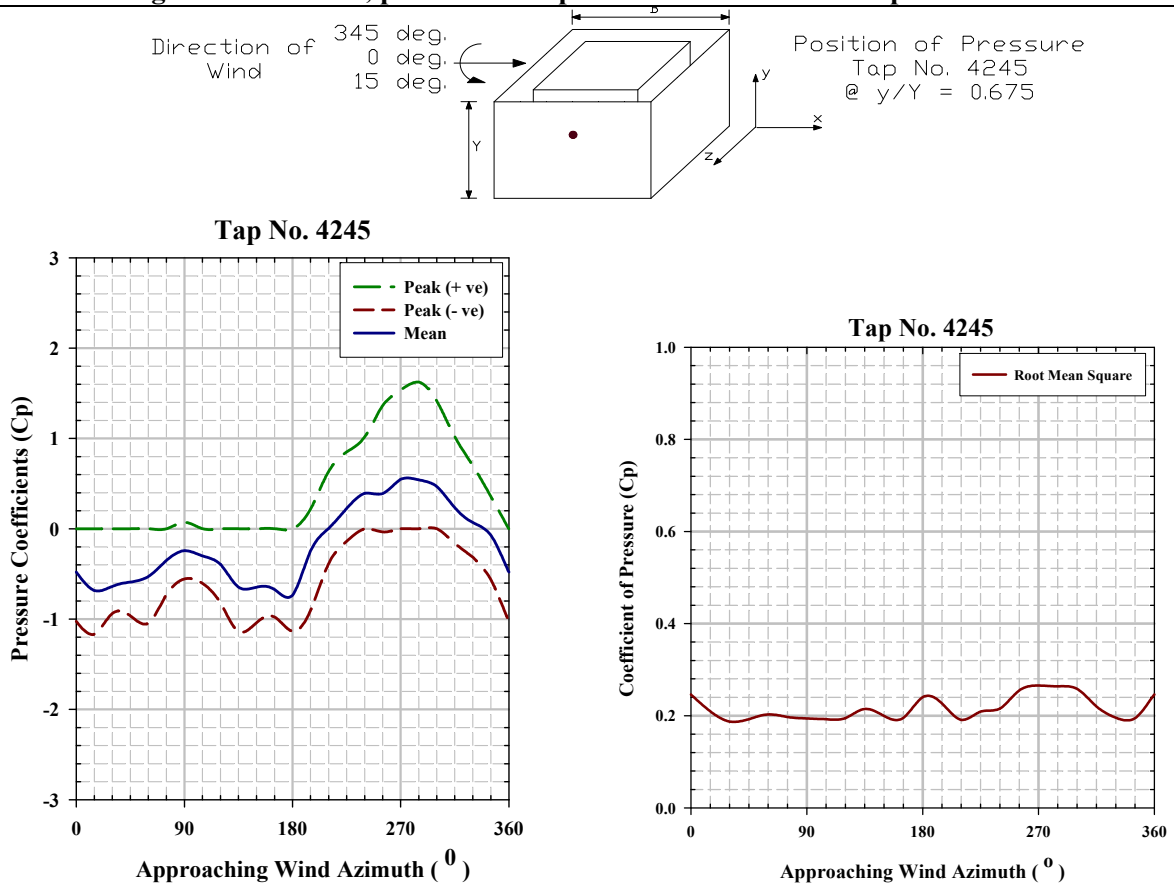

Figure 4B.28 Mean, peak and rms pressure coefficients for tap number 4245

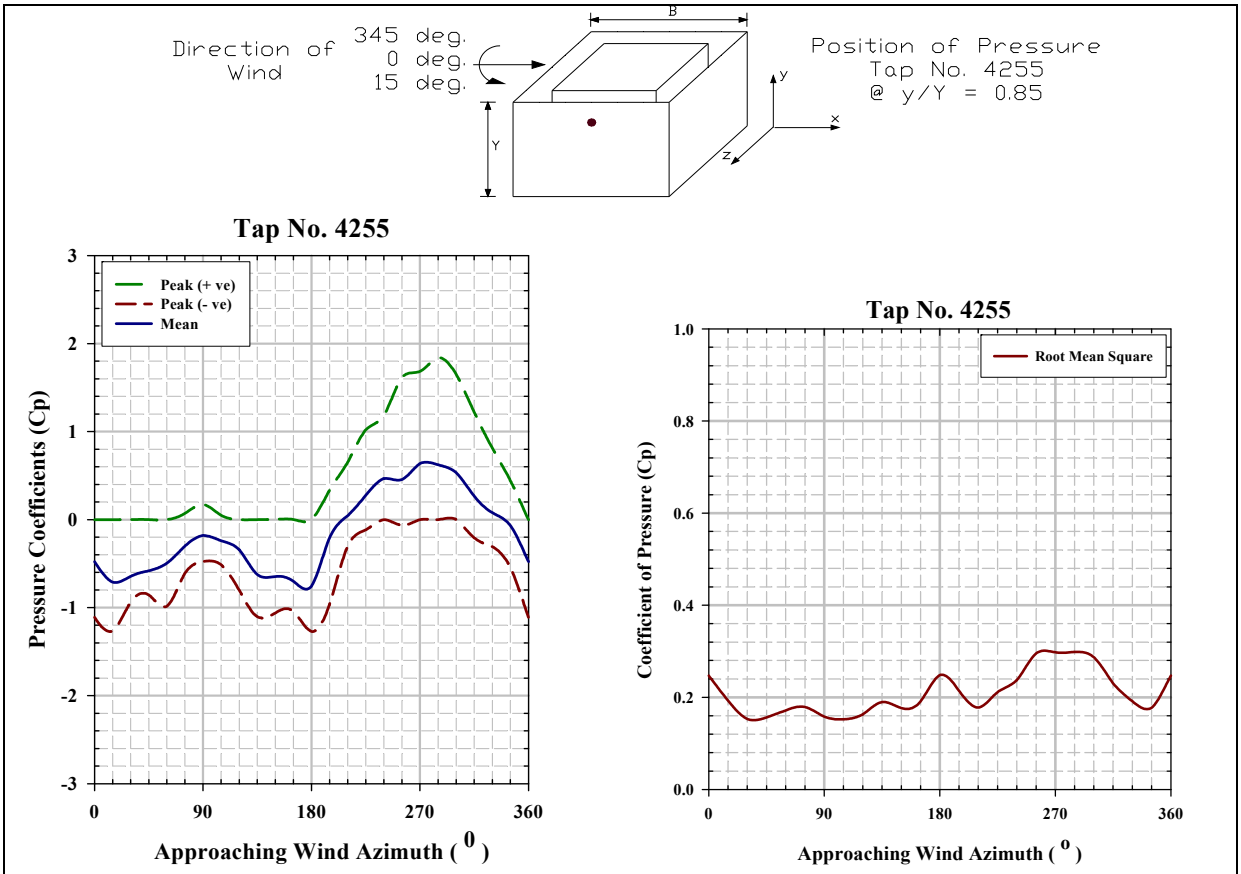

Figure 4B.29 Mean, peak and rms pressure coefficients for tap number 4255

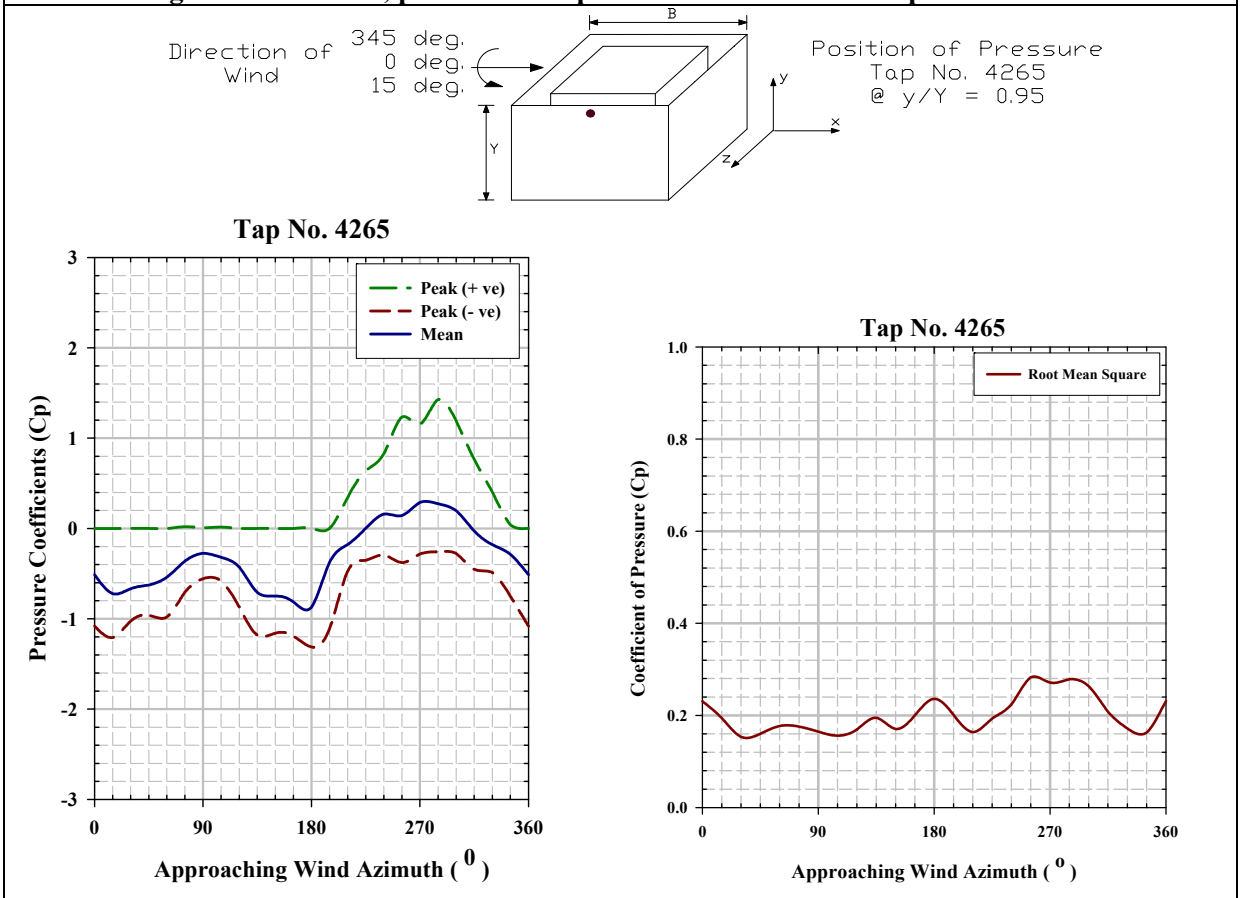

Figure 4B.30 Mean, peak and rms pressure coefficients for tap number 4265

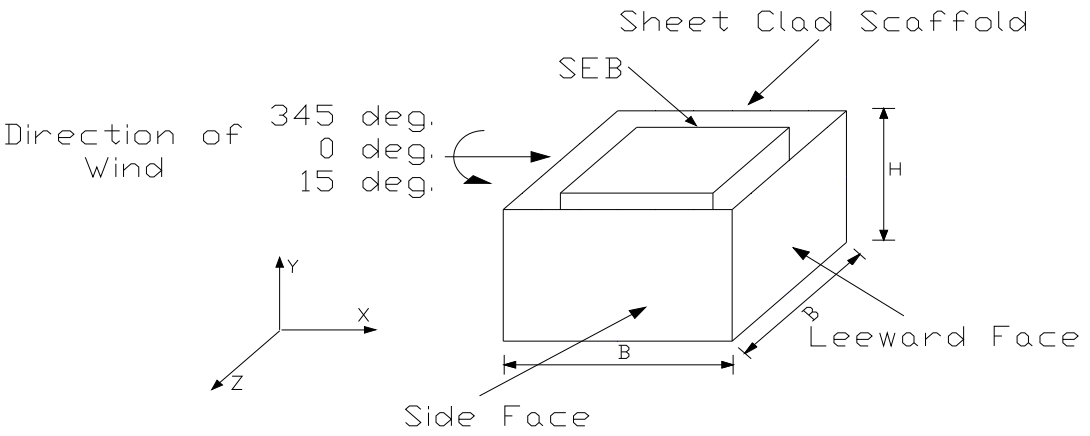

Figure 5.1 Scaled cubical SEB surrounded by sheet clad scaffold

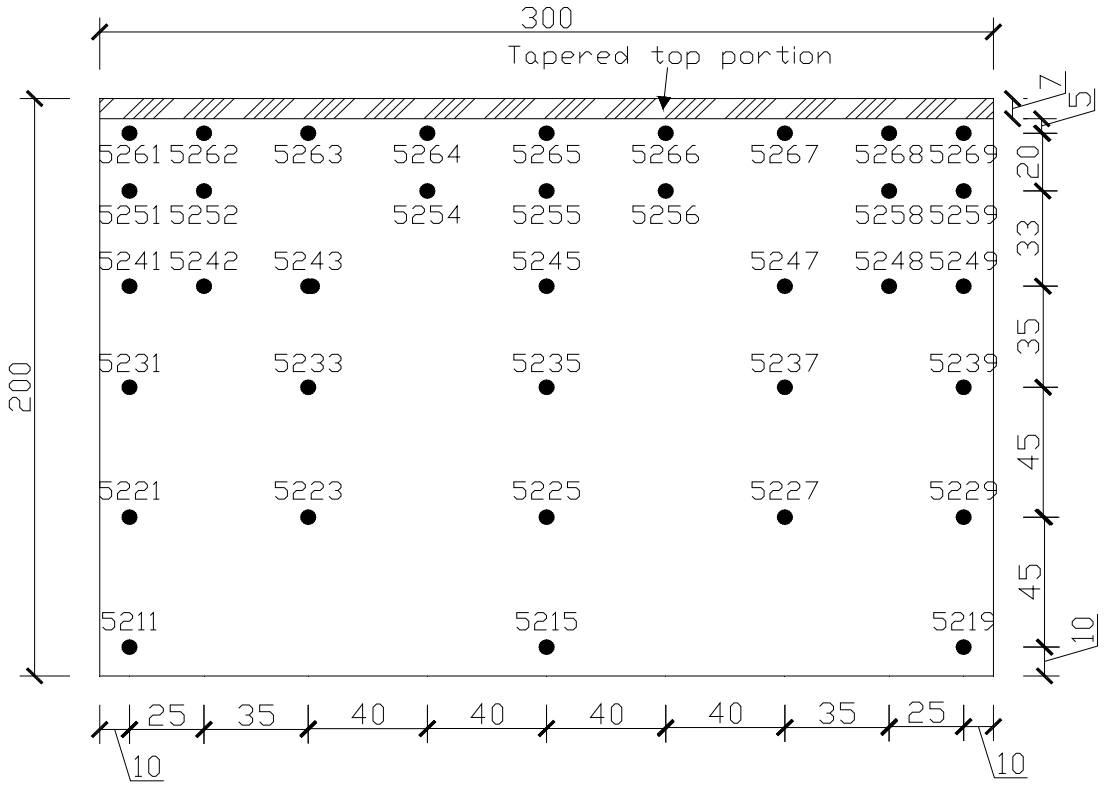

Figure 5.2 Pressure tap locations on the inner face of the sheet clad scaffold

Pressure Coefficient Contours on the Windward Inner Face of the Sheet Clad Scaffold for Type A Terrain

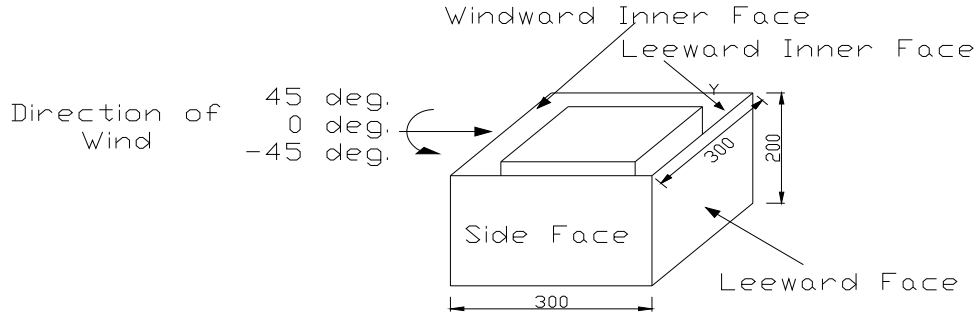

Figure 5A.1 Angle of attack of wind on windward outer face of the sheet clad scaffold surrounding SEB, direction of which varies from 45° to -45°

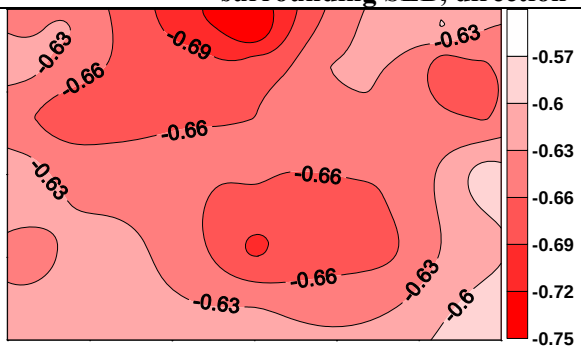

Figure 5A.2 Pressure coefficient contours on the windward inner face of the sheet clad scaffold when θ= 45°

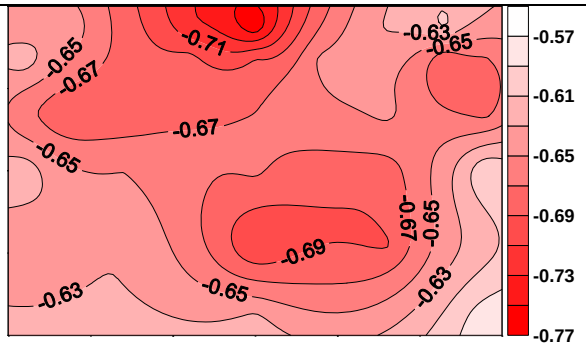

Figure 5A.3 Pressure coefficient contours on the windward inner face of the sheet clad scaffold when θ= 30°

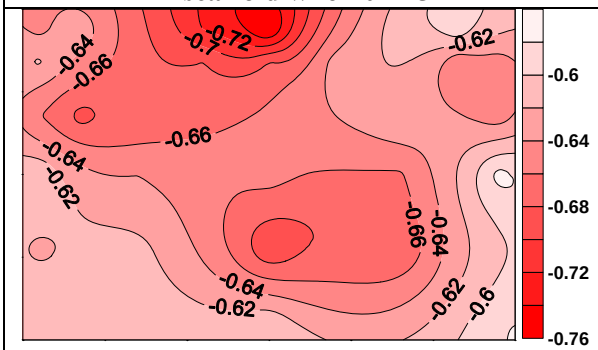

Figure 5A.4 Pressure coefficient contours on the windward inner face of the sheet clad scaffold when θ= 15°

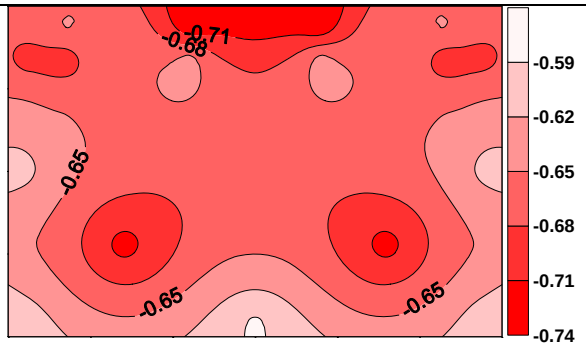

Figure 5A.5 Pressure coefficient contours on the windward inner face of the sheet clad scaffold when θ= 0°

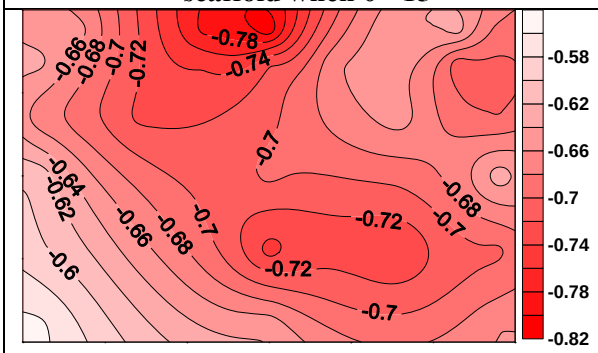

Figure 5A.6 Pressure coefficient contours on the windward inner face of the sheet clad scaffold when θ= -15°

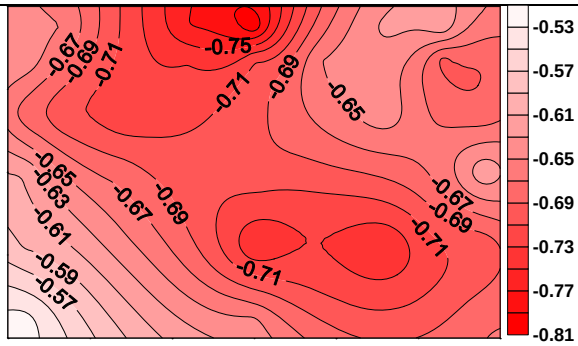

Figure 5A.7 Pressure coefficient contours on the windward inner face of the sheet clad scaffold when θ= -30°

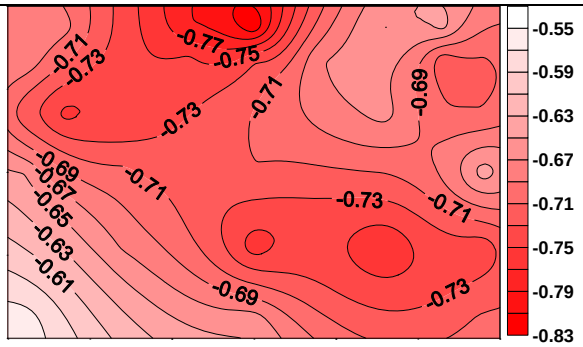

Figure 5A.8 Pressure coefficient contours on the windward inner face of the sheet clad scaffold when θ= -45°

Pressure Coefficient Contours on the Side Inner Face of the Sheet Clad Scaffold for Type A Terrain

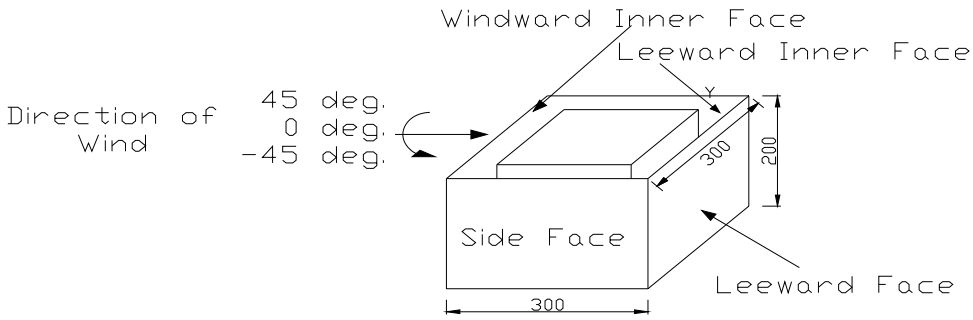

Figure 5A.9 Angle of attack of wind on windward outer face of the sheet clad scaffold surrounding SEB, direction of which varies from 45° to -45°

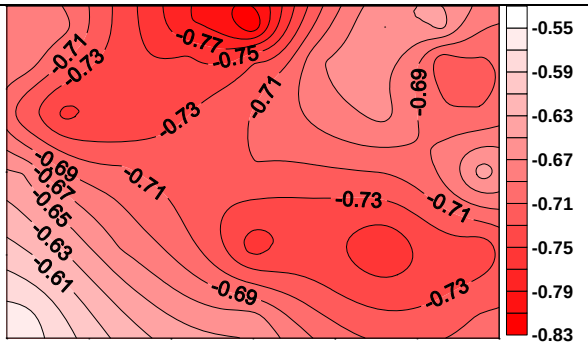

Figure 5A.10 Pressure coefficient contours on the side inner face of the sheet clad scaffold when θ= 45°

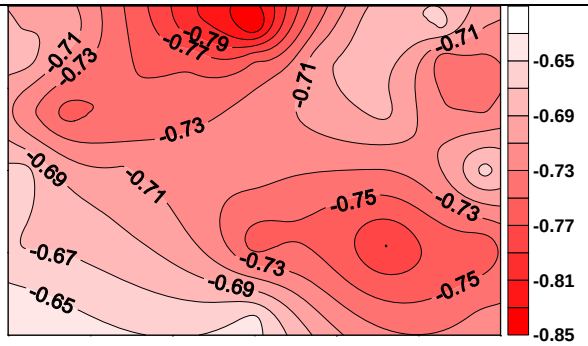

Figure 5A.11 Pressure coefficient contours on the side inner face of the sheet clad scaffold when θ= 30°

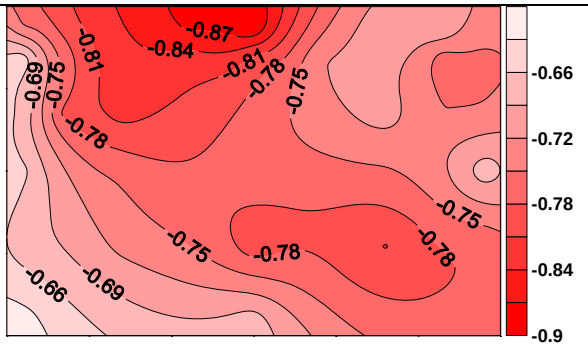

Figure 5A.12 Pressure coefficient contours on the side inner face of the sheet clad scaffold when θ= 15°

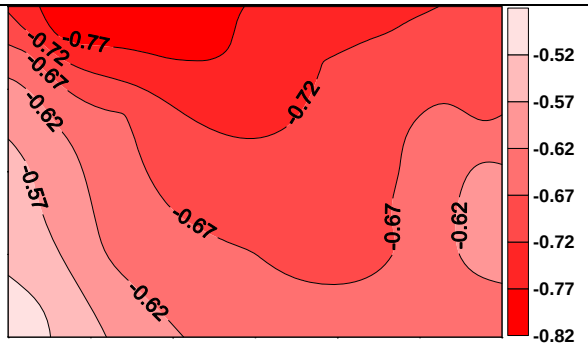

Figure 5A.13 Pressure coefficient contours on the side inner face of the sheet clad scaffold when θ= 0°

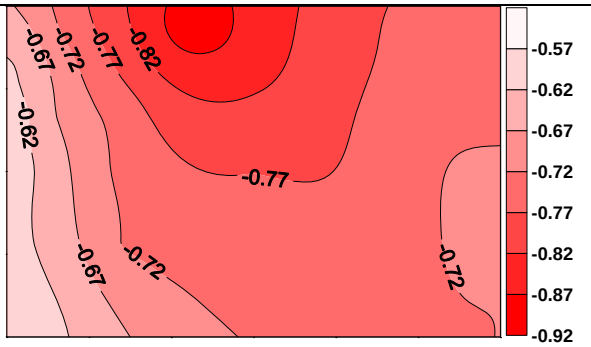

Figure 5A.14 Pressure coefficient contours on the side inner face of the sheet clad scaffold when θ= -15°

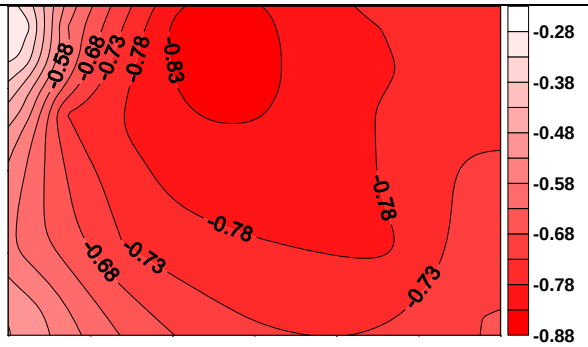

Figure 5A.15 Pressure coefficient contours on the side inner face of the sheet clad scaffold when θ= -30°

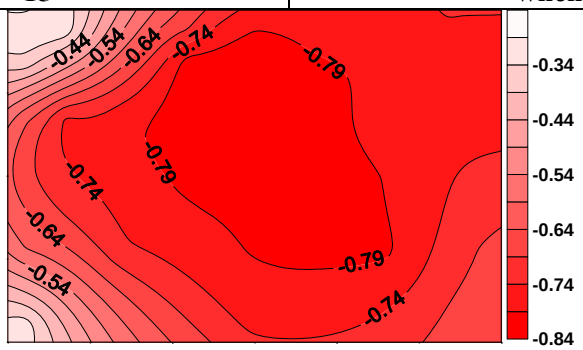

Figure 5A.16 Pressure coefficient contours on the side inner face of the sheet clad scaffold when θ= -45°

Pressure Coefficient Contours on the Leeward Inner Face of the Sheet Clad Scaffold for Type A Terrain

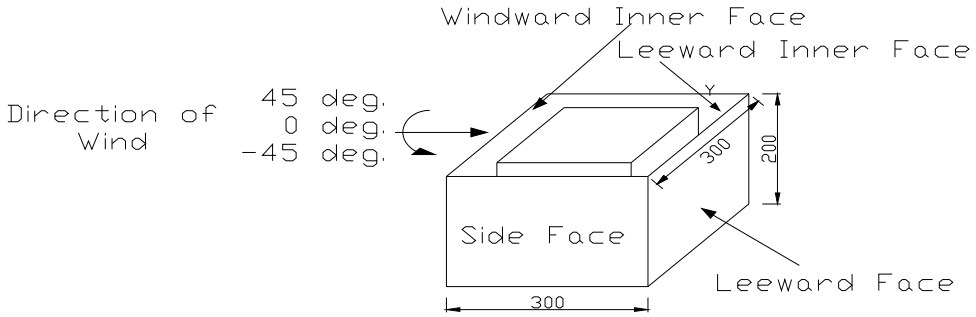

Figure 5A.17 Angle of attack of wind on windward outer face of the elevated sheet clad scaffold surrounding SEB, direction of which varies from 45° to -45°

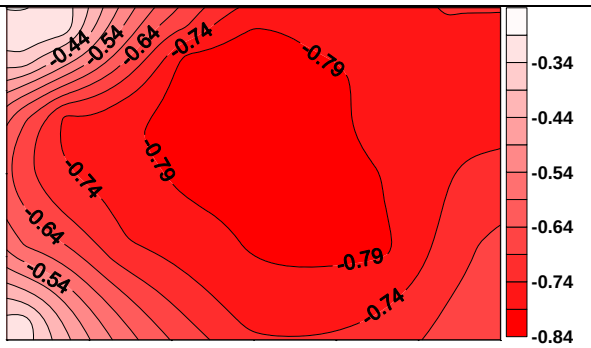

Figure 5A.18 Pressure coefficient contours on the leeward inner face of the sheet clad scaffold when θ= 45°

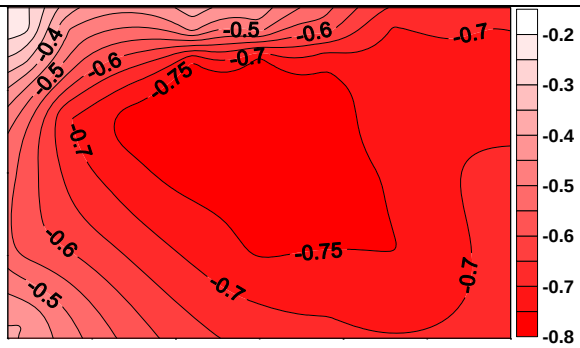

Figure 5A.19 Pressure coefficient contours on the leeward inner face of the sheet clad scaffold when θ= 30°

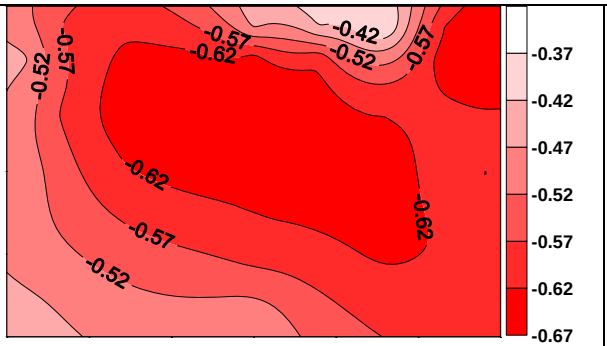

Figure 5A.20 Pressure coefficient contours on the leeward inner face of the sheet clad scaffold when θ= 15°

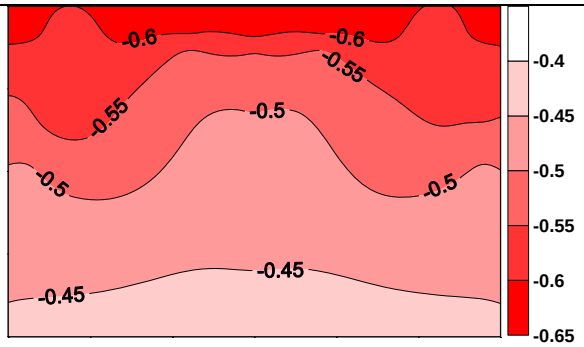

Figure 5A.21 Pressure coefficient contours on the leeward inner face of the sheet clad scaffold when θ= 0°

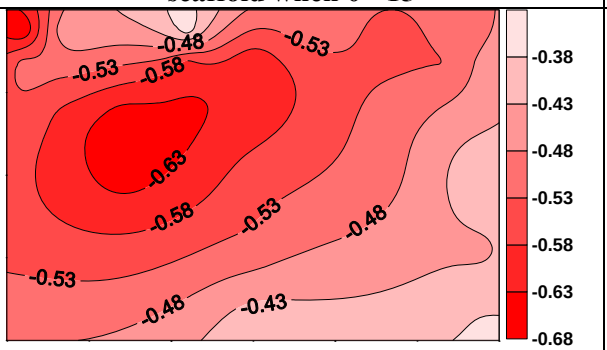

Figure 5A.22 Pressure coefficient contours on the leeward inner face of the sheet clad scaffold when θ= -15°

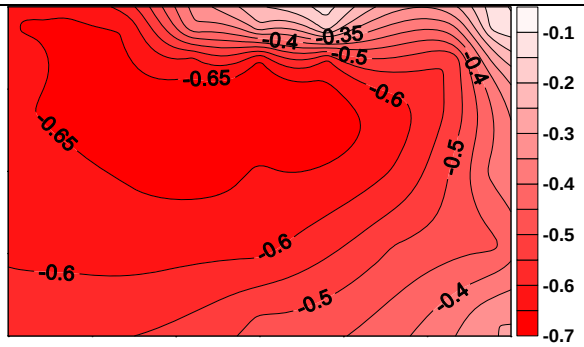

Figure 5A.23 Pressure coefficient contours on the leeward inner face of the sheet clad scaffold when θ= -30°

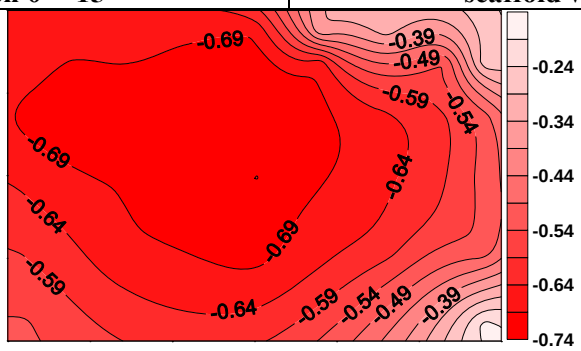

Figure 5A.24 Pressure coefficient contours on the leeward inner face of the sheet clad scaffold when θ= -45°

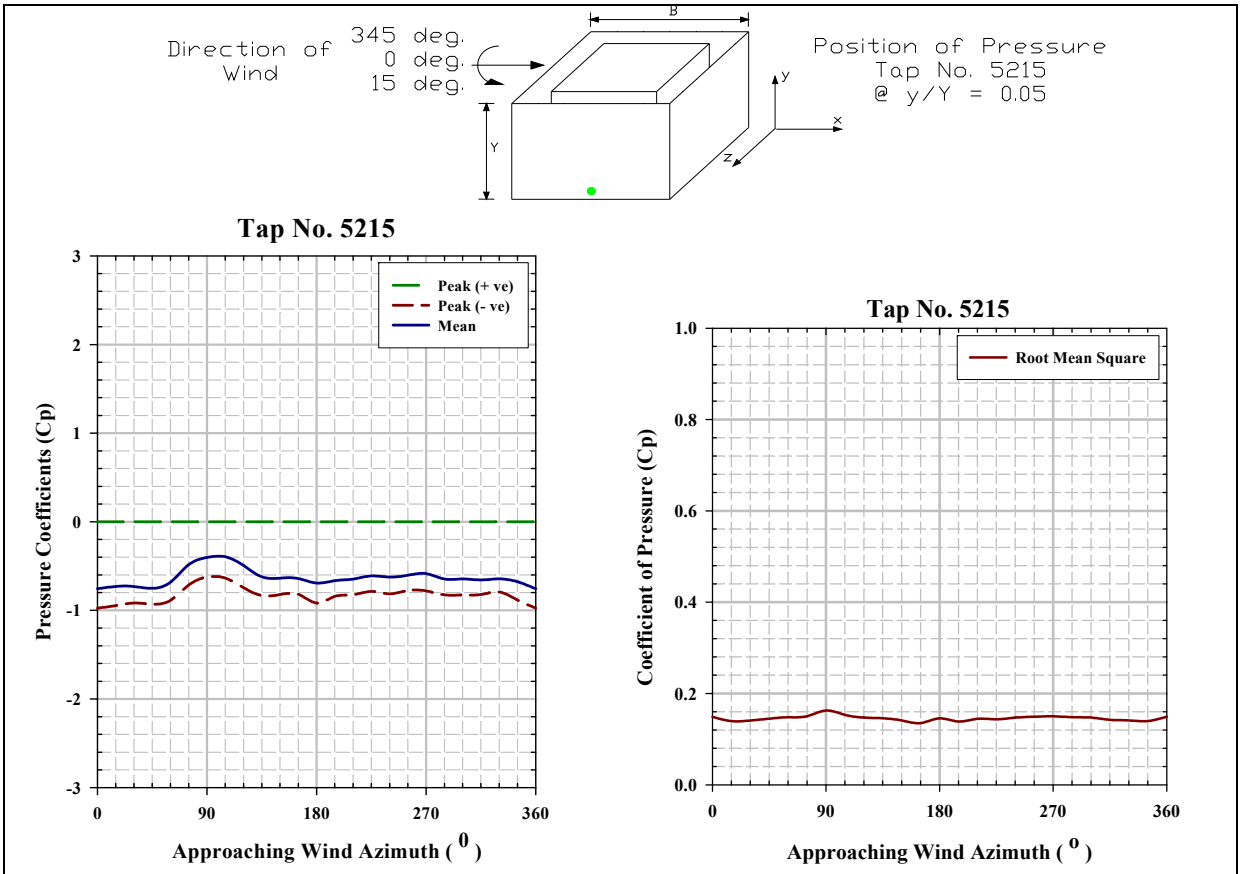

Figure 5A.25 Mean, peak and rms pressure coefficients for tap number 5215

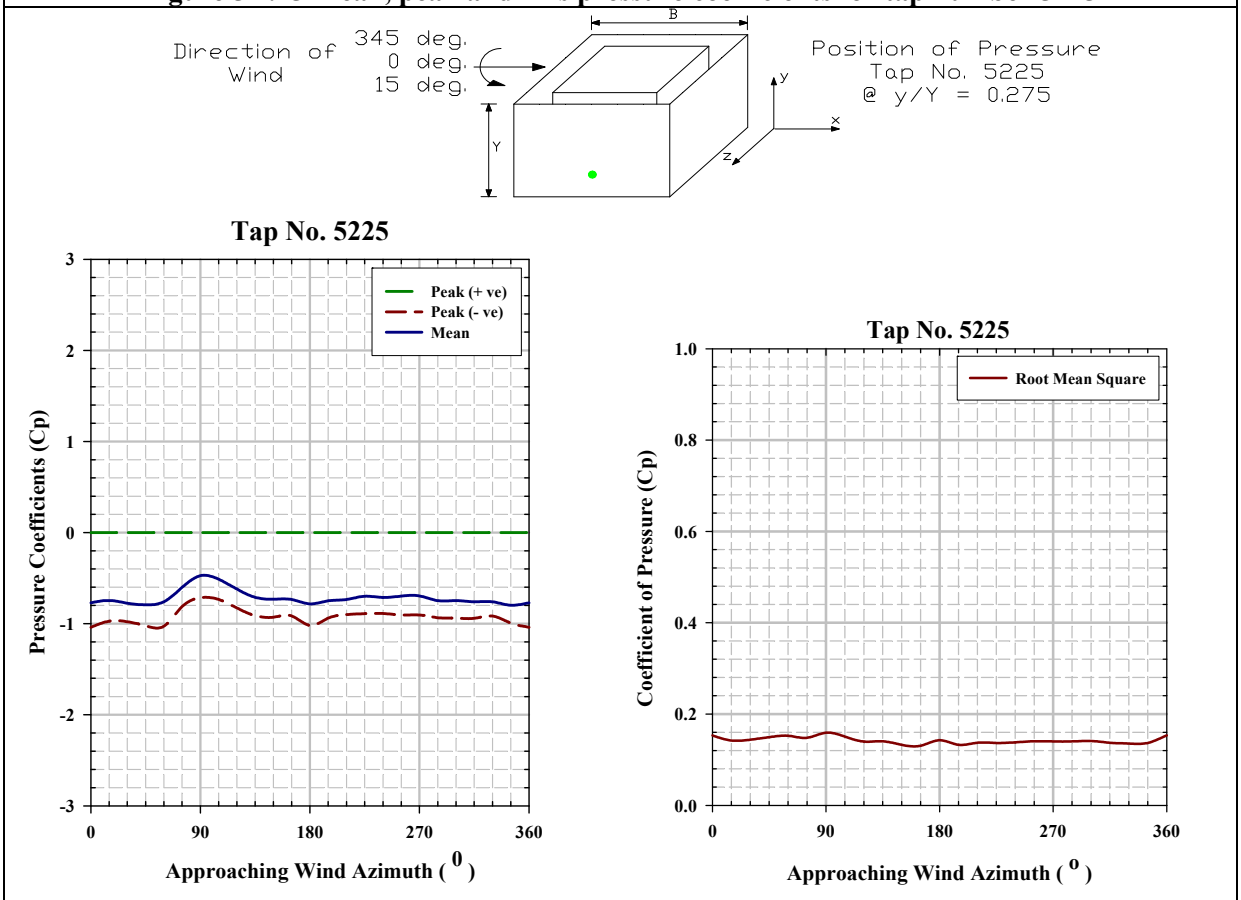

Figure 5A.26 Mean, peak and rms pressure coefficients for tap number 5225

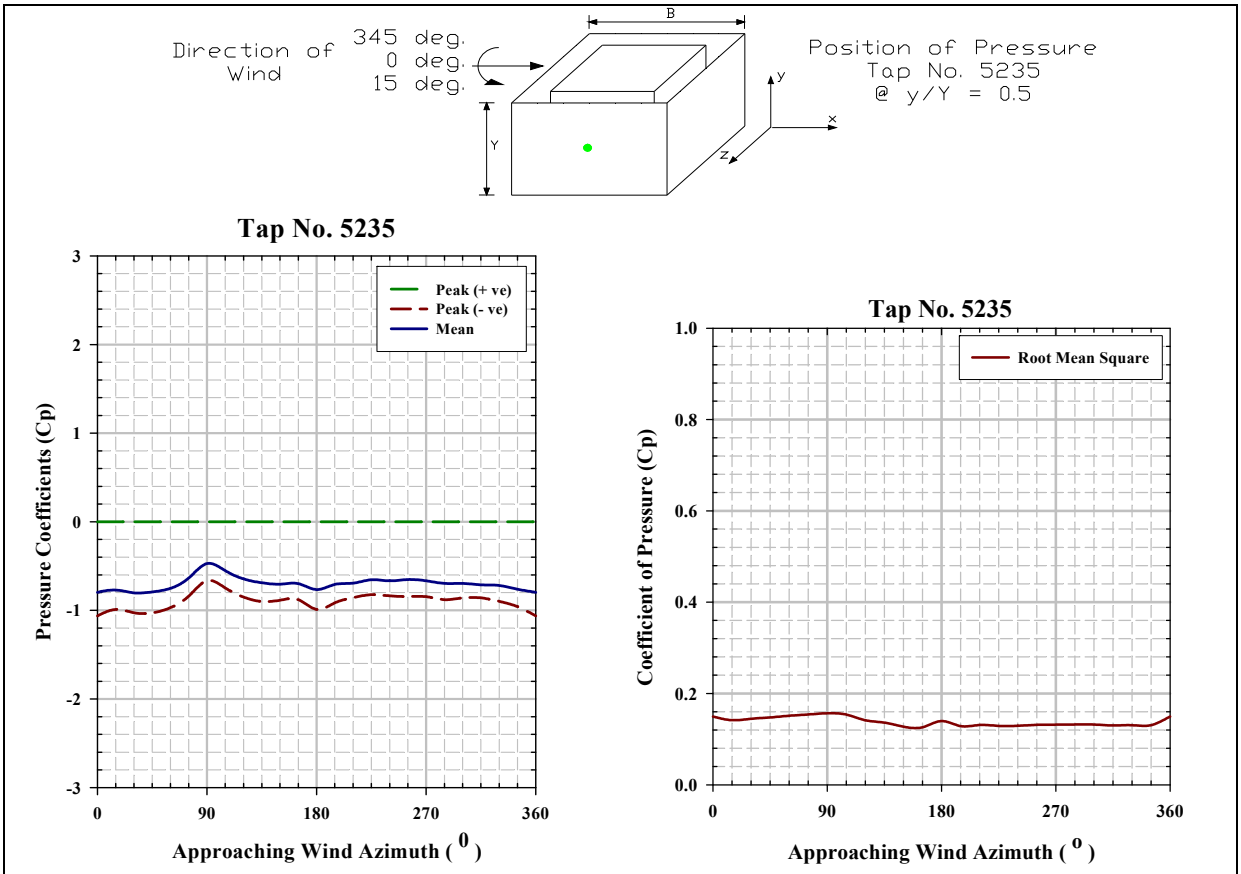

Figure 5A.27 Mean, peak and rms pressure coefficients for tap number 5235

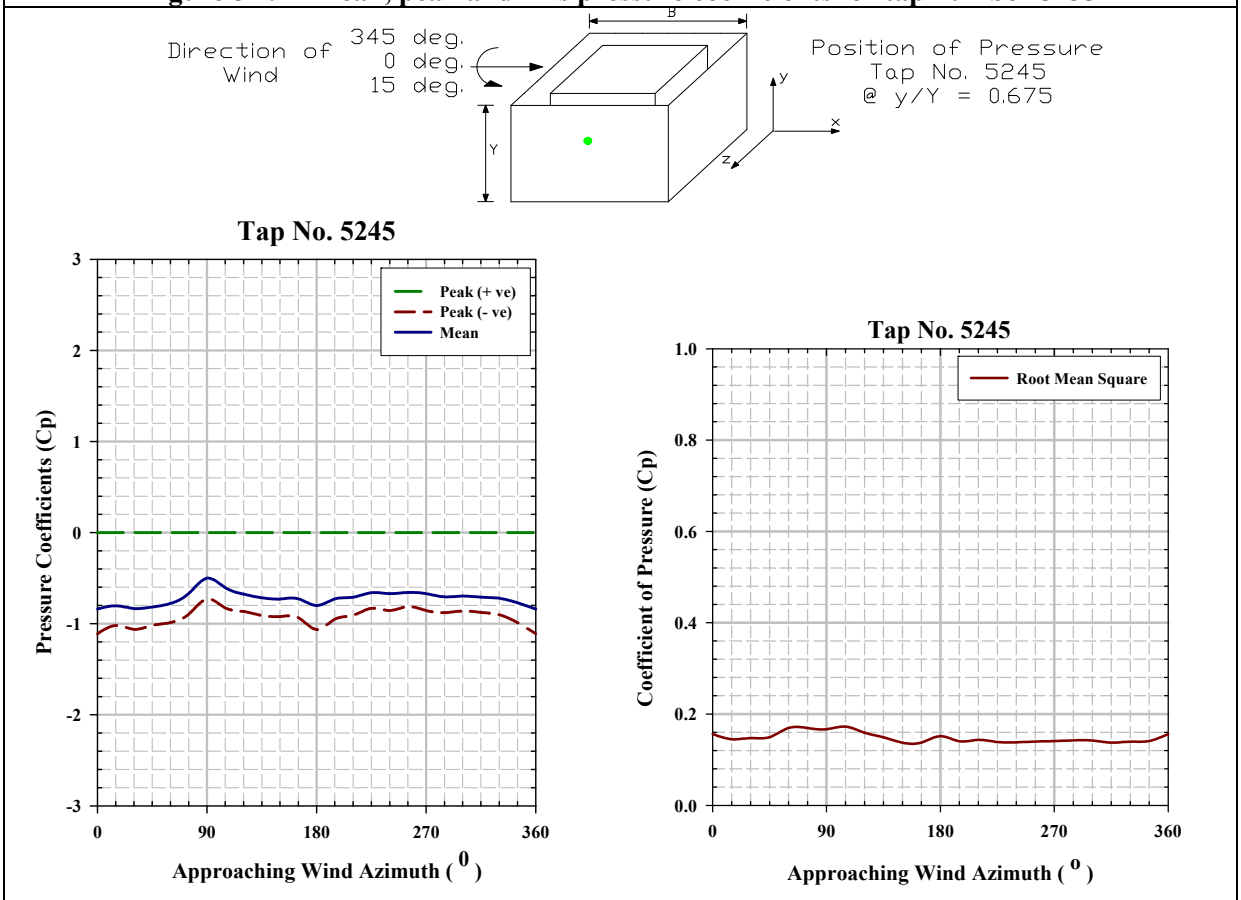

Figure 5A.28 Mean, peak and rms pressure coefficients for tap number 5245

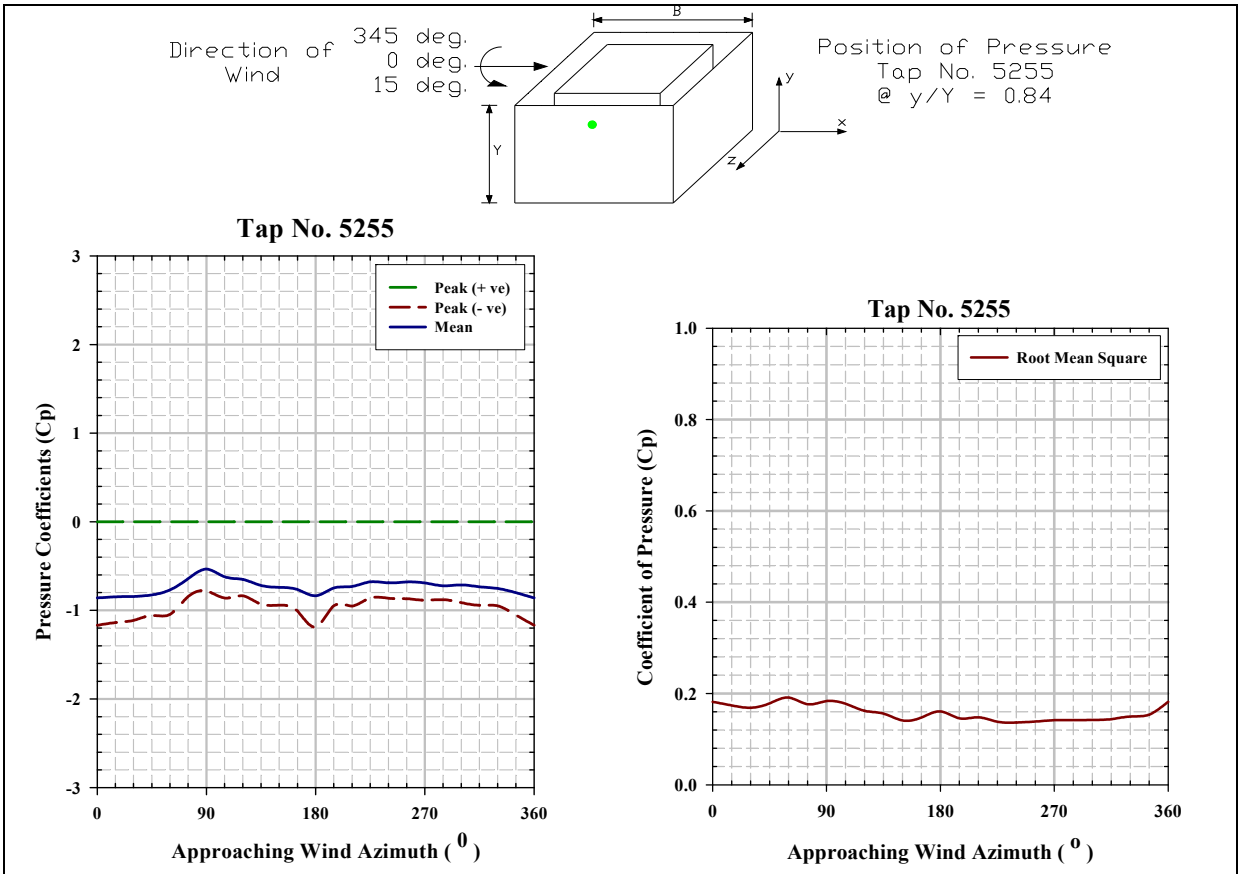

Figure 5A.29 Mean, peak and rms pressure coefficients for tap number 5255

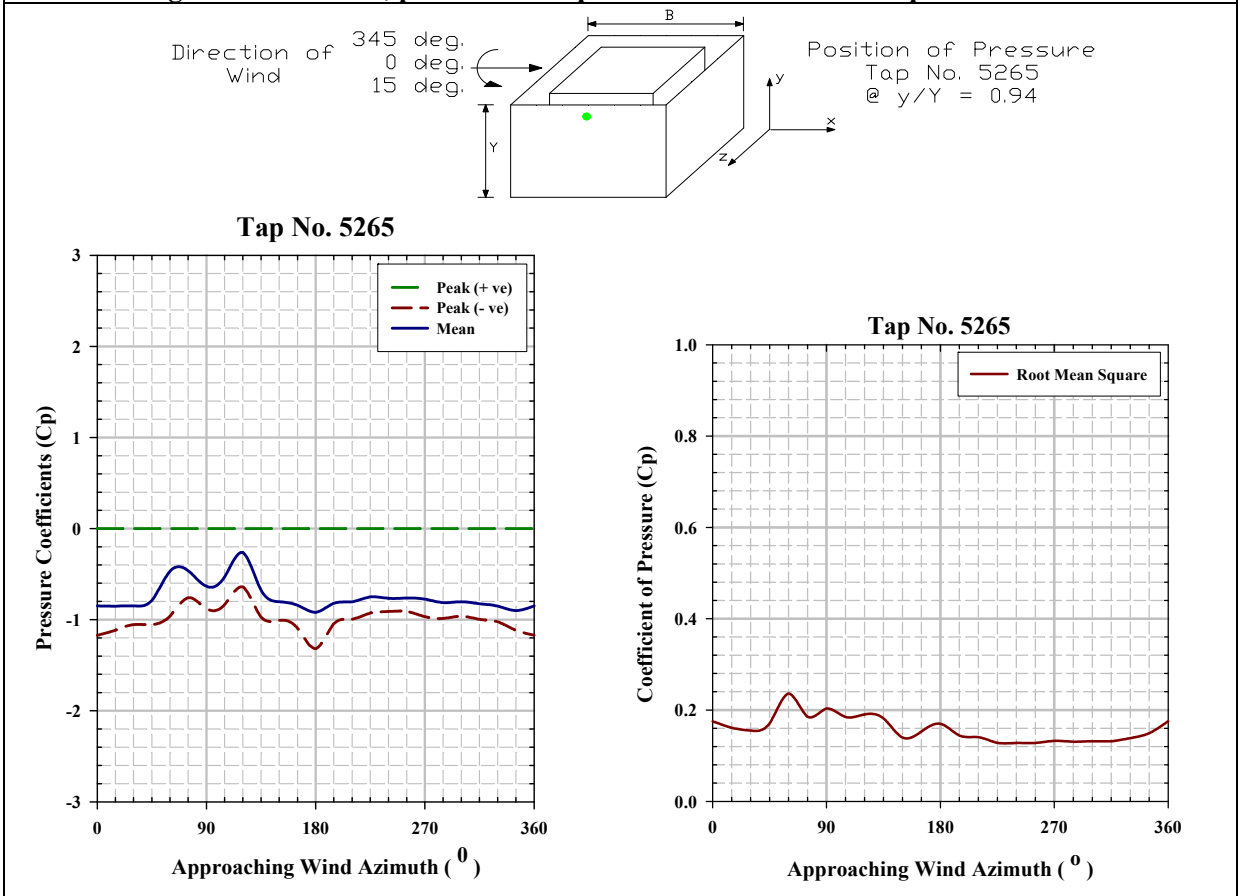

Figure 5A.30 Mean, peak and rms pressure coefficients for tap number 5265

Pressure Coefficient Contours on the Windward Inner Face of the Sheet Clad Scaffold for Type B Terrain

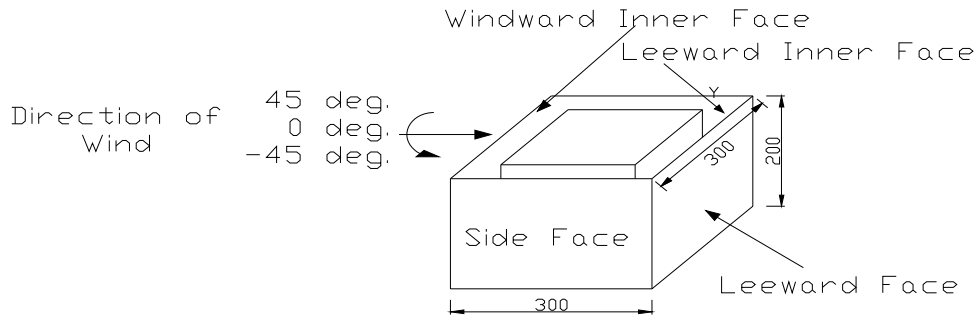

Figure 5B.1 Angle of attack of wind on windward outer face of the sheet clad scaffold surrounding SEB, direction of which varies from 45° to -45°

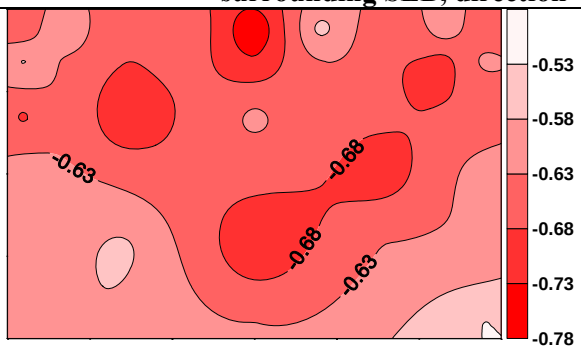

Figure 5B.2 Pressure coefficient contours on the windward inner face of the sheet clad scaffold when θ= 45°

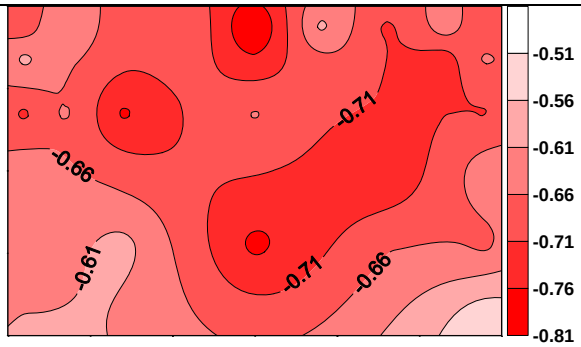

Figure 5B.3 Pressure coefficient contours on the windward inner face of the sheet clad scaffold when θ= 30°

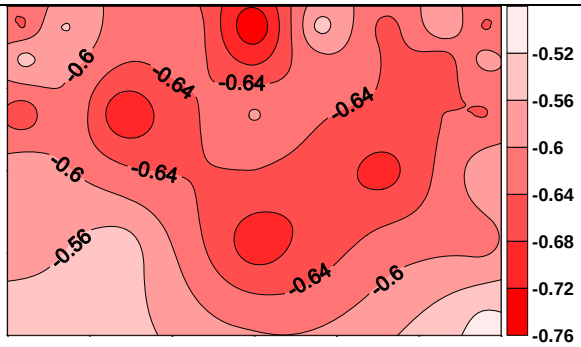

Figure 5B.4 Pressure coefficient contours on the windward inner face of the sheet clad scaffold when θ= 15°

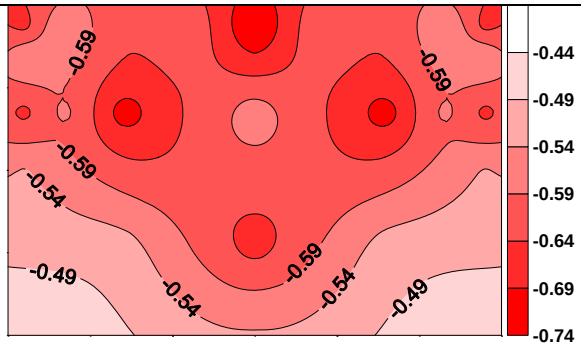

Figure 5B.5 Pressure coefficient contours on the windward inner face of the sheet clad scaffold when θ= 0°

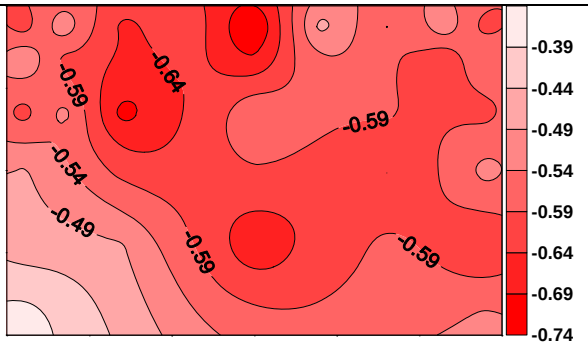

Figure 5B.6 Pressure coefficient contours on the windward inner face of the sheet clad scaffold when θ= -15°

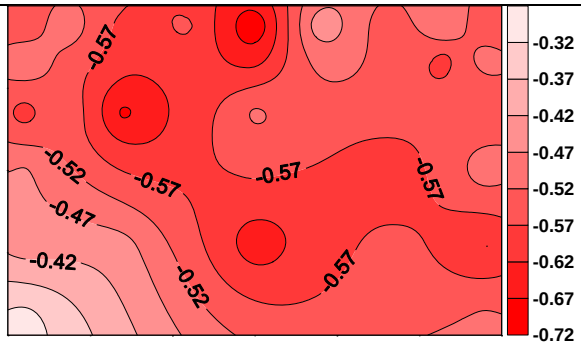

Figure 5B.7 Pressure coefficient contours on the windward inner face of the sheet clad scaffold when θ= -30°

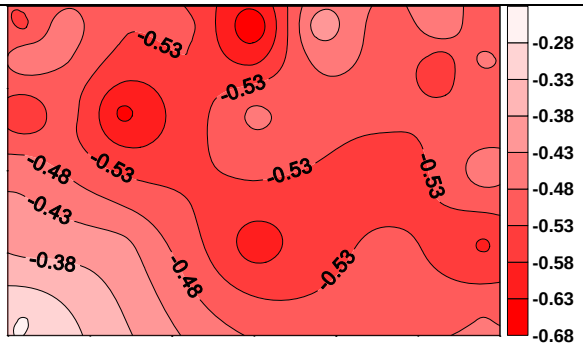

Figure 5B.8 Pressure coefficient contours on the windward inner face of the sheet clad scaffold when θ= -45°

Pressure Coefficient Contours on the Side Inner Face of the Sheet Clad Scaffold for Type B Terrain

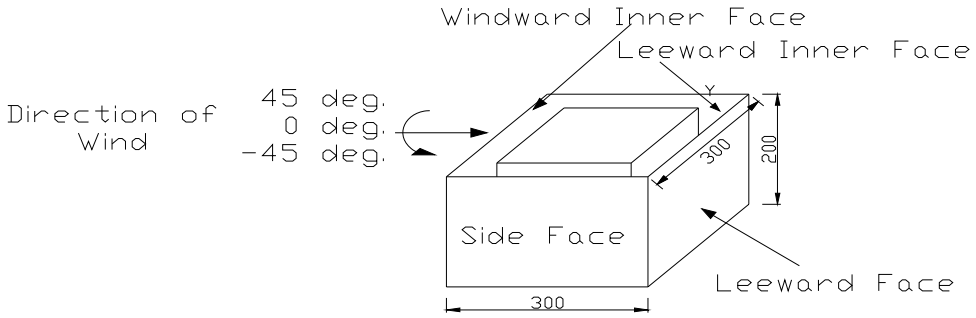

Figure 5B.9 Angle of attack of wind on windward outer face of the sheet clad scaffold surrounding SEB, direction of which varies from 45° to -45°

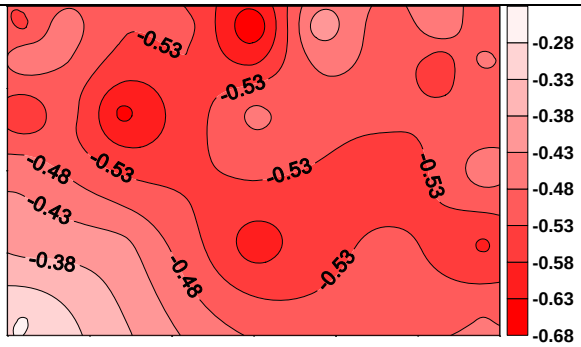

Figure 5B.10 Pressure coefficient contours on the side inner face of the sheet clad scaffold when θ= 45°

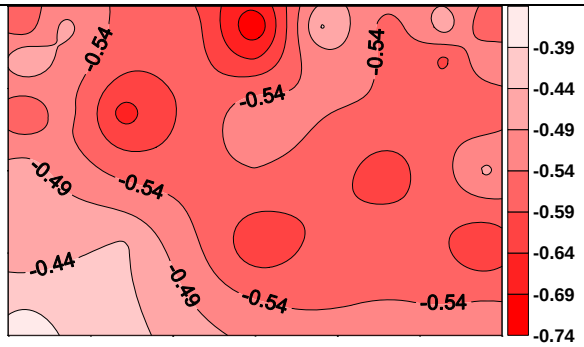

Figure 5B.11 Pressure coefficient contours on the side inner face of the sheet clad scaffold when θ= 30°

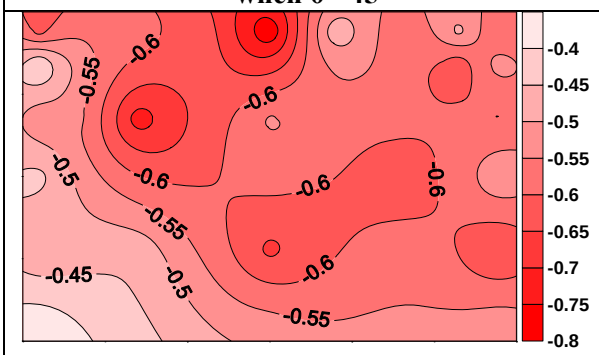

Figure 5B.12 Pressure coefficient contours on the side inner face of the sheet clad scaffold when θ= 15°

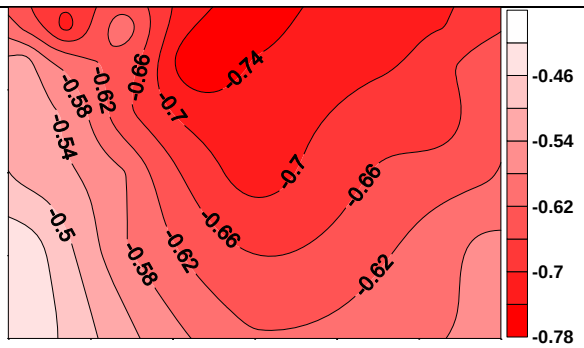

Figure 5B.13 Pressure coefficient contours on the side inner face of the sheet clad scaffold when θ= 0°

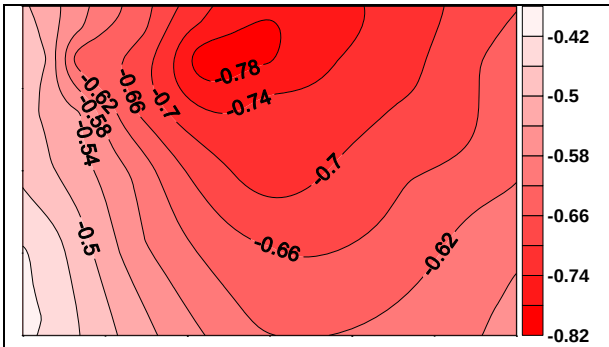

Figure 5B.14 Pressure coefficient contours on the side inner face of the sheet clad scaffold when θ= -15°

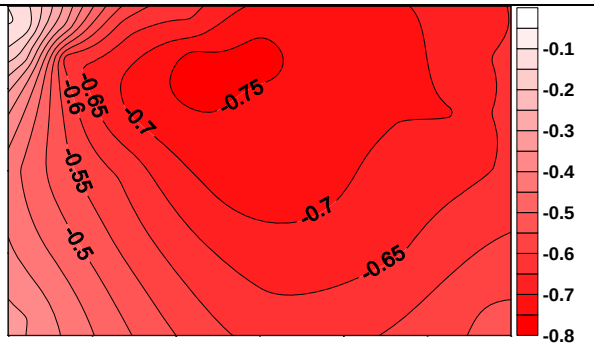

Figure 5B.15 Pressure coefficient contours on the side inner face of the sheet clad scaffold when θ= -30°

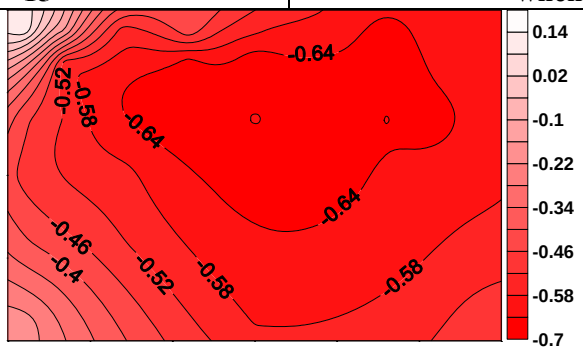

Figure 5B.16 Pressure coefficient contours on the side inner face of the sheet clad scaffold when θ= -45°

Pressure Coefficient Contours on the Leeward Inner Face of the Sheet Clad Scaffold

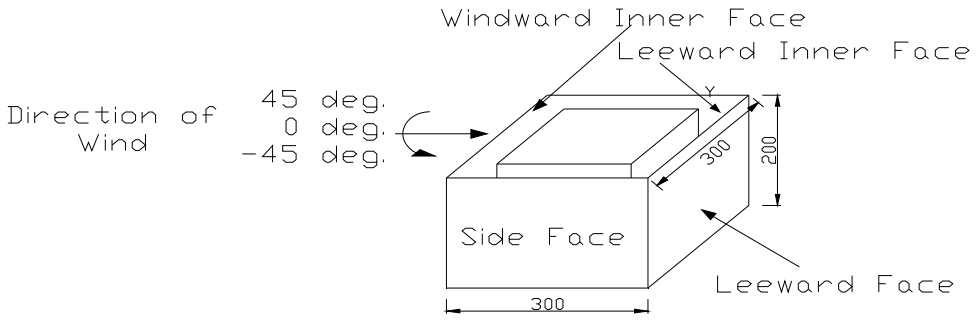

Figure 5B.17 Angle of attack of wind on windward outer face of the elevated sheet clad scaffold surrounding SEB, direction of which varies from 45° to -45°

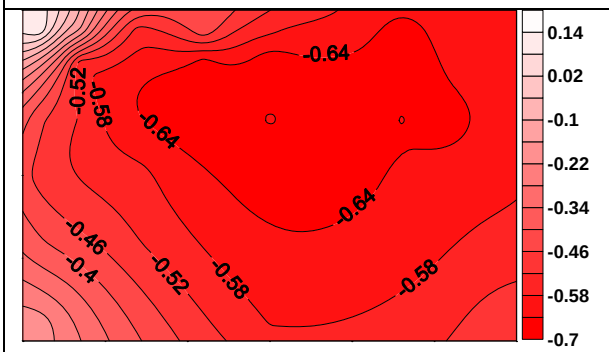

Figure 5B.18 Pressure coefficient contours on the leeward inner face of the sheet clad scaffold when θ= 45°

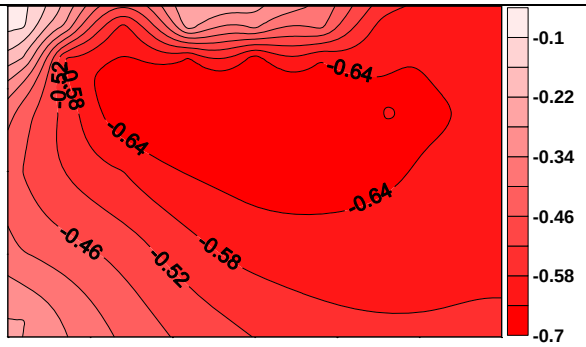

Figure 5B.19 Pressure coefficient contours on the leeward inner face of the sheet clad scaffold when θ= 30°

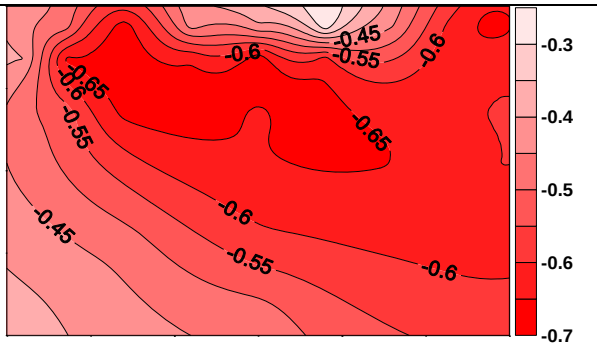

Figure 5B.20 Pressure coefficient contours on the leeward inner face of the sheet clad scaffold when θ= 15°

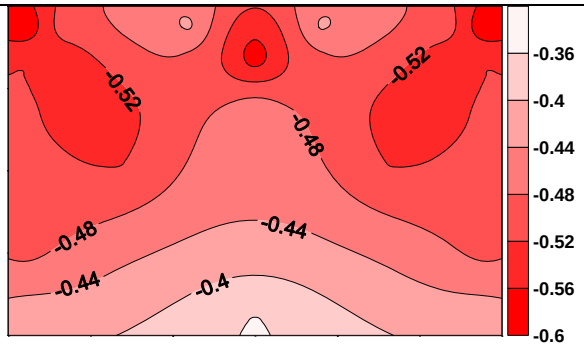

Figure 5B.21 Pressure coefficient contours on the leeward inner face of the sheet clad scaffold when θ= 0°

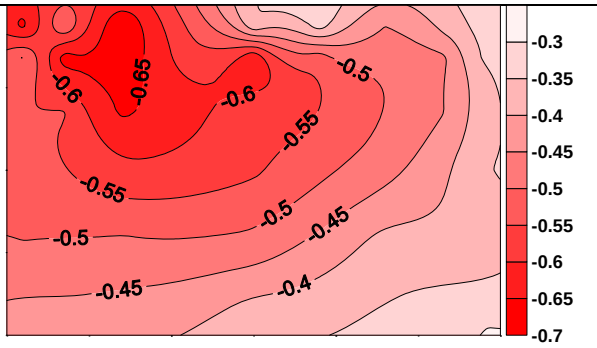

Figure 5B.22 Pressure coefficient contours on the leeward inner face of the sheet clad scaffold when θ= -15°

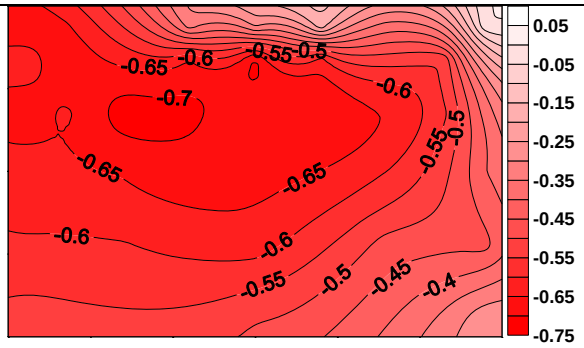

Figure 5B.23 Pressure coefficient contours on the leeward inner face of the sheet clad scaffold when θ= -30°

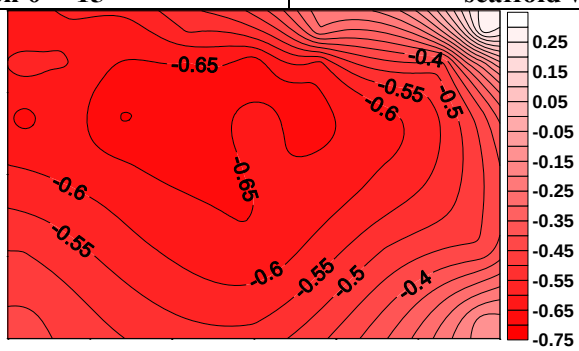

Figure 5B.24 Pressure coefficient contours on the leeward inner face of the sheet clad scaffold when θ= -45°

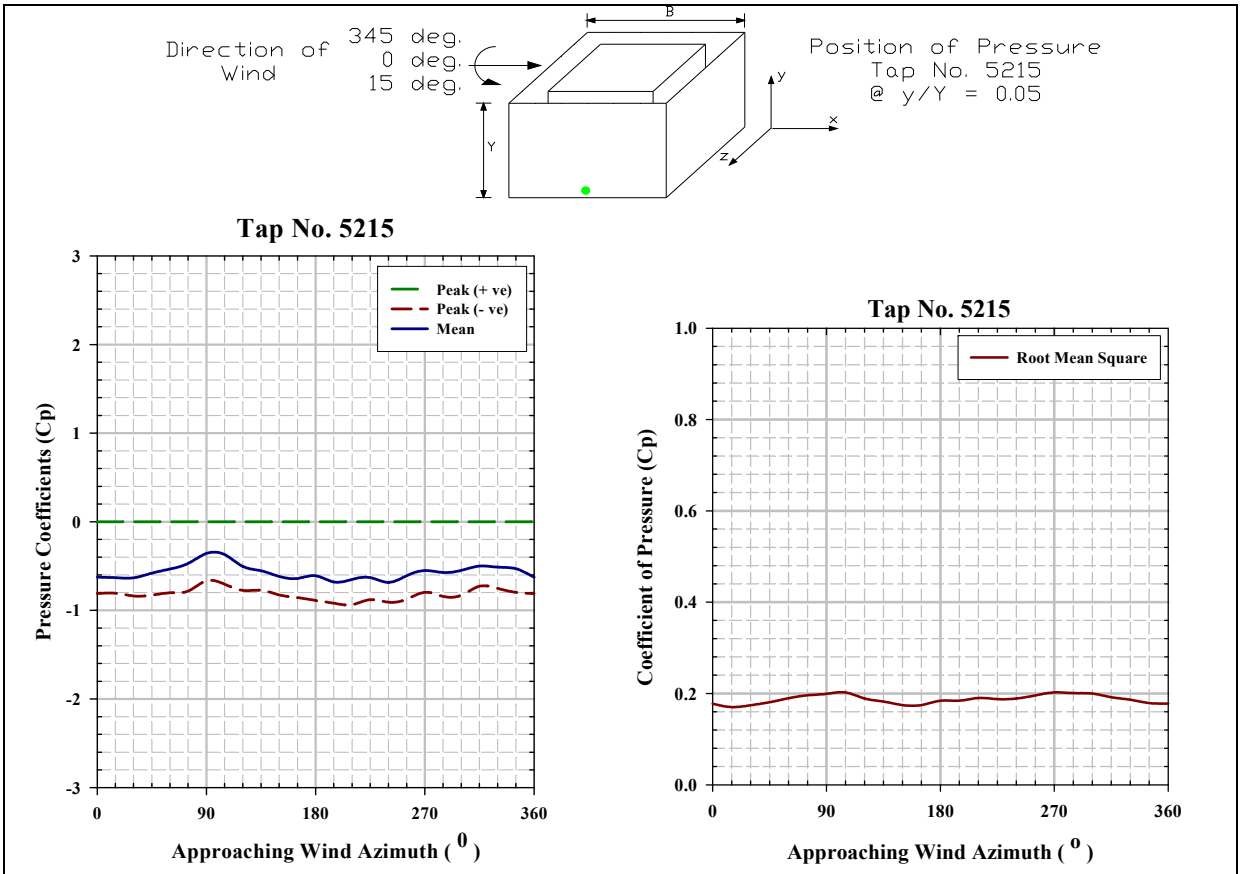

Figure 5B.25 Mean, peak and rms pressure coefficients for tap number 5215

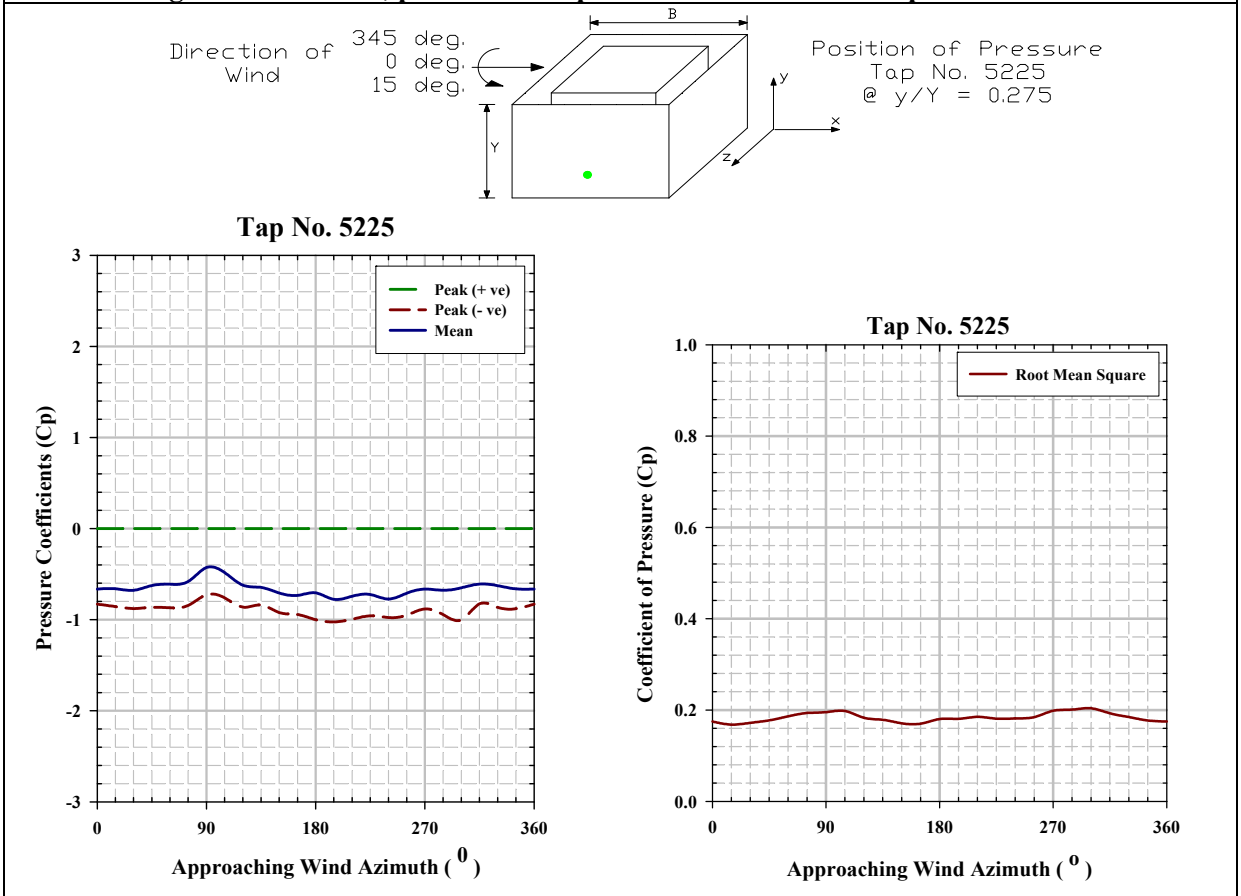

Figure 5B.26 Mean, peak and rms pressure coefficients for tap number 5225

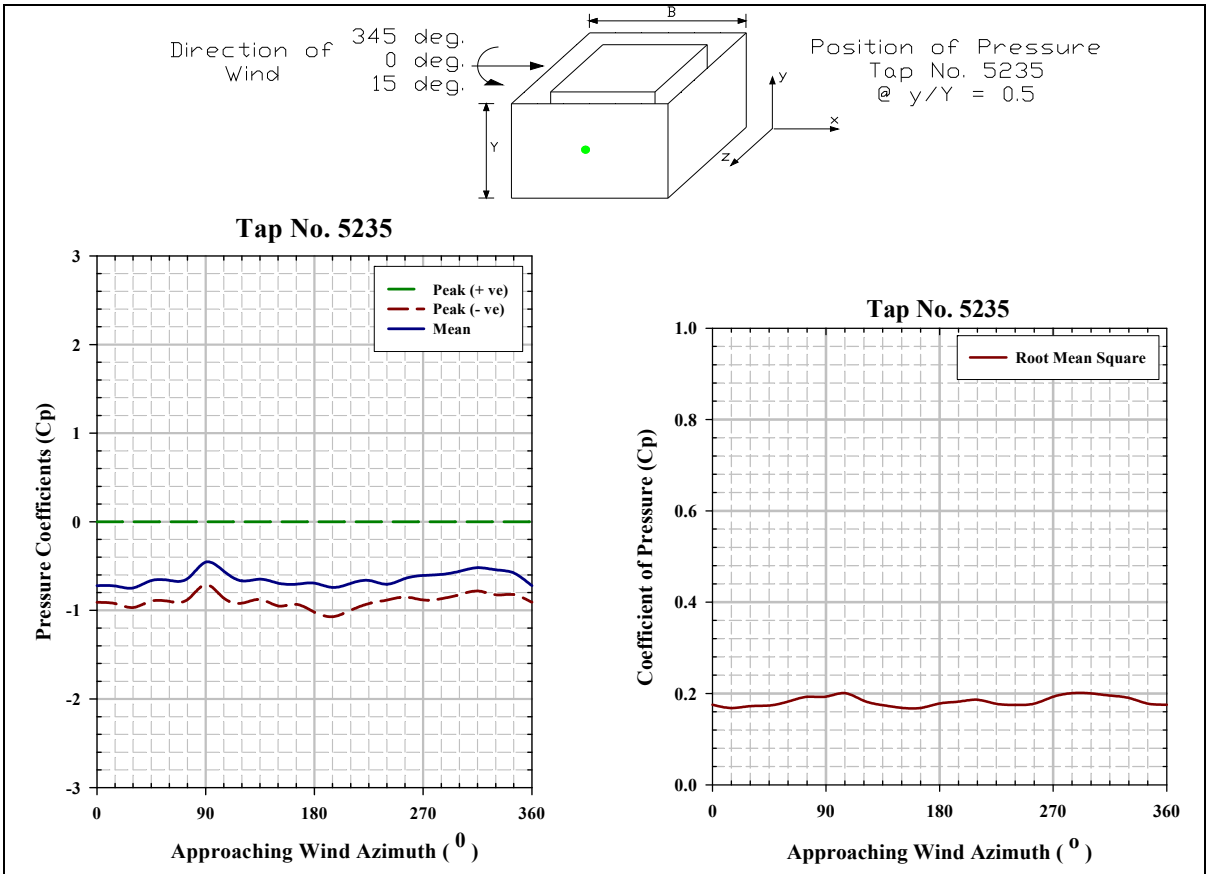

Figure 5B.27 Mean, peak and rms pressure coefficients for tap number 5235

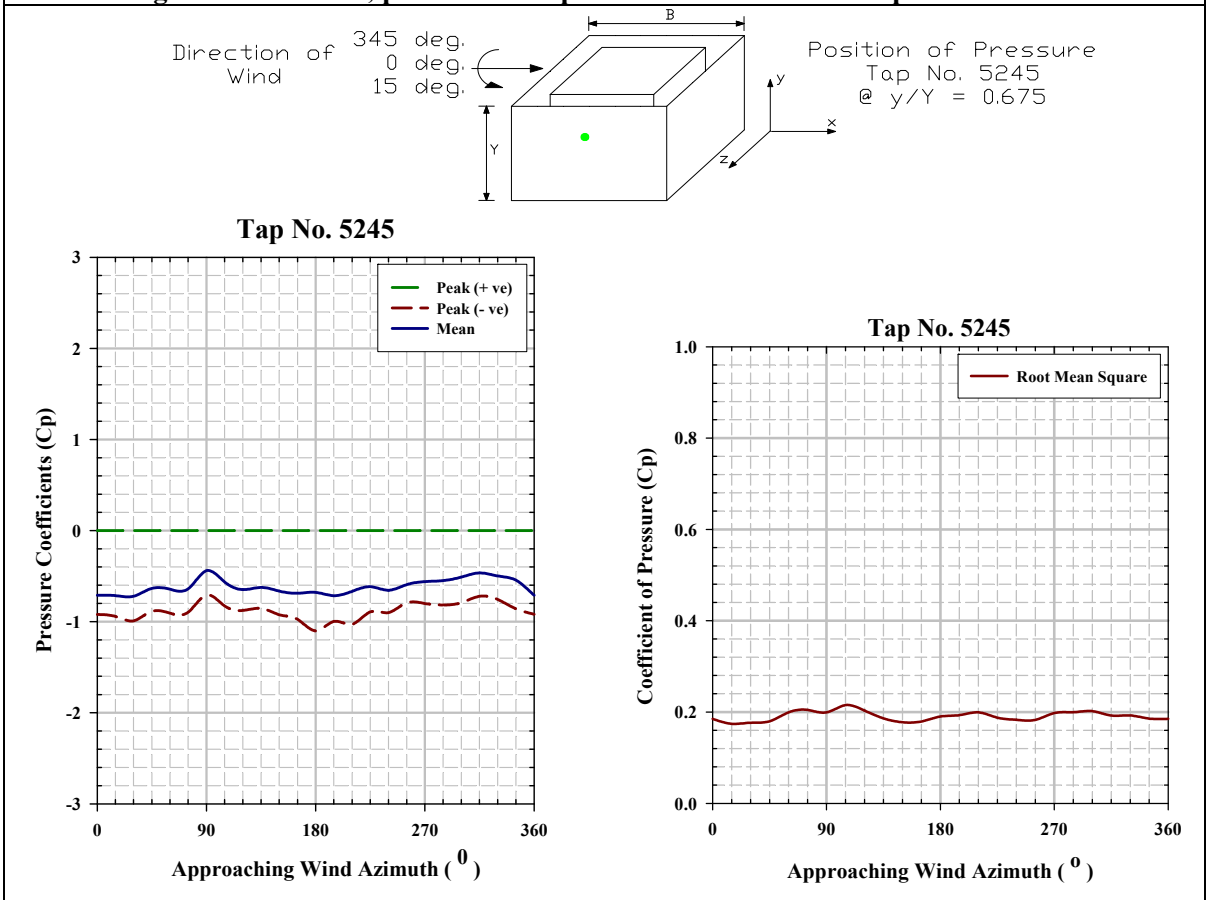

Figure 5B.28 Mean, peak and rms pressure coefficients for tap number 5245

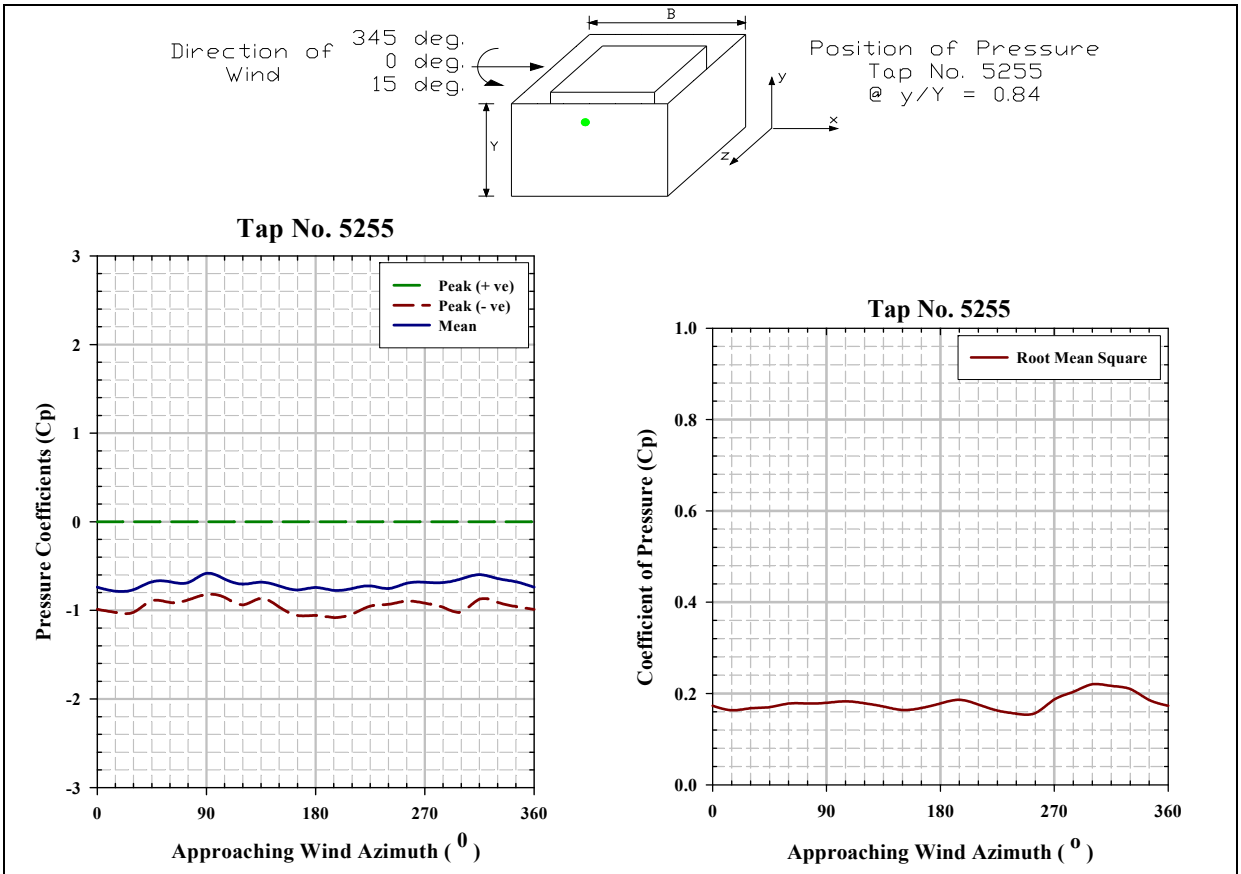

Figure 5B.29 Mean, peak and rms pressure coefficients for tap number 5255

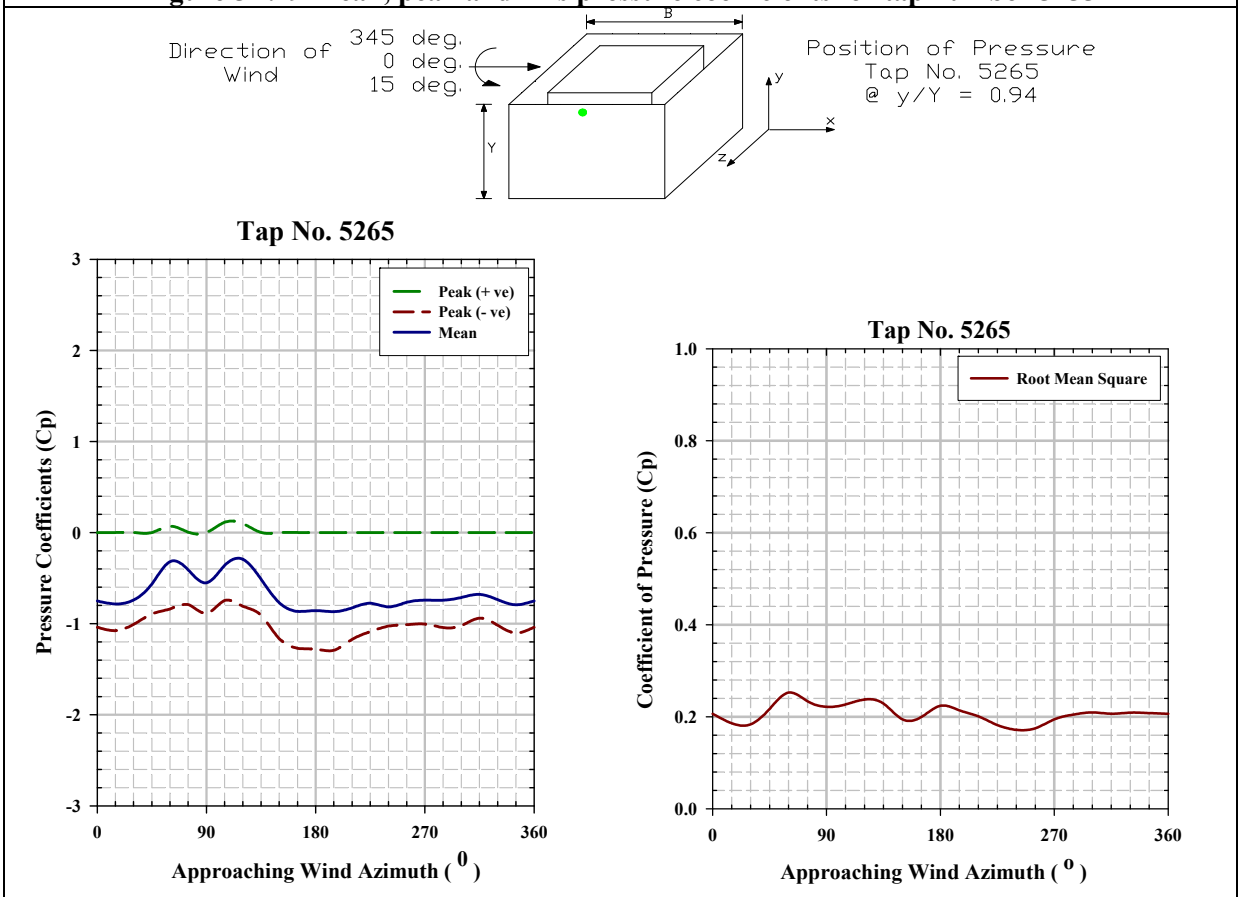

Figure 5B.30 Mean, peak and rms pressure coefficients for tap number 5215

EXPERIMENT-6

Pressure Coefficients on the Outer Face of the Elevated Sheet Clad Scaffold

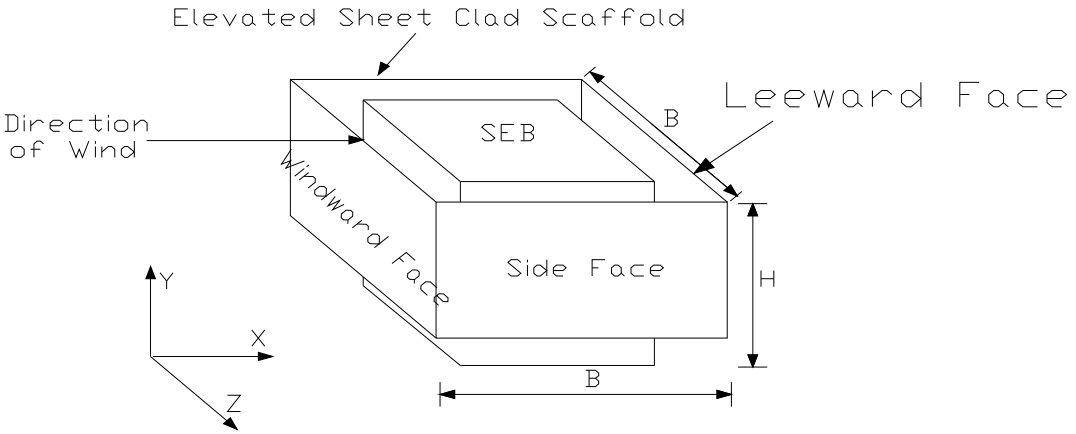

Figure 6.1 Scaled cubical SEB surrounded by elevated sheet clad scaffold

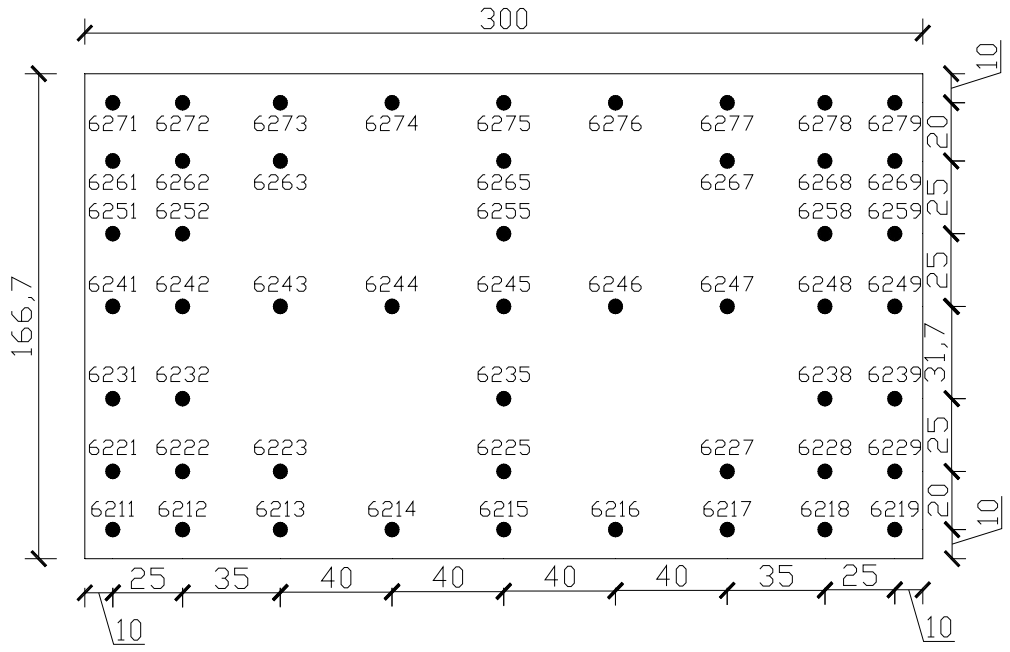

Figure 6.2 Pressure tap locations on the outer face of the elevated sheet clad scaffold

Pressure Coefficient Contours on the Windward Outer Face of the Elevated Sheet Clad Scaffold for Type A Terrain

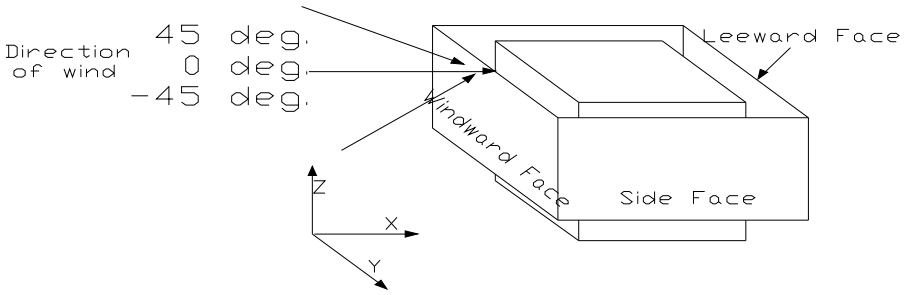

Figure 6A.1 Angle of attack of wind on windward outer face of the elevated sheet clad scaffold surrounding SEB, direction of which varies from 45° to -45°

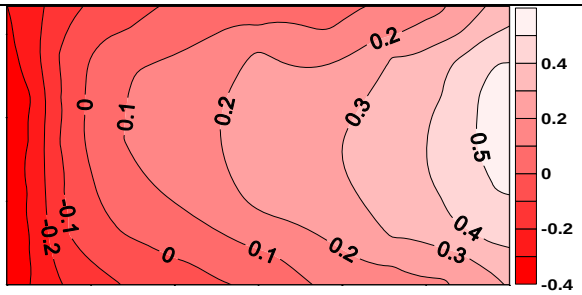

Figure 6A.2 Pressure coefficient contours on the windward outer face of the elevated sheet clad scaffold when θ= 45°

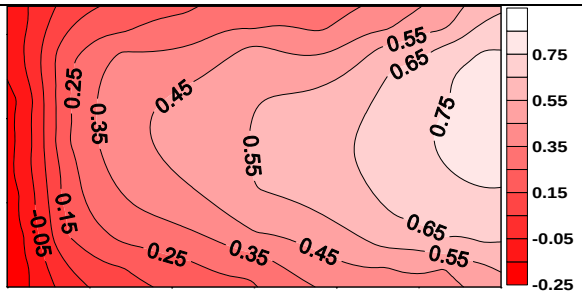

Figure 6A.3 Pressure coefficient contours on the windward outer face of the elevated sheet clad scaffold when θ= 30°

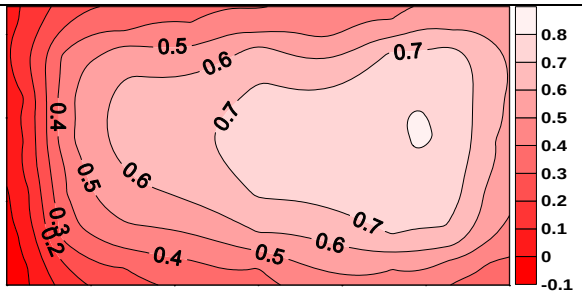

Figure 6A.4 Pressure coefficient contours on the windward outer face of the elevated sheet clad scaffold when θ= 15°

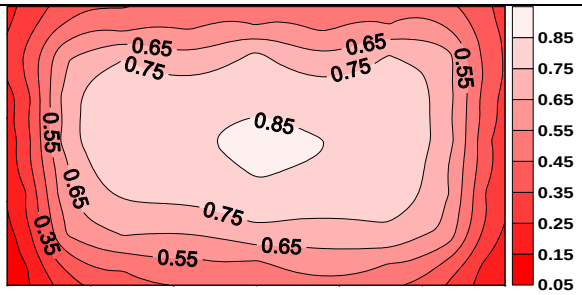

Figure 6A.5 Pressure coefficient contours on the windward outer face of the elevated sheet clad scaffold when θ= 0°

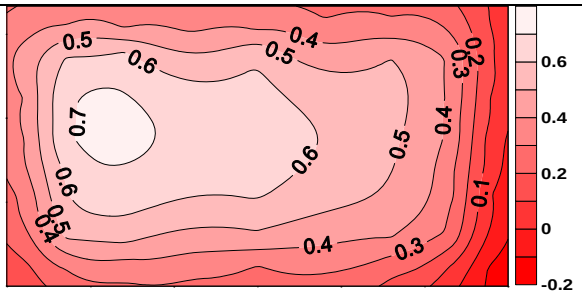

Figure 6A.6 Pressure coefficient contours on the windward outer face of the elevated sheet clad scaffold when θ= -15°

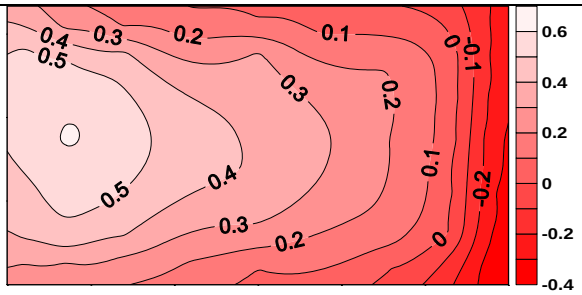

Figure 6A.7 Pressure coefficient contours on the windward outer face of the elevated sheet clad scaffold when θ= -30°

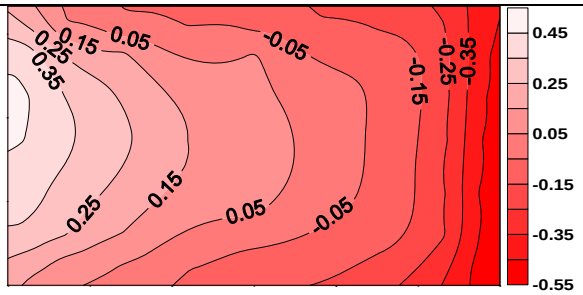

Figure 6A.8 Pressure coefficient contours on the windward outer face of the elevated sheet clad scaffold when θ= -45^o

Pressure Coefficient Contours on the Side Outer Face of the Elevated Sheet Clad Scaffold for Type A Terrain

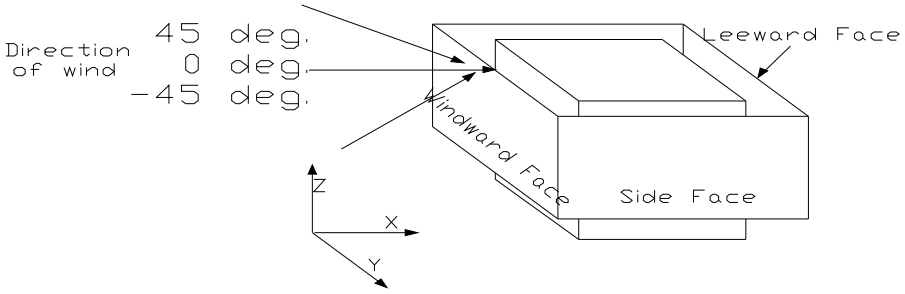

Figure 6A.9 Angle of attack of wind on windward outer face of the elevated sheet clad scaffold surrounding SEB, direction of which varies from 45^o to -45^o

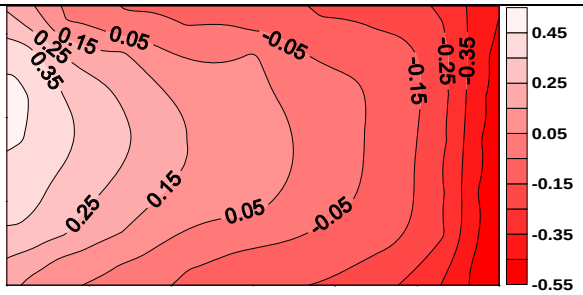

Figure 6A.10 Pressure coefficient contours on the side outer face of the elevated sheet clad scaffold when θ= 45^o

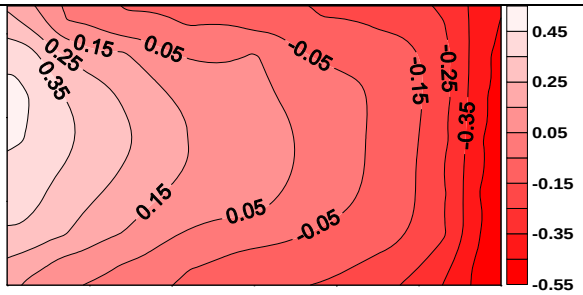

Figure 6A.11 Pressure coefficient contours on the side outer face of the elevated sheet clad scaffold when θ= 30^o

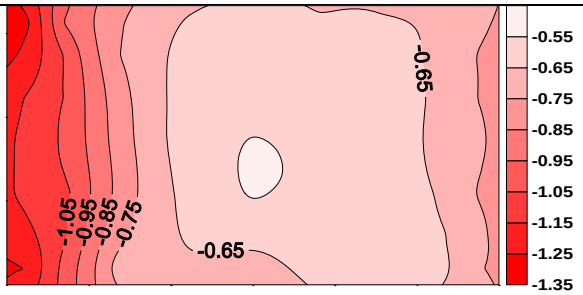

Figure 6A.12 Pressure coefficient contours on the side outer face of the elevated sheet clad scaffold when θ= 15^o

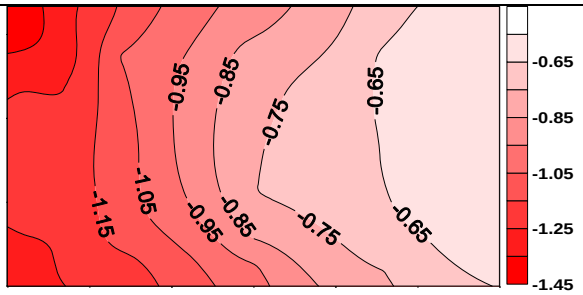

Figure 6A.13 Pressure coefficient contours on the side outer face of the elevated sheet clad scaffold when θ= 0^o

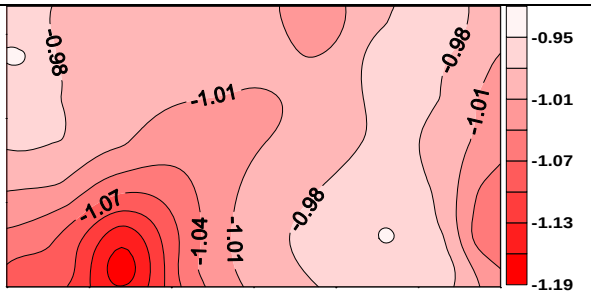

Figure 6A.14 Pressure coefficient contours on the side outer face of the elevated sheet clad scaffold when θ= -15^o

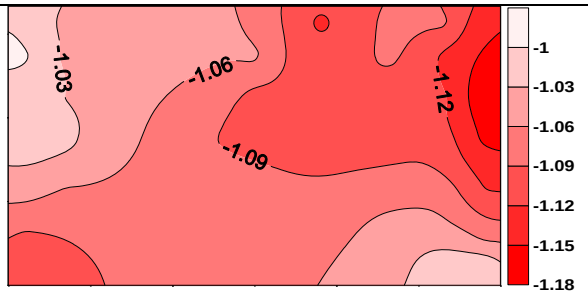

Figure 6A.15 Pressure coefficient contours on the windward outer face of the elevated sheet clad scaffold when θ= -30^o

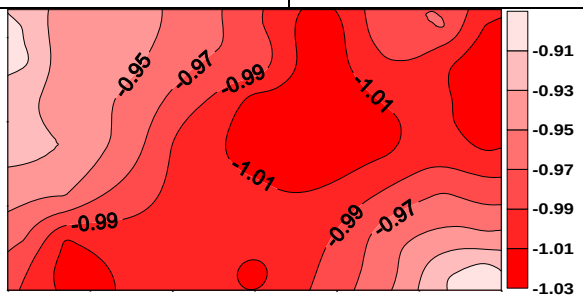

Figure 6A.16 Pressure coefficient contours on the side outer face of the elevated sheet clad scaffold when θ= -45^o

Pressure Coefficient Contours on the Leeward Outer Face of the Elevated Sheet Clad Scaffold for Type A Terrain

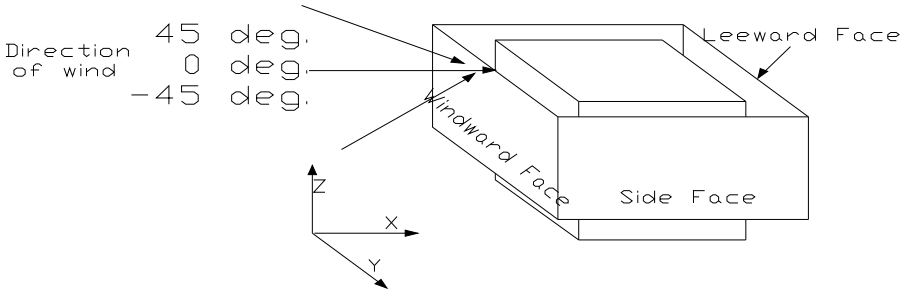

Figure 6A.17 Angle of attack of wind on windward outer face of the elevated sheet clad scaffold surrounding SEB, direction of which varies from 45^o to -45^o

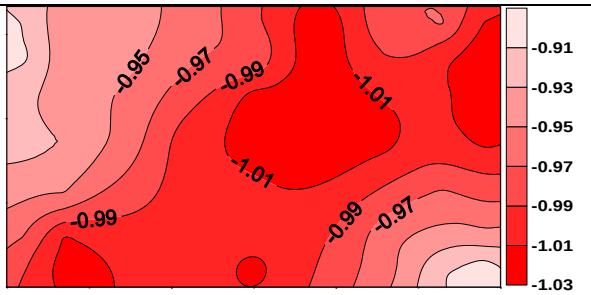

Figure 6A.18 Pressure coefficient contours on the leeward outer face of the elevated sheet clad scaffold when θ= 45^o

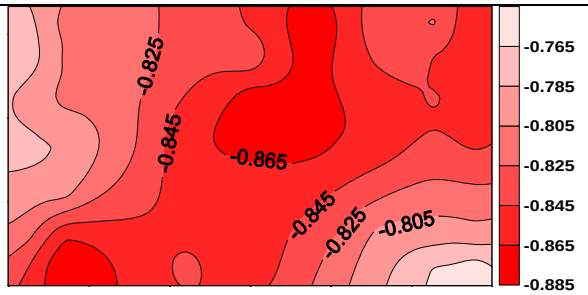

Figure 6A.19 Pressure coefficient contours on the leeward outer face of the elevated sheet clad scaffold when θ= 30^o

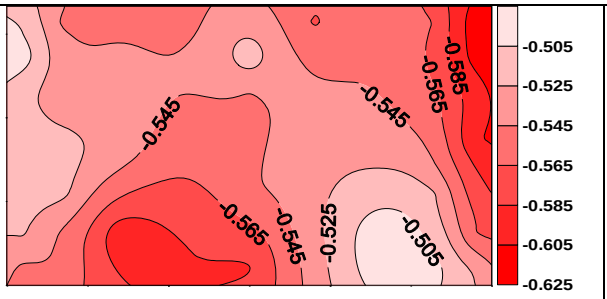

Figure 6A.20 Pressure coefficient contours on the leeward outer face of the elevated sheet clad scaffold when θ= 15^o

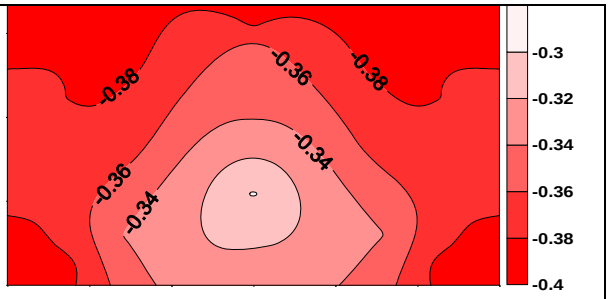

Figure 6A.21 Pressure coefficient contours on the leeward outer face of the elevated sheet clad scaffold when θ= 0^o

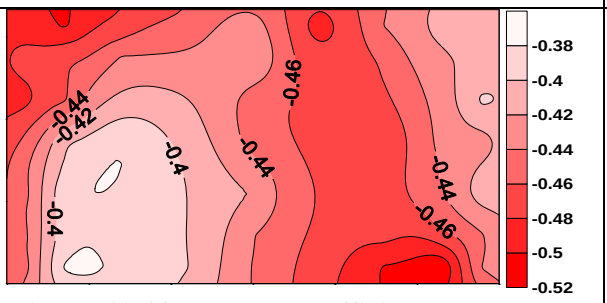

Figure 6A.22 Pressure coefficient contours on the leeward outer face of the elevated sheet clad scaffold when θ= -15^o

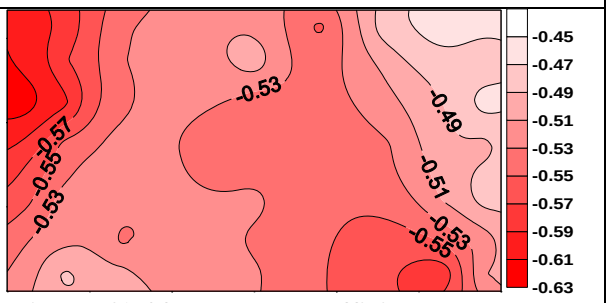

Figure 6A.23 Pressure coefficient contours on the leeward outer face of the elevated sheet clad scaffold when θ= -30^o

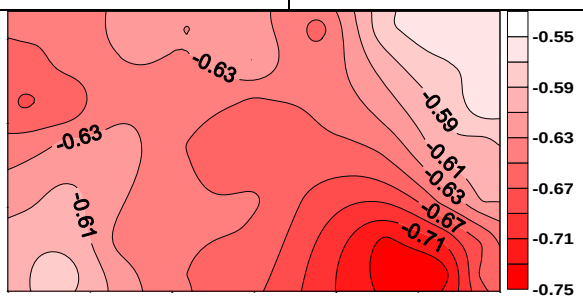

Figure 6A.24 Pressure coefficient contours on the leeward outer face of the elevated sheet clad scaffold when θ= -45^o

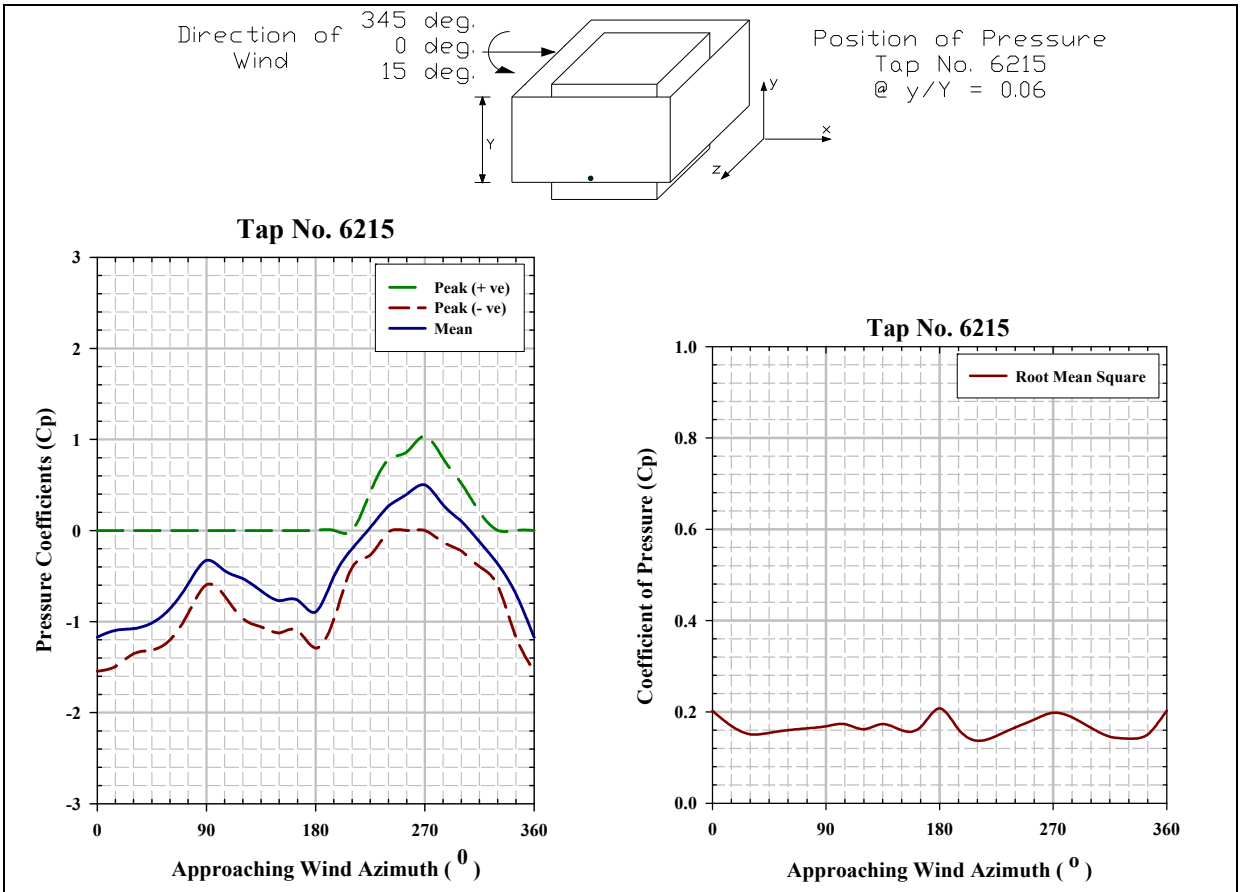

Figure 6A.25 Mean, peak and rms pressure coefficients for tap number 6215

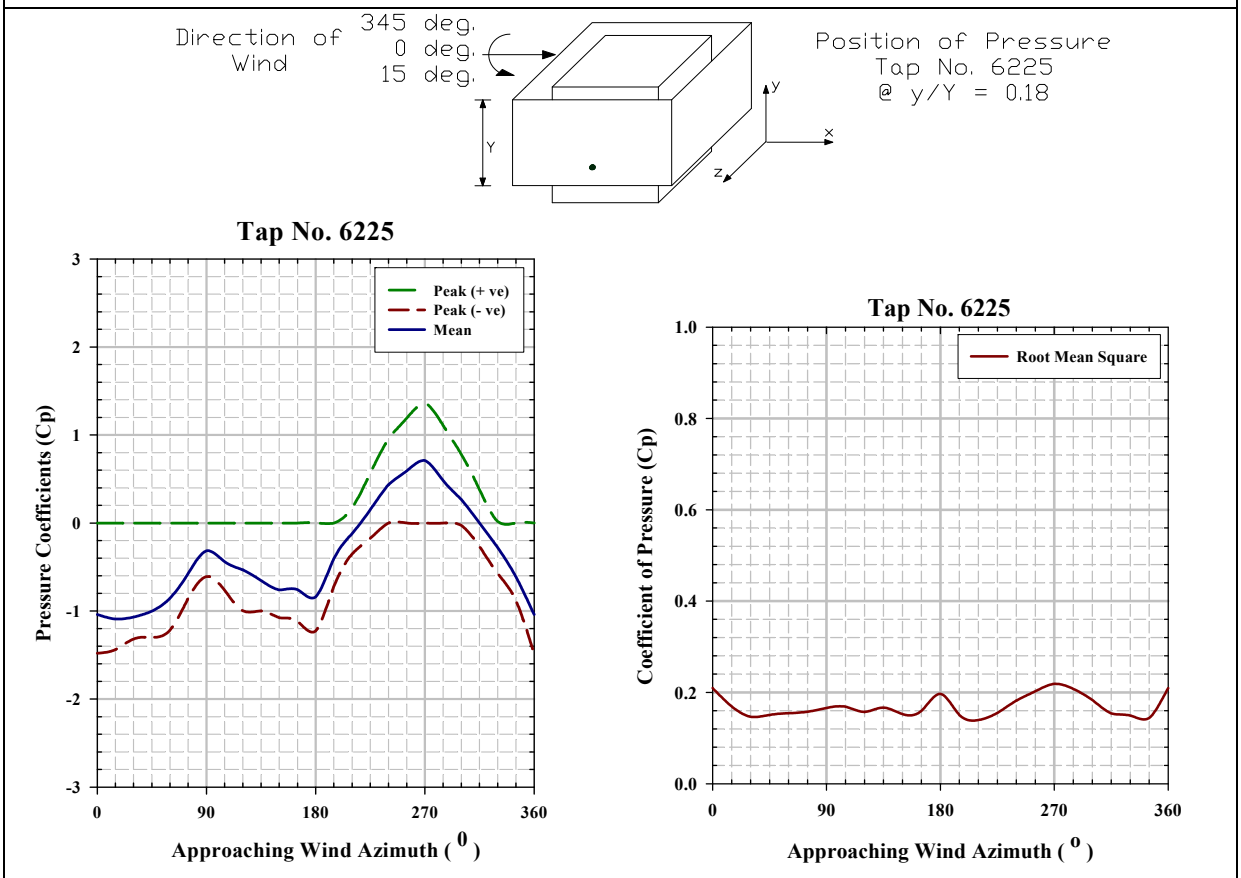

Figure 6A.26 Mean, peak and rms pressure coefficients for tap number 6225

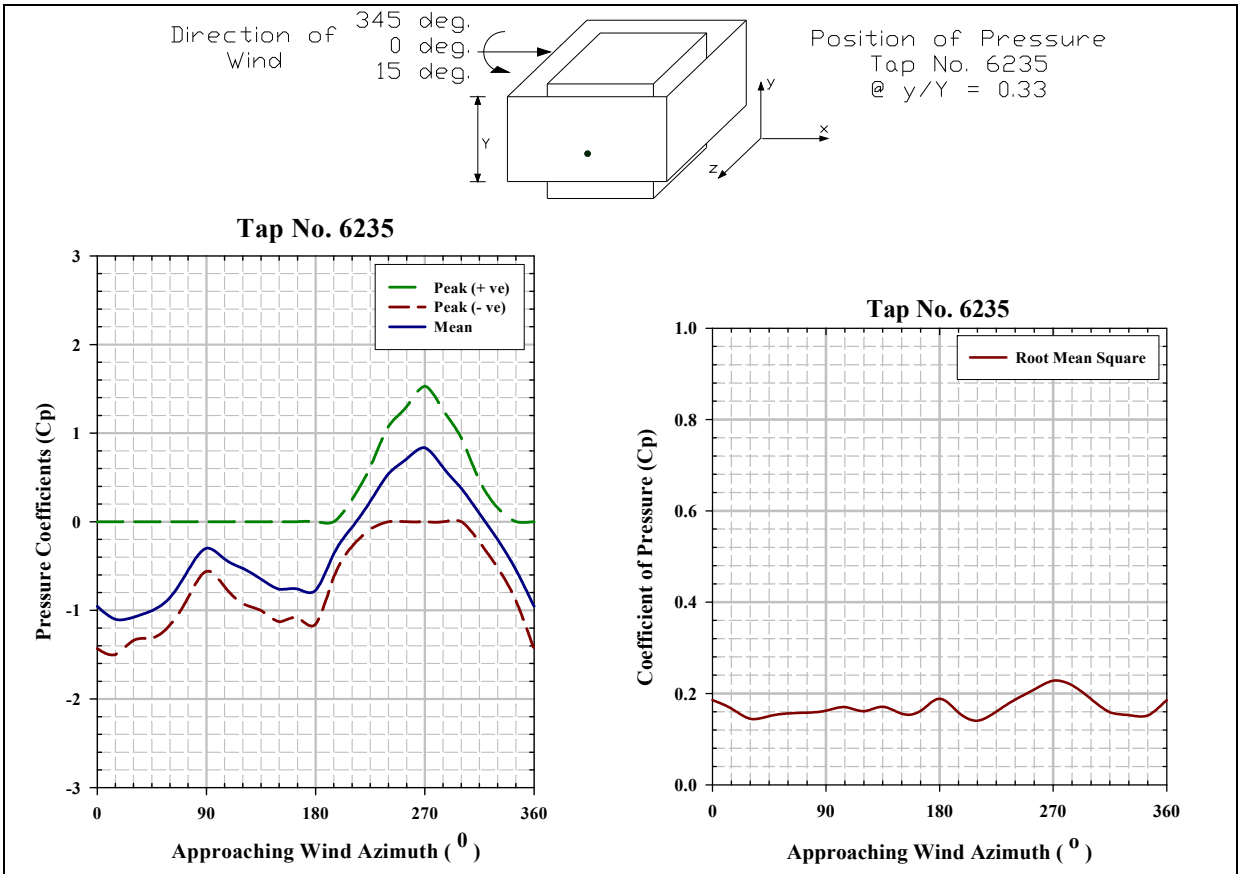

Figure 6A.27 Mean, peak and rms pressure coefficients for tap number 6235

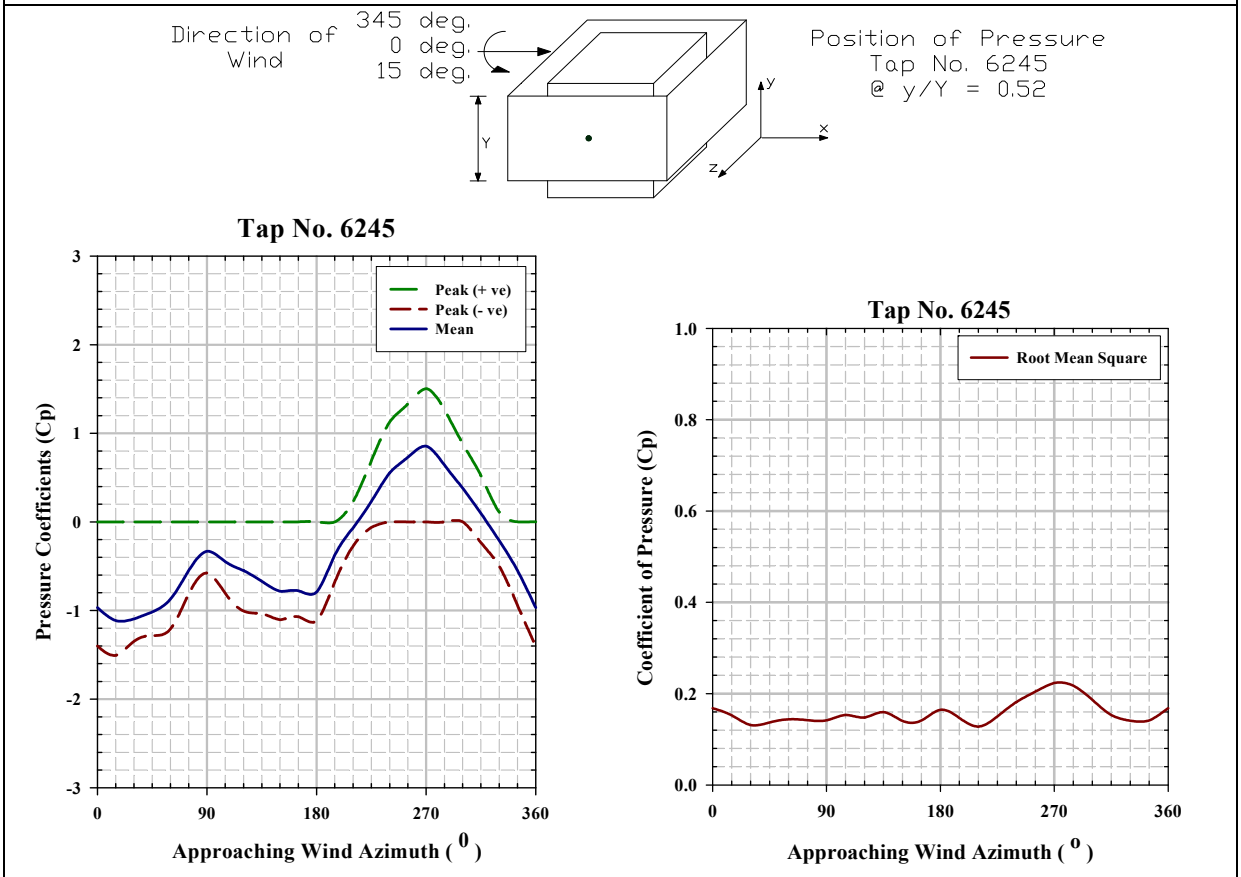

Figure 6A.28 Mean, peak and rms pressure coefficients for tap number 6245

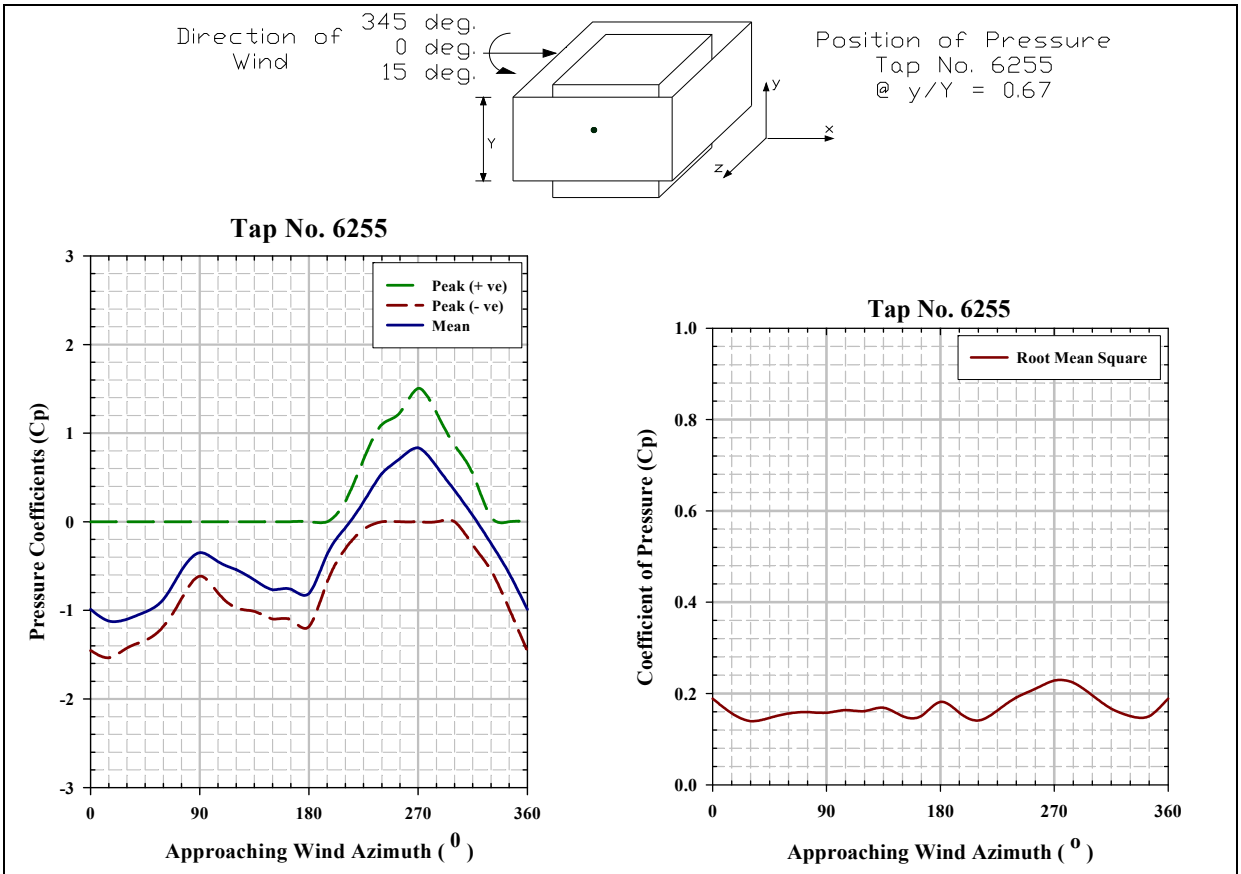

Figure 6A.29 Mean, peak and rms pressure coefficients for tap number 6255

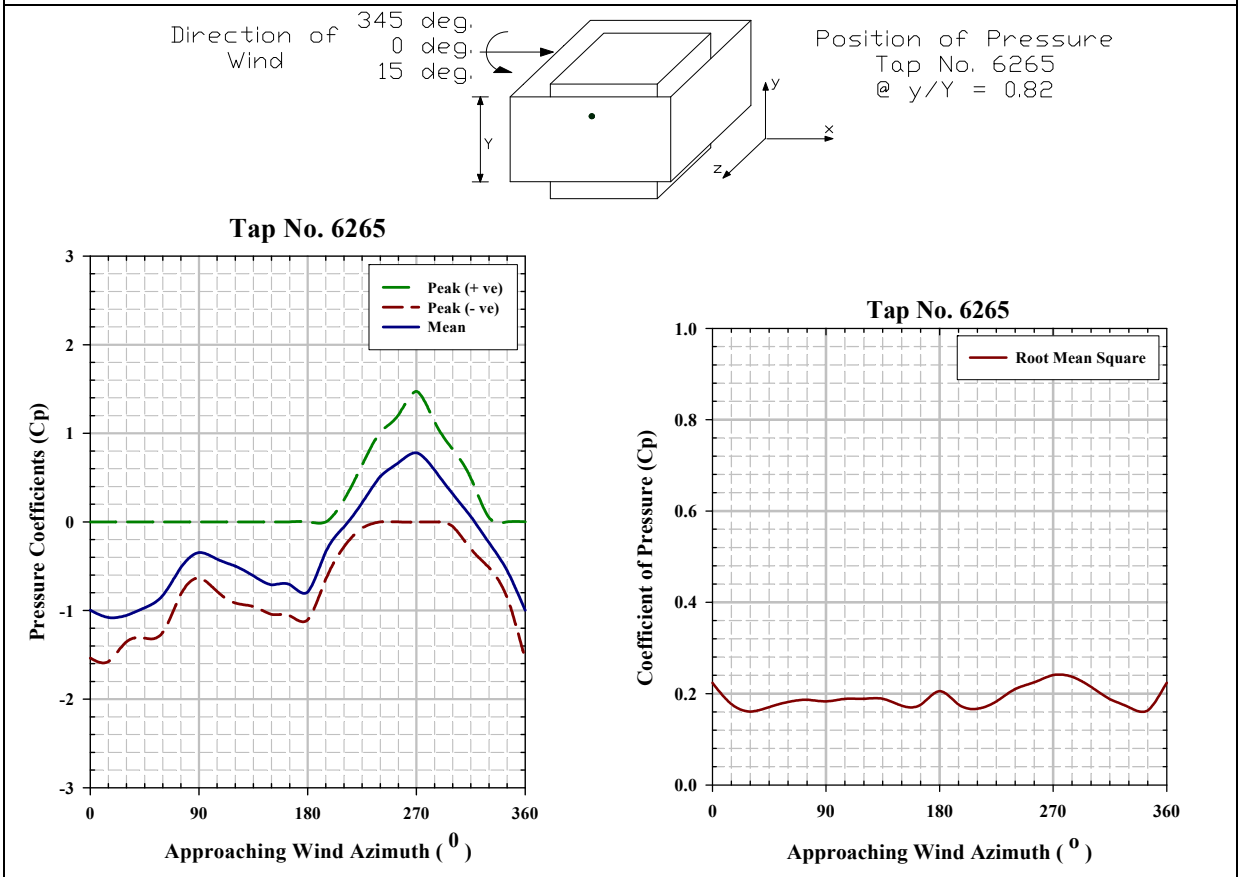

Figure 6A.30 Mean, peak and rms pressure coefficients for tap number 6265

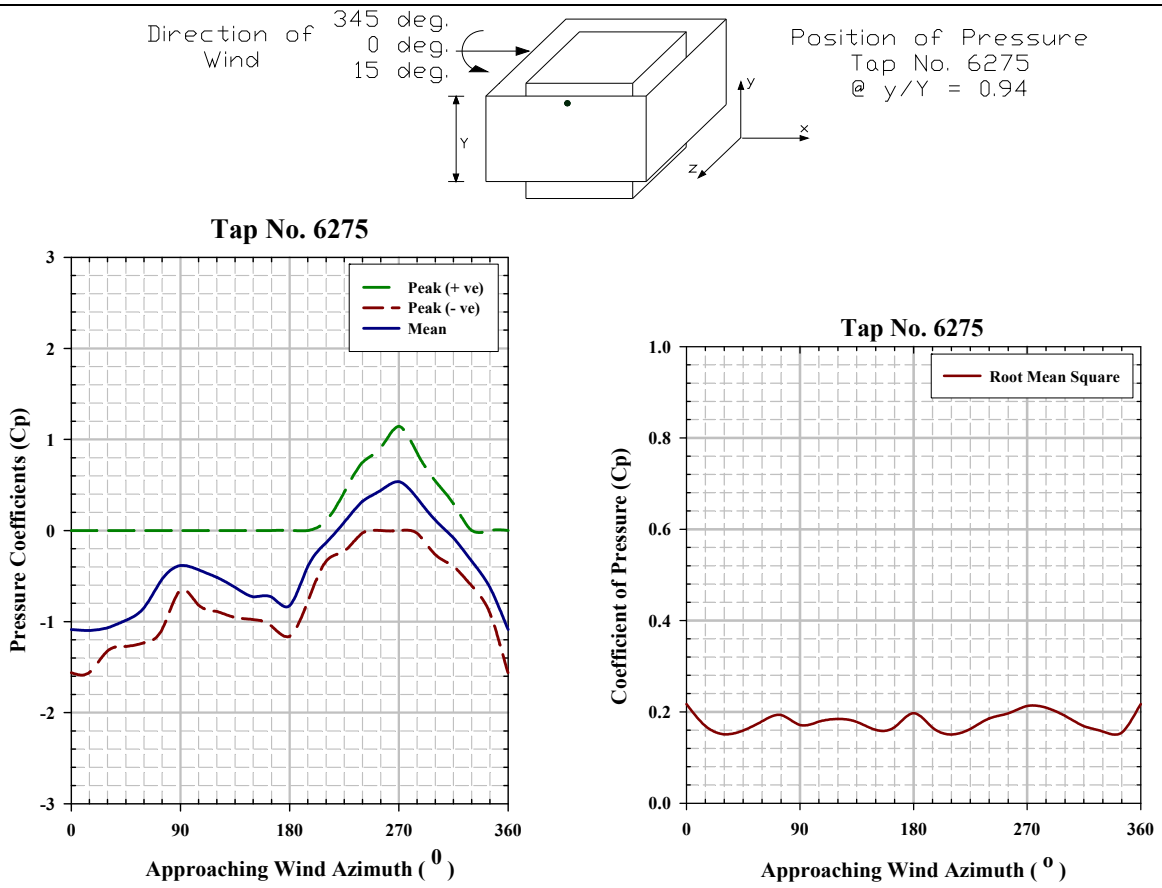

Figure 6A.31 Mean, peak and rms pressure coefficients for tap number 6275

Pressure Coefficient Contours on the Windward Outer Face of the Elevated Sheet Clad Scaffold for Type B Terrain

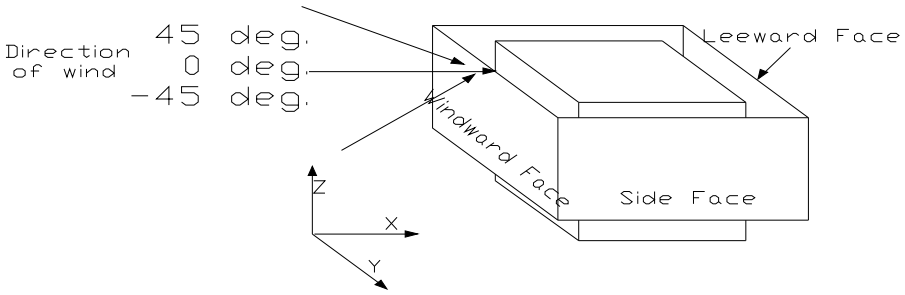

Figure 6B.1 Angle of attack of wind on windward outer face of the elevated sheet clad scaffold surrounding SEB, direction of which varies from 45° to -45°

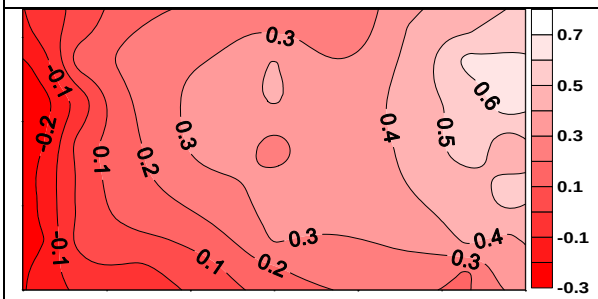

Figure 6B.2 Pressure coefficient contours on the windward outer face of the elevated sheet clad scaffold when θ= 45°

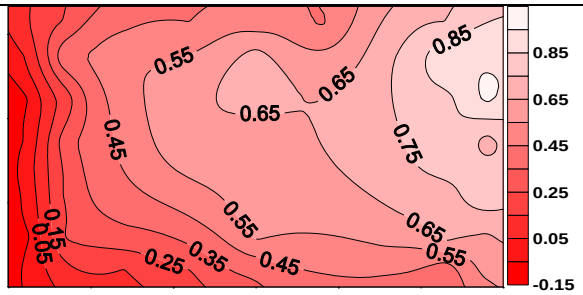

Figure 6B.3 Pressure coefficient contours on the windward outer face of the elevated sheet clad scaffold when θ= 30°

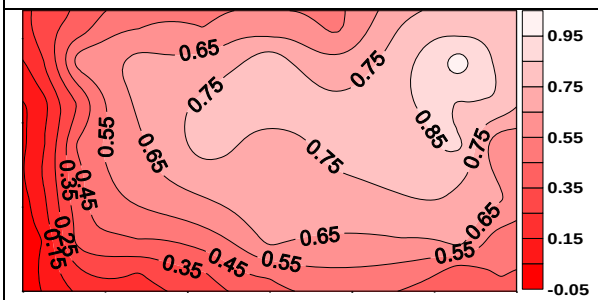

Figure 6B.4 Pressure coefficient contours on the windward outer face of the elevated sheet clad scaffold when θ= 15°

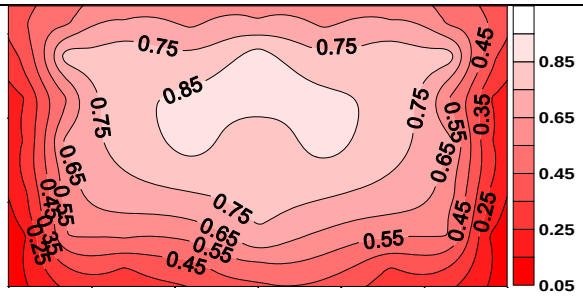

Figure 6B.5 Pressure coefficient contours on the windward outer face of the elevated sheet clad scaffold when θ= 0°

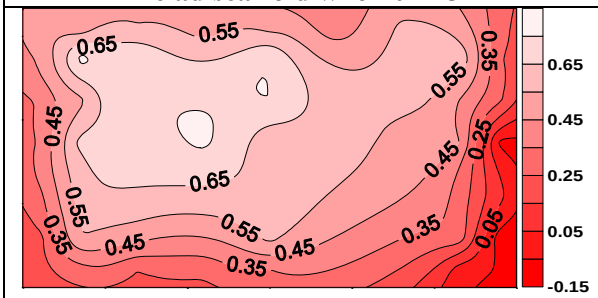

Figure 6B.6 Pressure coefficient contours on the windward outer face of the elevated sheet clad scaffold when θ= -15°

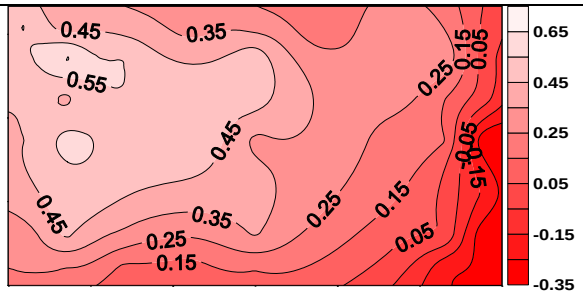

Figure 6B.7 Pressure coefficient contours on the windward outer face of the elevated sheet clad scaffold when θ= -30°

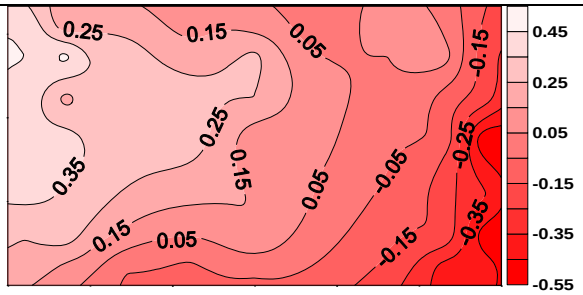

Figure 6B.8 Pressure coefficient contours on the windward outer face of the elevated sheet clad scaffold when θ= -45^o

Pressure Coefficient Contours on the Side Outer Face of the Elevated Sheet Clad Scaffold

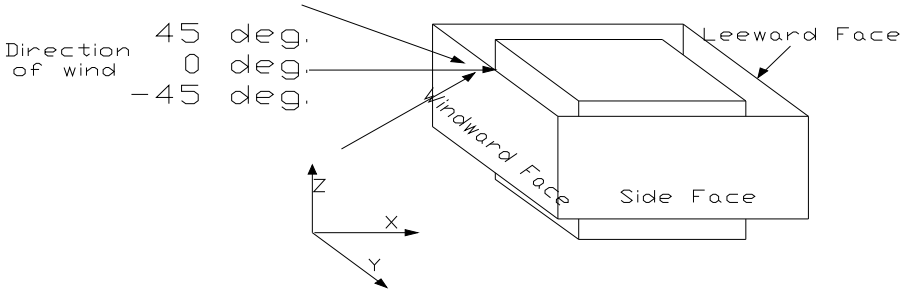

Figure 6B.9 Angle of attack of wind on windward outer face of the elevated sheet clad scaffold surrounding SEB, direction of which varies from 45^o to -45^o

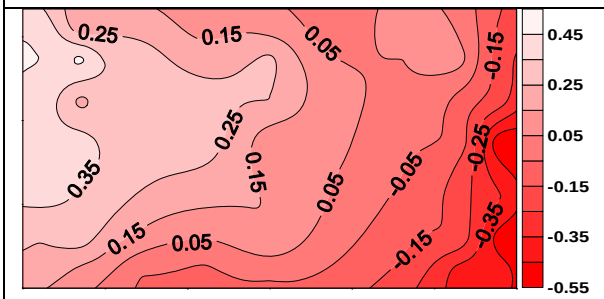

Figure 6B.10 Pressure coefficient contours on the side outer face of the elevated sheet clad scaffold when θ= 45^o

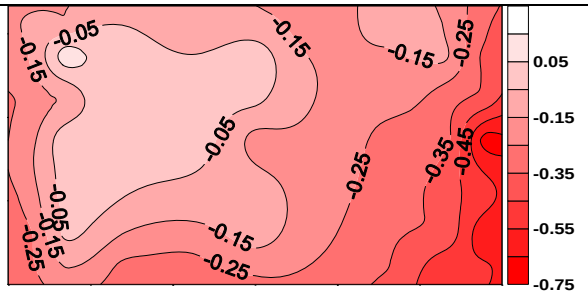

Figure 6B.11 Pressure coefficient contours on the side outer face of the elevated sheet clad scaffold when θ= 30^o

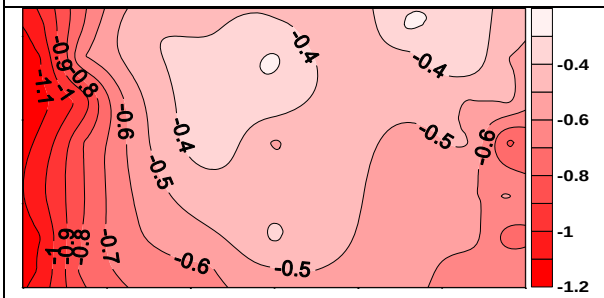

Figure 6B.12 Pressure coefficient contours on the side outer face of the elevated sheet clad scaffold when θ= 15^o

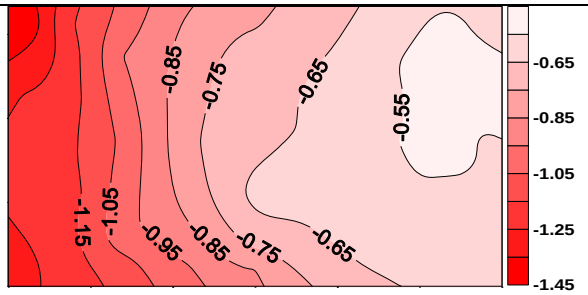

Figure 6B.13 Pressure coefficient contours on the side outer face of the elevated sheet clad scaffold when θ= 0^o

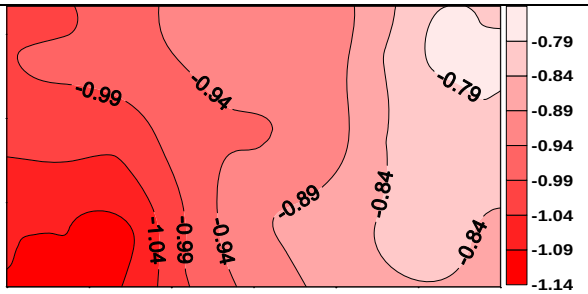

Figure 6B.14 Pressure coefficient contours on the side outer face of the elevated sheet clad scaffold when θ= -15^o

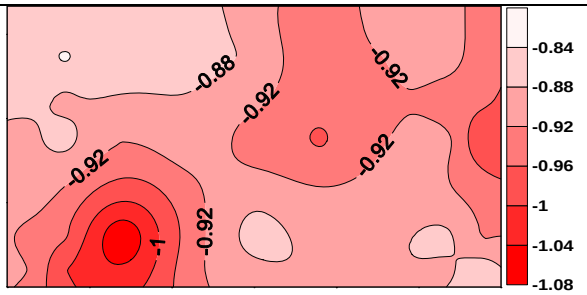

Figure 6B.15 Pressure coefficient contours on the windward outer face of the elevated sheet clad scaffold when θ= -30^o

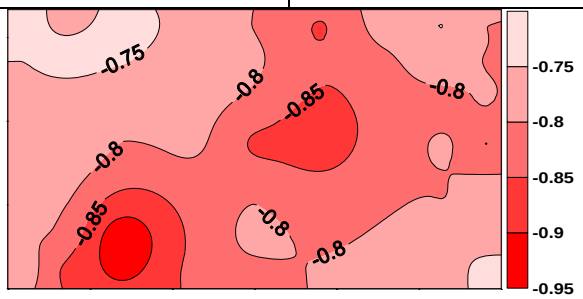

Figure 6B.16 Pressure coefficient contours on the side outer face of the elevated sheet clad scaffold when θ= -45^o

Pressure Coefficient Contours on the Leeward Outer Face of the Elevated Sheet Clad Scaffold for Type B Terrain

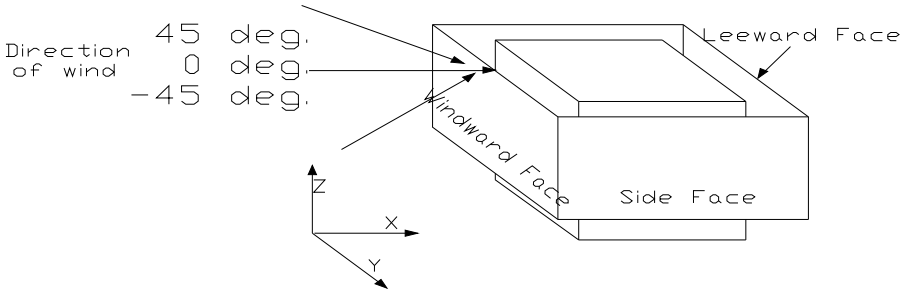

Figure 6B.17 Angle of attack of wind on windward outer face of the elevated sheet clad scaffold surrounding SEB, direction of which varies from 45^o to -45^o

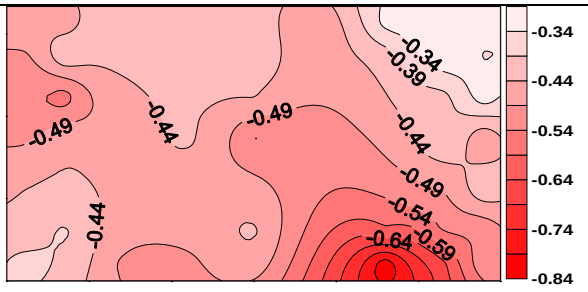

Figure 6B.18 Pressure coefficient contours on the leeward outer face of the elevated sheet clad scaffold when θ= 45^o

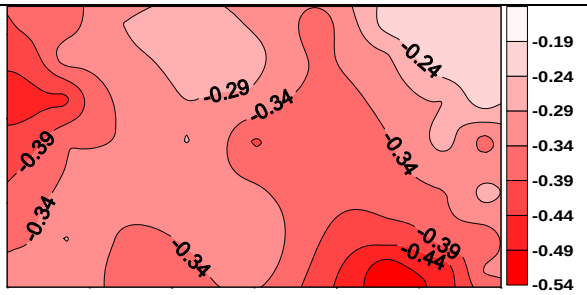

Figure 6B.19 Pressure coefficient contours on the leeward outer face of the elevated sheet clad scaffold when θ= 30^o

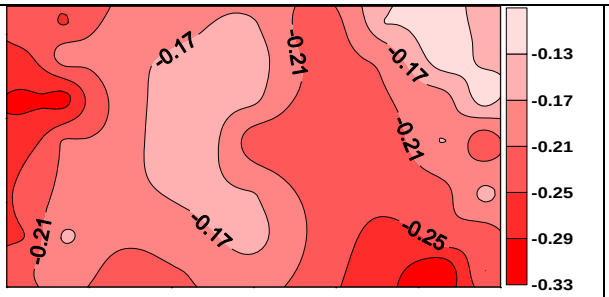

Figure 6B.20 Pressure coefficient contours on the leeward outer face of the elevated sheet clad scaffold when θ= 15^o

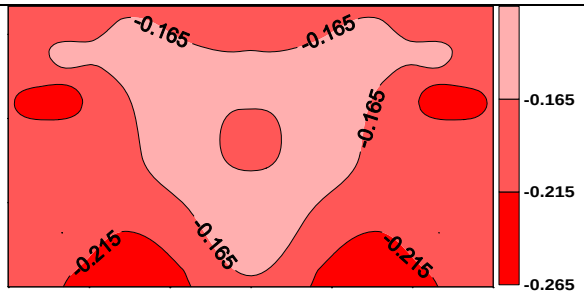

Figure 6B.21 Pressure coefficient contours on the leeward outer face of the elevated sheet clad scaffold when θ= 0^o

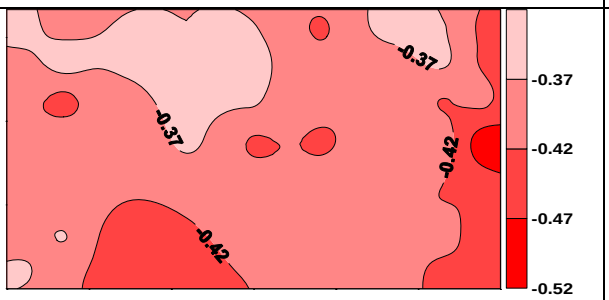

Figure 6B.22 Pressure coefficient contours on the leeward outer face of the elevated sheet clad scaffold when θ= -15^o

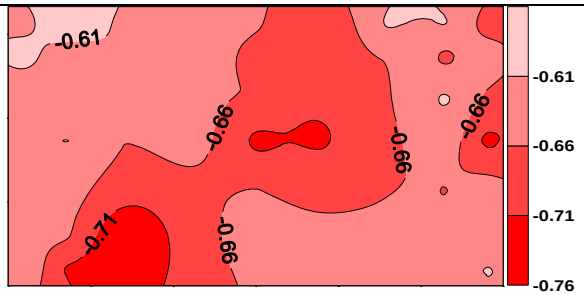

Figure 6B.23 Pressure coefficient contours on the leeward outer face of the elevated sheet clad scaffold when θ= -30^o

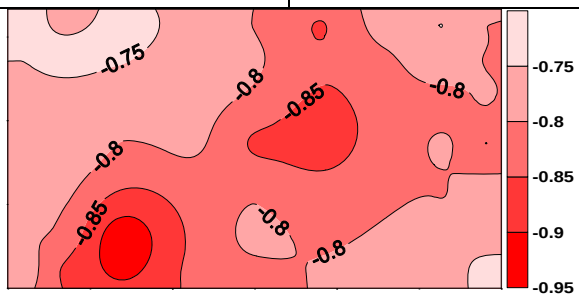

Figure 6B.24 Pressure coefficient contours on the leeward outer face of the elevated sheet clad scaffold when θ= -45^o

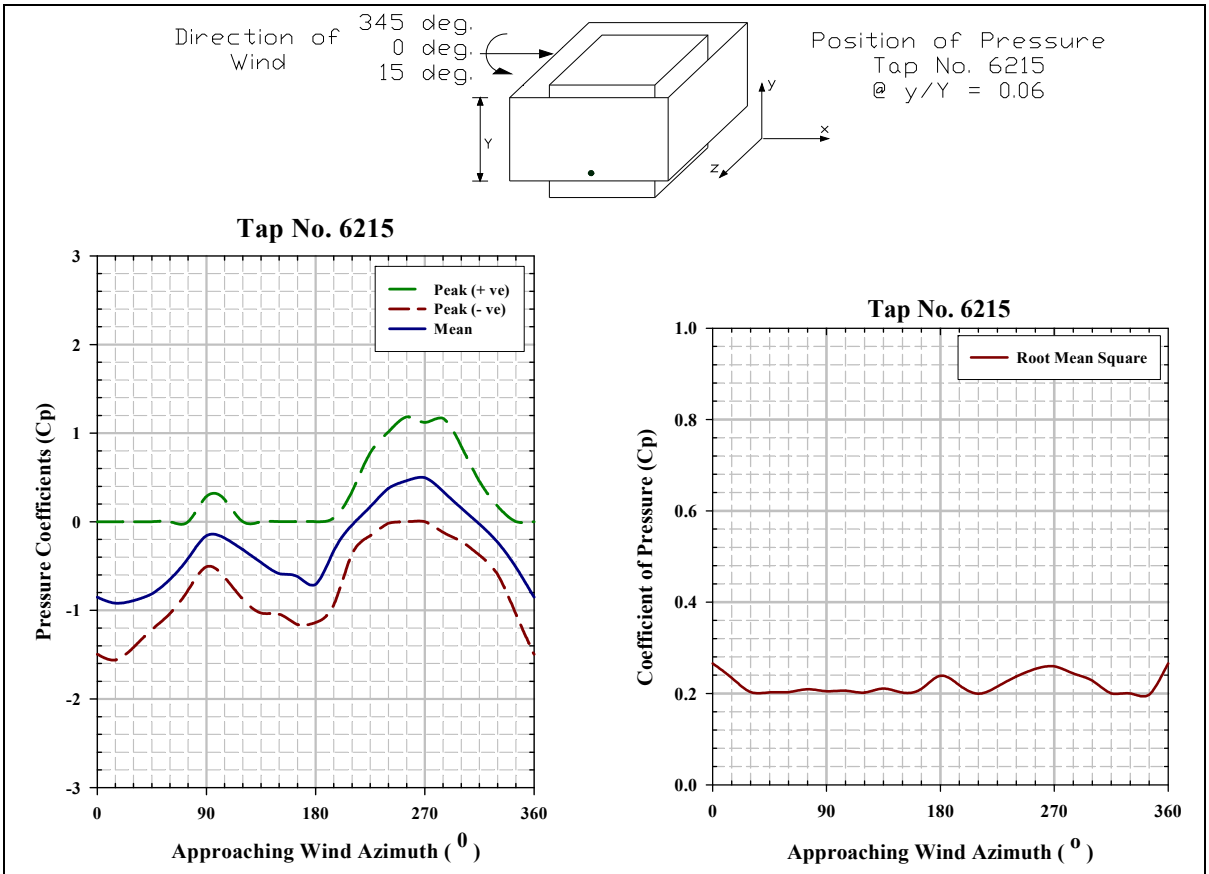

Figure 6B.25 Mean, peak and rms pressure coefficients for tap number 6215

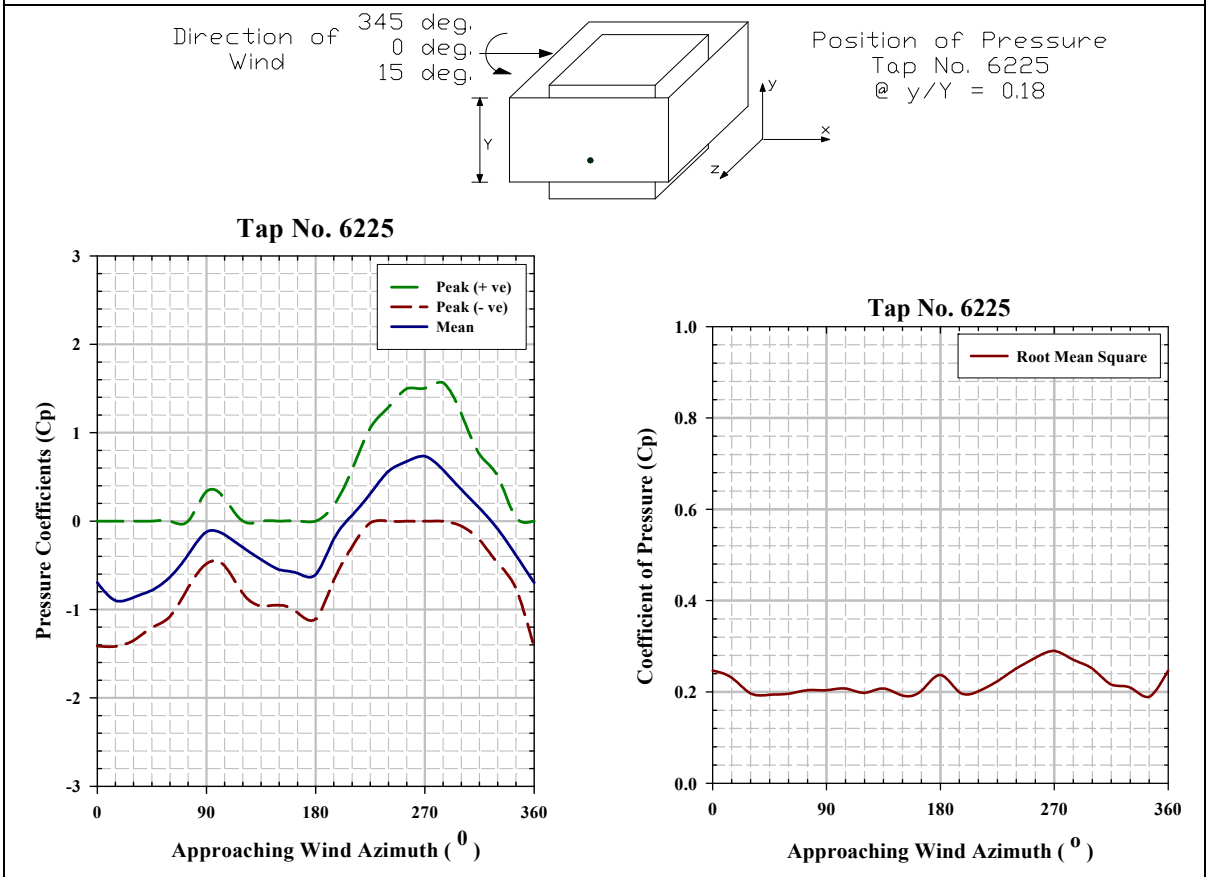

Figure 6B.26 Mean, peak and rms pressure coefficients for tap number 6225

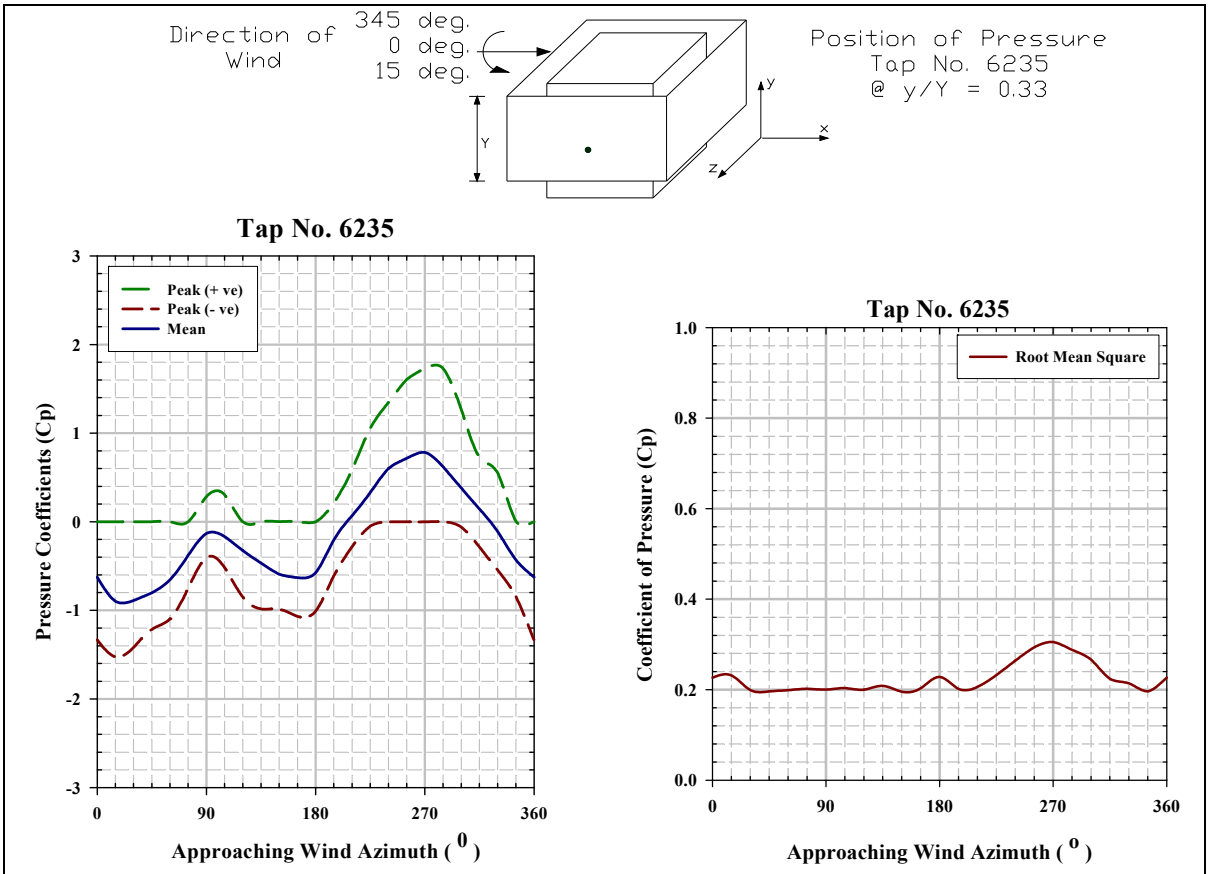

Figure 6B.27 Mean, peak and rms pressure coefficients for tap number 6235

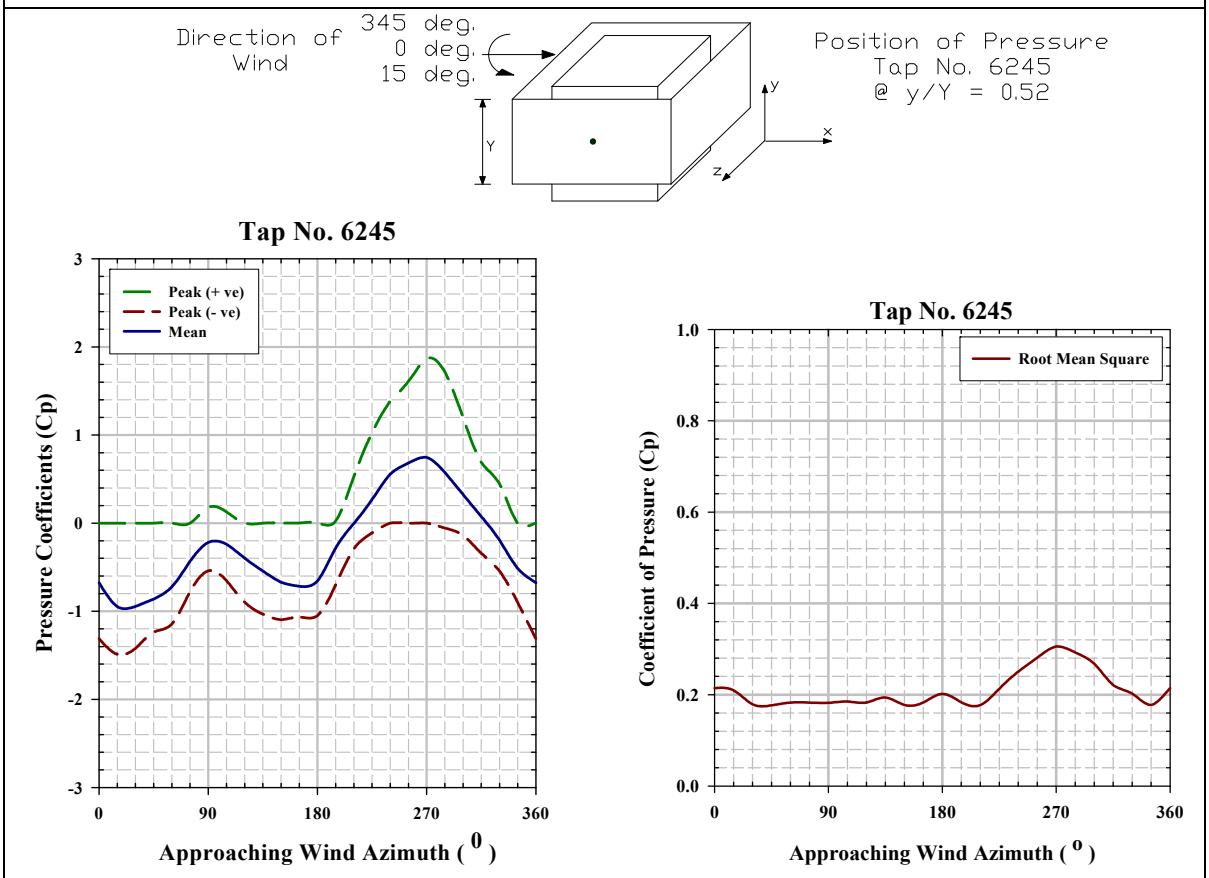

Figure 6B.28 Mean, peak and rms pressure coefficients for tap number 6245

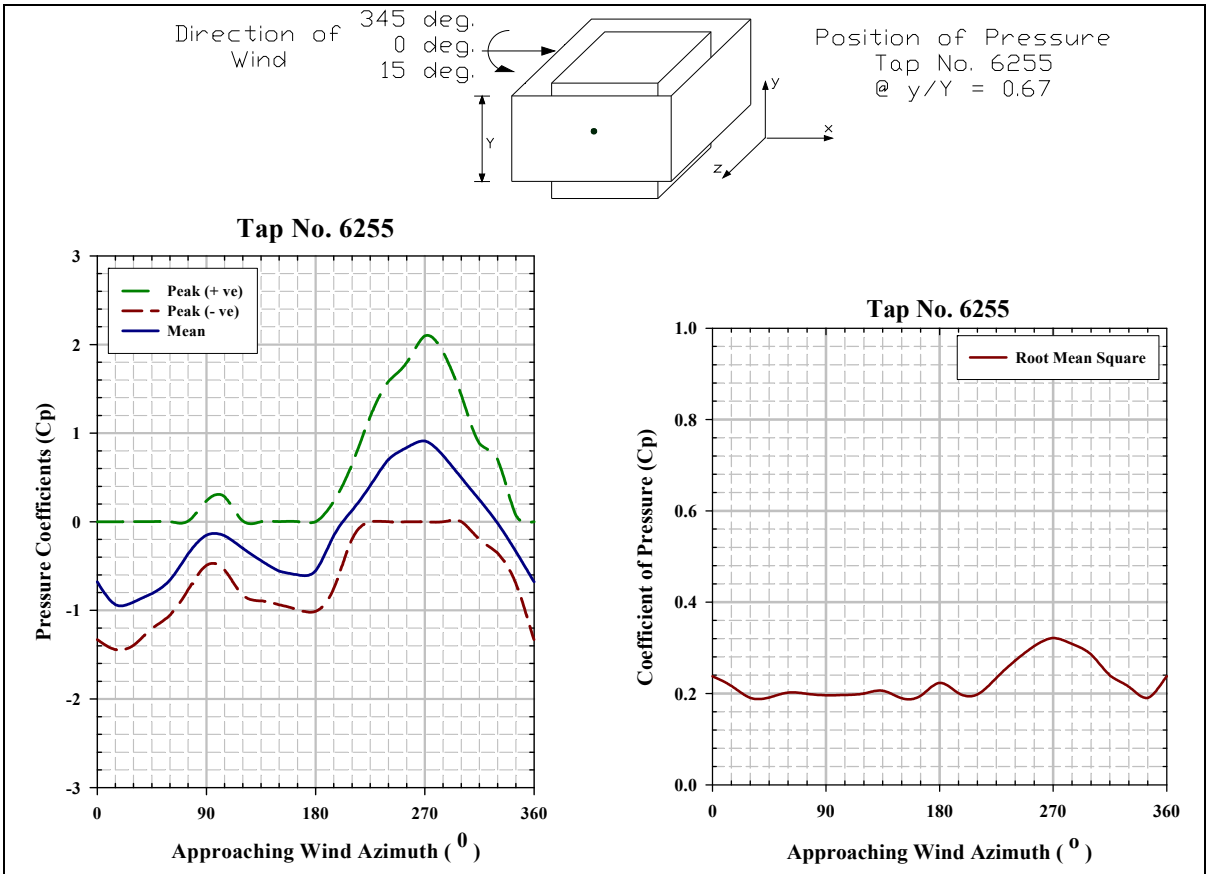

Figure 6B.29 Mean, peak and rms pressure coefficients for tap number 6255

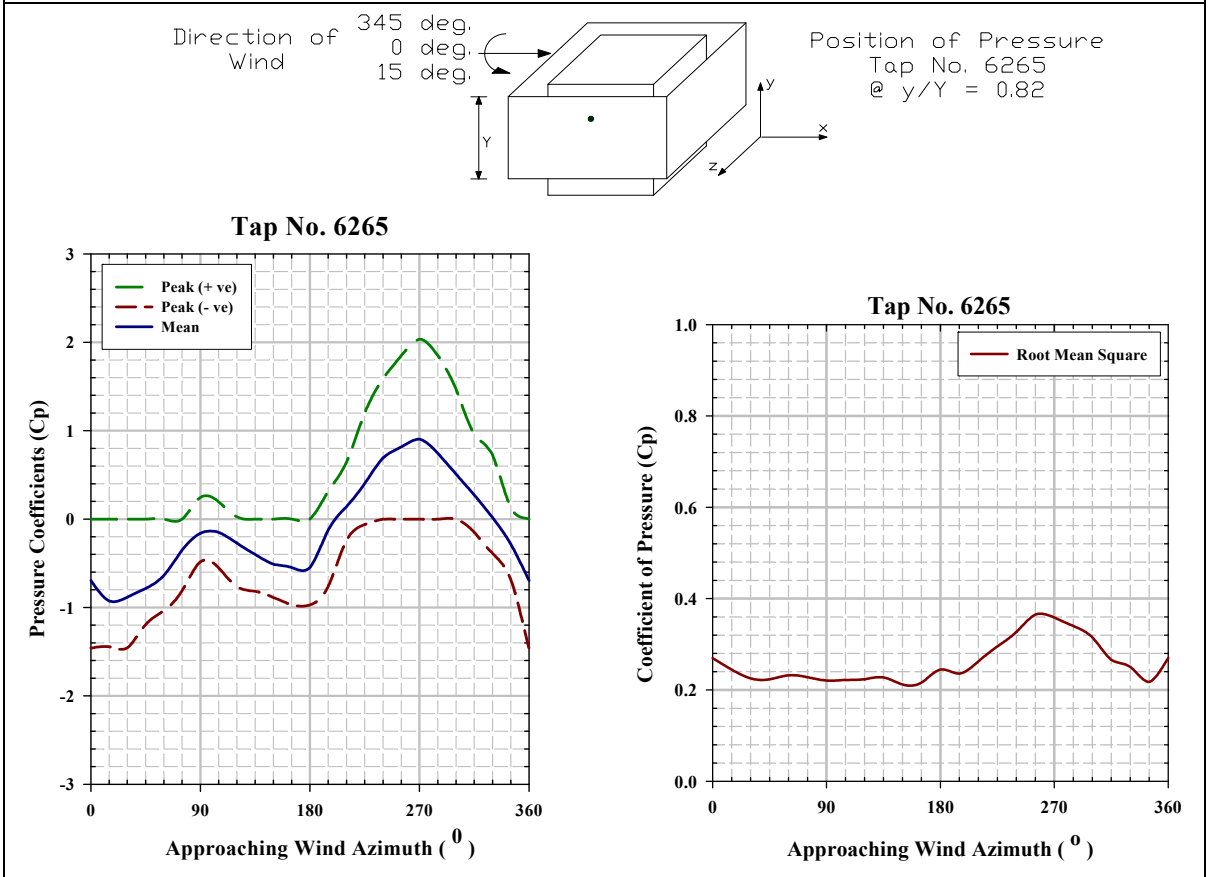

Figure 6B.30 Mean, peak and rms pressure coefficients for tap number 6265

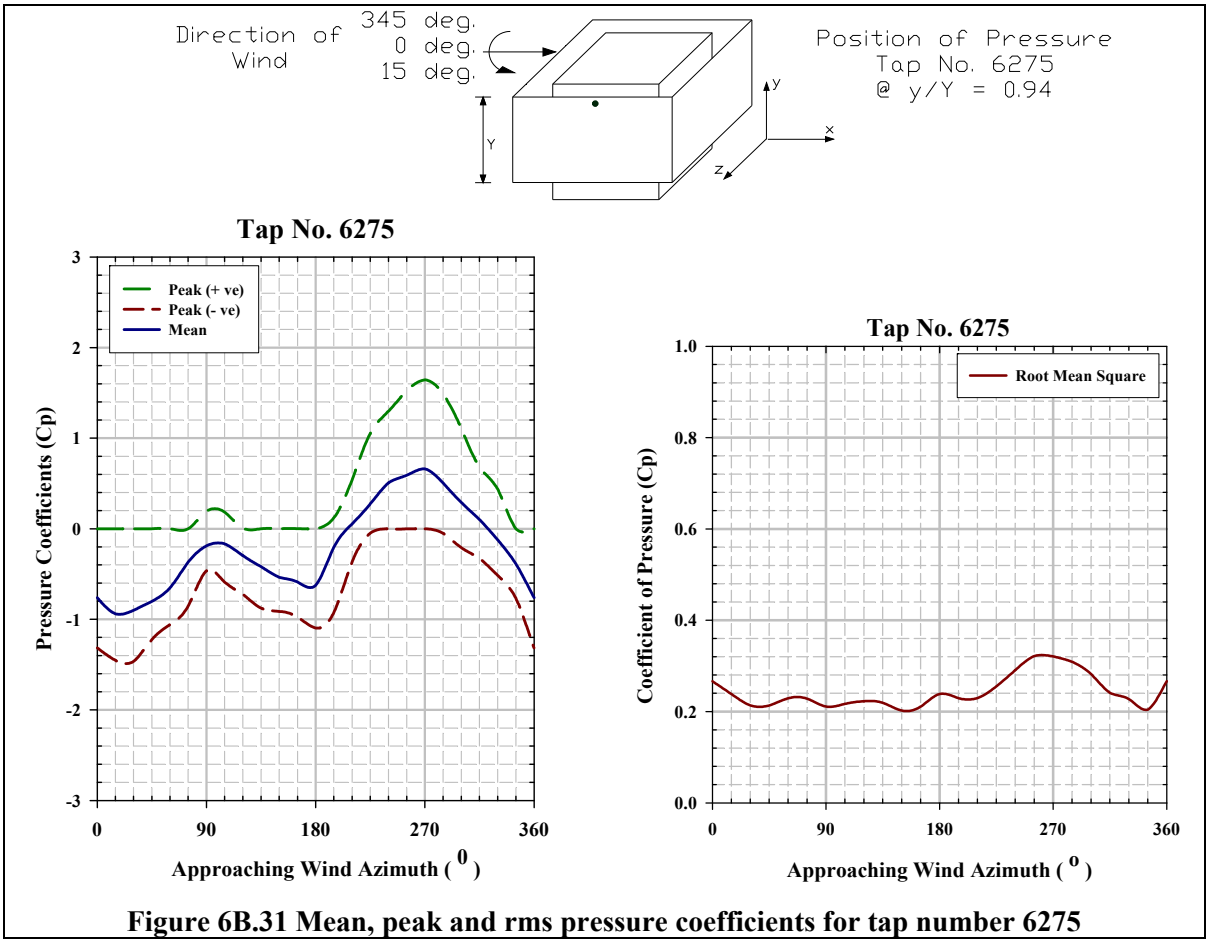

Figure 6B.31 Mean, peak and rms pressure coefficients for tap number 6275

EXPERIMENT-7

Pressure Coefficients on the Inner Face of the Elevated Sheet Clad Scaffold

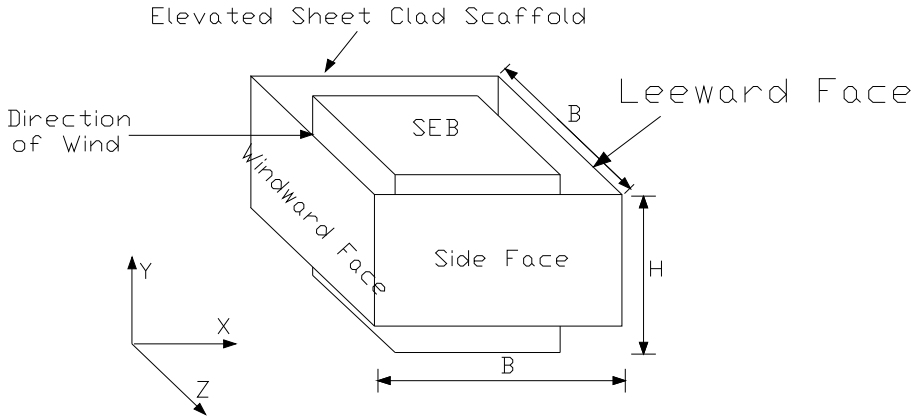

Figure 7.1 Scaled cubical SEB surrounded by elevated sheet clad scaffold

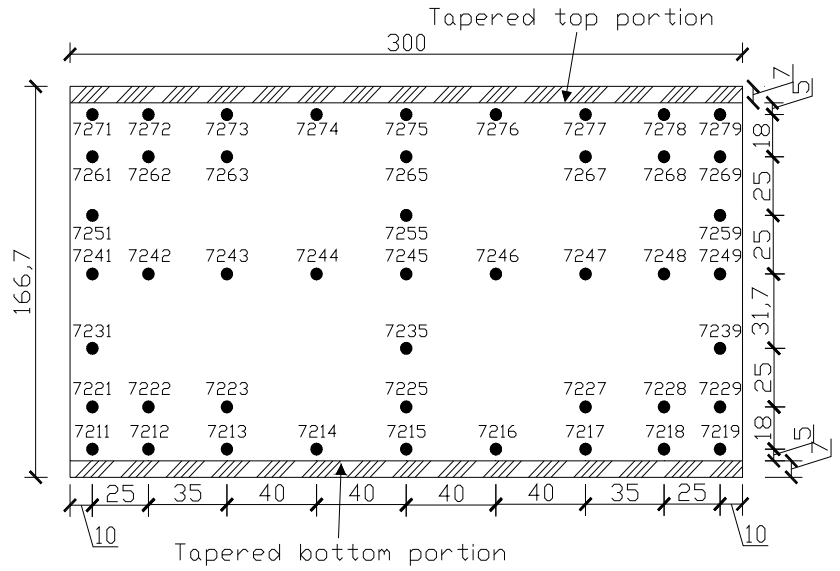

Figure 7.2 Pressure tap locations on the inner face of the elevated sheet clad scaffold

Pressure Coefficient Contours on the windward Inner Face of the Elevated Sheet Clad Scaffold for Type A Terrain

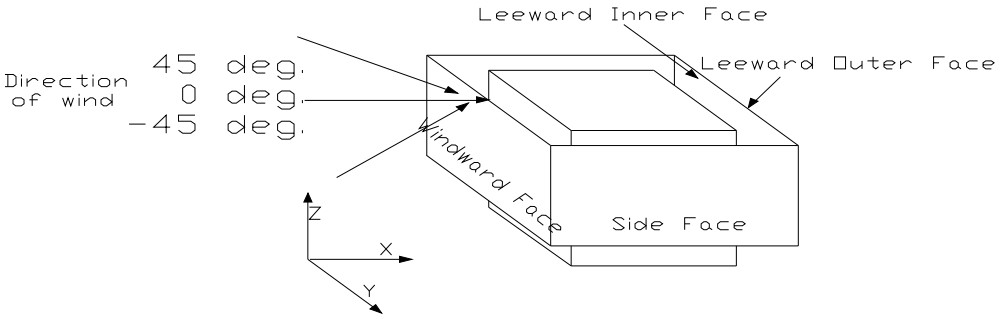

Figure 7A.1 Angle of attack of wind on windward outer face of the elevated sheet clad scaffold surrounding SEB, direction of which varies from 45° to -45°

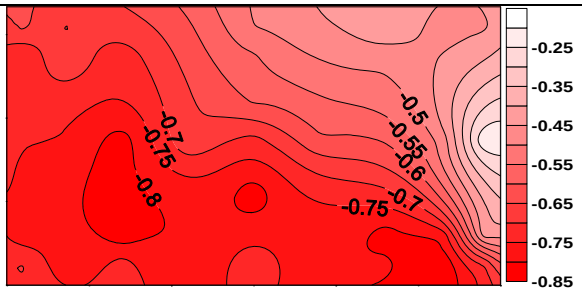

Figure 7A.2 Pressure coefficient contours on the windward inner face of the elevated sheet clad scaffold when θ= 45°

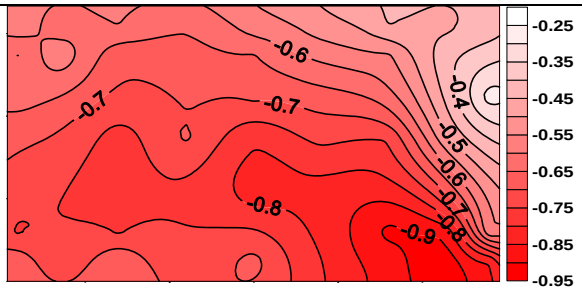

Figure 7A.3 Pressure coefficient contours on the windward inner face of the elevated sheet clad scaffold when θ= 30°

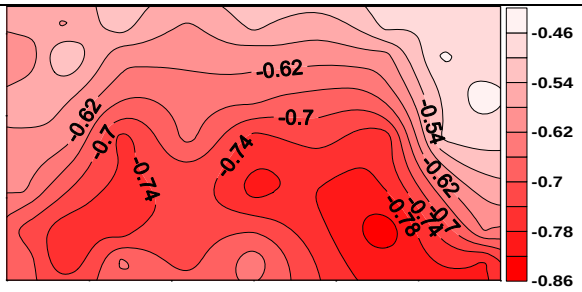

Figure 7A.4 Pressure coefficient contours on the windward inner face of the elevated sheet clad scaffold when θ= 15°

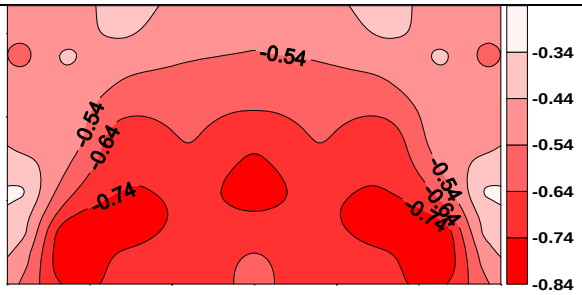

Figure 7A.5 Pressure coefficient contours on the windward inner face of the elevated sheet clad scaffold when θ= 0°

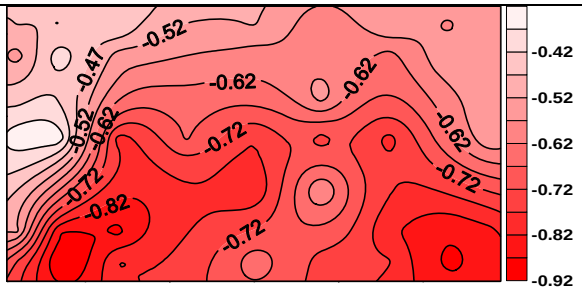

Figure 7A.6 Pressure coefficient contours on the windward inner face of the elevated sheet clad scaffold when θ= -15°

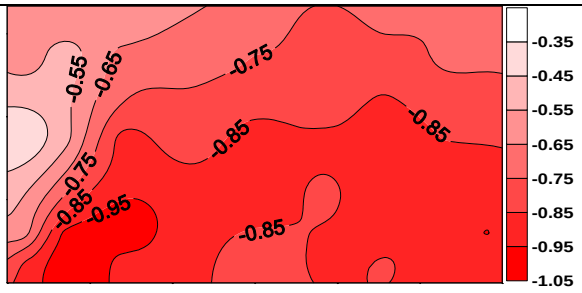

Figure 7A.7 Pressure coefficient contours on the windward inner face of the elevated sheet clad scaffold when θ= -30°

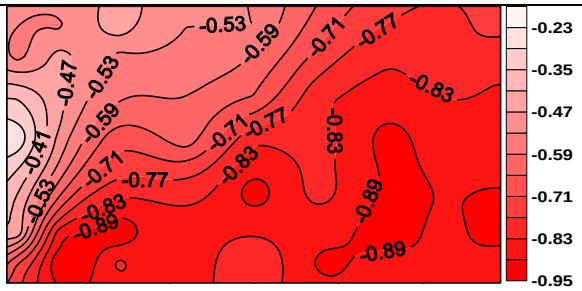

Figure 7A.8 Pressure coefficient contours on the windward inner face of the elevated sheet clad scaffold when θ= -45°

Pressure Coefficient Contours on the Side Inner Face of the Elevated Sheet Clad Scaffold for Type A Terrain

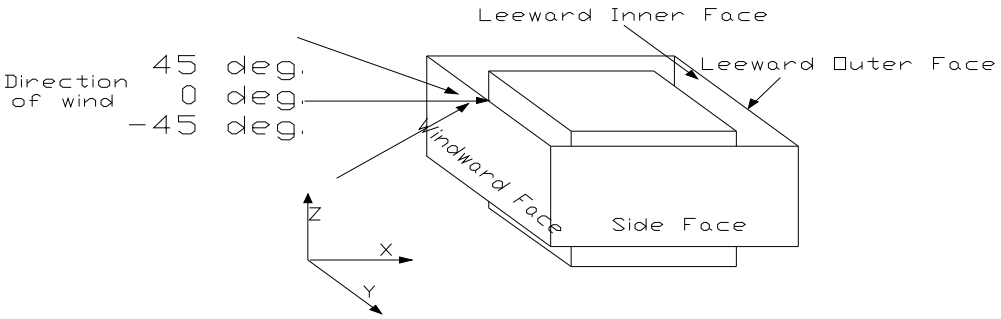

Figure 7A.9 Angle of attack of wind on windward outer face of the elevated sheet clad scaffold surrounding SEB, direction of which varies from 45° to -45°

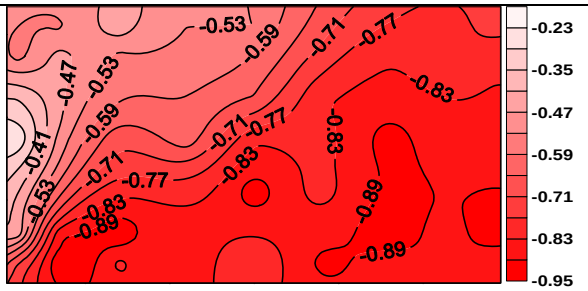

Figure 7A.10 Pressure coefficient contours on the side inner face of the elevated sheet clad scaffold when θ= 45°

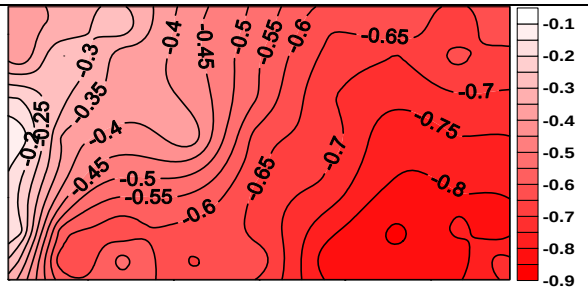

Figure 7A.11 Pressure coefficient contours on the side inner face of the elevated sheet clad scaffold when θ= 30°

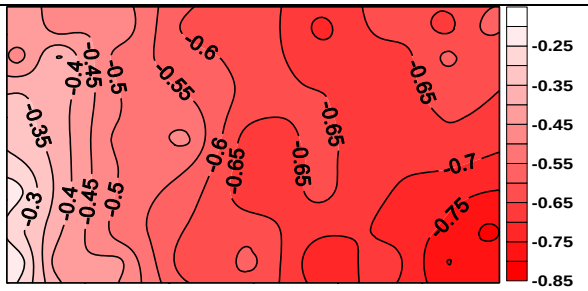

Figure 7A.12 Pressure coefficient contours on the side inner face of the elevated sheet clad scaffold when θ= 15°

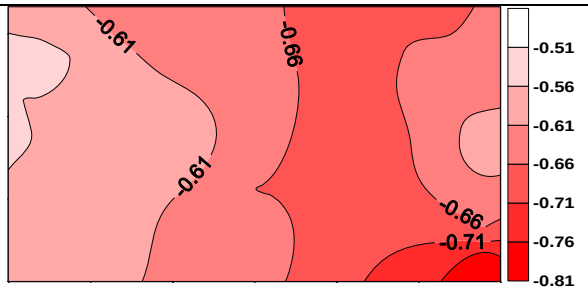

Figure 7A.13 Pressure coefficient contours on the side inner face of the elevated sheet clad scaffold when θ= 0°

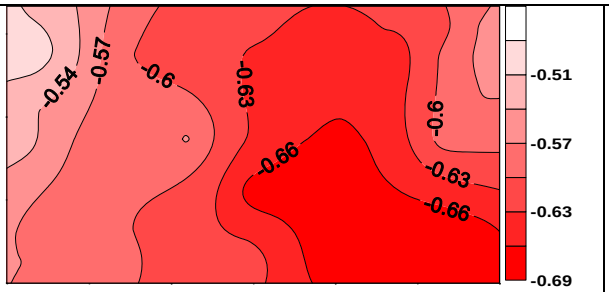

Figure 7A.14 Pressure coefficient contours on the side inner face of the elevated sheet clad scaffold when θ= -15^o

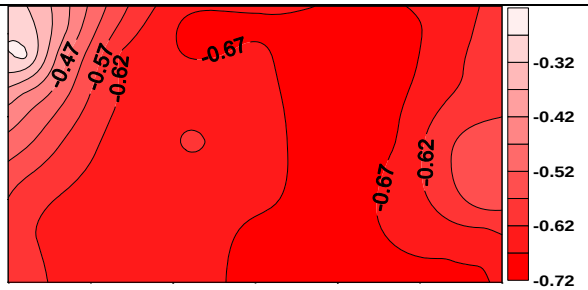

Figure 7A.15 Pressure coefficient contours on the side inner face of the elevated sheet clad scaffold when θ= -30^o

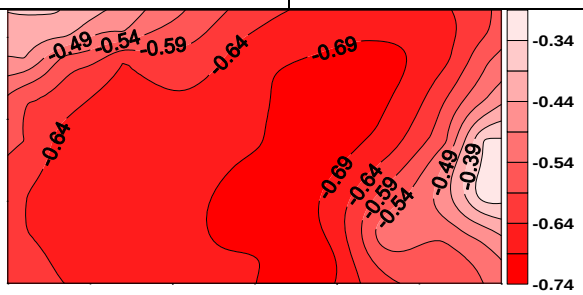

Figure 7A.16 Pressure coefficient contours on the side inner face of the elevated sheet clad scaffold when θ= -45^o

Pressure Coefficient Contours on the Leeward Inner Face of the Elevated Sheet Clad Scaffold for Type A Terrain

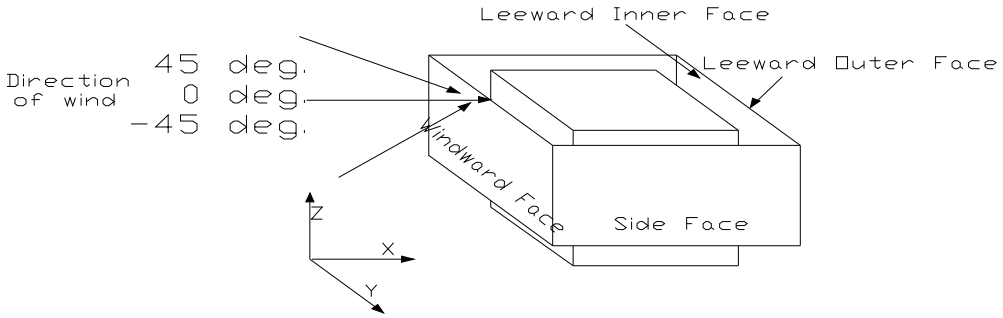

Figure 7A.17 Angle of attack of wind on windward outer face of the elevated sheet clad scaffold surrounding SEB, direction of which varies from 45^o to -45^o

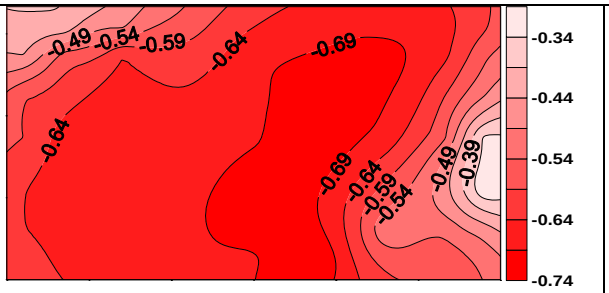

Figure 7A.18 Pressure coefficient contours on the leeward inner face of the elevated sheet clad scaffold when θ= 45^o

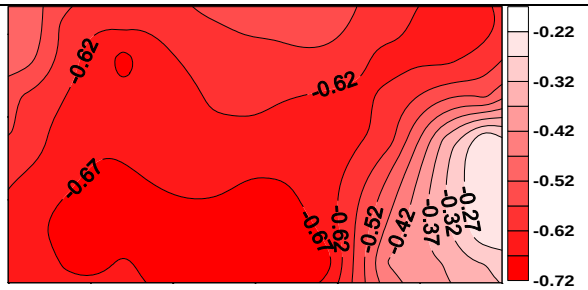

Figure 7A.19 Pressure coefficient contours on the leeward inner face of the elevated sheet clad scaffold when θ= 30^o

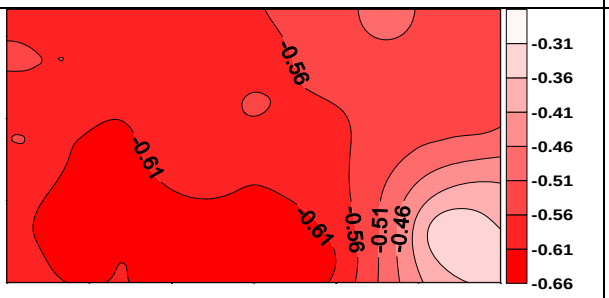

Figure 7A.20 Pressure coefficient contours on the leeward inner face of the elevated sheet clad scaffold when θ= 15^{o}

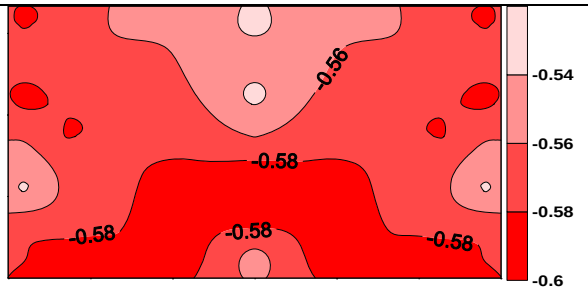

Figure 7A.21 Pressure coefficient contours on the leeward inner face of the elevated sheet clad scaffold when θ= 0^{o}

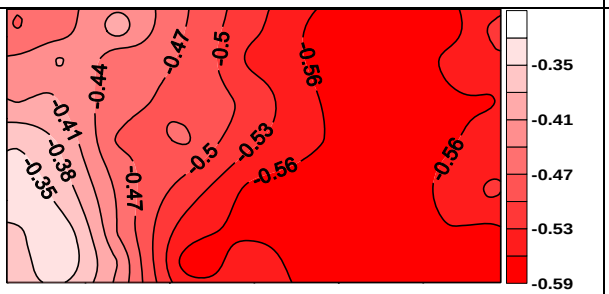

Figure 7A.22 Pressure coefficient contours on the leeward inner face of the elevated sheet clad scaffold when θ= 15^{o}

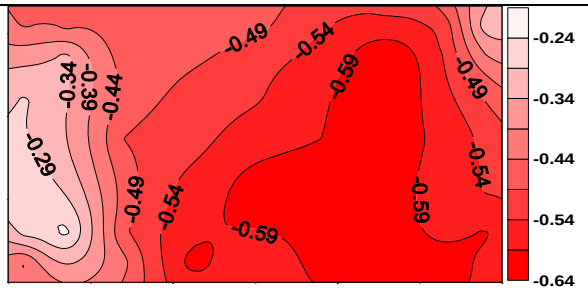

Figure 7A.23 Pressure coefficient contours on the leeward inner face of the elevated sheet clad scaffold when θ= 30^{o}

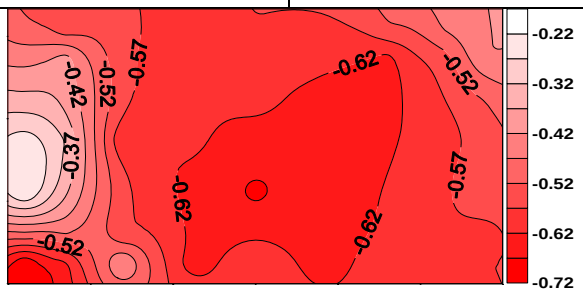

Figure 7A.24 Pressure coefficient contours on the leeward inner face of the elevated sheet clad scaffold when θ= 45^{o}

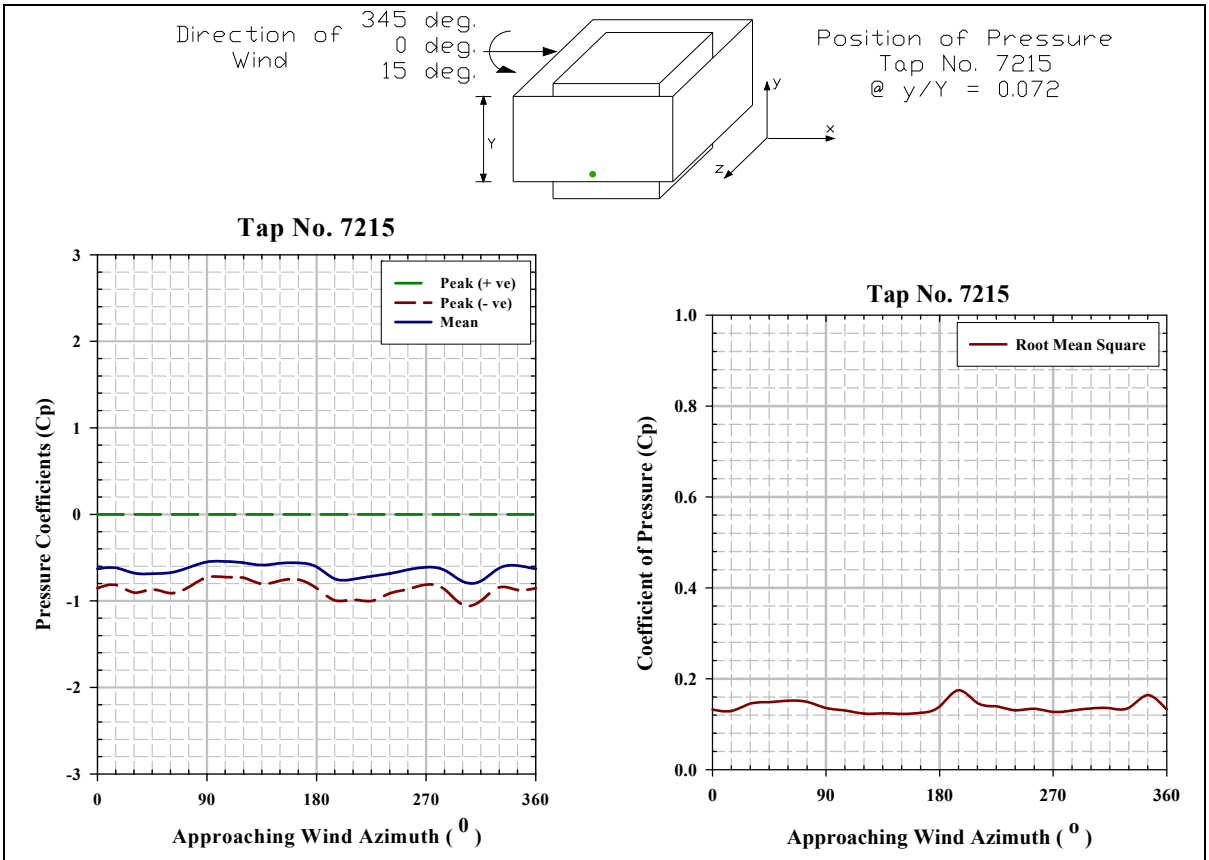

Figure 7A.25 Mean, peak and rms pressure coefficients for pressure tap number 7215

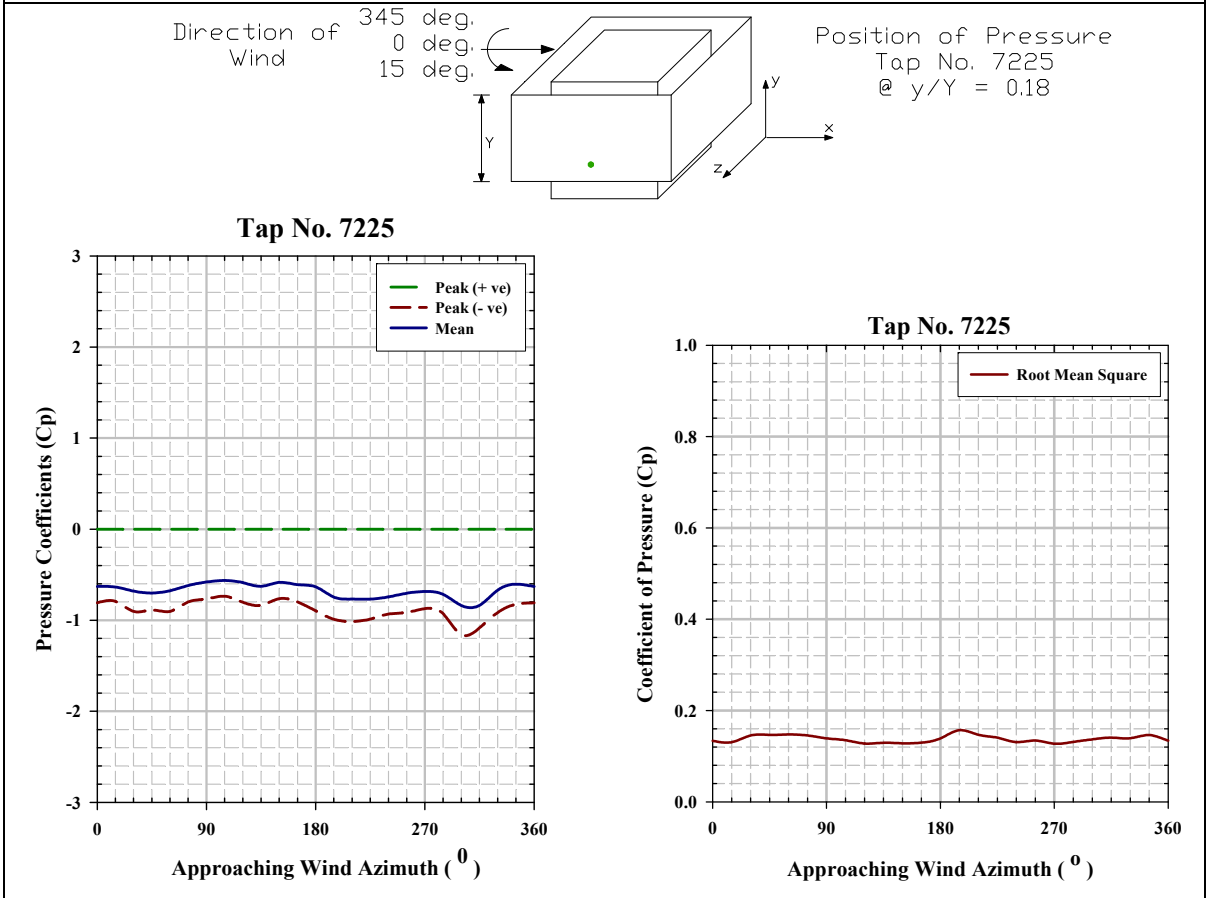

Figure 7A.26 Mean, peak and rms pressure coefficients for pressure tap number 7225

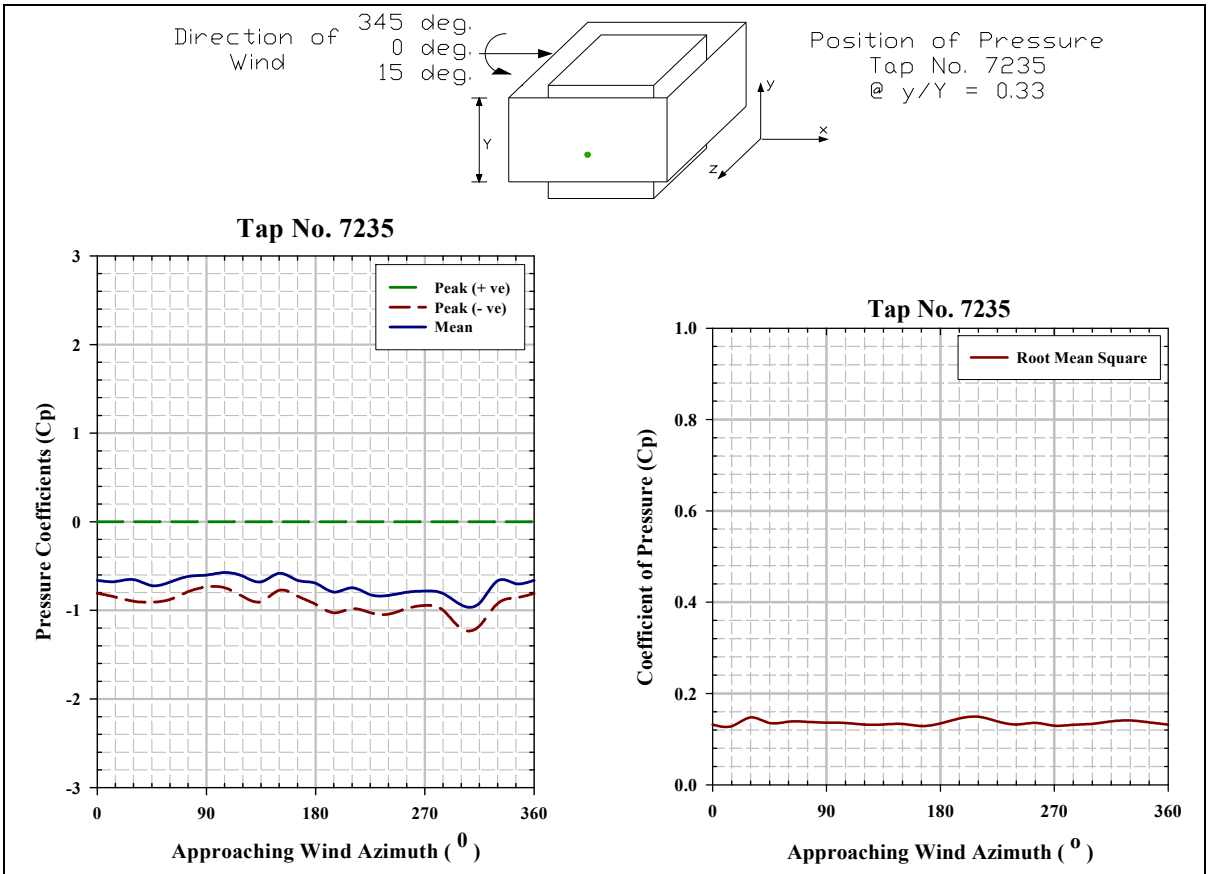

Figure 7A.27 Mean, peak and rms pressure coefficients for pressure tap number 7235

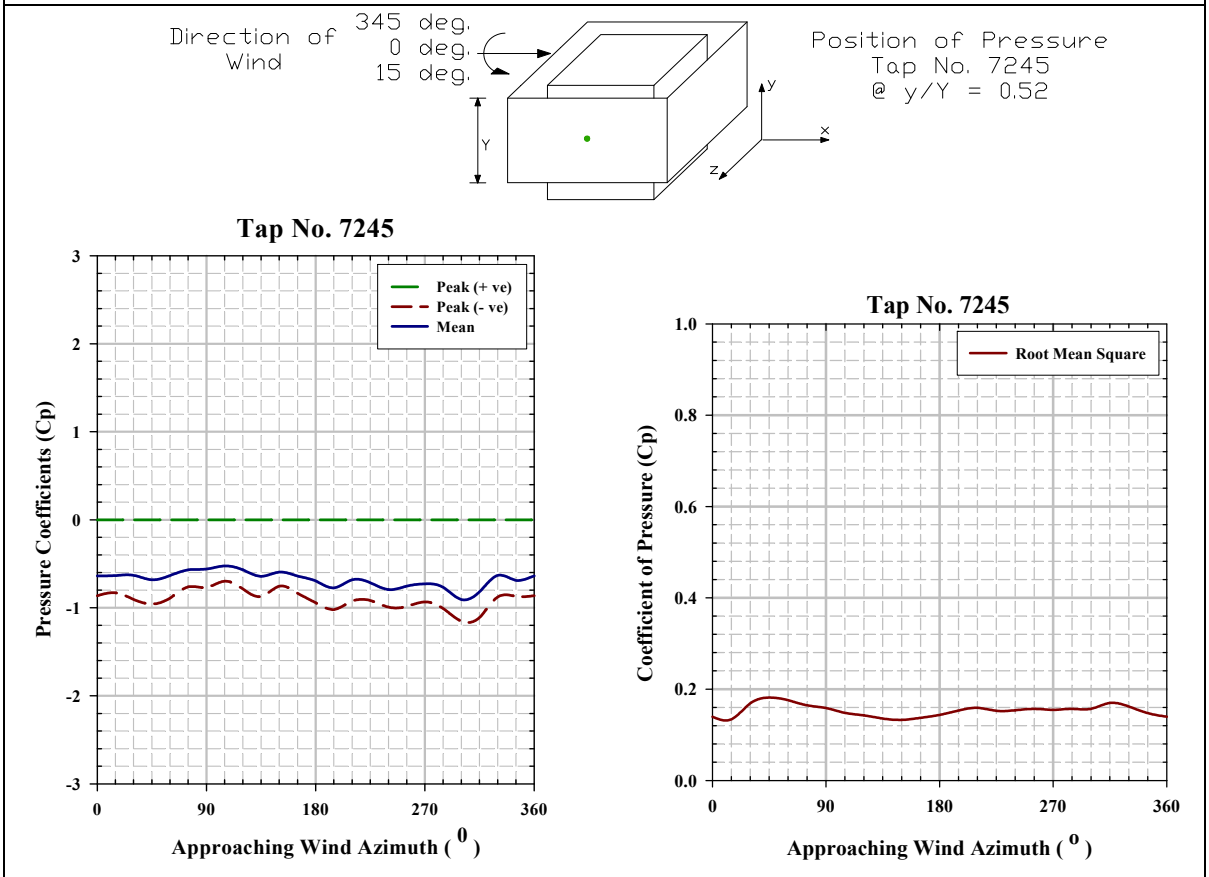

Figure 7A.28 Mean, peak and rms pressure coefficients for pressure tap number 7245

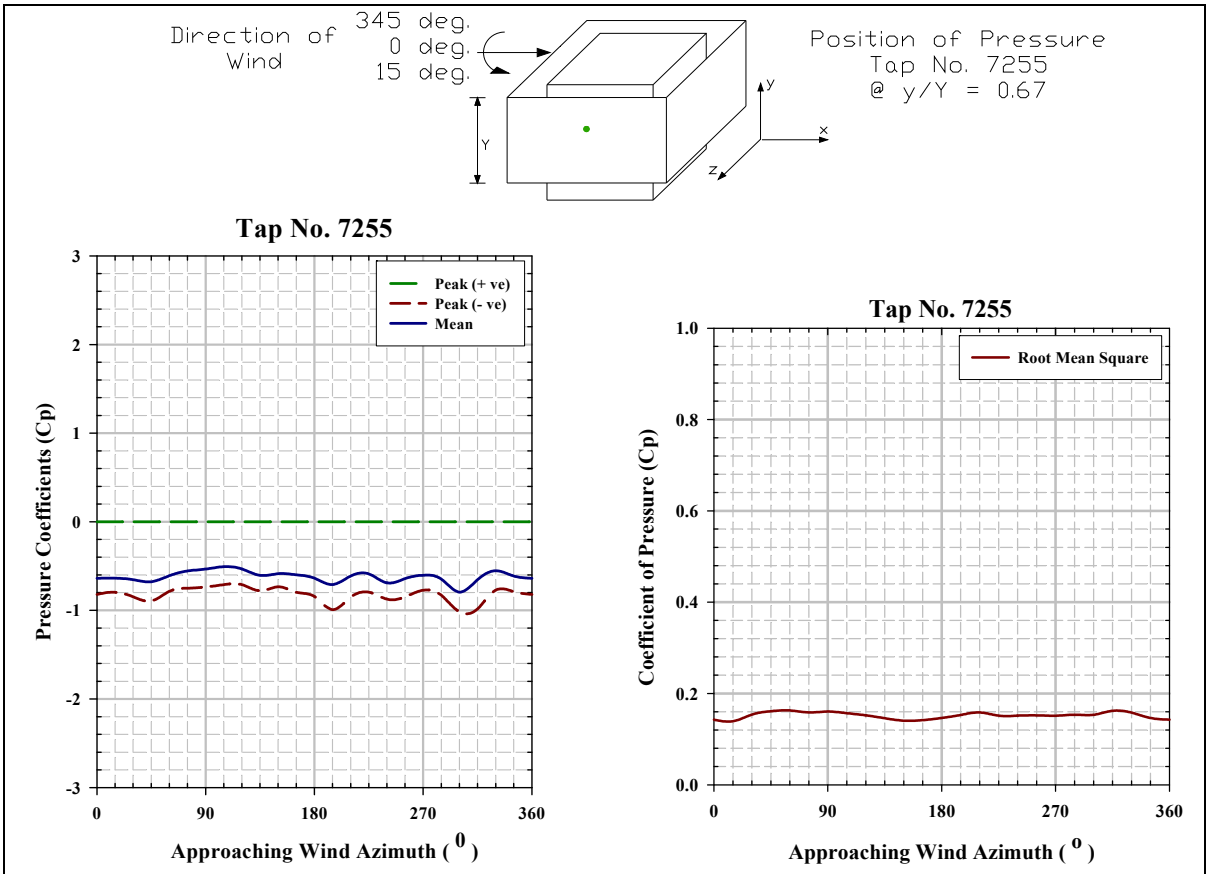

Figure 7A.29 Mean, peak and rms pressure coefficients for pressure tap number 7255

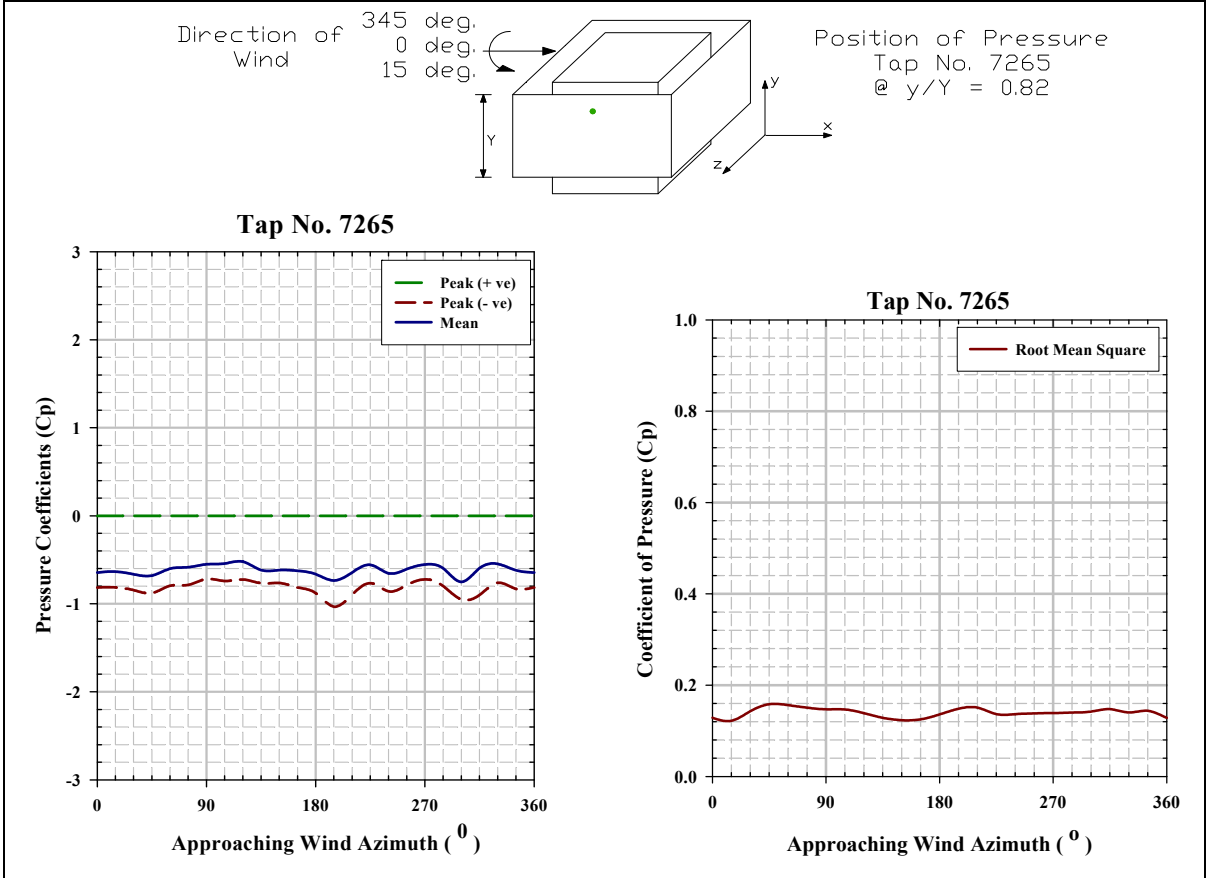

Figure 7A.30 Mean, peak and rms pressure coefficients for pressure tap number 7265

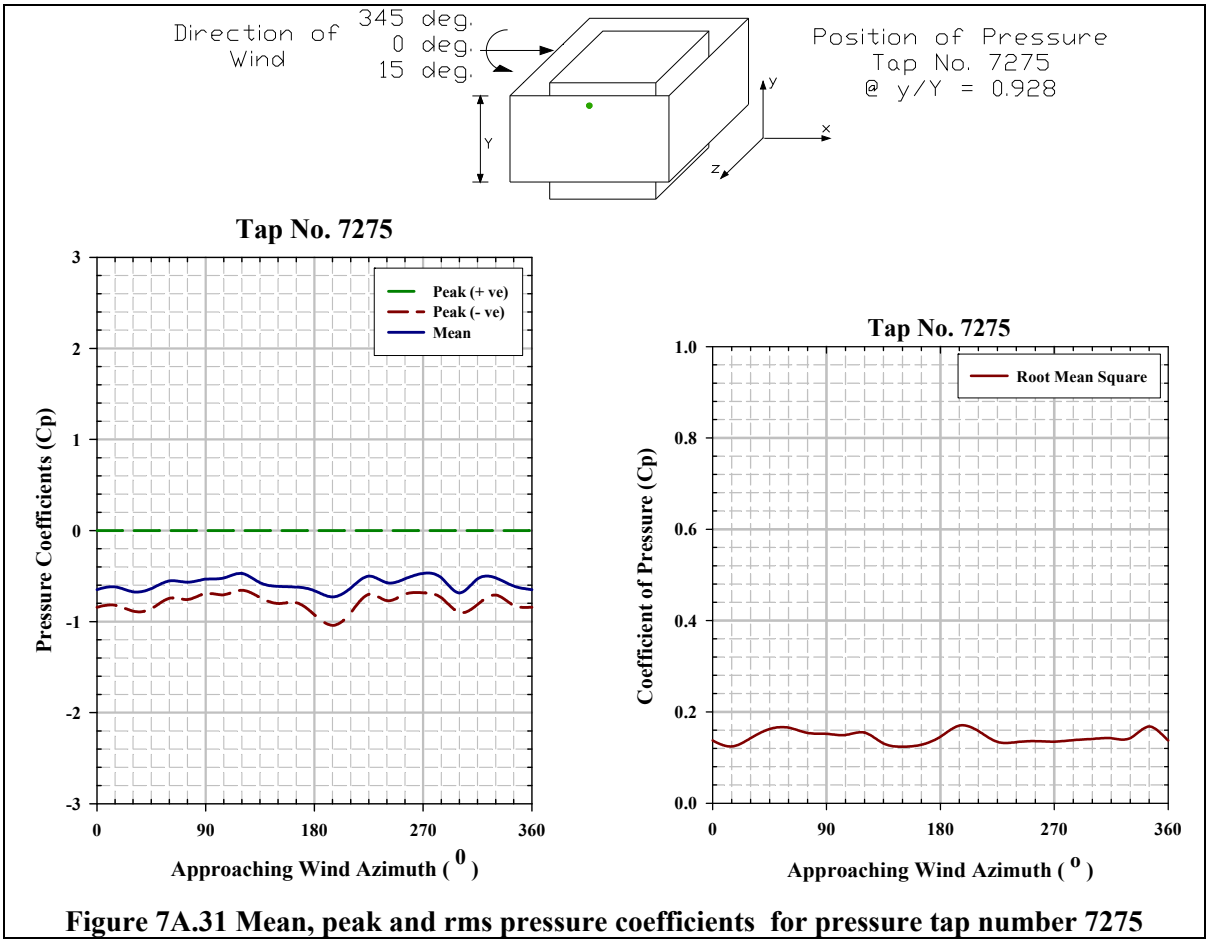

Figure 7A.31 Mean, peak and rms pressure coefficients for pressure tap number 7275

Pressure Coefficient Contours on the windward Inner Face of the Elevated Sheet Clad Scaffold for Type B Terrain

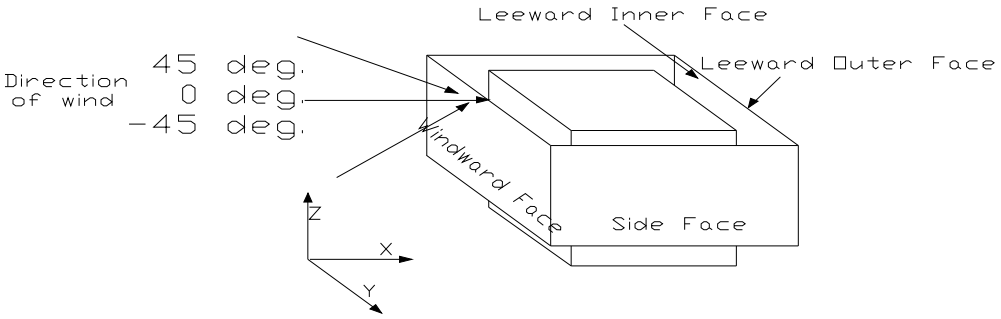

Figure 7B.1 Angle of attack of wind on windward outer face of the elevated sheet clad scaffold surrounding SEB, direction of which varies from 45° to -45°

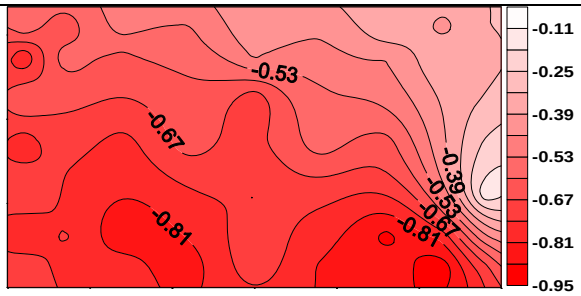

Figure 7B.2 Pressure coefficient contours on the windward inner face of the elevated sheet clad scaffold when θ= 45°

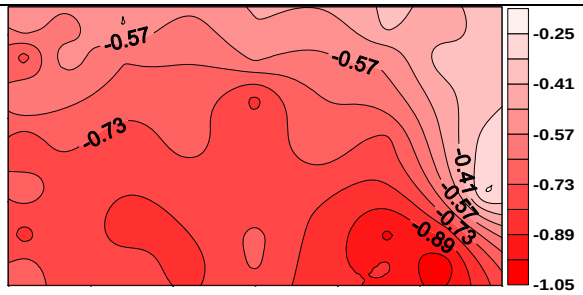

Figure 7B.3 Pressure coefficient contours on the windward inner face of the elevated sheet clad scaffold when θ= 30°

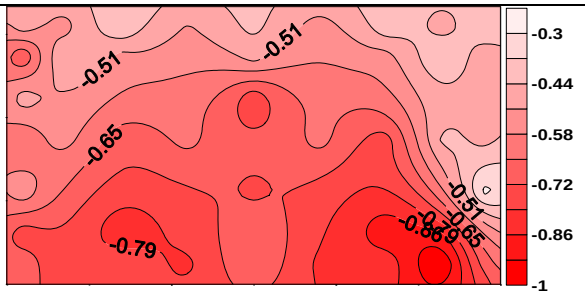

Figure 7B.4 Pressure coefficient contours on the windward inner face of the elevated sheet clad scaffold when θ= 15°

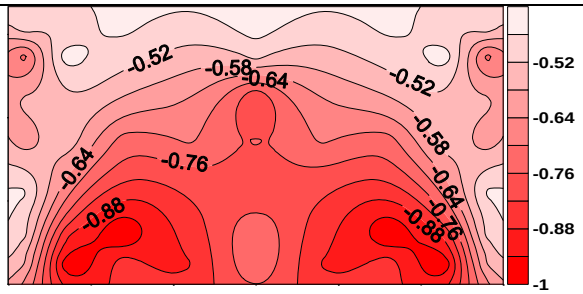

Figure 7B.5 Pressure coefficient contours on the windward inner face of the elevated sheet clad scaffold when θ= 0°

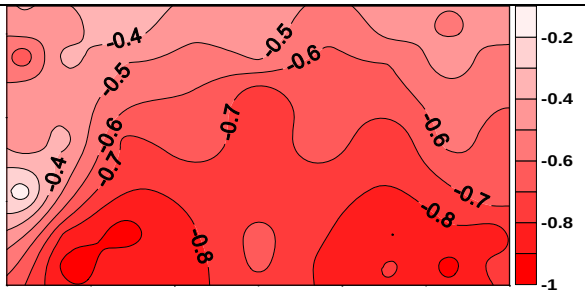

Figure 7B.6 Pressure coefficient contours on the windward inner face of the elevated sheet clad scaffold when θ= -15°

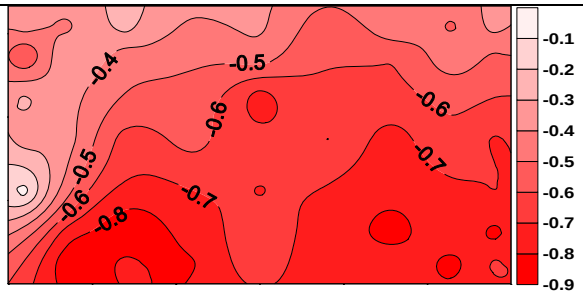

Figure 7B.7 Pressure coefficient contours on the windward inner face of the elevated sheet clad scaffold when θ= -30°

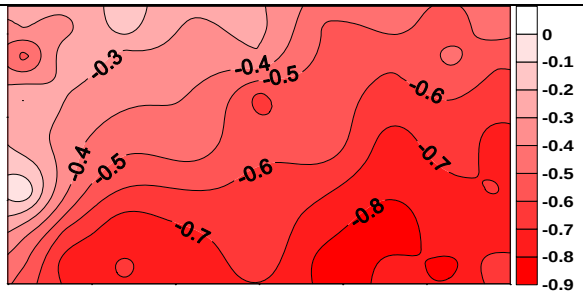

Figure 7B.8 Pressure coefficient contours on the windward inner face of the elevated sheet clad scaffold when θ= -45^o

Pressure Coefficient Contours on the Side Inner Face of the Elevated Sheet Clad Scaffold for Type B Terrain

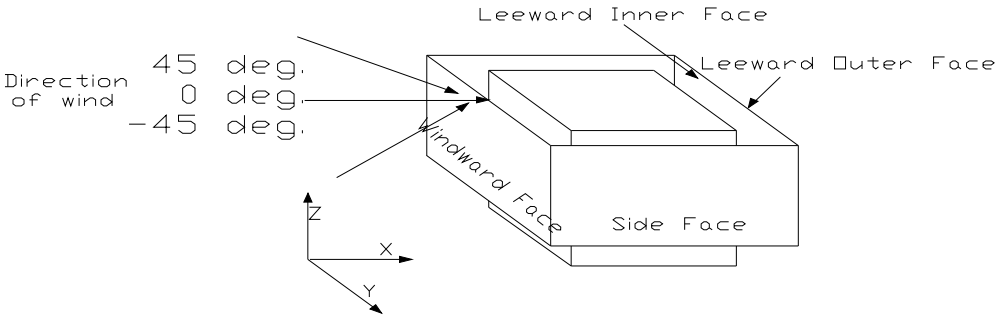

Figure 7B.9 Angle of attack of wind on windward outer face of the elevated sheet clad scaffold surrounding SEB, direction of which varies from 45^o to -45^o

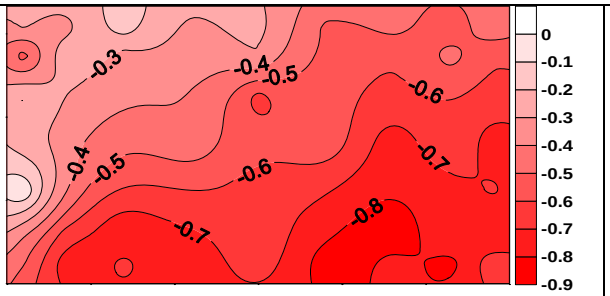

Figure 7B.10 Pressure coefficient contours on the side inner face of the elevated sheet clad scaffold when θ= 45^o

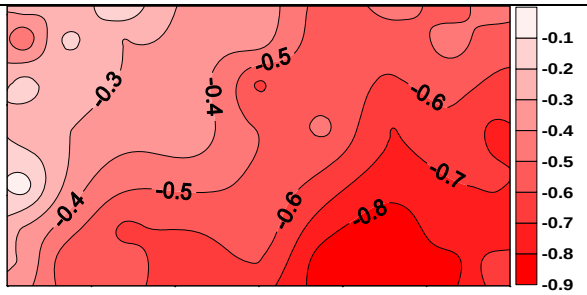

Figure 7B.11 Pressure coefficient contours on the side inner face of the elevated sheet clad scaffold when θ= 30^o

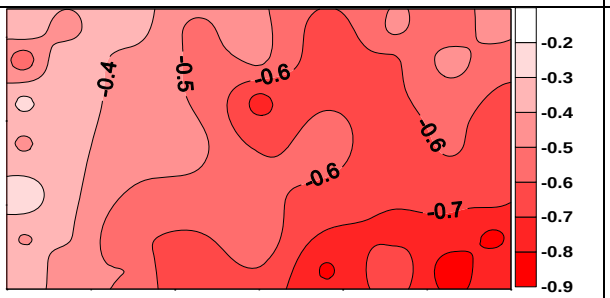

Figure 7B.12 Pressure coefficient contours on the side inner face of the elevated sheet clad scaffold when θ= 15^o

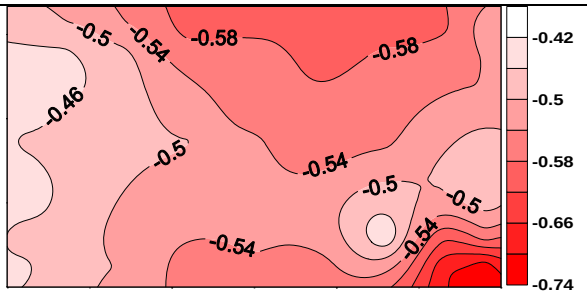

Figure 7B.13 Pressure coefficient contours on the side inner face of the elevated sheet clad scaffold when θ= 0^o

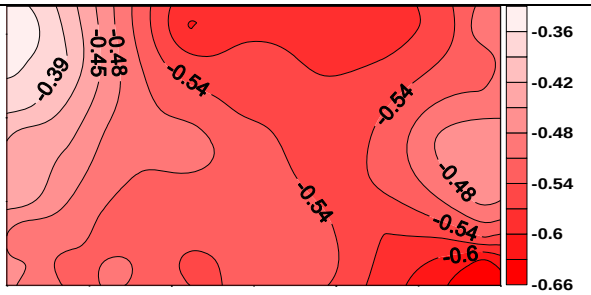

Figure 7B.14 Pressure coefficient contours on the side inner face of the elevated sheet clad scaffold when θ= -15°

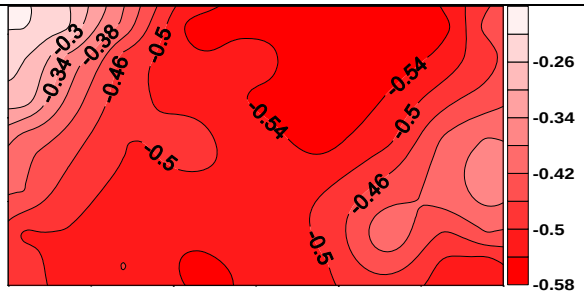

Figure 7B.15 Pressure coefficient contours on the side inner face of the elevated sheet clad scaffold when θ= -30°

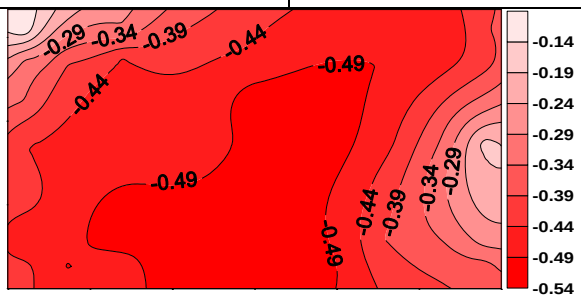

Figure 7B.16 Pressure coefficient contours on the side inner face of the elevated sheet clad scaffold when θ= -45°

Pressure Coefficient Contours on the Leeward Inner Face of the Elevated Sheet Clad Scaffold for Type B Terrain

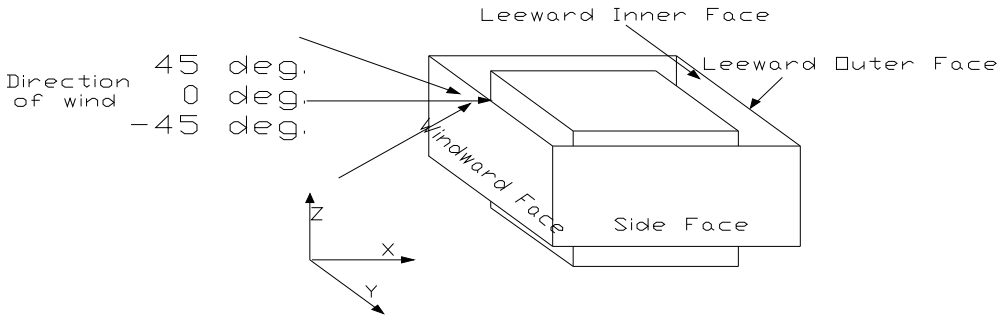

Figure 7B.17 Angle of attack of wind on windward outer face of the elevated sheet clad scaffold surrounding SEB, direction of which varies from 45° to -45°

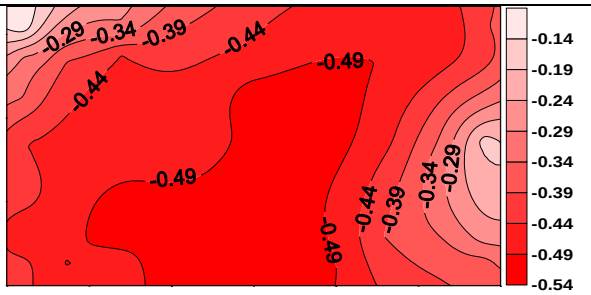

Figure 7B.18 Pressure coefficient contours on the leeward inner face of the elevated sheet clad scaffold when θ= 45°

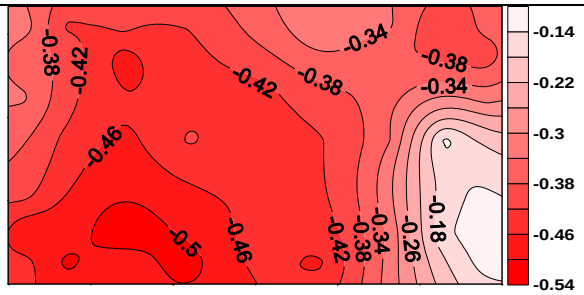

Figure 7B.19 Pressure coefficient contours on the leeward inner face of the elevated sheet clad scaffold when θ= 30°

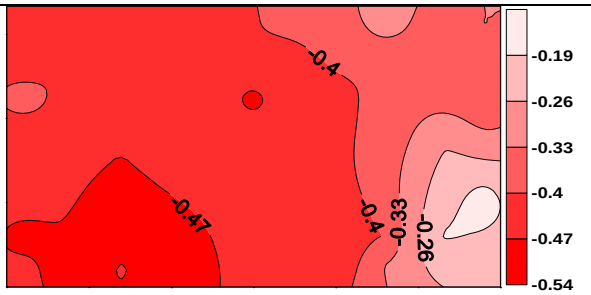

Figure 7B.20 Pressure coefficient contours on the leeward inner face of the elevated sheet clad scaffold when θ= 15^o

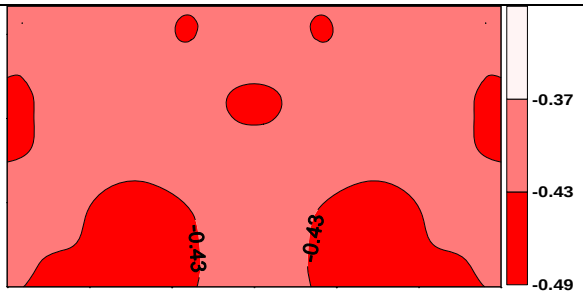

Figure 7B.21 Pressure coefficient contours on the leeward inner face of the elevated sheet clad scaffold when θ= 0^o

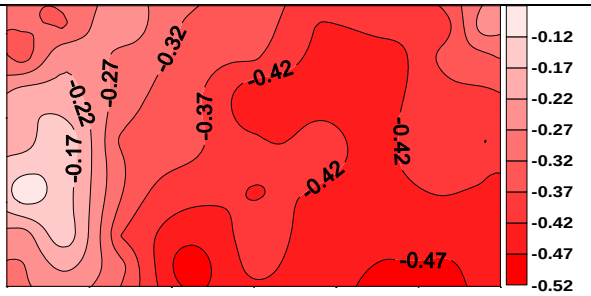

Figure 7B.22 Pressure coefficient contours on the leeward inner face of the elevated sheet clad scaffold when θ= 15^o

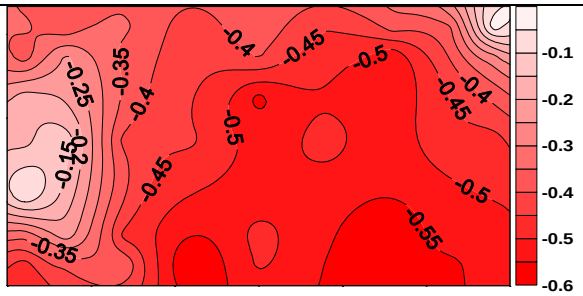

Figure 7B.23 Pressure coefficient contours on the leeward inner face of the elevated sheet clad scaffold when θ= 30^o

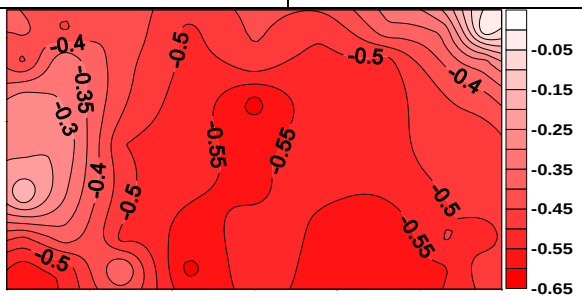

Figure 7B.24 Pressure coefficient contours on the leeward inner face of the elevated sheet clad scaffold when θ= 45^o

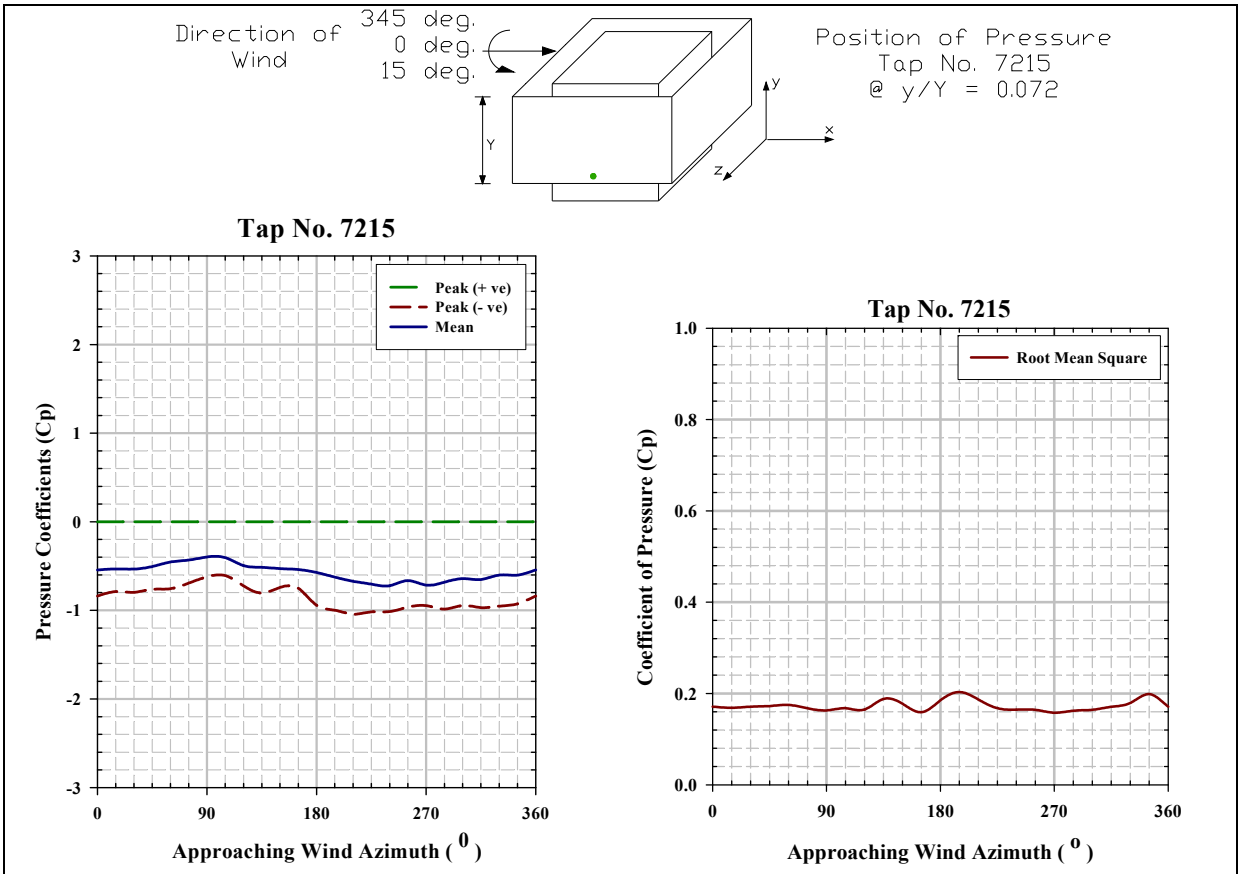

Figure 7B.25 Mean, peak, rms pressure coefficients for tap number 7215

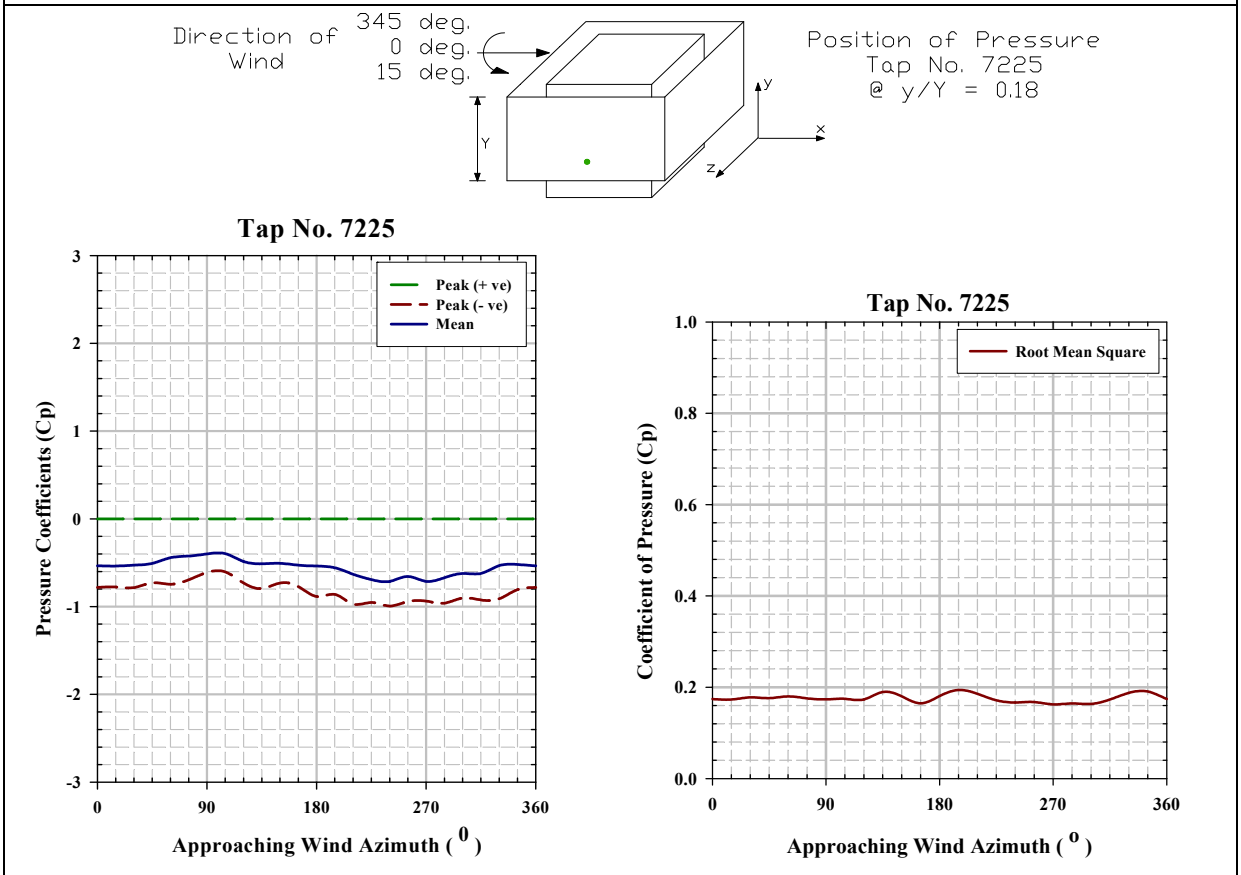

Figure 7B.26 Mean, peak, rms pressure coefficients for tap number 7225

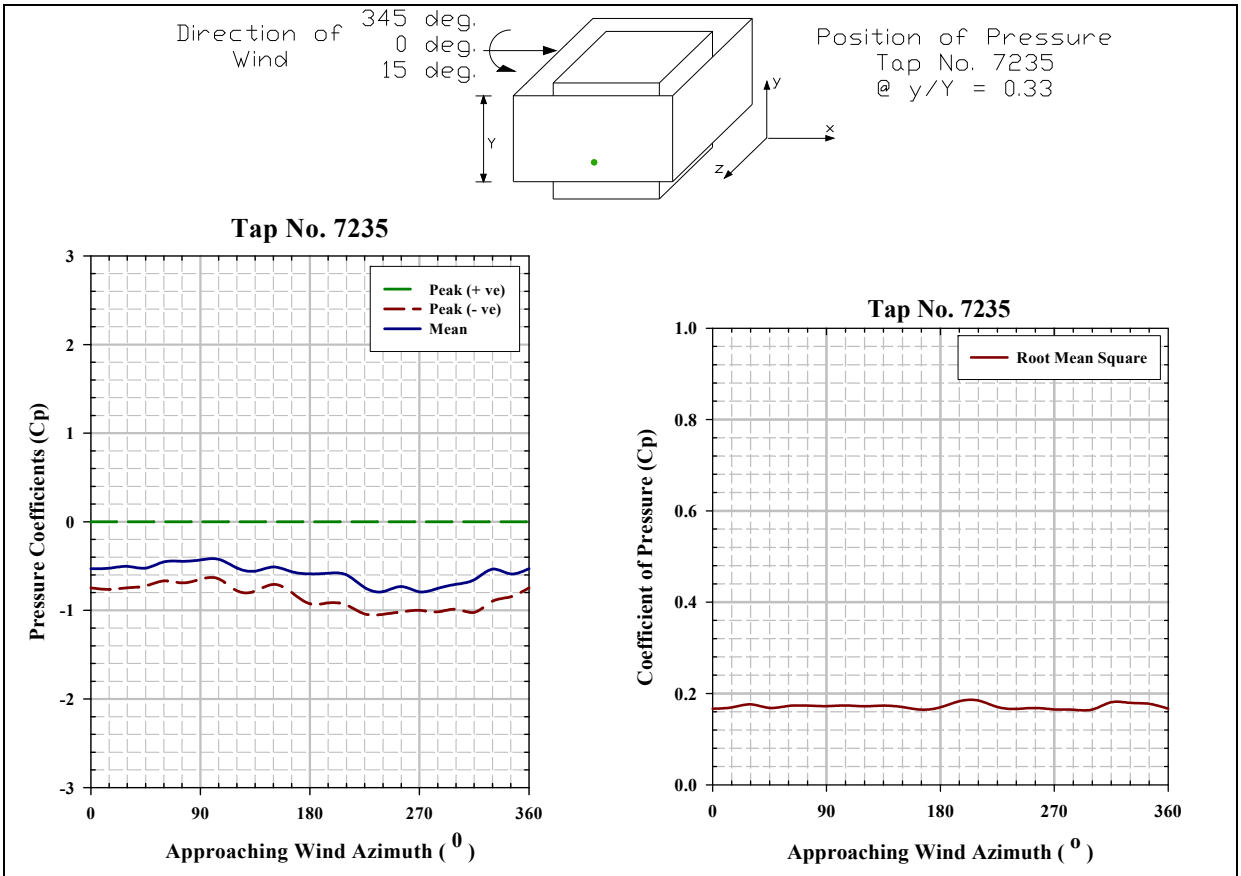

Figure 7B.27 Mean, peak, rms pressure coefficients for tap number 7235

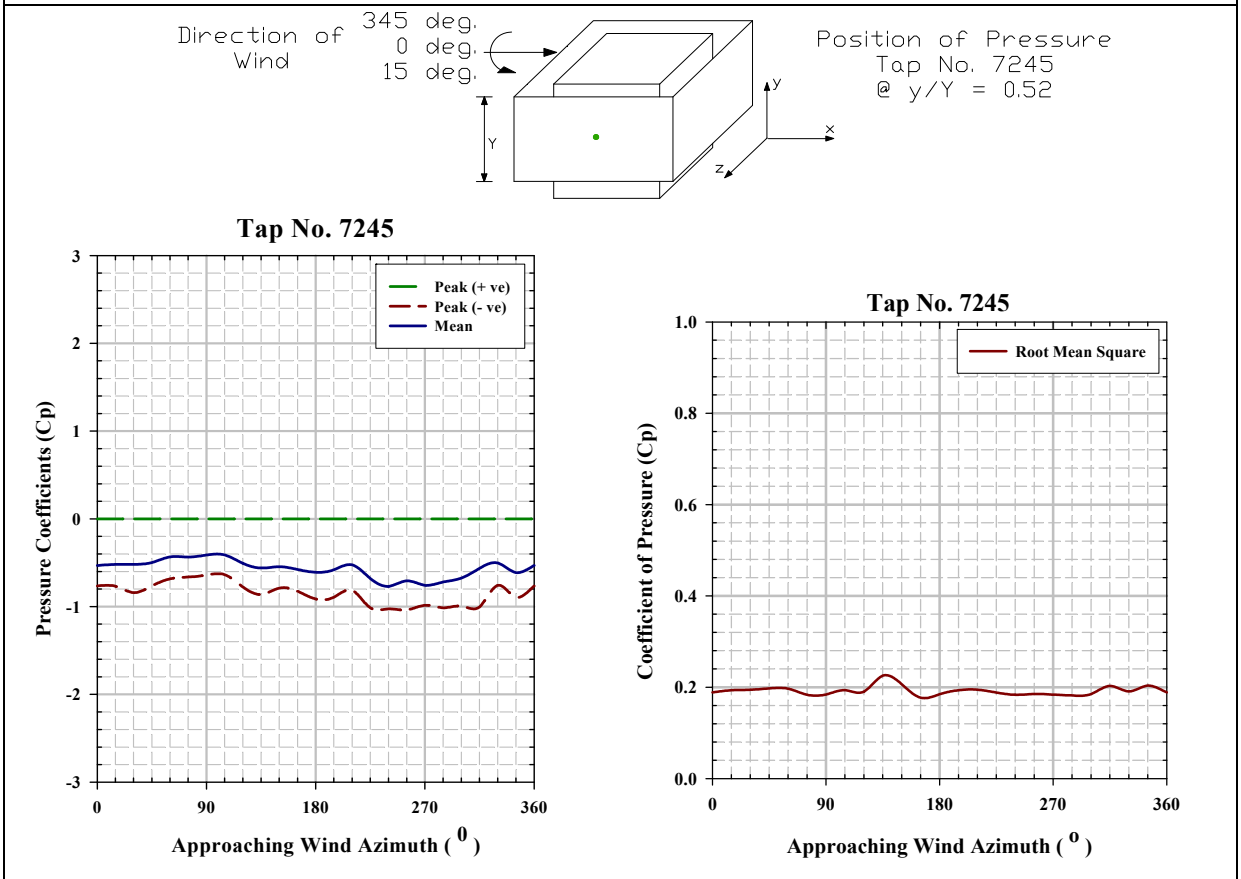

Figure 7B.28 Mean, peak, rms pressure coefficients for tap number 7245

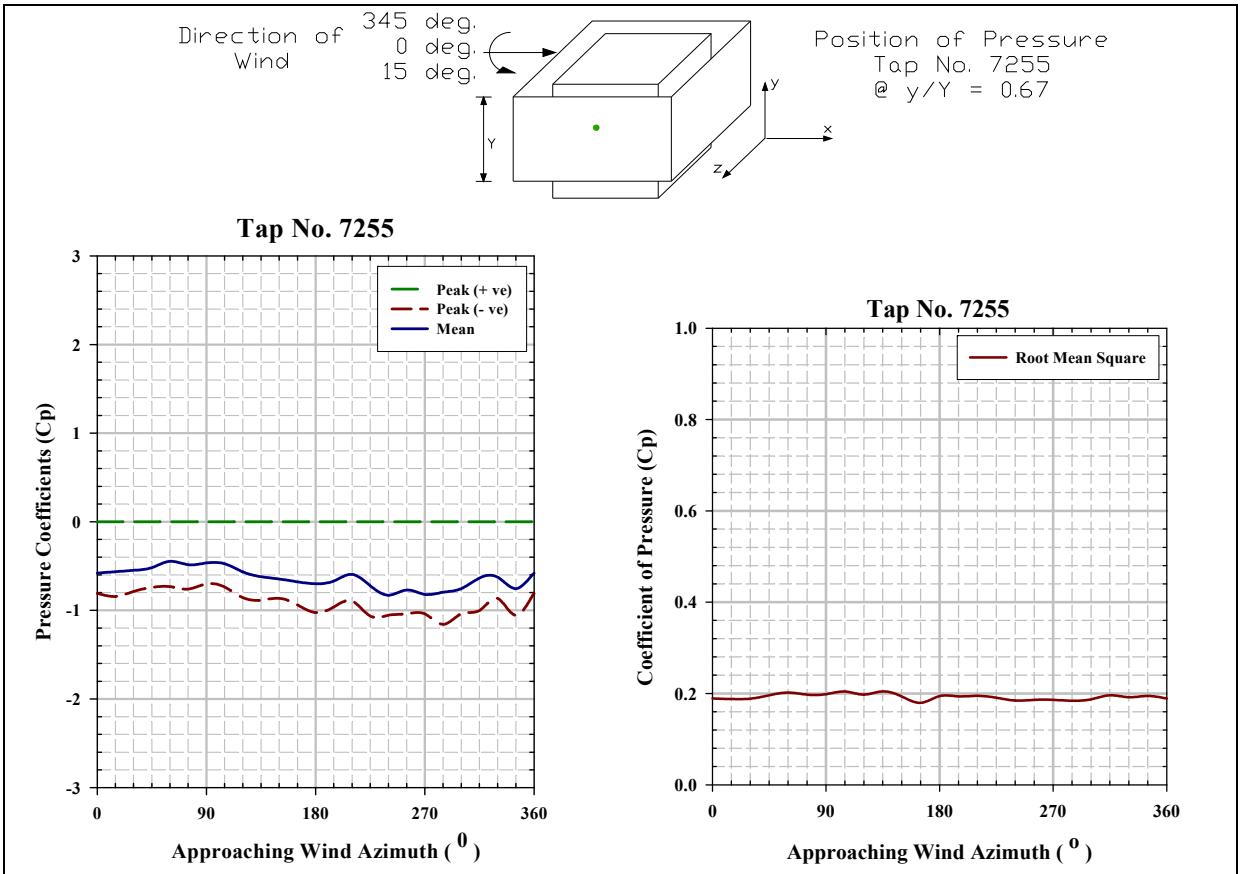

Figure 7B.29 Mean, peak, rms pressure coefficients for tap number 7255

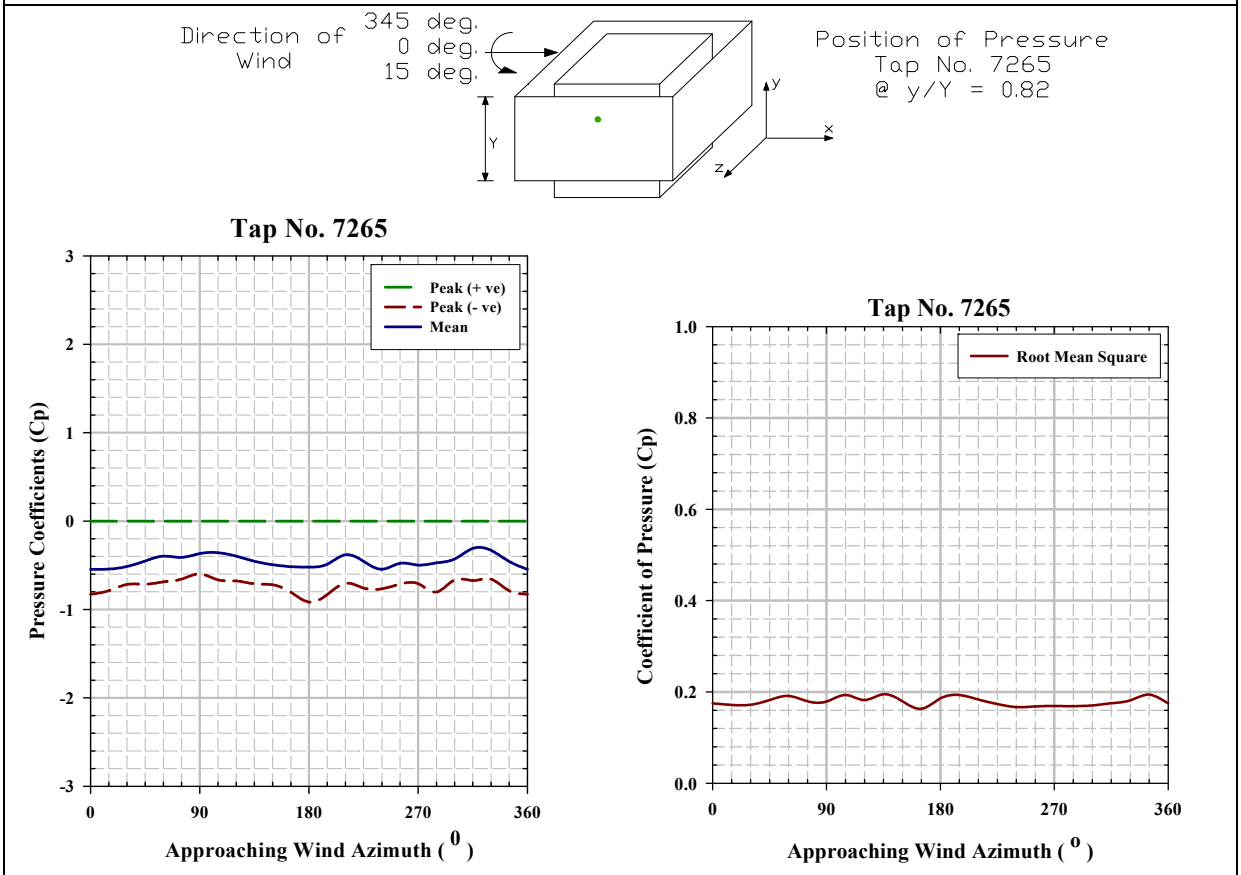

Figure 7B.30 Mean, peak, rms pressure coefficients for tap number 7265

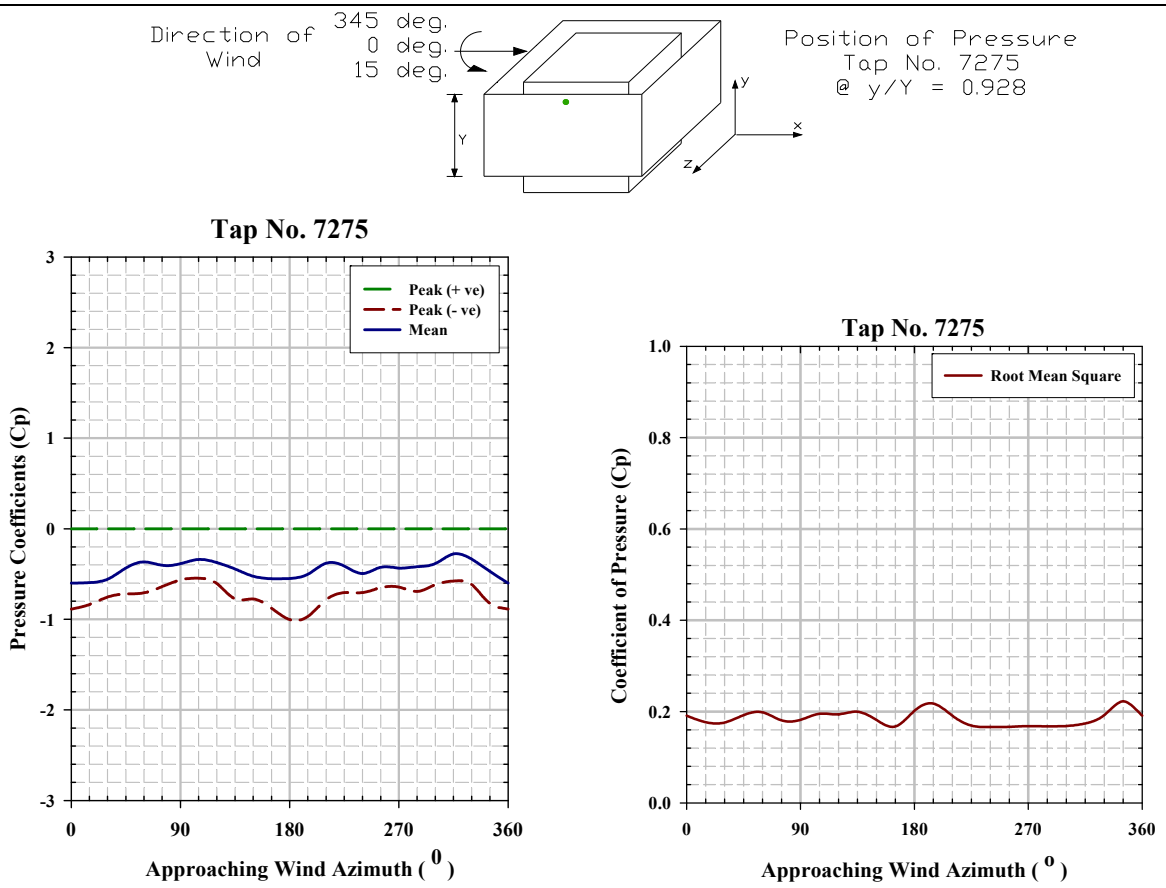

Figure 7B.31 Mean, peak, rms pressure coefficients for tap number 7275